BULLETIN OF RUSSIAN STATE MEDICAL UNIVERSITY

BIOMEDICAL JOURNAL OF PIROGOV RUSSIAN NATIONAL RESEARCH MEDICAL UNIVERSITY

Indexed in Scopus. CiteScore 2018: 0.16

Indexed in WoS. JCR 2018: 0.13

Five-year h-index is 3

Indexed in RSCI. IF 2017: 0.326

Listed in HAC 27.01.2016 (no. 1760)

Open access to archive

BULLETIN OF RSMU 6, 2019

ВЕСТНИК РГМУ

Contents
Содержание

EFFECTIVENESS OF MULTIDISCIPLINARY TEAM AS A NEW MODEL OF AFTER STROKE PATIENTS' REHABILITATION

Ivanova GE[1,2,9], Melnikova EV[1,5,8], Shmonin AA[1,5,8], Verbitskaya EV[5], Belkin AA[1,3], Bodrova RA[1,4,7], Lebedev PV[1], Maltseva MN[1,5], Prokopenko SV[1,6], Prosvirnina MS[1,8], Sarana AM[1], Stakhovskaya LV[1,2], Suvorov AYu[1,2,9] ✉, Khasanova DR[1,4,7], Shamalov NA[1,2,9]

[1] All-Russian Union Rehabilitators, Moscow, Russia
[2] Pirogov Russian National Research Medical University, Moscow, Russia
[3] Ural State Medical University, Ekaterinburg, Russia
[4] Kazan State Medical Academy, Kazan, Russia
[5] Pavlov First Saint Petersburg State Medical University, Saint Petersburg, Russia
[6] Krasnoyarsk State Medical University, Krasnoyarsk, Russia
[7] Kazan State Medical University, Kazan, Russia
[8] City Hospital № 26, Saint Petersburg, Russia
[9] Federal Centre of Cerebrovascular Pathology and Stroke, Moscow, Russia

Modern papers on treatment and rehabilitation of stroke patients describe the advantages and effectiveness of certain medical rehabilitation types, but these data are not enough to evaluate the efficiency of the whole rehabilitation system. The study was aimed to investigate the potential of the patient-centered problem-oriented multidisciplinary three-stage system for medical rehabilitation of stroke patients. The study included 1021 patients over 18 affected with ischemic or hemorrhagic stroke in the acute phase. All patients had a disability of admission at the time (but no persisting disability in their history). Two models of rehabilitation measures were compared in two consecutive phases of the study. The linear model of rehabilitation assistance was mainly implemented in phase 1, and the multidisciplinary model was implemented in phase 2. The patients' condition was evaluated using the Modified Rankin Scale (mRS) at the end of rehabilitation. Comparison of the 1st and 2nd phase results demonstrated that the number of patients with mRS score 0–1 in the 2nd phase was lower by 18%. The proportion of patients with positive dynamics was significantly higher in the 2nd phase than in the 1st phase, (16 and 30% respectively). In the 2nd phase there were significantly more patients who demonstrated improvement by 1–4 (mRS score). Thus, the use of a multidisciplinary model provides a significant benefit compared with a linear rehabilitation model.

ОЦЕНКА ЭФФЕКТИВНОСТИ РАБОТЫ МУЛЬТИДИСЦИПЛИНАРНОЙ БРИГАДЫ КАК НОВОЙ МОДЕЛИ ОКАЗАНИЯ РЕАБИЛИТАЦИОННОЙ ПОМОЩИ ПАЦИЕНТАМ С ЦЕРЕБРАЛЬНЫМ ИНСУЛЬТОМ

Г. Е. Иванова[1,2,9], Е. В. Мельникова[1,5,8], А. А. Шмонин[1,5,8], Е. В. Вербицкая[5], А. А. Белкин[1,3], Р. А. Бодрова[1,4,7], П. В. Лебедев[1], М. Н. Мальцева[1,5], С. В. Прокопенко[1,6], М. С. Просвирнина[1,8], А. М. Сарана[1], Л. В. Стаховская[1,2], А. Ю. Суворов[1,2,9] ✉, Д. Р. Хасанова[1,4,7], Н. А. Шамалов[1,2,9]

[1] Общероссийская общественная организация содействия развитию медицинской реабилитологии «Союз реабилитологов России», Москва, Россия
[2] Российский национальный исследовательский медицинский университет имени Н. И. Пирогова, Москва, Россия
[3] Уральский государственный медицинский университет, Екатеринбург, Россия
[4] Казанская государственная медицинская академия, Казань, Россия
[5] Первый Санкт-Петербургский государственный медицинский университет имени И. П. Павлова, Санкт-Петербург, Россия
[6] Красноярский государственный медицинский университет имени В. Ф. Войно-Ясенецкого, Красноярск, Россия
[7] Казанский государственный медицинский университет, Казань, Россия
[8] Городская больница № 26, Санкт-Петербург, Россия
[9] Федеральный центр цереброваскулярной патологии и инсульта, Москва, Россия

В современных работах по лечению и реабилитации пациентов с инсультом описывают преимущества и эффективность отдельных видов медицинской реабилитации, но этих данных недостаточно для оценки эффективности реабилитационной системы в целом. Целью нашего исследования было изучить эффективность пациент-центрированной проблемно-ориентированной мультидисциплинарной трехэтапной системы медицинской реабилитации пациентов с инсультом. В исследовании принял участие 1021 пациент старше 18 лет с ОНМК по ишемическому или геморрагическому типу в острейшем периоде. Все пациенты имели ограничение жизнедеятельности на момент поступления (без стойкой инвалидизации в анамнезе). Проводили сравнение двух моделей реабилитационных мероприятий, которые осуществляли в две последовательные фазы. В фазе 1 реализовывали преимущественно модель линейной формы оказания реабилитационной помощи, а в фазе 2 — мультидисциплинарную модель. Состояние пациентов оценивали по модифицированной шкале Рэнкина (mRS) в конце курса реабилитации. Сравнение результатов, полученных в первую и вторую фазы исследования, показало, что количество пациентов с оценкой по шкале mRS 0–1 балл в фазе 2 было на 18% меньше. Доля пациентов, имевших положительную динамику, также была значимо выше в фазе 2, чем в фазе 1 (16 и 30% соответственно). Пациентов, продемонстрировавших улучшение на 1–4 балла, в фазе 2 было значимо больше. Таким образом, применение мультидисциплинарной модели по сравнению с линейной моделью реабилитации обеспечивает значимое улучшение.

Various terms are used in the literature to describe the work of a multidisciplinary team (MDT) in medical rehabilitation [1–3]. It is written in the White Book on Physical and Rehabilitation Medicine (PRM) in Europe, that the rehabilitation team should work using a multi-professional, interdisciplinary, team-based approach [4–6]. In Russia, this principle is called multidisciplinary [1].

The study was aimed to investigate the efficiency of a patient-centered, problem-oriented multidisciplinary three-stage system of medical rehabilitation of patients with stroke compared with the linear rehabilitatopn model in the framework of a multi-center study.

METHODS

The study protocol was published earlier [7–9].

The study design was comparative, consistent and included two phases. The study involved 22 medical organizations of the first, second and third stages of medical rehabilitation from 8 regions of the Russian Federation: St. Petersburg, the Tver Region, the Sverdlovsk Region, the Republic of Tatarstan, the Krasnoyarsk Region, Chuvash Republic, Perm Krai. The staffing and equipment of all centers complied with the order of medical rehabilitation (order of the Ministry of Health of the Russian Federation № 1705н dated 29.12.2012) [10] and with the order of medical care for patients with stroke (order of the Ministry of Health of the Russian Federation № 928н dated 15.11.2012) [11].

Comparative study if the biomedical and biopsychosocial medical rehabilitation models, implemented in phases 1 and 2, was published earlier [8, 9]. Phase 1 was the work of a rehabilitation MDT that implemented a biomedical rehabilitation model (all specialists worked separately, without discussing the problems of patients at the MDT meetings). Neurologists directed the patients to physical therapists, speech-language pathologists, physiatrists and psychologists. Functional impairments were described in accordance with accepted forms and formalized records in the patient history. Rehabilitation diagnosis was not made, rehabilitation goal was not formulated. To assess the condition of the patient, only the International Classification Of Diseases (ICD-10) was used. The International Classification of Functioning, Disability and Health (ICF) was not used. During the 1st phase all MDT specialists were trained at 5 medical universities of the Ministry

of Health of the Russian Federation and one university of the Ministry of Education and Science of the Russian Federation (Pirogov Russian National Research Medical University, Pavlov First Saint Petersburg State Medical University, Ivanovo State Medical Academy, Krasnoyarsk State Medical University and Lobachevsky State University of Nizhny Novgorod). All centers used the same training program.

The training program included blocks on general issues of medical rehabilitation, as well as blocks on particular issues of cardiological and neurological rehabilitation, rehabilitation traumatology, on psychological correction, occupational therapy, physical therapy, speech-language therapy. Specialists were trained to organize and conduct a multidisciplinary rehabilitation process, to use ICF, to draw up the rehabilitation diagnosis and plan. The program involved training of specialists in basic rehabilitation interventions in accordance with Russian clinical recommendations [12] nd recommendations of the European Society of Physical and Rehabilitation Medicine (ESPRM) [4–6, 13–21].

The main group of specialists, who developed the training programs for the project participants and organized the educational process, was previously trained by the ESPRM specialists [7] according to the training program on physical and rehabilitation medicine. The training program was modular. The training programs available in Russia were supplemented by modules on medical and social rehabilitation as well as the other modules. Training and re-training were a key element of the study.

Phase 2 implementing the new rehabilitation model began after the completion of MDT specialists training. To assess the conformity of the educational bases of universities with the implemented training models, a clinical bases' audit was conducted by Russian and European specialists. It was concluded that all clinical training facilities for MDT specialists were complied with the rehabilitation organization order, the research protocol and European standards of rehabilitation [22].

In phase 2, medical organizations worked in accordance with principles, implementing a patient-centered, problem-oriented multidisciplinary (bio-psychosocial) approach [8]. The occupational therapist or a specialist who fulfilled the functional duties of an occupational therapist after special training (specialist with basic higher pedagogical, psychological or medical education) was included in the MDT. The program for

Table 1. List of scales used in the phase 2

Specialist	Scale
Rehabilitation physician (neurologist)	National Institutes of Health Stroke Scale (NIHSS)
	Modified Rankin Scale (mRS)
	Pain Visual Analogue Scale (VAS)
	Modified Ashworth Scale (MAS)
Psychologist	Montreal Cognitive Assessment (MoCA)
	Hospital Anxiety and Depression Scale (HADS)
Speech-language pathologist	Scale designed by L.I. Wasserman for estimating the degree of speech disorders in patients with local brain injuries
	Mann Assessment of Swallow Ability (MASA)
Emergency	National Institutes of Health Stroke Scale (NIHSS)
	Glasgow Coma Scale
Physical therapist	Medical Research Council scale (MRC)
	Berg Balance Scale (BBS)
	Functional Independence Measure (FIM)
	Frenchay Arm Test
	Quality of life assessment using EuroQ-5D questionnaire

re-training of exercise therapy methodologists also included modules on physical therapy.

MDT worked in accordance with the ESPRM standards. All specialists met and discussed the patient's problems at the MDT meeting, set the goal of rehabilitation and drew up a rehabilitation plan. Rehabilitation diagnosis was used for coordination. Clinical psychologists and psychotherapists were actively involved to provide a patient-centered approach.

To evaluate the role of the MDT specialists, rehabilitation assessment scales were used [23]. Scales and questionnaires were distributed in accordance with the competencies of specialists to describe the main necessary for rehabilitation patient functioning indicators (Table 1). If the changes had been revealed that could be evaluated using certain scale, then such a scale was used in case of the feasibility of the assessment (for example, it is impossible to evaluate cognitive function or anxiety in a patient with a decreased consciousness). However, some scales were used regardless of the severity of the patient's condition (mRS, Rivermead Mobility Index, NIHSS and Glasgow Coma Scale). Assessment was carried out at the beginning and at the end of hospitalization at all three study stages. Specialists were allowed to use other scales and questionnaires, which were not analyzed separately.

When transferring a patient from the intensive care unit or vascular unit to the medical rehabilitation unit, only the Glasgow Coma Scale was excluded from the list of scales.

After the rehabilitation completion (1.5 years), a delayed assessment of the patient's condition based on a telephone interview with the patient or his close relatives was carried out using a modified set of tests and scales. For telephone interviewing, a group of specialists trained to perform telephone surveys was created. The training included psychologist's lectures on the psychological features of performing surveys, lectures on conflict management as well as training on mRS implementation in telephone surveys for rehabilitation physicians. After training all specialists passed the exam. The following indices were chosen for telephone assessment: mRS, Rivermead Mobility Index, adverse events and EQ-5D. During the interview, specialists had access to the patients' database, so they could use information about the patient's condition at various stages of rehabilitation to increase the interview effectiveness. The interviewers did not know to what phase of the study the patients they interacted with belonged. Patients also did not know what phase of the study they were included in. Thus, the study could be considered double blind.

Two mRS score values were selected as intermediate points of the study: the value obtained at the 1st stage of rehabilitation, and the value obtained 1.5 years (18 months) after the rehabilitation. The mRS was chosen as a universal indicator of the patient's health, disability and the patient's independence, since the scale allows one to describe any degree of disability regardless of the cause (not only related to stroke).

The study included patients with acute ischemic or hemorrhagic stroke who had a disability at the time (minimum mRS score 2) and who had not have a disability prior to stroke (score 2 or more). That is, patients without previous persistent disabilities who were independent before stroke according to information obtained from patient or his relatives were included into the study.

Inclusion criteria: ischemic or hemorrhagic stroke acute period (within 21 days from the onset), provided that surgery is not required; age over 18. Exclusion criteria: mRS score over 1 before stroke; conducting or planning of any surgery (except thrombectomy); isolated subarachnoid hemorrhage; transient ischemic attack; impaired consciousness upon admission (coma score 2 or more).

The protocol of stroke patients' survey during medical rehabilitation at all stages in phase 1 and phase 2 was published earlier [8]. After the 1st stage rehabilitation completion, the patients were directed to the 2nd and 3rd stage, depending on the level of vital activity restoration and the need of further rehabilitation. Thus, the patients with mRS score 4–5 were directed to the 2nd stage of rehabilitation, and the patients with mRS score 2–3 were directed to the 3rd stage. All patients directed to the 2nd and 3rd stages of rehabilitation had good prospects for recovery and a prognosis of full or partial functioning restoration, or a prognosis of adaptation and compensation. Patients with a prognosis of nursing and palliative care were transferred to appropriate facilities or discharged. Patients with mRS score 0–1 were also discharged, since they had no disability and did not need rehabilitation. The sampling was continuous.

Thus, patients received a three-stage medical rehabilitation in accordance with the multidisciplinary problem-oriented and patient-centered model in phase 2 or in accordance with the biomedical model in phase 1, which made it possible to compare the two systems of rehabilitation organization. The protocol of patients' examination used in phases 1 and 2 was the same. It was based on the current rules and regulations of the Russian Federation [10–11]) as well as clinical scales that had shown validity in Russian and foreign studies on the stroke patients rehabilitation.

ICF-reader application (developed by Shmonin AA, Maltseva MN, Melnikova EV; Saint-Petersburg, Russia) was used as an electronic registration card patients' data collection. The application was installed in all centers participating in the study; it worked in accordance with the network principle. Any registered employee could enter the application, see the patient's data and perform the assessment. The application also promoted multidisciplinary approach because of better information sharing. Due to the ICF-reader software, the research organizers could conduct an electronic audit [9, 23].

Statistical analysis was performed using the SAS software (SAS Institute Inc.; USA). The Shapiro–Wilk test was used for assessment the distribution normality. Analysis of variance (ANOVA) was used to compare the main quantitative indicators in a normal distribution. Mixed-design analysis of variance (MixedANOVA) was implemented for repeated measurements in a normal distribution. Pairwise analysis of the groups was carried out only if there were significant differences according to the Breslow–Day test. For pairwise comparisons, the Tukey–Cramer test was used. McNemar's test was applied to contingency tables with a dichotomous trait. For a distribution other than normal, the Mann–Whitney U test was used for unrelated samples, and the Wilcoxon test was used for related samples. To analyze the qualitative data, the Fisher exact test and the Pearson χ^2 test were used, depending on the number of indicators. The differences were considered significant when $p < 0.05$.

The study was registered as a clinical trial in the international ClinicalTrials.gov registry with the following name: The Pilot Project Development Of Medical Rehabilitation System in Russian Federation (DOME) (NCT02793934).

RESULTS

There were 1021 patients registered in the electronic system. Prior to the study, the groups of patients were comparable in severity and major epidemiological parameters (Table 2). In

phase 2, there was a greater number of patients with a specified stroke pathogenetic variant. Disability before stroke, as well as the the proportion of patients who received reperfusion therapy during the stroke acute period in phases 1 and 2 were comparable.

At the beginning of the study, all patients had similar indices values (Table 3).

The main endpoint of the study was the mRS score at the end of rehabilitation (Fig. 1). In the phase 2, an 18% increase in the proportion of patients without disabilities was observed (mRS 0–1) compared with phase 1 ($p < 0.0001$). The mRS score in the 1st group in the end of rehabilitation was 3 (2; 4), and in the 2nd group it was 2 (1; 3) (Mann–Whitney U test, $p < 0.01$).

Table 2. Comparison of two groups of patients with stroke before the start of the study

Indicator	Phase 1	Phase 2	Significance
Nimber of patients	498	523	–
Sex (F : M)	1 : 1.5	1 : 1.2	0.06
Age	68 ± 12	68 ± 14	0.32
Smoke	14%	15%	0.26
Ischemic stroke	91.2%	92.7%	0.21
Hemorrhagic stroke	8.8%	7.3%	
Alcohol addiction	4.5%	3.2%	0.16
Ischemic stroke history	20%	18%	0.23
Hemorrhagic stroke history	1%	1%	0.23
Disability history			
mRS score before stroke 0	81.8%	84.0%	0.33
mRS score before stroke 1	18.0%	16.0%	
mRS score before stroke 2	0.2%	0.0%	
Reperfusion therapy			
Intravenous fibrinolytic therapy	3.5%	1.5%	0.14
Thrombectomy	0.6%	0.6%	
Ischemik stroke pathogenesis variant			
NYD	**11.7%**	**8.0%**	< 0.05
Atherothrombosis	56.9%	51.4%	
Cardioembolic stroke	13.3%	19.2%	
Lacunar stroke	**7.8%**	**13.2%**	
Rare causes of stroke	0.2%	0.2%	
Other	1.2%	0.7%	

Note: phase 1 — biomedical rehabilitation model; phase 2 — multidisciplinary patient-centered problem-oriented rehabilitation model.

Table 3. Comparison of two groups of patients with stroke before the start of the study

Scales					Phase 1	Phase 2	Significance, Tukey–Kramer test
NIHSS					6 (4; 10)	5 (3; 9)	>0.05
MoCa					17.5 (8; 21)	18 (9; 23)	0.3287
Frenchay arm test					2 (0; 4)	3 (0; 5)	0.0765
FIM					81 (56; 97)	76 (52; 95)	0.8394
BBS					25 (5; 38)	16 (0; 37)	0.1582
MRC	Hand	Right		Proximal	3 (0; 4)	3 (0; 4)	0.5086
				Distal	3 (0; 4)	3 (0; 4)	0.3538
		Left		Proximal	3 (0; 4)	3 (0; 4)	0.0038
				Distal	3 (0; 4)	3 (0; 4)	0.0022
	Leg	Right		Proximal	3 (0; 4)	3 (0; 4)	0.5207
				Distal	3 (0; 4)	3 (0; 4)	0.3081
		Left		Proximal	3 (0; 4)	3 (0; 4]	0.0056
				Distal	3 (0; 4)	3 (0; 4)	0.0016
MASA					179 (169; 180)	180 (177; 180)	0.5601
L. I. Wasserman psychodiagnostic scale					6 (0; 25)	0 (0; 24)	0.6027
EuroQ-5D					10 (8; 13)	11 (10; 15)	0.3648
HADS	Depression				6 (3; 12)	8 (4; 11)	0.427
	Anxiety				7 (3; 11)	6 (4; 10)	0.9971

In phase 2, the best improvement was demonstrated by patients with score 4, 3, and 2 at the moment of admission (p = 0.0009, 0.0019 and 0.001 respectively). Patients with mRS score 5 and 1 did not have any advantage in the 1st stage during rehabilitation in phase 2 compared with phase 1. Phase 2 rehabilitation was more effective in patients with moderate severity and disability. In severe patients and patients with no disability (mRS score 1), the efficiency remained the same as when using the biomedical model.

Assessment scales were the secondary endpoints роли (Table 4). By the time of the 1st stage rehabilitation completion, the severity in accordance with the NIHSS scale in groups 1 and 2 was comparable (p > 0.05). The FIM score, reflecting changes in self-care, mobility, communication and social activity, showed that the 2nd group patients recovered better.

The Frenchay test (Table 4) in phase 2 revealed an improvement in the patients's condition. The number of patients with score 5 (complete restoration of hand function) was 20% more in phase 2 than in phase 1. In addition, there were less patients with the score below 0, 1, 2, and 3 points in phase 2 (patients could not complete the test or made many mistakes) than in phase 1. Analysis using the Pearson χ^2 test revealed no significant differences (p = 0.0604).

Assessment using the Berg Balance Scale (Table 4) revealed a significant improvement by the end of rehabilitation in patients of the 1st (p < 0.0001), and 2nd groups (p < 0.0001). The improvement was more pronounced in the 2nd group, however, the Tukey–Cramer test demonstrated that the differences were not significant (p = 0.0859). The analysis (excluding patients with normal score at the start of the experiment) showed an increase in the proportion of patients with a low risk of falling (score 41–56) by the time the hospital stay was completed in phase 2 (59%) compared with phase 1 (47.3%). There was a decrease in the proportion of patients with an average risk of falling (21–40 points) from 39 to 19% in phase 2 (Pearson χ^2 test; p = 0.0077).

Assessment using MASA and L.I. Wasserman demonstrated the ceiling effect. By the time of the 1st stage rehabilitation completion, it was found that patients of both groups achieved an almost complete functional restoration of swallowing (200,

maximum MASA score) by median and interquartile range; therefore, there were no significant differences between the groups. By the end of the 1st stage rehabilitation, the patients of both groups achieved almost complete restoration of speech, therefore, there were no significant differences between the groups, although the median values were higher in group 2.

Assessment of cognitive functions was carried out using MoCa. In phase 2, better cognitive functions' recovery was observed than in phase 1 (p < 0.0001). The improvement was significant both in group 1 (p < 0.0001) and in group 2 (p < 0.0001).

Assessment of the anxiety level using the HADS scale did not reveal any significant differences between groups 1 and 2 (p = 0.5422). Higher level of depression was detected in phase 2 (p = 0.0318). Removing of patients with a normal HADS score from a sample at the beginning of the study showed that the increase in the HADS score was due to a significant increase in the proportion of patients subclinical depression (phase 1, 18%; phase 2, 44%; p = 0.0129). The number of patients with clinical depression (HADS) in the phases 1 and 2 was the same (28.3 and 28.8% respectively).

The use of the EuroQ-5D revealed a comparable quality of life in both groups, there were no significant differences (p = 0.0887). The best indicators were observed in the 2nd group. During hospitalization at the 1st stage, both in group 1 (p = 0.0896) and in group 2 (p = 0.567) he quality of life did not improve, which indicated lack of said indicator sensitivity at the 1st stage of the study.

A pairwise comparison (Mann–Whitney U test) showed that hospitalization was shorter in phase 2 (14 (12; 19) patient days) compared with phase 1 (16 (14; 20) patient days; p < 0.001). Recalculation of the hospitalization duration in absolute terms demonstrated that in phase 2 there was a reduction (saving) in the length of hospitalization by 38% (patient days) compared with phase 1. In phase 2, MDT specialists were advised to regulate the hospitalization duration on their own, without any limitations. Due to the introduction of a patient-centered problem-oriented multidisciplinary rehabilitation, some patients became able to remain at the 1st stage longer, because there was a need for a longer rehabilitation. Some patients became
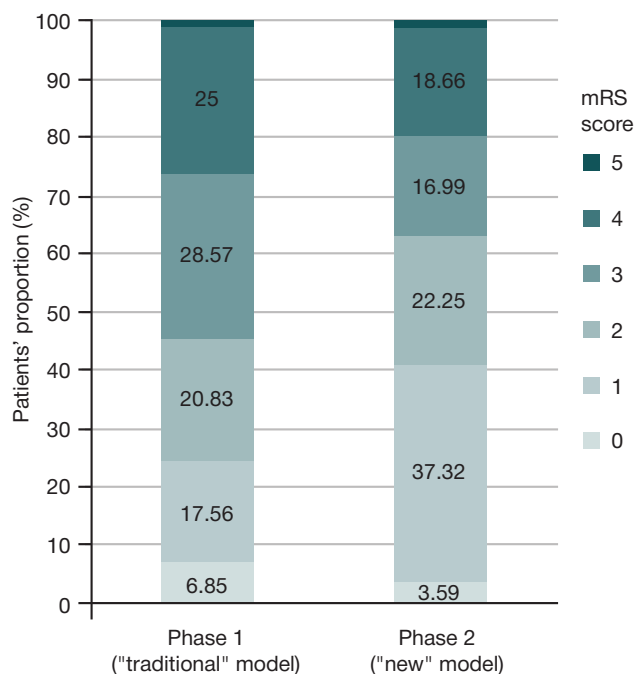
Fig. 1. Results of stroke patients rehabilitation at the end of the 1st stage (Pearson χ^2 test; p < 0.0001)

able to be discharged earlier if the goals of the rehabilitation program were achieved at the 1st stage. The principle of "unlimited" hospitalization periods allowed us to reduce the duration of hospitalization. Reducing the hospitalization duration at the 1st stage (taking into account the cost of care for patients with stroke in various regions from 75,000 to 180,000 rubles) should be regarded as ROI.

To evaluate the stroke patients' condition 1.5 years after rehabilitation using a biopsychosocial patient-centered and problem-oriented model, the analysis included information on the 237 people status received from patients or their relatives. The main reason for the patient's inaccessibility for a call was the lack of a phone number (the patient did not leave a phone number, specialists did not add it to the database) or the number change. Twenty nine people refused to talk and did not explain the reason (12%). The time between the onset and the telephone interview was comparable in both groups (Table 5), 21 (19; 23) months in the 1st group, 20 (18; 22) months in the 2nd group.

The average duration of a telephone conversation was 7 (5; 9) minutes. The most of patients and their relatives were positive and willing to communicate. In both groups, the interviewers spoke more often with patients' relatives than patients themselves.

An analysis of the interviewer's role and the assessment of the patient's condition were carried out. It was found that the results obtained by all specialists were the same and corresponded to the real patients' condition. The number of refuses to talk in all interviewers was also comparable. The data obtained were significant and did not depend on the researcher.

According to a telephone survey (Table 5), 89% patients underwent the 2nd stage rehabilitation in phase 1, and 81% patients in phase 2 ($p = 0.324$). The 3rd stage rehabilitation was received by 50% phase 1 patients and 53% phase 2

patients ($p = 0.7$). In phase 2, patients received rehabilitation in the institutions where the MDT specialists were trained. The 57% patients were directed to the 2nd and 3rd stages of rehabilitation immediately, avoiding getting home. This means that there was no break between the medical rehabilitation stages.

Since not all patients (only 237 people) were included in the sample, a comparison was made of the groups of patients who took part in a telephone interview according using the baseline indicators for the 1st stage (Table 5). The disability prior to stroke baseline assessment obtained using mRS and the patient's history, was comparable in both groups ($p > 0.05$). The mRS disability score was also the same in the beginning of the 1st stage ($p = 0.967$), which allowed us to compare the groups.

mRS assessment was the main endpoint of the study, it was performed by phone. The disability score in stroke patients after 1.5 years was in lower 2nd group than in the 1st group (Fisher exact test; $p < 0.05$) (Fig. 2). The Mann–Whitney U test showed that in the 1st group the mRS score was 3 (2; 4), and in the second group it was 2 (1; 3) ($p = 0.026$).

Mortality in both groups was comparable and did not differ significantly (1st group, 15.5 %, 2nd group, 16 % (Pearson χ^2 test, $p = 0.532$). Multidisciplinary rehabilitation together with specialized and high-tech medical care did not affect mortality within 1.5 years after a stroke.

The patients' quality of life in accordance to EuroQ-5D and VAS EuroQ-5D y the end of the study was comparable in both groups ($p = 0.1293$ and $p = 0.0903$) (Table 5). However, a subanalysis showed that when using a patient-centered, problem-oriented multidisciplinary rehabilitation, the anxiety level in accordance with EuroQ-5D was lower (Mann–Whitney U test; $p = 0,0045$).

Rivermead Mobility Index score was better with a patient-centered, problem-oriented multidisciplinary rehabilitation

Table 4. Results of stroke patients condition evaluation at the end of the 1st stage of rehabilitation

Scales				Significance, pairwise comparison			Significance, before and after rehabilitation on the 1st stage		Tests
				Phase 1	Phase 2	Tukey–Kramer test	Phase 1	Phase 2	
NIHSS				5 (3; 7)	3 (2; 7)	> 0.05	< 0.0001	< 0.0001	Tukey–Kramer test
FIM				100 (76; 114)	118 (103;125)	< 0.0001	< 0.0001	< 0.0001	Tukey–Kramer test
Frenchay arm test				5 (3; 5)	5 (4.5; 5)	1.0	0.0041		Wilcoxon test
							0.0604		χ^2
BBS				42 (27; 51)	50.5 (35; 54)	0.0859	< 0.0001	< 0.0001	Tukey–Kramer test
MRC	Hand	Right	Proximal	3 (0; 5)	4 (0; 5)	0.0355			Mann–Whitney U test
			Distal	3 (0; 5)	4 (0; 5)	0.0062			Mann–Whitney U test
		Left	Proximal	3 (0; 5)	3 (0; 5)	< 0.0001			Mann–Whitney U test
			Distal	3 (0; 5)	4 (0; 5)	< 0.0001			Mann–Whitney U test
	Leg	Right	Proximal	4 (0; 5)	4 (0; 5)	0.110			Mann–Whitney U test
			Distal	4 (0; 5)	4 (0; 5)	0.0236			Mann–Whitney U test
		Left	Proximal	4 (0; 5)	4 (0; 5)	0.0003			Mann–Whitney U test
			Distal	3 (0; 4)	3 (0; 4)	< 0.0001			Mann–Whitney U test
MASA				180 (178; 180)	180 (178; 180)	0.8284	0.0033	0.0594	Tukey–Kramer test
L. I. Wasserman psychodiagnostic scale				2 (0; 10)	0 (0; 2)	0.5578	0.0387	0.086	Tukey–Kramer test
MoCa				21.5 (15; 25)	23 (19; 26)	< 0.0001	$p < 0.0001$	$p < 0.0001$	Tukey–Kramer test
HADS	Depression			4 (2; 7)	7 (3; 10)	0.0318	0.0009	0.2435	Tukey–Kramer test
	Anxiety			4 (2; 7)	5 (3; 7)	0.5422	< 0.0001	0.1048	Tukey–Kramer test
EuroQ-5D				8.5 (6; 10)	7 (5; 10)	0.0887	0.0896	0.567	Tukey–Kramer test
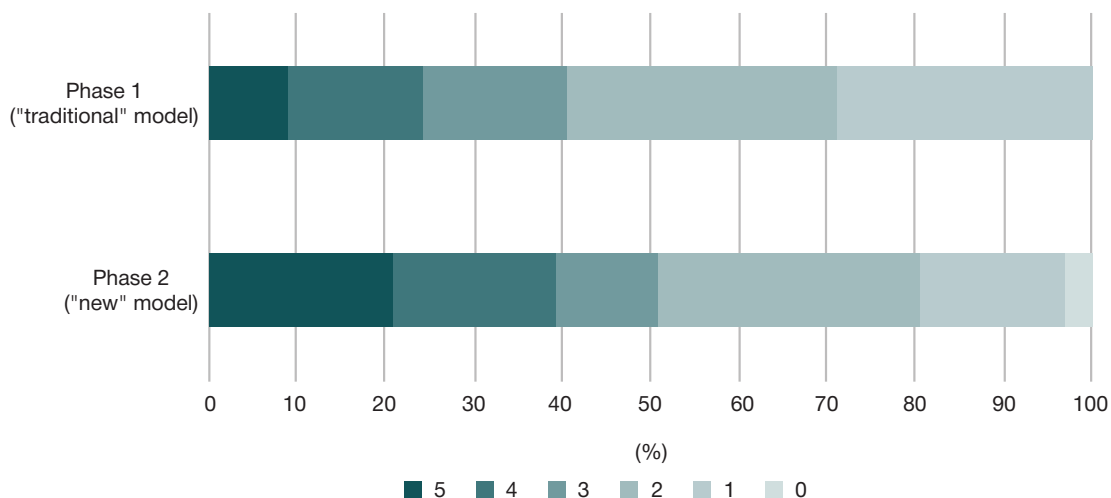
Fig. 2. mRS assessment carried out 1.5 years after stroke (score obtained during the telephone interview)

(14 (9; 14)) than with a biomedical model (13.5 (7; 14), $p = 0.04$), i.e. patients became more mobile 1.5 years after the stroke.

The proportion of patients who were constantly under the doctor's care (Table 5) was greater in phase 2, the differences were not significant ($p = 0.123$). In the phases 1 and 2 the same number of patients was controlled by neurologist, physician and other doctors ($p = 0.123$). Patient-centered problem-oriented multidisciplinary rehabilitation did not affect the patient's commitment to control his condition with doctor's assistance after completing 3-stage rehabilitation. Ten percent of patients who underwent rehabilitation according to the biomedical model refused to take drugs after the completion of treatment in medical institutions. When using a patient-centered problem-oriented multidisciplinary rehabilitation, patients refused less often (4% patients), however, there were no significant defferences ($p = 0.23$). Blood pressure was not controlled by 7% patients who underwent rehabilitation according to the biomedical model, and by 4% patients who underwent rehabilitation according to a multidisciplinary problem-oriented and patient-centered model ($p = 0.73$).

DISCUSSION

Introduction of a patient-centered problem-oriented multidisciplinary rehabilitation at the 1st stage of treatment and rehabilitation in our study provided a significant decrease in the level of dependence in the daily life of stroke patients compared to the traditional rehabilitation model. The effect of the new rehabilitation model was associated with the rehabilitation optimization, better rehabilitation organization, focus on functional outcome, greater involvement of the patient and his relatives in the rehabilitation process, as well as greater patient's interest.

The patients' condition changes analysis (mRS) demonstrated that the proportion of patients who showed deterioration during the 1st stage of medical rehabilitation in phase 2 was less than in phase 1. Deterioration was associated with pneumonia, urinary tract infections, pulmonary embolism, progression of cerebral edema, etc. Significant improvement (by 3 and 4) was possible only at the 1st stage of rehabilitation, in patients who had functional disorders associated with "quick-fix" causes (stress, pain, brain edema, intoxication, acute infection, etc.). The use of a problem-oriented patient-centered and multidisciplinary rehabilitation model provides significant improvement, fewer patients show a deterioration during the rehabilitation.

The results obtained using the FIM scale emphasize the features of the rehabilitation intervention, which, in case of impossibility of function restoring, improves functioning due to the active patient's participation. FIM also reflects the efficiency of the occupational therapy and physical therapy specialists.

Assessment using the Frenchay test demonstrated that the scale was not so sensitive and did not fully reflect the effects of rehabilitation. It may be necessary to use more sensitive evaluation instruments (for example, the ARAT test).

The Berg Balance Scale showed the effectiveness of the physical therapists' work in phase 2. Assessment using MASA and L. I. Wasserman scale for estimating the degree of speech disorders in patients with local brain injuries demonstrated the ceiling effect. Good speech and swallowing recovery were associated with the effective work of speech-language pathologists in both phase 1 and phase 2.

In patients with stroke, cognitive impairment could be both a manifestation of a stroke and premorbid disorders associated with cerebrovascular risk factors. In some cases, a combination of one and the other could be present. The best recovery of cognitive functions (MoCa) in phase 2 demonstrated the advantage of the patient-centered problem-oriented approach in the work of MDT psychologists.

Assessment using the HADS scale used for screening assessment of emotional disturbances in patients with cerebral stroke revealed a higher level of subclinical depression in the phase 2 patients. That could be due to a higher level of patient's awareness and difficulty in adaptation during phase 2, which, among other things, was evidenced by a better restoration of cognitive functions in phase 2. It is likely that the use of a wider range of diagnostic tools will allow us to study the manifestations of emotional disturbances in patients with cerebral stroke during the recovery period better.

Evaluation using EuroQ-5D showed a comparable level of quality of life in both groups. The lack of improvement in the quality of life at the 1st stage could be due to the necessity of a hospital stay, communication with strangers and other factors. A delayed assessment may provide an opportunity to obtain objective information about the patients' quality of life.

Hospitalization period duration change and, as a result, the economic efficiency of rehabilitation indicates the impossibility of introducing the fixed periods of hospitalization for rehabilitation patients, since the needs of patients with stroke, and therefore the duration of rehabilitation, can be different. It is necessary to link the duration of hospitalization with the rehabilitation potential implementation and the rehabilitation goals achievement set upon admission of the patient to each stage.

Table 5. Groups of patients' baseline indicators and results obtained during the telephone interview

Scales and questionnaires	Phase 1		Phase 2	Significance	Test
Time between entering the 1st stage and the telephone interview, months	21 (19; 23)		20 (18; 22)	0.09	Mann–Whitney U test
mRS score before stroke 0	80%		79%	0.47	Fisher's exact test
mRS score before stroke 1	20%		21%		
Relatives answered the call	73%		66%	0.194	
Patient answered the call himself	27%		34%		
mRS score when entering the 1st stage	3 (3; 4)		3 (3; 4)	0.967	Mann–Whitney U test
mRS score 0	When entering the 1st stage	0%	0%	0.109	Fisher's exact test
mRS score 1		0%	0%		
mRS score 2		14%	12%		
mRS score 3		29%	30%		
mRS score 4		43%	45%		
mRS score 5		14%	13%		
Rivermead Mobility Index	13.5 (7; 14)		14 (9; 14)	0.04	Mann–Whitney U test
Total EuroQ-5D	7 (5; 10)		6 (5; 8)	0.1293	
VAS EuroQ-5D, %	50 (20; 70)		50 (50; 70)	0.0903	
EuroQ-5D Mobility	2 (1; 2)		2 (1; 2)	0.5097	
EuroQ-5D Self-care	1 (1; 2)		1 (1; 2)	0.1517	
EuroQ-5D Usual activities	2 (1; 2)		1 (1; 2)	0.2346	
EuroQ-5D Pain/discomfort	2 (1; 2)		1 (1; 2)	0.125	
EuroQ-5D Anxiety/depression	2 (1; 2)		1 (1; 2)	0.0045	
Underwent rehabilitation at the 2nd stage	89.25%		81.33%	0.342	
Underwent rehabilitation at the 3rd stage	50.00%		52.78%	0.7	
Obesity	37.78%		34.78%	0.251	
Was under no doctor's care	33.33%		27.14%	0.123	
Was under neurologist's care	22.22%		20.00%		
Was under physician's care	30.00%		22.86%		
Was under other doctor's care	14.44%		30.00%		
Did not receive any medicine	10.11%		4.29%	0.23	
Did not control blood pressure	6.74%		4.29%	73	

An equal number of patients who received rehabilitation in the 2nd and 3rd stages contributed to the objectivity of the study, since the amount of care received by patients of phases 1 and 2 is the same. However, the quality of care received by patients in the 2nd and 3rd stages of the study in the institutions where the teams implemented the multidisciplinary patient-centered problem-oriented model was significantly higher.

Analysis of the main study endpoints demonstrated that patient-centered, problem-oriented multidisciplinary medical rehabilitation was more effective than traditional rehabilitation of patients with stroke. It was shown that the rehabilitation effect maintained at least for 1.5 years, which indicated its persistence. Most of phase 1 patients did not pass to the 2nd and 3rd stage of rehabilitation immediately and "dropped out" of observation. After the 1st stage discharge patients registered in the waiting list and received rehabilitation after months and years when the rehabilitation efficiency became lower. In phase 2, the number of patients who received rehabilitation at the second and third stages in the participating institutions was significantly larger. However, given the small sample size in phase 1 of the study, no statistical analysis was performed. In phase 2, a continuity ensuring system was created, which, with an equal amount of assistance provided, demonstrated higher quality and better effect of rehabilitation treatment.

The convenience of data collecting trough telephone interviews using a number of scales is noteworthy. Telephone interviews allow one to evaluate the patient's mobility using the Rivermead Mobility Index, to obtain information on complications and recurrent events, as well as mortality and disability severity (mRS). During the telephone interviews, we managed to obtain valuable information about the patients' condition and the persistence of the rehabilitation, which could be used to create databases on the volume and quality of medical care provided.

CONCLUSION

Three-stage patient-centered, problem-oriented, multidisciplinary model is more cost-efficient, since the model ensures better recovery of patients after stroke, improves the quality of life and patient adherence to treatment, reduces secondary healthcare costs, and helps to reduce the cost of specialized and high-tech medical care for said category of patients.

References

1. Sycheva AV. Multidisciplinary approach in the recovery treatment of the consequences of cerebral stroke [dissertation]. M., 2008. Russian.
2. Stroke Unit Trialists' Collaboration. Organised inpatient (stroke unit) care for stroke. Cochrane Database Syst Rev. 2013 Sep 11; 9: CD000197.
3. Turner-Stokes L, Pick A, Nair A, Disler PB, Wade DT. Multi-disciplinary rehabilitation for acquired brain injury in adults of working age. Cochrane Database Syst Rev. 2015 Dec 22; 12: CD004170,
4. European Physical and Rehabilitation Medicine Bodies Alliance. White Book on Physical and Rehabilitation Medicine (PRM) in Europe. Chapter 8. The PRM specialty in the healthcare system and society. Eur J Phys Rehabil Med. 2018; 54 (2): 261–78.
5. European Physical and Rehabilitation Medicine Bodies Alliance. White Book on Physical and Rehabilitation Medicine (PRM) in Europe. Chapter 7. The clinical field of competence: PRM in practice. Eur J Phys Rehabil Med. 2018; 54 (2): 230–60.
6. European Physical and Rehabilitation Medicine Bodies Alliance. White Book on Physical and Rehabilitation Medicine (PRM) in Europe. Chapter 6. Knowledge and skills of PRM physicians. Eur J Phys Rehabil Med. 2018; 54 (2): 214–29.
7. Ivanova GE, Aronov DM, Belkin AA, Belyaev AF, Bodrova RA, Bubnova MG, et al. Pilot Project "Development of Medical Rehabilitation System in the Russian Federation». Journal of Restorative Medicine. 2016; (2): 2–6.
8. Ivanova GE, Belkin AA, Belyaev AF, Bodrova RA, Bujlova TV, Melnikova EV, et al. Pilot project "Development of medical rehabilitation system in the Russian Federation." General Principles and Protocol. Journal of the Ivanovsky Medical Academy. 2016; 21 (1): 6–11.
9. Ivanova GE, Belkin AA, Belyaev AF, Bodrova RA, Melnikova EV, Prokopenko SV, et al. Pilot project "Development of medical rehabilitation system in the Russian Federation." System of monitoring and monitoring the effectiveness of medical rehabilitation in case of acute disorders of cerebral circulation. Journal of the Ivanovsky Medical Academy. 2016; 21 (1): 19–22.
10. On the procedure for organizing medical rehabilitation. Pub. L. of the Ministry of Healthcare of the Russian Federation № 1705n (Dec. 29, 2012).
11. On approval of the procedure for medical care for patients with Stroke. Pub. L. of the Ministry of Healthcare of the Russian Federation № 928n (Nov. 15, 2012).
12. Zabolotskih IB, Shifman EM, redaktory. Klinicheskie rekomendacii. Anesteziologija-reanimatologija. M.: GJeOTAR-Media, 2016; p. 873–928. Russian.
13. European Physical and Rehabilitation Medicine Bodies Alliance. White Book on Physical and Rehabilitation Medicine (PRM) in Europe. Chapter 11. Challenges and perspectives for the future of PRM. Eur J Phys Rehabil Med. 2018; 54 (2): 311–21.
14. European Physical and Rehabilitation Medicine Bodies Alliance. White Book on Physical and Rehabilitation Medicine (PRM) in Europe. Chapter 10, Science and research in PRM: specificities and challenges. Eur J Phys Rehabil Med. 2018; 54 (2): 287–310.
15. European Physical and Rehabilitation Medicine Bodies Alliance. White Book on Physical and Rehabilitation Medicine (PRM) in Europe. Chapter 9. Education and continuous professional development: shaping the future of PRM. Eur J Phys Rehabil Med. 2018; 54 (2): 279–86.
16. European Physical and Rehabilitation Medicine Bodies Alliance. White Book on Physical and Rehabilitation Medicine (PRM) in Europe. Chapter 5. The PRM organizations in Europe: structure and activities. Eur J Phys Rehabil Med. 2018; 54 (2): 198–213.
17. European Physical and Rehabilitation Medicine Bodies Alliance. White Book on Physical and Rehabilitation Medicine (PRM) in Europe. Chapter 4. History of the specialty: where PRM comes from. Eur J Phys Rehabil Med. 2018; 54 (2): 186–97.
18. European Physical and Rehabilitation Medicine Bodies Alliance. White Book on Physical and Rehabilitation Medicine (PRM) in Europe. Chapter 3. A primary medical specialty: the fundamentals of PRM. Eur J Phys Rehabil Med. 2018; 54 (2): 177–85.
19. European Physical and Rehabilitation Medicine Bodies Alliance. White Book on Physical and Rehabilitation Medicine in Europe. Chapter 2. Why rehabilitation is needed by individual and society. Eur J Phys Rehabil Med. 2018; 54 (2): 166–76.
20. European Physical and Rehabilitation Medicine Bodies Alliance. White Book on Physical and Rehabilitation Medicine (PRM) in Europe. Chapter 1. Definitions and concepts of PRM. Eur J Phys Rehabil Med. 2018; 54 (2): 156–65.
21. European Physical and Rehabilitation Medicine Bodies Alliance. White Book on Physical and Rehabilitation Medicine in Europe. Introductions, Executive Summary, and Methodology. Eur J Phys Rehabil Med. 2018; 54 (2): 125–55.
22. Ivanova GE, Melnikova EV, Shmonin AA, Aronov DM, Belkin AA, Belyaev AF, et al. Pilot project "Development of medical rehabilitation system in the Russian Federation". Protocol of the second phase of the project. Scientific notes of PSPbGMU. 2016; (2): 27–34.
23. Ivanova GE, Melnikova EV, Shmonin AA, Verbitskaya EV, Aronov DM, Belkin AA, et al. Pilot Project "Development of Medical Rehabilitation System in the Russian Federation": Preliminary Results at the First and Second Stages. Journal of Restorative Medicine. 2017; 2 (78): 10–15.

Литература

1. Сычева А. В. Мультидисциплинарный подход при восстановительном лечении последствий церебрального инсульта [диссертация]. М., 2008.
2. Stroke Unit Trialists' Collaboration. Organised inpatient (stroke unit) care for stroke. Cochrane Database Syst Rev. 2013 Sep 11; 9: CD000197.
3. Turner-Stokes L, Pick A, Nair A, Disler PB, Wade DT. Multi-disciplinary rehabilitation for acquired brain injury in adults of working age. Cochrane Database Syst Rev. 2015 Dec 22; 12: CD004170,
4. European Physical and Rehabilitation Medicine Bodies Alliance. White Book on Physical and Rehabilitation Medicine (PRM) in Europe. Chapter 8. The PRM specialty in the healthcare system and society. Eur J Phys Rehabil Med. 2018; 54 (2): 261–78.
5. European Physical and Rehabilitation Medicine Bodies Alliance. White Book on Physical and Rehabilitation Medicine (PRM) in Europe. Chapter 7. The clinical field of competence: PRM in practice. Eur J Phys Rehabil Med. 2018; 54 (2): 230–60.
6. European Physical and Rehabilitation Medicine Bodies Alliance. White Book on Physical and Rehabilitation Medicine (PRM) in Europe. Chapter 6. Knowledge and skills of PRM physicians. Eur J Phys Rehabil Med. 2018; 54 (2): 214–29.
7. Иванова Г. Е., Аронов Д. М., Белкин А. А., Беляев А. Ф., Бодрова Р. А., Бубнова М. Г. и др. Пилотный проект «Развитие системы медицинской реабилитации в РФ». Вестник восстановительной медицины. 2016; (2): 2–6.
8. Иванова Г. Е., Белкин А. А., Беляев А. Ф., Бодрова Р. А., Буйлова Т. В., Мельникова Е. В. и др. Пилотный проект «Развитие системы медицинской реабилитации в Российской Федерации». Общие принципы и протокол. Вестник Ивановской медицинской академии. 2016; 21 (1): 6–11.
9. Иванова Г. Е., Белкин А. А., Беляев А. Ф., Бодрова Р. А., Мельникова Е. В., Прокопенко С. В. и др. Пилотный проект «Развитие системы медицинской реабилитации в Российской Федерации». Система контроля и мониторирования эффективности медицинской реабилитации при острых нарушениях мозгового кровообращения. Вестник Ивановской медицинской академии. 2016; 21 (1): 19-22.
10. Приказ Министерства здравоохранения Российской Федерации № 1705н от 29.12.2012. «О порядке организации

медицинской реабилитации».

11. Приказ Министерства здравоохранения Российской Федерации № 928н от 15.11.2012. «Об утверждении порядка медицинской помощи больным с нарушениями мозгового кровообращения».

12. Заболотских И. Б., Шифман Е. М., редакторы. Клинические рекомендации. Анестезиология-реаниматология. М.: ГЭОТАР-Медиа, 2016; с. 873–928.

13. European Physical and Rehabilitation Medicine Bodies Alliance. White Book on Physical and Rehabilitation Medicine (PRM) in Europe. Chapter 11. Challenges and perspectives for the future of PRM. Eur J Phys Rehabil Med. 2018; 54 (2): 311–21.

14. European Physical and Rehabilitation Medicine Bodies Alliance. White Book on Physical and Rehabilitation Medicine (PRM) in Europe. Chapter 10, Science and research in PRM: specificities and challenges. Eur J Phys Rehabil Med. 2018; 54 (2): 287–310.

15. European Physical and Rehabilitation Medicine Bodies Alliance. White Book on Physical and Rehabilitation Medicine (PRM) in Europe. Chapter 9. Education and continuous professional development: shaping the future of PRM. Eur J Phys Rehabil Med. 2018; 54 (2): 279–86.

16. European Physical and Rehabilitation Medicine Bodies Alliance. White Book on Physical and Rehabilitation Medicine (PRM) in Europe. Chapter 5. The PRM organizations in Europe: structure and activities. Eur J Phys Rehabil Med. 2018; 54 (2): 198–213.

17. European Physical and Rehabilitation Medicine Bodies Alliance. White Book on Physical and Rehabilitation Medicine (PRM) in Europe. Chapter 4. History of the specialty: where PRM comes from. Eur J Phys Rehabil Med. 2018; 54 (2): 186–97.

18. European Physical and Rehabilitation Medicine Bodies Alliance. White Book on Physical and Rehabilitation Medicine (PRM) in Europe. Chapter 3. A primary medical specialty: the fundamentals of PRM. Eur J Phys Rehabil Med. 2018; 54 (2): 177–85.

19. European Physical and Rehabilitation Medicine Bodies Alliance. White Book on Physical and Rehabilitation Medicine in Europe. Chapter 2. Why rehabilitation is needed by individual and society. Eur J Phys Rehabil Med. 2018; 54 (2): 166–76.

20. European Physical and Rehabilitation Medicine Bodies Alliance. White Book on Physical and Rehabilitation Medicine (PRM) in Europe. Chapter 1. Definitions and concepts of PRM. Eur J Phys Rehabil Med. 2018; 54 (2): 156–65.

21. European Physical and Rehabilitation Medicine Bodies Alliance. White Book on Physical and Rehabilitation Medicine in Europe. Introductions, Executive Summary, and Methodology. Eur J Phys Rehabil Med. 2018; 54 (2): 125–55.

22. Иванова Г. Е., Мельникова Е. В., Шмонин А. А., Аронов Д. М., Белкин А. А., Беляев А. Ф. и др. Пилотный проект «Развитие системы медицинской реабилитации в Российской Федерации». Протокол второй фазы проекта. Ученые записки ПСПбГМУ им. акад. И. П. Павлова. 2016; (2): 27–34.

23. Иванова Г. Е., Мельникова Е. В., Шмонин А. А., Вербицкая Е. В., Аронов Д. М., Белкин А. А. и др. Пилотный проект «Развитие системы медицинской реабилитации в Российской Федерации»: предварительные результаты на первом и втором этапах. Вестник восстановительной медицины. 2017; 2 (78): 10–15.

QUALITY OF LIFE OF PATIENT WITH MULTIPLE CEREBRAL ANEURYSMS AFTER ENDOVASCULAR TREATMENT: ASSESSMENT BY THE CRITERIA OF INTERNATIONAL CLASSIFICATION OF FUNCTIONING

Oleynik AA[1] ✉, Ivanova NE[1], Oleynik EA[1], Ivanov AYu[2,3]

[1] Almazov Medical Research Centre, St. Petersburg, Russia

[2] St. Petersburg State Pediatric Medical University, St. Petersburg, Russia

[3] North-Western State Medical University named after I. I. Mechnikov, St. Petersburg, Russia

The rate of mortality and disability associated with aneurysmal subarachnoid hemorrhage (SAH) is high. Patients with multiple cerebral aneurysms (MCA) require repeated surgeries more often and they are likely to develop aneurysms de novo and suffer their rupture. This study aimed to apply the International Classification of Functioning (ICF) to assess the quality of life (QOL) of MCA patients after endovascular treatment, late postoperative period. The study involved patients who underwent endovascular treatment and had multiple (>2) cerebral aneurysms (141 people). All patients underwent 1–6 endovascular surgeries; complications developed in 7.1% (10/141) of cases. The patients' QOL was assessed against the ICF 6 to 24 months post-surgery. We found that at such time points treatment results deteriorate in a number of domains, namely those associated with pain, memory, motor coordination, limb strength. Patients with ruptured aneurysms showed worse results for locomotion-related domains than patients with unruptured aneurysms ($p < 0.05$), in patients with aneurysms having a pseudotumor type of flow, by domains associated with dysfunction of the cranial nerves responsible for innervation of the eye muscles ($p < 0.001$) ($p < 0.001$). Patients with ruptured MCA were more active in the late post-surgery period, which was revealed by comparing that period's data to the baseline pre-surgery records ($p < 0.05$). The severity of activity disorders depended on surgery complications, patient age ($p < 0.05$), complications that developed during the acute SAH stage ($p < 0.001$).

Keywords: multiple cerebral aneurysms, quality of life, endovascular treatment, late aneurysms treatment results, optimization of medical rehabilitation

✉ **Correspondence should be addressed:** Anna A. Oleynik
ul. Mayakovskogo, 12, St. Petersburg, 191014; doctor.an.an@mail.ru

ОЦЕНКА КАЧЕСТВА ЖИЗНИ ПО МЕЖДУНАРОДНОЙ КЛАССИФИКАЦИИ ФУНКЦИОНИРОВАНИЯ ПРИ МНОЖЕСТВЕННЫХ ЦЕРЕБРАЛЬНЫХ АНЕВРИЗМАХ ПОСЛЕ ЭНДОВАСКУЛЯРНОГО ЛЕЧЕНИЯ

А. А. Олейник[1] ✉, Н. Е. Иванова[1], Е. А. Олейник[1], А. Ю. Иванов[2,3]

[1] Национальный медицинский исследовательский центр имени В. А. Алмазова, Санкт-Петербург, Россия

[2] Санкт-Петербургский государственный педиатрический медицинский университет, Санкт-Петербург, Россия

[3] Северо-Западный государственный медицинский университет имени И. И. Мечникова, Санкт-Петербург, Россия

Аневризматическое субарахноидальное кровоизлияние (САК) ассоциировано с высокой летальностью и инвалидизацией больных. Пациенты с множественными церебральными аневризмами (МА) чаще подвержены неоднократным оперативным вмешательствам, у них имеется вероятность образования аневризм de novo и их разрыва. Целью исследования было оценить качество жизни (КЖ) пациентов с помощью Международной классификации функционирования (МКФ) в отдаленном послеоперационном периоде после эндоваскулярного лечения МА для определения пути оптимизации реабилитации. В исследовании приняли участие оперированные эндоваскулярно пациенты с множественными (> 2) церебральными аневризмами (141 человек). Всем пациентам было выполнено 1–6 эндоваскулярных операций, осложнения лечения возникли в 7,1% (10/141). КЖ определяли в сроки от 6 до 24 месяцев после операции, используя МКФ. Выявлено, что в отдаленном послеоперационном периоде результаты были хуже по доменам, связанным с болью, памятью, координацией движений, силой конечностей. При геморрагическом типе течения результаты по доменам, связанным с передвижением, были хуже по сравнению с другими типами течения ($p < 0,05$), а при псевдоопухолевом — по доменам, связанным с нарушением функции черепно-мозговых нервов, отвечающих за иннервацию мышц глаза ($p < 0,001$). По сравнению с показателями дооперационного периода в отдаленном послеоперационном периоде выявлено повышение активности и участия больных с геморрагическим типом течения ($p < 0,05$). На выраженность нарушений активности влияли осложнения операций, возраст больных ($p < 0,05$), осложнения острого периода САК ($p < 0,001$).

Ключевые слова: множественные церебральные аневризмы, качество жизни, эндоваскулярное лечение, отдаленные результаты лечения аневризм, оптимизация медицинской реабилитации

✉ **Для корреспонденции:** Анна Анатольевна Олейник
ул. Маяковского, д. 12, г. Санкт-Петербург, 191014; doctor.an.an@mail.ru

Cerebral aneurysms are some of the most common causes of subarachnoid hemorrhage (SAH) [1–2]. Over the past 30 years, the approaches to SAH treatment have changed significantly [3]. Pathophysiological mechanisms of vasospasm and cerebral ischemia after SAH were investigated; understanding of these mechanisms allowed improving the acute period intensive care

methods and reducing the incidence of ischemic complications [4–5]. The achievements in the field of cerebral aneurysm surgery, including methods designed specifically for the acute SAH period, the improvement of the methods of endovascular treatment of aneurysms resulted in reduction of the number of repeated SAH occurrences [6]. Advancements in non-invasive diagnostics and the growing availability of magnetic resonance angiography, computed tomography angiography enabled detection of asymptomatic cerebral aneurysms [7]. Assesing the risk of hemorrhage from an aneurysm takes into account the morphological features of the aneurysm (size, shape, location), the only treatment remains surgical intervention [8]. The rate of occurrence of complications related to such surgery ranges from 3 to 29% [9–11]. However, to date the quality of life of patients after aneurysm surgery remains largely unresearched [12], regardless of such aneurysms staying asymptomatic or causing hemorrhage or have a pseudotumor course. It is known that up to 20–30% of patients acquire disabilities after intracranial hemorrhage [13]. The results of medical rehabilitation of SAH patients, as well as those suffering from post-surgery complications (ischemic or hemorrhagic), can be improved through optimization of rehabilitation algorithms by factoring in the principal neurological disorders [14]. Assessment of the quality of life of patients based on the International Classification of Functioning, Disability and Health (ICF) provides a holistic view of various aspects of their health [15]. This study aimed to apply the International Classification of Functioning (ICF) to assess the quality of life of MCA patients after endovascular treatment (late postoperative period); the goal was to discover the rehabilitation algorithms optimization paths.

METHODS

The study included MCA patients (n = 141) who received endovascular treatment at the Polenov Russian Research Institute of Neurosurgery in 2010–2018. Seventeen percent of the participants were male (24/141), 83% — female (117/141); the mean age of the patients was 54.16 ± 11.24 years. The inclusion criteria were: multiple (>2) cerebral aneurysms treated endovascularly; opportunity to register late results. The exclusion criteria were: age below 18 years; concomitant arteriovenous malformations; history of

microsurgical treatment of aneurysm. The number of aneurysms detected ranged from 2 to 6: 2 aneurysms in 62.4% of cases (88/141), 3 aneurysms in 26.2% (36/141), 4 — in 7.8% (11/141), 5 aneurysms in 2.8% (4/141), 6 — in 0.7% (1/141). All in all, we detected 349 aneurysms in 141 cases. Their size varied: 22.9% (80/349) were miliary (up to 3 mm) aneurysms, the size of 67.9% (237/349) was regular (4–15 mm), 5.2% (18/349) were large (16–25 mm) and 4.0% (14/349) — gigantic (> 25mm). As for the clinical course pre-surgery, 45.4% (64 cases) of patients suffered one or several subarachnoid hemorrhages, 7.1% (10 cases) had a pseudotumor that affected surrounding structures volumetrically, and in 47.5% (67 cases) of patients the condition developed asymptomatically (accidentally detected aneurysms). All patients had 1 to 6 endovascular surgeries (271 surgeries in total): endovascular occlusion of aneurysms with detachable coils — 42.4% (115/271), assisted (stent and balloon) endovascular occlusion of aneurysms with detachable coils — 32.8% (89/271), flow diverter — 24.7% (67/271). Complications after endovascular treatment (vasospasm, ischemic complications, hemorrhagic complications) occurred in 7.1% of cases (10/141), of which persistent neurological deficiency developed in 4.3% (6/141). We assessed the quality of life in the late period, 6 to 24 months post-surgery. For this purpose, we used the International Classification of Functioning, Disability and Health [15], focusing on the domains of body functions, activity and participation (Table 1).

All data were entered into a Microsoft Excel 7.0 spreadsheet. The clinical data obtained in the study were processed with STATISTICA for Windows 10.0 (StatSoft, Tulsa; USA). Mann-Whitney test, median χ^2 and the ANOVA module were used to compare the quantitative parameters (scores by ICF domains, Rankin scale, Extended Glasgow Outcome Scale, Barthel Index of Activities of Daily Living (by age groups), SAH complications status, surgery-related complications status, pre-surgery disease development groups). Wilcoxon test was applied to evaluate the dynamics of the activity and participation domain indicators before and after surgery. The findings were considered statistically significant at $p < 0.05$.

RESULTS

Figure 1 presents the assessment of neurological symptoms and patient complaints in the late postoperative period. Figure 2

Table 1. Domains of body functions, activity and participation, methods for their assessment

Body functions domains	Assessment method
b144 Memory functions	MMSE [16]
b2152 Functions of external muscles of the eye	Isolated assessment of the eye muscle function using the Kurtzke Functional Systems Scores*
b2702 Sensitivity to pressure	Scale score**
b167 Mental functions of language	Wasserman speech impairment scale [17]
b28010 Pain in head and neck	Visual analogue scale for pain assessment [18]
b320 Articulation functions	Severity assessment
b730 Muscle power functions	Muscle power assessment scale
b7602 Coordination of voluntary movements	GET UP AND GO TEST [19]
d450 Walking	Six-minute walk test [20]
d640 Doing housework	Rankin Scale [21], Extended Glasgow Outcome Scale [22]
d510 Washing oneself	Barthel Index of Activities of Daily Living [23], Rankin Scale
d540 Dressing	Barthel Index of Activities of Daily Living
d550 Eating	Barthel Index of Activities of Daily Living

Note: * — 0 — no changes; 1 — symptoms present, no function impairment (mild disorder detected through neurological examination, no complaints from the patient); 2 — mild impairments (mild eye movement disorder, the patient complains of double vision, there is paresis of any one of the eye external muscles); 3 — moderate impairments (moderate eye movement disorder, the patient complains of double vision); 4 — severe impairments (paralysis of one or more of the eye external muscles); ** — 0 — no impairments; 1 — mild impairments; 2 — moderate impairments; 3 — severe impairments; 4 — absolute impairments.

presents the assessment of activity and participation domains by the "capacity" and "performance" qualifiers.

The ICF allows a systematic assessment of the state of body functions, with a single impairments severity scale; therefore, we established that the scores registered in the pain (b28010) and memory function (b144) domains were low more often than those describing the status in the voluntary movements coordination (b7602) and muscle power (b7302) domains. In the activity and participation section, the impairments were registered more often in the walking (d450) and housework (d640) domains.

Assessing the impairments detected in the late post-surgery period through the lens of pre-surgery aneurysm development pattern, we established that we found that in patients with ruptured aneurysms, the movement (b 7302, d4602, d640) domains indicators were significantly worse compared to the other types of multiple aneurysms development patterns ($p < 0.05$). Cranial nerves innervating the eye muscles (III, IV, VI) were significantly more often impaired in the group that had the aneurysms developing pseudotumors, even in the late postoperative period ($p < 0.001$). In other domains, we registered no significant difference between the MCA development patterns groups ($p > 0.05$). Assessment of the cephalgic syndrome post-surgery revealed no significant difference in patients with ruptured and unruptured aneurysms. This fact underscores the importance of a detailed study of the cephalgic syndrome structure and its causes.

Comparing the pre-surgery data and those obtained in the late post-surgery period, we discovered that the patients with ruptured MCA enjoyed enjoyed a better quality of life in domains d4602 (Moving around outside the home and other buildings; Fig. 3) ($p = 0.004$) and d640 (Doing housework) ($p = 0.03$).

The severity of activity impairments (assessed with the Barthel Index of Activities of Daily Living, Rankin Scale, Extended Glasgow Outcome Scale) depended on post-surgery complications ($p < 0.05$), patient age from 51 to 60 years ($p < 0.05$), acute SAH period complications (p < 0.001).

The following complications were registered in the late postoperative period: aneurysm rupture — 1.4% (2/141, with focal neurological symptoms), vascular thrombosis — 2.1% (3/141, with focal neurological symptoms in one case). Due to the presence of an unoperated aneurysm that caused intracranial hemorrhage the patients were referred to surgery with subsequent rehabilitation measures.

Thus, using the ICF to score impairments allows qualifying the rehabilitation courses for such patients.

DISCUSSION

The results of our study confirm findings of other researchers [24–26]: a history of subarachnoid hemorrhages in patients with both single and multiple aneurysms negatively affect their functional status. Same as ours, a number of other reports describe the following factors that influence functional outcomes: age of patients at the time of hemorrhage [24], intraparenchymal hemorrhage [24–25], large and gigantic size of the aneurysm [25]. However, unlike other researchers, we did not register as such factors the medial cerebral artery localization of the aneurysm [24, 30] and intraventricular hemorrhage [27].

In the recent years, it became customary to apply the ICF to evaluate the results of treatment and/or rehabilitation in cases with disorders and injuries of the nervous system [28] and other body systems [29]. However, there is an insufficient number of studies addressing application of the ICF in the context of assessment of the results of endovascular treatment of MCA patients. The ICF was used to classify the determinants when summarizing data from various studies investigating QOL deterioration determinants in SAH survivors [30]. It was found that the determinants associated with body structure and
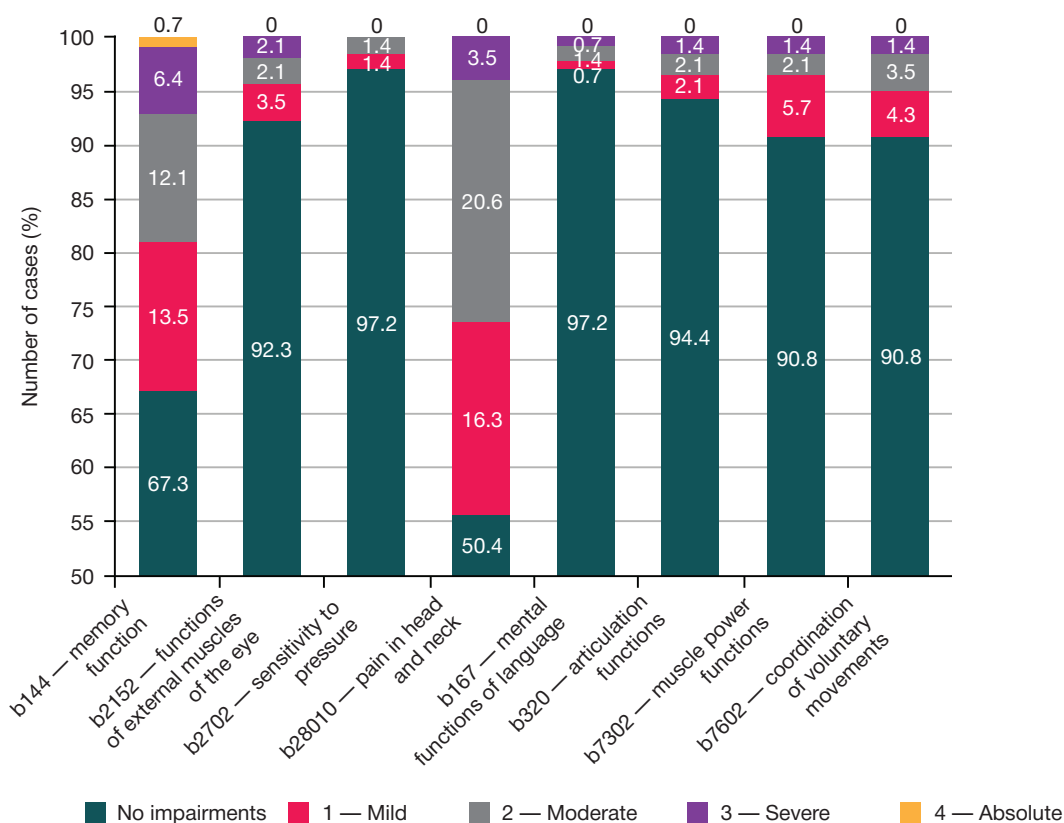
Fig. 1. Assessment by the body function domains, MCA patients, late postoperative period
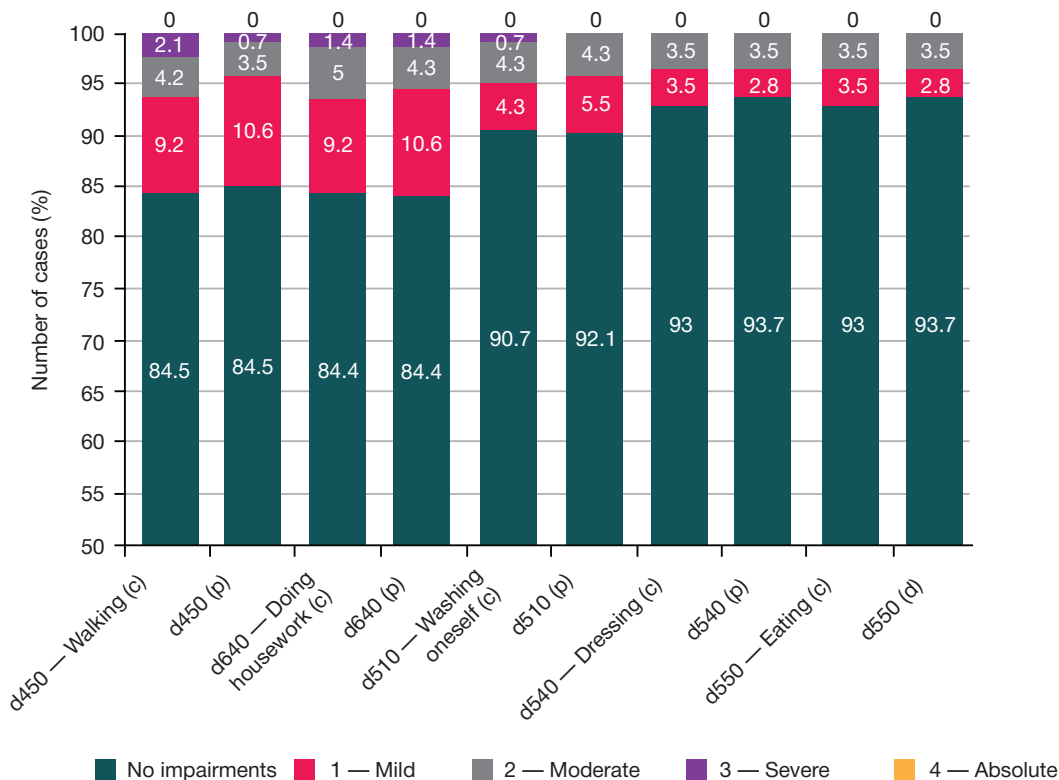
Fig. 2. Assessment by the activity and participation domains, "capacity" (c) and "performance" (p) qualifiers, MCA patients, late postoperative period
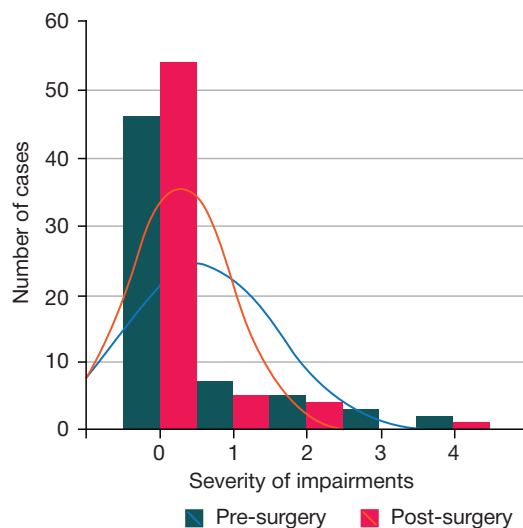
Fig. 3. Assessment by the d4602 domain (Moving around outside the home and other buildings), patients with hemorrhagic course MCA, pre-surgery and late post-surgery

functions (clinical condition at admission, low spirit), activity limitations (physical disability, cognitive status complaints) and personal factors (female sex, advanced age) negatively affect QOL post-SAH. Our study confirms that the QOL of patients with impaired body functions (b7302, b2152) deteriorates.

CONCLUSIONS

In the late postoperative period after endovascular treatment of MCA, a history of SAH and the presence of large aneurysms following the pseudotumor pattern are the factors that negatively affect the QOL of the patients. There is a risk of another SAH linked to the possibility of aneurysm formation de novo and aneurysm recanalization. Thus, further rehabilitation measures should account for neuroimaging data obtained in the late postoperative period. Application of the ICF to assess status of the patient's body functions, activity and participation, allow formulating the goals of rehabilitation, evaluating the results of endovascular treatment and further rehabilitation measures. Using separate scales disallows systematic analysis of the patient's condition. A single description of the severity of impairments is not only convenient in the context of evaluating the results, it also enables research efforts and comparison thereof.

References

1. Krylov VV, redaktor. Hirurgija anevrizm golovnogo mozga. V treh tomah. Tom I. M.: Izd-vo IP «T. A. Alekseeva», 2011; 432 s. Russian.

2. Azarov MV, Kupatadze DD, Nabokov VV. Sindrom Klippelja-Trenone, jetiologija, patogenez, diagnostika i lechenie. Pediatrija. 2018; 9 (2): 78–86. Russian.

3. La Pira B, Singh TD, Rabinstein AA, Lanzino G. Time Trends in Outcomes After Aneurysmal Subarachnoid Hemorrhage Over the Past 30 Years. Mayo Clin Proc. 2018 Dec; 93 (12): 1786–93.

4. Diringer MN, Zazulia AR. Aneurysmal Subarachnoid Hemorrhage: Strategies for Preventing Vasospasm in the Intensive Care Unit. Semin Respir Crit Care Med. 2017 Dec; 38 (6): 760–7.

5. Goroshhenko SA, Ivanova NE, Rozhchenko LV, Zabrodskaja YuM, Razmologova AYu, Kondratev AN, i dr. Jekstrapontinnyj mielinoliz, razvivshijsja posle anevrizmaticheskogo subarahnoidal'nogo krovoizlijanija (sluchaj iz praktiki i obzor literatury). Voprosy nejrohirurgii. 2016; (6): 82–7. Russian.

6. Anxionnat R, Tonnelet R, Derelle AL, Liao L, Barbier C, Bracard S. Endovascular treatment of ruptured intracranial aneurysms: Indications, techniques and results. Diagn Interv Imaging. 2015 Jul–Aug; 96 (7–8): 667–75.

7. Krylov VV, Eliava ShSh, Yakovlev SB, Kheyreddin AS, Belousova OB, Polunina NA. Klinicheskie rekomendacii po lecheniju nerazorvavshihsja bessimptomnyh anevrizm golovnogo mozga. Voprosy nejrohirurgii. 2016; 80 (5): 124–35. Russian.

8. Wiebers DO, Whisnant JP, Huston J 3rd, Meissner I, Brown RD Jr, Piepgras DG, et al. International Study of Unruptured Intracranial Aneurysms Investigators. Unruptured intracranial aneurysms: natural history, clinical outcome, and risks of surgical and endovascular treatment. Lancet. 2003 Jul 12; 362 (9378): 103–10.

9. Ihn YK, Shin SH, Baik SK, Choi IS. Complications of endovascular treatment for intracranial aneurysms: Management and prevention. Interv Neuroradiol. 2018 Jun; 24 (3): 237–45.

10. Oishi H, Yamamoto M, Shimizu T, Yoshida K, Arai H. Endovascular therapy of 500 small asymptomatic unruptured intracranial aneurysms. AJNR Am J Neuroradiol. 2012 May; 33 (5): 958–64.

11. Kim DY, Park JC, Kim JK, Sung YS, Park ES, Kwak JH, Choi CG, Lee DH. Microembolism after Endovascular Treatment of Unruptured Cerebral Aneurysms: Reduction of its Incidence by Microcatheter Lumen Aspiration. Neurointervention. 2015 Sep; 10 (2): 67–73.

12. Dammann P, Wittek P, Darkwah Oppong M, Hütter BO, Jabbarli R, et al. Relative health-related quality of life after treatment of unruptured intracranial aneurysms: long-term outcomes and influencing factors. Ther adv neurol disord. 2019; (12): 1–12.

13. le Roux AA, Wallace MC. Outcome and cost of aneurysmal subarachnoid hemorrhage. Neurosurg Clin N Am. 2010 Apr; 21 (2): 235–46.

14. Geyh S, Cieza A, Schouten J, Dickson H, Frommelt P, Omar Z, et al. ICF Core Sets for stroke. J Rehabil Med. 2004 Jul; (44 Suppl): 135–41.

15. World Health Organization. International Classification of Functioning, Disability and Health: ICF. Geneva: WHO; 2001.

16. Folstein MF, Folstein SE, McHugh PR. «Mini-mental state» a practical method for grading the cognitive state of patients for the clinician. Journal of Psychiatric Research. 1975; 12 (3): 189–98.

17. Vasserman LI, Dorofeeva SA, Meerson YaA. Metody nejropsihologicheskoj diagnostiki. Prakticheskoe rukovodstvo. SPb.: Strojlespechat', 1997. Russian.

18. Scott J, Huskisson EC. Graphic representation of pain. Pain. 1976; 2 (2): 175–84.

19. Mathias S, Nayak US, Isaacs B. Balance in elderly patients: the "get-up and go" test. Arch Phys Med Rehabil. 1986 Jun; 67 (6): 387–9.

20. American Thoracic Society statement: guidelines for the six-minute walk test. Am J Respir Crit Care Med. 2002; 166 (1): 111–7.

21. Bonita R, Beaglehole R. Modification of Rankin Scale: Recovery of motor function after stroke. Stroke. 1988 Dec; 19 (12): 1497–500.

22. Wilson JT, Pettigrew LE, Teasdale GM. Structured interviews for the Glasgow Outcome Scale and the extended Glasgow Outcome Scale: guidelines for their use. J Neurotrauma. 1998; (15): 573–85.

23. Mahoney F, Barthel D. Functional evaluation: the Barthel Index. Md Med J. 1965; (14): 61–5.

24. Preiss M, Netuka D, Koblihova J, Bernardova L, Charvat F, Kratochvilova D, et al. Quality of life 1 year after aneurysmal subarachnoid hemorrhage in good outcome patients treated by clipping or coiling. J Neurol Surg A Cent Eur Neurosurg. 2012 Aug; 73 (4): 217–23.

25. Andersen CR, Fitzgerald E, Delaney A, Finfer S. Systematic Review of Outcome Measures Employed in Aneurysmal Subarachnoid Hemorrhage (aSAH). Clin res neurocritical care. 2019; 30 (3): 534–41.

26. AlMatter M, Aguilar Péreza M, Bhogal P, Hellstern V, Ganslandt O, Henkes H. Results of interdisciplinary management of 693 patients with aneurysmal subarachnoid hemorrhage: Clinical outcome and relevant prognostic factors. Clin Neurol Neurosurg. 2018 Apr; (167): 106–11.

27. Visser-Meily JMA, Rhebergen ML, Rinkel GJE, van Zandvoort MJ, Post MWM. Long-term health related quality of life after aneurysmal subarachnoid hemorrhage; relationship with psychological symptoms and personality characteristics. Stroke. 2009; (40): 1526–9.

28. Bodrova RA, Auhadeev YeI, Tihonov IV. Opyt primenenija mezhdunarodnoj klassifikacii funkcionirovanija v ocenke jeffektivnosti reabilitacii pacientov s posledstvijami porazhenija CNS. Prakticheskaja medicina. 2013; 1 (66): 98–100. Russian.

29. Ponomarenko GN, Shoshmin AV, Besstrashnova YaK, Cherkashina IV. Planirovanie i ocenka jeffektivnosti reabilitacii bol'nyh osteoartrozom: ispol'zovanie bazovogo nabora Mezhdunarodnoj klassifikacii funkcionirovanija, ogranichenij zhiznedejatel'nosti i zdorov'ja. Voprosy kurortologii, fizioterapii i lechebnoj fizicheskoj kul'tury. 2017; (1): 4–8. Russian.

30. Passier PE, Visser-Meily JM, Rinkel GJ, Lindeman E, Post MW. Determinants of health-related quality of life after aneurysmal subarachnoid hemorrhage: a systematic review. Qual Life Res. 2013 Jun; 22 (5): 1027–43.

Литература

1. Крылов В. В., редактор. Хирургия аневризм головного мозга. В трех томах. Том I. М.: Изд-во ИП «Т. А. Алексеева», 2011; 432 с.

2. Азаров М. В., Купатадзе Д. Д., Набоков В. В. Синдром Клиппеля-Треноне, этиология, патогенез, диагностика и лечение. Педиатрия. 2018; 9 (2): 78–86.

3. La Pira B, Singh TD, Rabinstein AA, Lanzino G. Time Trends in Outcomes After Aneurysmal Subarachnoid Hemorrhage Over the Past 30 Years. Mayo Clin Proc. 2018 Dec; 93 (12): 1786–93.

4. Diringer MN, Zazulia AR. Aneurysmal Subarachnoid Hemorrhage: Strategies for Preventing Vasospasm in the Intensive Care Unit. Semin Respir Crit Care Med. 2017 Dec; 38 (6): 760–7.

5. Горощенко С. А., Иванова Н. Е., Рожченко Л. В., Забродская Ю. М., Размологова А. Ю., Кондратьев А. Н. и др. Экстрапонтинный миелинолиз, развившийся после аневризматического субарахноидального кровоизлияния (случай из практики и обзор литературы). Вопросы нейрохирургии. 2016; (6): 82–7.

6. Anxionnat R, Tonnelet R, Derelle AL, Liao L, Barbier C, Bracard S. Endovascular treatment of ruptured intracranial aneurysms: Indications, techniques and results. Diagn Interv Imaging. 2015 Jul–Aug; 96 (7–8): 667–75.

7. Крылов В. В., Элиава Ш. Ш., Яковлев С. Б., Хейреддин А. С., Белоусова О. Б., Полунина Н. А. Клинические рекомендации

по лечению неразорвавшихся бессимптомных аневризм головного мозга. Вопросы нейрохирургии. 2016; 80 (5): 124–35.

8. Wiebers DO, Whisnant JP, Huston J 3rd, Meissner I, Brown RD Jr, Piepgras DG, et al. International Study of Unruptured Intracranial Aneurysms Investigators. Unruptured intracranial aneurysms: natural history, clinical outcome, and risks of surgical and endovascular treatment. Lancet. 2003 Jul 12; 362 (9378): 103–10.

9. Ihn YK, Shin SH, Baik SK, Choi IS. Complications of endovascular treatment for intracranial aneurysms: Management and prevention. Interv Neuroradiol. 2018 Jun; 24 (3): 237–45.

10. Oishi H, Yamamoto M, Shimizu T, Yoshida K, Arai H. Endovascular therapy of 500 small asymptomatic unruptured intracranial aneurysms. AJNR Am J Neuroradiol. 2012 May; 33 (5): 958–64.

11. Kim DY, Park JC, Kim JK, Sung YS, Park ES, Kwak JH, Choi CG, Lee DH. Microembolism after Endovascular Treatment of Unruptured Cerebral Aneurysms: Reduction of its Incidence by Microcatheter Lumen Aspiration. Neurointervention. 2015 Sep; 10 (2): 67–73.

12. Dammann P, Wittek P, Darkwah Oppong M, Hütter BO, Jabbarli R, et al. Relative health-related quality of life after treatment of unruptured intracranial aneurysms: long-term outcomes and influencing factors. Ther adv neurol disord. 2019; (12): 1–12.

13. le Roux AA, Wallace MC. Outcome and cost of aneurysmal subarachnoid hemorrhage. Neurosurg Clin N Am. 2010 Apr; 21 (2): 235–46.

14. Geyh S, Cieza A, Schouten J, Dickson H, Frommelt P, Omar Z, et al. ICF Core Sets for stroke. J Rehabil Med. 2004 Jul; (44 Suppl): 135–41.

15. World Health Organization. International Classification of Functioning, Disability and Health: ICF. Geneva: WHO; 2001.

16. Folstein MF, Folstein SE, McHugh PR. «Mini-mental state» a practical method for grading the cognitive state of patients for the clinician. Journal of Psychiatric Research. 1975; 12 (3): 189–98.

17. Вассерман Л. И., Дорофеева С. А., Меерсон Я. А. Методы нейропсихологической диагностики. Практическое руководство. СПб.: Стройлеспечать, 1997.

18. Scott J, Huskisson EC. Graphic representation of pain. Pain. 1976; 2 (2): 175–84.

19. Mathias S, Nayak US, Isaacs B. Balance in elderly patients: the "get-up and go" test. Arch Phys Med Rehabil. 1986 Jun; 67 (6): 387–9.

20. American Thoracic Society statement: guidelines for the six-minute walk test. Am J Respir Crit Care Med. 2002; 166 (1):

111–7.

21. Bonita R, Beaglehole R. Modification of Rankin Scale: Recovery of motor function after stroke. Stroke. 1988 Dec; 19 (12): 1497–500.

22. Wilson JT, Pettigrew LE, Teasdale GM. Structured interviews for the Glasgow Outcome Scale and the extended Glasgow Outcome Scale: guidelines for their use. J Neurotrauma. 1998; (15): 573–85.

23. Mahoney F. Barthel D. Functional evaluation: the Barthel Index. Md Med J. 1965; (14): 61–5.

24. Preiss M, Netuka D, Koblihova J, Bernardova L, Charvat F, Kratochvilova D, et al. Quality of life 1 year after aneurysmal subarachnoid hemorrhage in good outcome patients treated by clipping or coiling. J Neurol Surg A Cent Eur Neurosurg. 2012 Aug; 73 (4): 217–23.

25. Andersen CR, Fitzgerald E, Delaney A, Finfer S. Systematic Review of Outcome Measures Employed in Aneurysmal Subarachnoid Hemorrhage (aSAH). Clin res neurocritical care. 2019; 30 (3): 534–41.

26. AlMatter M, Aguilar Péreza M, Bhogal P, Hellstern V, Ganslandt O, Henkes H. Results of interdisciplinary management of 693 patients with aneurysmal subarachnoid hemorrhage: Clinical outcome and relevant prognostic factors. Clin Neurol Neurosurg. 2018 Apr; (167): 106–11.

27. Visser-Meily JMA, Rhebergen ML, Rinkel GJE, van Zandvoort MJ, Post MWM. Long-term health related quality of life after aneurysmal subarachnoid hemorrhage; relationship with psychological symptoms and personality characteristics. Stroke. 2009; (40): 1526–9.

28. Бодрова Р. А., Аухадеев Э. И., Тихонов И. В. Опыт применения международной классификации функционирования в оценке эффективности реабилитации пациентов с последствиями поражения ЦНС. Практическая медицина. 2013; 1 (66): 98–100.

29. Пономаренко Г. Н., Шошмин А. В., Бесстрашнова Я. К., Черкашина И. В. Планирование и оценка эффективности реабилитации больных остеоартрозом: использование базового набора Международной классификации функционирования, ограничений жизнедеятельности и здоровья. Вопросы курортологии, физиотерапии и лечебной физической культуры. 2017; (1): 4–8.

30. Passier PE, Visser-Meily JM, Rinkel GJ, Lindeman E, Post MW. Determinants of health-related quality of life after aneurysmal subarachnoid hemorrhage: a systematic review. Qual Life Res. 2013 Jun; 22 (5): 1027–43.

INTERICTAL EPILEPTIFORM ACTIVITY IN SLEEP AND WAKEFULNESS IN PATIENTS WITH TEMPORAL LOBE EPILEPSY

Broutian AG ✉, Belyakova-Bodina AI, Dolgova SM, Pushkar TN, Abramova AA

Research Center of Neurology, Moscow, Russia

Sleep is an important activator of epileptiform activity, with epileptiform discharge (ED) probability varying among sleep stages. The aim of our study was to analyze the association between epileptiform activity and sleep stages or wakefulness in adults with temporal discharges. We analyzed 32 long-term overnight EEG recordings. All focal discharges were marked, and the entire sleep was staged. Absolute general epileptiform discharge index (EDI), defined as a ratio of total ED number to the full recording time in hours, as well as absolute EDIs for REM, N1, N2 and N3 stages were calculated. The majority of patients (28) had the highest EDI in N3. EDI increased significantly while sleep progressed to deeper stages, reaching its peak in N3. In REM sleep, EDI sharply declined ($p < 0.01$) reaching the levels of wakefulness. Increasing synchronization of cortical neurons is thought to be the major mechanism of EDI rise in NREM sleep. Hence, N3 seems to be the most sensitive stage to capture EDs, which highlights the importance of deep sleep recording in patients with temporal epilepsy.

Keywords: electroencephalography, sleep, epileptiform activity, epilepsy, temporal lobe epilepsy

✉ **Correspondence should be addressed:** Amayak G. Broutian
Leningradsky Prospect, 33, Moscow, 125284; abroutian@mail.ru

ИНТЕРИКТАЛЬНАЯ ЭПИЛЕПТИФОРМНАЯ АКТИВНОСТЬ ВО СНЕ И В БОДРСТВОВАНИИ У ПАЦИЕНТОВ С ВИСОЧНОЙ ЭПИЛЕПСИЕЙ

А. Г. Брутян ✉, А. И. Белякова-Бодина, С. М. Долгова, Т. Н. Пушкарь, А. А. Абрамова

Научный центр неврологии, Москва, Россия

Сон является значимым активатором эпилептиформной активности, при этом вероятность регистрации разрядов может меняться в зависимости от стадии и глубины сна. Целью исследования было оценить зависимость эпилептиформной активности от уровня бодрствования и глубины сна в популяции взрослых пациентов с височной локализацией разрядов. Нами было проанализировано 32 продолженных ЭЭГ-мониторинга с записью ночного сна, в которых были отмечены все фокальные разряды, а также проводилось стадирование сна. Определяли общий индекс эпилептиформной активности, как отношение общего количества разрядов к длительности исследования в часах, а также индивидуальные индексы эпилептиформной активности для бодрствования и каждой из стадий сна: для REM-фазы и N1, N2 и N3 стадий NREM-сна. У подавляющего числа пациентов (28) максимальный индекс зарегистрирован в стадии N3. По мере перехода к более глубоким стадиям сна, индекс разрядов последовательно и достоверно увеличивался, достигая максимальных величин в стадии N3 ($p < 0,01$). В фазу REM-сна индекс резко снижался ($p < 0,01$), приближаясь к значениям, зарегистрированным в бодрствовании. Основным механизмом, который приводит к увеличению индекса эпилептиформной активности в NREM-сне, может быть нарастающая синхронизация корковых нейронов с увеличением доли медленной активности в ЭЭГ. Таким образом, стадия N3 является наиболее информативной в плане регистрации фокальных разрядов, что диктует необходимость достижения достаточной глубины сна при проведении диагностических ЭЭГ исследований у пациентов с височными формами эпилепсии.

Ключевые слова: электроэнцефалография, сон, эпилептиформная активность, эпилепсия, височная эпилепсия

✉ **Для корреспонденции:** Амаяк Грачевич Брутян
Ленинградский проспект, д. 33, г. Москва, 125284; abroutian@mail.ru

The likelihood of developing epileptic seizures depending on the level of wakefulness and sleep depth is largely determined by the epilepsy and seizure type [1, 2]. For example, in juvenile myoclonic epilepsy seizures typically occur after awakening while in autosomal dominant nocturnal frontal lobe epilepsy they only happen during sleep. Sleep is also known to be a significant activator of interictal epileptiform activity in electroencephalography (EEG), which is more common for focal discharges than for generalized ones [3].

Sleep, however, is not a homogeneous state; it consists of several states changing in a cyclic manner. These states differ in depth, physiological parameters, and EEG patterns.

A remarkable example is epileptic encephalopathy with continuous spikes and waves during sleep (CSWS) in which epileptic discharges almost replace the physiological patterns of non-rapid eye movements sleep (NREM sleep) and disappear during rapid eye movements (REM) sleep.

Thus, the probability of epileptiform activity is expected to depend on sleep stage. Furthermore, ED number during a certain sleep stage should be related to the duration of this sleep stage. For example, stage 2 prevails in a healthy person's sleep, which may mislead an EEG interpreter into thinking that EDs are the most prevalent during this stage.

Epileptiform discharge index (EDI) is described for both generalized and focal forms of epilepsy [4–8]. Studies on focal discharges differ in number of patients, discharge localization and epileptiform activity index calculation methods. In the majority of studies, discharges were calculated in 5 to 20-minute intervals of wakefulness and each stage of sleep. Both discharge localization and calculation methods can affect the results [4–8].

Temporal epilepsy is the most common, comprising two thirds of all focal epilepsies [9]. The aim of this study was to assess the effect of various stages of sleep on interictal epileptiform activity in a relatively homogeneous group of adults with temporal lobe epilepsy by counting and analyzing EDs throughout the entire EEG recordings.

METHODS

We scanned video EEG recordings obtained in the Research Center of Neurology from February 2018 through June 2019 to select overnight recordings only. We found 709 recordings which were 10 to 12 hours long and included night sleep, evening and morning wakefulness. Initially, 142 recordings with focal epileptiform activity regardless of the disease duration and antiepileptic drug regimen were chosen. Inclusion criteria were the following: 1) only temporal ED localisation; 2) in case of repeated recordings, the first one was analyzed; 3) all sleep stages were present; 4) manual ED detection only, no automatic algorithms were used; 5) at least 10 EDs in a recording. Exclusion criteria were: 1) epileptic seizures during recording; 2) more than 500 EDs. Recordings with epileptic seizures were excluded due to their potential effect on EDI. Recordings with more than 500 EDs were excluded because of the technical limitations of ED manual detection. Finally, 32 recordings that met all the criteria were included in our study. Among the included patients there were 17 females and 15 males, aged 19 to 79 years (median 41 years).

EEG was recorded with scalp electrodes placed according to 10–20 international system with additional EKG channel. In 11 recordings, an inferior temporal chain (F9, F10, T9, T10, P9, P10) was used as well. EEG was recorded with NicOne (Natus, USA) and BePlus LTM (EBNeuro; Italy) systems. Recordings started between 20:00 and 21:00 and ended between 07:00 and 08:00. Photic stimulation and 5-minute hyperventilation were performed in the beginning of the recordings and after awakening in the morning. Epileptiform activity was defined according to 2017 revised glossary of EEG terms [10]. Total number of EDs varied from 13 to 401 (median 72 EDs). 27 patients (84%) showed unilateral EDs, 5 patients showed bilateral EDs. Number of patients with left-sided or predominantly left-sided EDs (17) was comparable to the number of patients (15) with right-sided or predominantly right-sided EDs.

Sleep was staged using 30-second epochs in accordance with American Academy of Sleep Medicine Manual for the Scoring of Sleep and Associated Events [11]. Since we did not use electrooculographic (EOG) electrodes and electromyographic (EMG) chin electrodes, REM sleep was identified based on indirect signs, such as ocular artefacts in frontal channels, muscle artifacts and REM-sleep-specific EEG patterns [11]. In this paper, we used traditional designations for sleep stages and wakefulness: Wake for wakefulness, N1 for stage 1, N2 for stage 2, N3 for stage 3 (slow-wave sleep), REM for REM sleep. Figure 1 shows an example of a hypnogram with ED marks.

We created hypnograms and marked EDs on them for each recording and calculated the following indices: 1) absolute general EDI, defined as a ratio of total ED count to the full recording time in hours; 2) absolute EDI for wakefulness and each sleep stage (N1, N2, N3, REM), defined as a ratio of ED count during stage to its duration in hours. For bilateral EDs, average EDI from both sides were calculated. The range of absolute EDIs was substantial. Since our study mainly focused on the trends of EDIs in relation to sleep stages and wakefulness, we did additional normalization, calculating relative EDIs, defined as a ratio of absolute stage EDI to absolute general EDI. Further in the text, EDI should be regarded as relative EDI, unless otherwise specified.

STATISTICA 12.6 software (Statsoft, Dell Software; USA) was used for statistical processing of the results. We applied the Shapiro–Wilk normality test for distribution characteristics, Mann–Whitney test for independent samples and Wilcoxon test
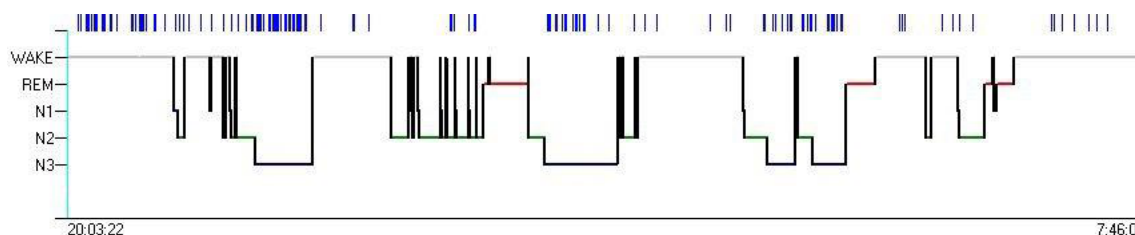
Fig. 1. An example of a hypnogram with ED marks. X-axis shows astronomical time. Y-axis shows sleep stages and wakefulness. Blue vertical lines in the top are ED marks. Wake, wakefulness periods; N1, stage 1; N2, stage 2; N3, stage 3 (slow-wave sleep); REM, REM sleep
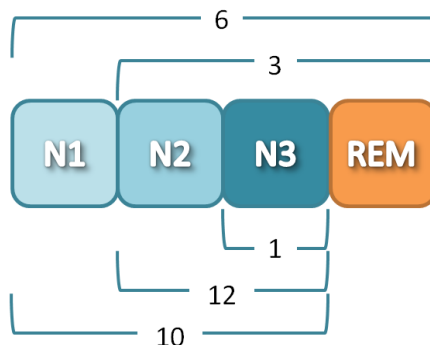
Fig. 2. Registered combinations of sleep stages with EDs. Combinations of sleep stages with EDs are highlighted with braces. Numbers in the middle of the braces reflect the number of patients with certain ED distribution

Table 1. The number of recordings having EDs in certain sleep stages or wakefulness and average relative EDIs

Stage	Wake	N1	N2	N3	REM
Number of patients with/without discharges at this stage	18/14	16/16	31/1	32/0	9/23
Number of patients with maximum discharges at this stage	2	0	1	28	1
Relative discharge index, median [lower; upper quartile]	0.03 [0; 0.23]	0.11 [0; 0.89]	1.19 [0.64; 1.64]	3.92 [2.74; 6.64]	0.19 [0; 0.06]

for dependent samples. Spearman's rank correlation coefficient was used to calculate the correlation. The differences were considered statistically significant at $p < 0.05$.

RESULTS

18 patients (56%) had EDs while being awake, 16 patients (50%) had EDs in N1, 31 patients (97%) had EDs in N2, all the patients had EDs in N3 and 9 patients (28%) had EDs in REM sleep (Table 1). The combinations of wakefulness and sleep stages with EDs varied (Fig. 2). No recording showed EDs exclusively in wakefulness, N1, N2 or REM. Nevertheless, one recording revealed EDs only in N3.

Stages with the largest EDI were identified. 28 patients (87.5%) had the largest EDI in N3, 2 patients had the largest EDI in wakefulness period, 1 patient had the largest EDI in N2, 1 patient had the largest EDI in REM, no patients were shown to have the largest EDI in N1.

Relative EDIs with trends are shown in Fig. 3. The median EDIs were: 0.03 for wakefulness periods, 0.11 for N1, 0.19 for N2, 3.92 for N3, 0.19 for REM (Table 1, Fig. 4). Application of the Wilcoxon signed-rank test revealed a significantly higher EDI in NREM sleep compared to that of wakefulness: $p < 0.05$ for N1 and $p < 0.01$ for N2 and N3, with difference from REM

being not significant. N3 EDI was significantly larger than EDI for other stages. EDI for REM was significantly smaller than EDI for each NREM sleep stage. EDI for REM had no significant difference from EDI for wakefulness period.

We divided our sample into 2 groups according to the total ED number: patients with small ED number (14 to 75 EDs) and large ED number (75 to 401 EDs). We compared EDIs between these groups and found no significant difference.

We performed correlation analysis for absolute stage/ EDIs and found significant correlation between EDI for N1 and REM, N1 and N2, and N2 and N3.

There was no significant EDI difference between left and right side temporal discharges in either wakefulness or sleep.

DISCUSSION

Our study showed N3 EDIs to be substantially higher than EDIs in other stages. ED predominance in slow-wave sleep was shown in earlier studies, in which EDI was analyzed for each sleep stage [6–8, 12–14]. There were no patients without EDs in N3 in our study, and EDs in N3 were on average three times more probable than in N2. Comparing stages that harbored the majority of EDs within a single EEG recording revealed even greater difference, as recordings with the majority of EDs in N3
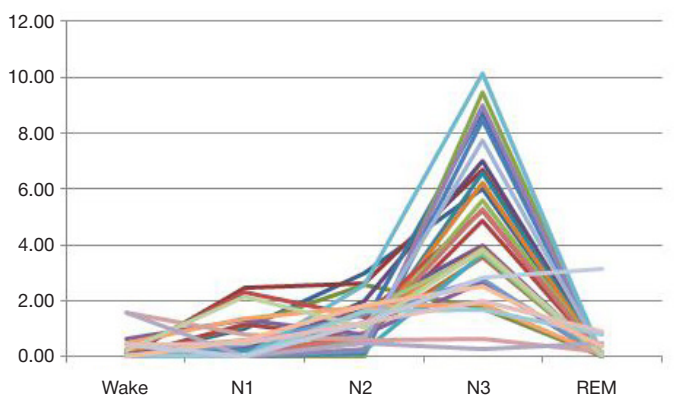
Fig. 3. Trends of EDIs for each sleep stage and wakefulness in patients with temporal discharges
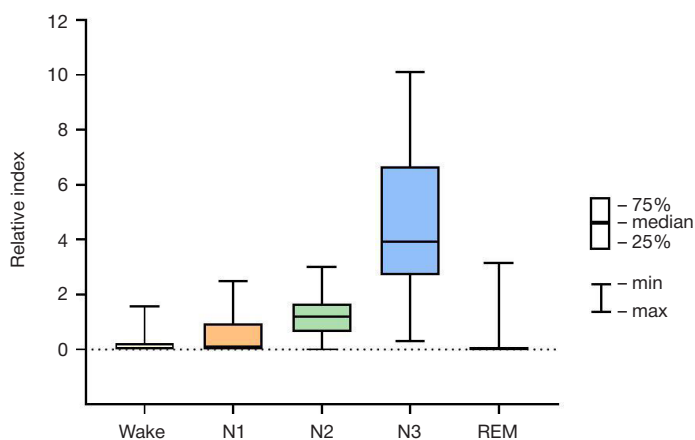
Fig. 4. Relative EDIs for each sleep stage and wakefulness in patients with temporal discharges

had a share of 87.5%. Analyzing the numerical data (Table 1) and EDI trending (Fig. 3), we observed a burst in N3. Similar to N3, EDI in N2, being smaller than in N3, was still significantly larger than in wakefulness, N1 and REM. We found no previous studies that showed significant difference in EDIs for N1 and N2. The lack of such statistical significance in earlier studies may be attributed to the method of ED marking, which was performed in selected intervals of EEG recordings rather than throughout the whole recordings [8, 15, 16].

Hence, we observed EDI increasing with sleep progression from REM to N1, N2 and N3.

Such EDI changes through the sleep stages may be explained by increased synchronization of neural networks in NREM sleep. Scalp EEG electrodes are known to require quite a large number of cortical neurons to discharge synchronously. Experimental data suggest that such synchronously discharging neurons should occupy at least an area of 6–8 cm². Slow activity, mainly that of delta range, is known to reflect high synchronization of cortical neurons. A characteristic feature of N3 is high-amplitude delta activity occupying at least 20% of an epoch. However, thorough analysis may reveal gradual increase of slow-wave activity occurring already in N2. Apart from slow-wave activity not sufficient to meet N3 criteria, N2 is characterized by the presence of K-complexes which is the most important criterion of this sleep stage. K-complexes are relatively slow high-amplitude transients which may embed EDs, becoming the so-called epileptic K-complexes. Such epileptic K-complexes can be found in both generalized and focal epilepsy [17, 18]. Furthermore, nocturnal frontal lobe epilepsy seizures have been shown to be associated with K-complexes [19]. Hence, an increased probability of EDs in NREM sleep may be considered as a consequence of increased synchronization of neural networks. This is supported by studies which showed positive correlation between ED frequency and delta band power.

Despite sleep in general being the most potent ED activator, REM sleep harbored the least of sleep EDs, with the index of epileptiform activity being comparable to such of wakefulness. Our data are consistent with earlier studies of the effect of REM sleep on epileptiform activity [8, 14, 21, 22]. In all the studies, EDI in REM was the lowest among sleep stages. Compared to wakefulness, EDI in REM sleep was shown to be slightly lower in the majority of studies. Having no activating effect on epileptiform activity, REM sleep, however, has two aspects that draw our attention. Firstly, if occurring in REM sleep, EDs tend to be more localized, thus having greater localizing value than in other sleep stages [23, 24]. Secondly, REM sleep, being an integral part of healthy sleep, not only has no activating effect on epileptiform activity, but also reduces its probability. Thus, to some extent, activity of neural networks in REM sleep is protective, reducing the probability of not only EDs, but also seizures [3].

Our study results might have been affected by several factors. Firstly, we intentionally excluded patients with exceedingly large numbers of EDs, which were hard to be counted manually. In some earlier studies, ED counting was selective, i.e. EDs were marked in limited stretches of time (5–20 minutes to 1 hour) with further extrapolation to the entire EEG recording [8, 14, 15, 25]. We also occasionally use selective ED count in practice; however, we did not include recordings analyzed in such a way in order to avoid probable bias. Secondly, REM sleep duration might have been underestimated because of the lack of EMG channels reflecting the activity of mentalis muscle. Thirdly, wakefulness EDIs might have been overestimated, as 5-minute hyperventilation tests included in wakefulness periods increase the neuronal synchronization by reducing cerebral blood flow and thus may activate ED. Nevertheless, NREM sleep is a much stronger activator compared to hyperventilation [15]. Fourthly, the effect of antiepileptic therapy, time from the first seizure, seizure frequency and semiology, drug resistance and structural lesions on MRI was not analyzed.

From a practical point of view, our study highlights the importance of slow-wave sleep recording in EEG diagnostic investigations, especially if focal epilepsy is suspected. Short-term EEG, particularly 20-minute routine EEG, provide lower probability to record EDs, thus diminishing sensitivity of these tests in the diagnosis of epilepsy, especially its focal forms. As a result, a precise diagnosis and correct treatment initiation might be delayed.

CONCLUSIONS

Our study on a sample of patients with temporal epileptiform activity showed that relative EDI for focal discharges increases while NREM progresses from N1 to N3. In REM sleep, EDI drops significantly to the level comparable to wakefulness. The most likely mechanism behind the significant predominance of EDs in the slow-wave sleep is synchronization of cortical neurons. Lack of records describing the N3 stage, which is when the epileptiform activity reaches its maximum, or the insufficient duration of this stage significantly reduce the likelihood of epileptiform activity recording, and when the clinical manifestation is insufficiently convincing, this lack of information can lead to erroneous conclusions, and to a delay in making the correct diagnosis and proper treatment initiation.

References

1. Minecan D, Natarajan A, Marzec M, Malow B. Relationship of epileptic seizures to sleep stage and sleep depth. Sleep. 2002; 25 (8): 899–904.
2. Bazil CW. Seizure modulation by sleep and sleep state. Brain Res. 2019; (1703): 13–17.
3. Ng M, Pavlova M. Why are seizures rare in rapid eye movement sleep? Review of the frequency of seizures in different sleep stages. Epilepsy Res Treat. 2013; (2013): 932790.
4. Kellaway P, Frost JD, Crawley JW. Time modulation of spike–and–wave activity in generalized epilepsy. Ann Neurol. 1980; 8 (5): 491–500.
5. Halász P, Terzano MG, Parrino L. Spike–wave discharge and the microstructure of sleep–wake continuum in idiopathic generalised epilepsy. Neurophysiol Clin. 2002; 32 (1): 38–53.
6. Lieb JP, Joseph JP, Engel J, Walker J, Crandall PH. Sleep state and seizure foci related to depth spike activity in patients with temporal lobe epilepsy. Electroencephalogr Clin Neurophysiol. 1980; 49 (5–6): 538–57.
7. Sammaritano M, Gigli GL, Gotman J. Interictal spiking during wakefulness and sleep and the localization of foci in temporal lobe epilepsy. Neurology. 1991; 41 (2 (Pt 1): 290–7.
8. Clemens Z, Janszky J, Clemens B, Szucs A, Halász P. Factors affecting spiking related to sleep and wake states in temporal lobe epilepsy (TLE). Seizure. 2005; 14 (1): 52–7.
9. Semah F, Picot MC, Adam C, Broglin D, Arzimanoglou A, Bazin B, et al. Is the underlying cause of epilepsy a major prognostic factor for recurrence? Neurology. 1998; 51 (5): 1256–62.
10. Kane N, Acharya J, Benickzy S, Caboclo L, Finnigan S, Kaplan PW,

et al. A revised glossary of terms most commonly used by clinical electroencephalographers and updated proposal for the report format of the EEG findings. Revision 2017. Clin Neurophysiol Pract. 2017; (2): 170–85.

11. Berry RB, Brooks R, Gamaldo CE, Harding SM, Lloyd RM, Marcus CL, et al. The AASM Manual for the Scoring of Sleep and Associated Events: Rules, Terminology and Technical Specifications, Version 2.2. www.aasmnet.org. Darien, Illinois: American Academy of Sleep Medicine, 2015.

12. Malow BA, Kushwaha R, Lin X, Morton KJ, Aldrich MS. Relationship of interictal epileptiform discharges to sleep depth in partial epilepsy. Electroencephalogr Clin Neurophysiol. 1997; 102 (1): 20–6.

13. Clemens Z, Janszky J, Szucs A, Békésy M, Clemens B, Halász P. Interictal epileptic spiking during sleep and wakefulness in mesial temporal lobe epilepsy: a comparative study of scalp and foramen ovale electrodes. Epilepsia. 2003; 44 (2): 186–92.

14. Singh S, Shukla G, Goyal V, Srivastava AK, Singh MB, Vibha D, et al. Impact of sleep on the localizing value of video EEG in patients with refractory focal seizures — a prospective video–EEG with EOG and submental EMG study. Clin Neurophysiol. 2014; 125 (12): 2337–43.

15. Klein KM, Knake S, Hamer HM, Ziegler A, Oertel WH, Rosenow F. Sleep but not hyperventilation increases the sensitivity of the EEG in patients with temporal lobe epilepsy. Epilepsy Res. 2003; 56 (1): 43–9.

16. Yu YL, Yan YL, Tian SF, Feng ZH, Shi MT. Circadian rhythm of interictal epileptiform discharges and changes of spindles in patients with temporal lobe epilepsy. Biomed Res. 2018; 29 (6): 1263–7.

17. Geyer JD, Carney PR, Gilliam F. Focal epileptiform spikes in conjuction with K–complexes. J Clin Neurophysiol. 2006; 23 (5): 437–40.

18. Niedermeyer E. Epileptiform K complexes. Am J Electroneurodiagnostic Technol. 2008; 48 (1): 48–51.

19. ElHelou J, Navarro V, Depienne C, Fedirko E, LeGuern E, Baulac M, et al. K–complex–induced seizures in autosomal dominant nocturnal frontal lobe epilepsy. Clin Neurophysiol. 2008; 119 (10): 2201–4.

20. Ferrillo F, Beelke M, DeCarli F, Cossu M, Munari C, Rosadini G, et al. Sleep–EEG modulation of interictal epileptiform discharges in adult partial epilepsy: a spectral analysis study. Clin Neurophysiol. 2000; 111 (5): 916–23.

21. Malow BA, Lin X, Kushwaha R, Aldrich MS. Interictal spiking increases with sleep depth in temporal lobe epilepsy. Epilepsia. 1998; 39 (12): 1309–16.

22. Campana C, Zubler F, Gibbs S, deCarli F, Proserpio P, Rubino A1, et al. Suppression of interictal spikes during phasic rapid eye movement sleep: a quantitative stereo–electroencephalography study. J Sleep Res. 2017; 26 (5): 606–13.

23. Malow BA, Aldrich MS. Localizing value of rapid eye movement sleep in temporal lobe epilepsy. Sleep Med. 2000; 1 (1): 57–60.

24. Ochi A, Hung R, Weiss S, Widjaja E, To T, Nawa Y, et al. Lateralized interictal epileptiform discharges during rapid eye movement sleep correlate with epileptogenic hemisphere in children with intractable epilepsy secondary to tuberous sclerosis complex. Epilepsia. 2011; 52 (11): 1986–94.

25. Scarlatelli–Lima AV, Sukys–Claudino L, Watanabe N, Guarnieri R, Walz R, Lin K. How do people with drug–resistant mesial temporal lobe epilepsy sleep? A clinical and video–EEG with EOG and submental EMG for sleep staging study. eNeurologicalSci. 2016; (4): 34–41.

Литература

1. Minecan D, Natarajan A, Marzec M, Malow B. Relationship of epileptic seizures to sleep stage and sleep depth. Sleep. 2002; 25 (8): 899–904.

2. Bazil CW. Seizure modulation by sleep and sleep state. Brain Res. 2019; (1703): 13–17.

3. Ng M, Pavlova M. Why are seizures rare in rapid eye movement sleep? Review of the frequency of seizures in different sleep stages. Epilepsy Res Treat. 2013; (2013): 932790.

4. Kellaway P, Frost JD, Crawley JW. Time modulation of spike–and–wave activity in generalized epilepsy. Ann Neurol. 1980; 8 (5): 491–500.

5. Halász P, Terzano MG, Parrino L. Spike–wave discharge and the microstructure of sleep–wake continuum in idiopathic generalised epilepsy. Neurophysiol Clin. 2002; 32 (1): 38–53.

6. Lieb JP, Joseph JP, Engel J, Walker J, Crandall PH. Sleep state and seizure foci related to depth spike activity in patients with temporal lobe epilepsy. Electroencephalogr Clin Neurophysiol. 1980; 49 (5–6): 538–57.

7. Sammaritano M, Gigli GL, Gotman J. Interictal spiking during wakefulness and sleep and the localization of foci in temporal lobe epilepsy. Neurology. 1991; 41 (2 (Pt 1): 290–7.

8. Clemens Z, Janszky J, Clemens B, Szucs A, Halász P. Factors affecting spiking related to sleep and wake states in temporal lobe epilepsy (TLE). Seizure. 2005; 14 (1): 52–7.

9. Semah F, Picot MC, Adam C, Broglin D, Arzimanoglou A, Bazin B, et al. Is the underlying cause of epilepsy a major prognostic factor for recurrence? Neurology. 1998; 51 (5): 1256–62.

10. Kane N, Acharya J, Benickzy S, Caboclo L, Finnigan S, Kaplan PW, et al. A revised glossary of terms most commonly used by clinical electroencephalographers and updated proposal for the report format of the EEG findings. Revision 2017. Clin Neurophysiol Pract. 2017; (2): 170–85.

11. Berry RB, Brooks R, Gamaldo CE, Harding SM, Lloyd RM, Marcus CL, et al. The AASM Manual for the Scoring of Sleep and Associated Events: Rules, Terminology and Technical Specifications, Version 2.2. www.aasmnet.org. Darien, Illinois: American Academy of Sleep Medicine, 2015.

12. Malow BA, Kushwaha R, Lin X, Morton KJ, Aldrich MS. Relationship of interictal epileptiform discharges to sleep depth in partial epilepsy. Electroencephalogr Clin Neurophysiol. 1997; 102 (1): 20–6.

13. Clemens Z, Janszky J, Szucs A, Békésy M, Clemens B, Halász P. Interictal epileptic spiking during sleep and wakefulness in mesial temporal lobe epilepsy: a comparative study of scalp and foramen ovale electrodes. Epilepsia. 2003; 44 (2): 186–92.

14. Singh S, Shukla G, Goyal V, Srivastava AK, Singh MB, Vibha D, et al. Impact of sleep on the localizing value of video EEG in patients with refractory focal seizures — a prospective video–EEG with EOG and submental EMG study. Clin Neurophysiol. 2014; 125 (12): 2337–43.

15. Klein KM, Knake S, Hamer HM, Ziegler A, Oertel WH, Rosenow F. Sleep but not hyperventilation increases the sensitivity of the EEG in patients with temporal lobe epilepsy. Epilepsy Res. 2003; 56 (1): 43–9.

16. Yu YL, Yan YL, Tian SF, Feng ZH, Shi MT. Circadian rhythm of interictal epileptiform discharges and changes of spindles in patients with temporal lobe epilepsy. Biomed Res. 2018; 29 (6): 1263–7.

17. Geyer JD, Carney PR, Gilliam F. Focal epileptiform spikes in conjuction with K–complexes. J Clin Neurophysiol. 2006; 23 (5): 437–40.

18. Niedermeyer E. Epileptiform K complexes. Am J Electroneurodiagnostic Technol. 2008; 48 (1): 48–51.

19. ElHelou J, Navarro V, Depienne C, Fedirko E, LeGuern E, Baulac M, et al. K–complex–induced seizures in autosomal dominant nocturnal frontal lobe epilepsy. Clin Neurophysiol. 2008; 119 (10): 2201–4.

20. Ferrillo F, Beelke M, DeCarli F, Cossu M, Munari C, Rosadini G, et al. Sleep–EEG modulation of interictal epileptiform discharges in adult partial epilepsy: a spectral analysis study. Clin Neurophysiol. 2000; 111 (5): 916–23.

21. Malow BA, Lin X, Kushwaha R, Aldrich MS. Interictal spiking increases with sleep depth in temporal lobe epilepsy. Epilepsia. 1998; 39 (12): 1309–16.

22. Campana C, Zubler F, Gibbs S, deCarli F, Proserpio P, Rubino A1, et al. Suppression of interictal spikes during phasic rapid eye movement sleep: a quantitative stereo–electroencephalography study. J Sleep Res. 2017; 26 (5): 606–13.

23. Malow BA, Aldrich MS. Localizing value of rapid eye movement sleep in temporal lobe epilepsy. Sleep Med. 2000; 1 (1): 57–60.

24. Ochi A, Hung R, Weiss S, Widjaja E, To T, Nawa Y, et al. Lateralized interictal epileptiform discharges during rapid eye movement sleep correlate with epileptogenic hemisphere in children with intractable epilepsy secondary to tuberous sclerosis complex. Epilepsia. 2011; 52 (11): 1986–94.

25. Scarlatelli–Lima AV, Sukys–Claudino L, Watanabe N, Guarnieri R, Walz R, Lin K. How do people with drug–resistant mesial temporal lobe epilepsy sleep? A clinical and video–EEG with EOG and submental EMG for sleep staging study. eNeurologicalSci. 2016; (4): 34–41.

BRAIN-COMPUTER-INTERFACE TECHNOLOGY WITH MULTISENSORY FEEDBACK FOR CONTROLLED IDEOMOTOR TRAINING IN THE REHABILITATION OF STROKE PATIENTS

Bushkova YuV[1] ✉, Ivanova GE[1], Stakhovskaya LV[2], Frolov AA[3]

[1] Research Center of Cerebrovascular Pathology and Stroke, Ministry of Health of the Russian Federation, Moscow, Russia

[2] Pirogov Russian National Research Medical University, Moscow, Russia

[3] Institute of Higher Nervous Activity and Neurophysiology, Russian Academy of Sciences, Moscow, Russia

Motor recovery of the upper limb is a priority in the neurorehabilitation of stroke patients. Advances in the brain-computer interface (BCI) technology have significantly improved the quality of rehabilitation. The aim of this study was to explore the factors affecting the recovery of the upper limb in stroke patients undergoing BCI-based rehabilitation with the robotic hand. The study recruited 24 patients (14 men and 10 women) aged 51 to 62 years with a solitary supratentorial stroke lesion. The lesion was left-hemispheric in 11 (45.6%) patients and right-hemispheric in 13 (54.4%) patients. Time elapsed from stroke was 4.0 months (3.0; 12.0). The median MoCa score was 25.0 (23.0; 27.0). The rehabilitation course consisted of 9.5 sessions (8.0; 10.0). We established a significant moderate correlation between motor imagery performance (the MIQ-RS score) and the efficacy of patient-BCI interaction. Patients with high MIQ-RS scores (47.5 (32.0; 54.0) achieved a better control of the BCI-driven hand exoskeleton (63.0 (54.0; 67.0), $R = 0.67$; $p < 0.05$). Recovery dynamics were more pronounced in patients with high MIQ-RS scores: the median score on the Fugl-Meyer Assessment scale was 14 (8.0; 16.0) points vs 10 (6.0; 13.0) points in patients with low MIQ-RS scores. However, the difference was not significant. Thus, we established a correlation between a patient's ability for motor imagery (MIQ-RS) and the efficacy of patient-BCI interaction. A larger patient sample might be necessary to assess the effect of these factors on motor recovery dynamics.

Keywords: stroke, neurorehabilitation, brain-computer interface, ideomotor training

✉ **Correspondence should be addressed:** Yuliya V. Bushkova
Ostrovityanova, 1, str. 10, Moscow, 117342; Julijabush777@gmail.com

ТЕХНОЛОГИЯ ИНТЕРФЕЙСА МОЗГ–КОМПЬЮТЕР КАК КОНТРОЛИРУЕМЫЙ ИДЕОМОТОРНЫЙ ТРЕНИНГ В РЕАБИЛИТАЦИИ БОЛЬНЫХ ПОСЛЕ ИНСУЛЬТА

Ю. В. Бушкова[1] ✉, Г. Е. Иванова[1], Л. В. Стаховская[2], А. А. Фролов[3]

[1] Федеральный центр цереброваскулярной патологии и инсульта, Москва, Россия

[2] Российский национальный исследовательский университет имени Н. И. Пирогова, Москва, Россия

[3] Институт высшей нервной деятельности и нейрофизиологии, Москва, Россия

Восстановление функции руки у пациентов после инсульта является приоритетным направлением в нейрореабилитации. Развитие технологии интерфейса мозг–компьютер–экзоскелет кисти (ИМКЭ) качественно улучшило реабилитацию в этом направлении. Целью данного исследования было изучить факторы, влияющие на двигательное восстановление верхней конечности у пациентов после инсульта на фоне применения технологии ИМКЭ. Исследовали 24 пациента (14 мужчин, 10 женщин) в возрасте от 51 до 62 лет с единичным очагом инсультной этиологии, супратенториальной локализации. В 11 (45,6%) случаях левополушарное поражение, в 13 (54,4%) случаях — правополушарное. Давность инсульта — 4,0 (3,0; 12,0) месяца. Медиана MoCA 25,0 (23,0; 27,0). Курс занятий ИМКЭ включал 9,5 (8,0; 10,0) процедур. Выявлена значимая умеренная корреляция между успешностью моторного представления (MIQ-RS) и эффективностью взаимодействия пациентов с ИМКЭ кисти. Пациенты с высокими показателями MIQ-RS 47,5 (32,0; 54,0) достоверно лучше взаимодействовали с ИМКЭ 63,0 (54,0; 67,0), $R = 0,67$ ($p < 0,05$). У пациентов с высокими показателями MIQ-RS динамика двигательного восстановления была более выраженной: медиана ΔFugl-Meyer Assessment (FMA) составила 14 (8,0; 16,0) баллов против группы пациентов с низкими показателями MIQ-RS, ΔFMA — 10 (6,0; 13,0), но при этом не достигла статистически значимого уровня. Таким образом, выявлена взаимосвязь между способностью пациентов к моторному представлению (MIQ-RS) и эффективностью взаимодействия пациентов с ИМКЭ. Для выявления влияния этих факторов на динамику двигательного восстановления руки, вероятно, требуется продолжить исследование с большей выборкой.

Ключевые слова: инсульт, нейрореабилитация, интерфейс мозг–компьютер, идеомоторная тренировка

✉ **Для корреспонденции:** Юлия Владимировна Бушкова
ул. Островитянова, д. 1, стр. 10, г. Москва, 117342; Julijabush777@gmail.com

Stroke is one of the leading causes of lasting disabilities worldwide. Post-stroke motor and cognitive deficits impair patients' mobility and everyday activities, prevent their reintegration in the community and reduce their chances to return to work [1, 2].

A well-structured, gradual, specific, and adequate neurorehabilitation (NR) program can significantly mitigate stroke-related neurological deficit.

NR relies on the reserve capacity of the brain determined by the systemic organization of brain functions. As the patient relearns movement skills, their brain undergoes functional reorganization resulting in the restoration of or compensation for stroke-damaged functions. The ultimate goal of NR is true recovery. This sounds like a very adequate approach since it implies complete restoration of the affected function or the best improvement possible. The affected functions are regained due to the reorganization of intact functional systems enabled by the plasticity of the nervous system and the anatomic connections between its compartments.

Rehabilitation of neurology patients boasts a variety of methods aimed at initiating plasticity processes that make up for or replace the lost function. However, the majority of patients experience limited recovery after stroke. Advances in brain-computer interface (BCI) technology for activating the motor cortex that controls a specific movement, such as a BCI-controlled robotic hand, have substantially improved the quality of post-stroke rehabilitation [3, 4].

A BCI is directly operated by neurophysiological activity of the brain in such a way that neuromuscular pathways typically involved in the motion are bypassed [5]. A BCI-controlled robotic hand with visual and kinesthetic feedback harnesses the ability of patients to generate various EEG signals (the EEG µ-rhythm in the motor regions of the brain, in our case), allowing the brain to "connect" to external devices without involving neuromuscular pathways. The BCI rehabilitation device relies on the mental imagery (MI) of active movements. According to functional neuroimaging studies, MI activates cortical motor areas [6], except when stroke disrupts the ability of the brain to generate mental images [7].

It is known that repeated mental rehearsal of an action (ideomotor training, IT) promotes development of a motor skill under physiological conditions and recovery or regain of an impaired/lost skill in patients with nervous system pathology. An ideomotor task means a physical movement is performed mentally. This is also known as mental practice. The patient is asked to imagine a movement (such as reaching out with their hand, opening a hand, clenching a fist, grasping a cup, etc.) from a first- or third-person perspective. If the movement is imagined from the first-person perspective, the patient is very likely to perform it kinesthetically. If the task is performed from the third-person perspective, this type of imagery is visual [8]. In comparison with visual imagery, kinesthetic imagery is more reliably associated with a patient's ability to successfully interact with brain-computer interfaces [9].

There are a few major hypotheses about the mechanism underlying the effect of mental practice. One of them, the so-called psychoneuromuscular theory [10], is based on the assumption that mental practice activates muscles involved in performing the movement at the subthreshold level and consolidates the motor "script". According to another hypothesis, motor imagery evokes specific neurophysiological patterns in the motor cortex; these patterns are similar to those involved in implementing the actual movement. Functional MRI studies suggest that mental practice leads to the reorganization of the motor system in both brain hemispheres [6, 11].

Various dosage regimens of ideomotor training have been tested in randomized clinical trials. A statistically significant effect on the FMA and ARAT scales has been demonstrated for the following regimen: two 30-min sessions once a week repeated over the course of 6 weeks [12]. The program included functionally significant movements like reaching out or grasping an object, using writing utensils, etc.

However, the use of IT for regaining control of movement in adults after a catastrophic cerebral event produces controversial results [13]. Damage to motor function negatively affects both the patient's ability to execute movements and to imagine them. This could be due to post-stroke cognitive impairment [1,14].

Rehabilitation technologies based on motor imagery hold promise for patients with cerebral injury [12]. IT is seen as an adjunct to conventional rehabilitation. IT combined with physical therapy for patients with neurological deficits shapes the basis for *repetitive task-specific practice* (RTP). It has been shown that prolonged regular motor imagery training has a positive gradual and sustainable effect on neuronal plasticity [15].

Motor imagery is a subjective process and, therefore, is difficult to evaluate. One of the solutions lies in measuring desynchronization of sensorimotor EEG rhythms induced by motor imagery [4, 16]. Desynchronization of sensorimotor EEG rhythms can be used to detect the act of motor imagery, but its specificity remains understudied.

Another problem addressed in the literature is assessing a patient's ability for motor imagery [17]. This can be done using the *movement imagery questionnaire* (MIQ) adapted for the clinical population. MIQ and MIQ-R are normally used in athletes, whereas MIQ-RS, in individuals with motor deficit.

The BCI controlled robotic hand rehabilitation technology with multisensory visual and kinesthetic feedback can be described as controlled ideomotor training. This training is based on the enhancement of afferent stimulation of the upper limb by the mechanical force of the exoskeleton in response to *successful* performance of a mental task.

Thus, one of the crucial problems facing mental imagery research is detection of patients' ability to implement mental tasks because it determines the efficacy of interaction between the patient and the rehabilitation device.

The aim of this study was to explore the factors affecting motor recovery of the upper limb in stroke patients undergoing rehabilitation with a BCI-controlled robotic hand in the early rehabilitation period.

METHODS

The study was carried out by the Research Center of Cerebrovascular Pathology (Pirogov Russian National Research Medical University) at the facilities of Moscow City Clinical Hospital № 31 (Neurology Unit for stroke patients) from September 2018 to April 2019.

Inclusion criteria were as follows: patients of both sexes aged 18–80 years with a history of one subcortical stroke experienced < 2 years before the study, retained cognitive function (at least 22 points on the Montreal Cognitive Assessment scale, MoCA) [18], motor deficit of the upper limb (0 to 4 points on the Medical Research Council Scale for Muscle Strength) [19], and right-handedness according to the Edinburgh Handedness Inventory [20].

The following exclusion criteria were applied: older stroke (> 2 years before the study); left-handedness (the Edinburgh Handedness Inventory); pronounced reduction in cognitive function; sensory aphasia; severe motor aphasia; severe visual impairment that prevented the patient from following visual

instructions on the computer screen; excessive arm spasticity (4 points on the Ashworth scale, mAS) [21].

We analyzed performance of 24 patients: 14 (58.3%) men and 10 (41.7%) women. The median age was 56.5 (51.0; 62.0) years. Stroke was ischemic in 20 patients (83.3%) and hemorrhagic in 4 (16.7%) patients. In all the participants, stroke was localized to the supratentorial brain region (the location was confirmed by CT or MRI). The lesion was left-hemispheric in 11 (45.6%) patients and right-hemispheric in 13 (54.4%) patients. The median time elapsed from stroke was 4 months (3.0; 12.0). The MoCA median was 25.0 points (23.0; 27.0), corresponding to moderate cognitive deficit. Some of the participants were in inpatient care ($n = 11$); others were outpatients ($n = 13$). The BCIHE-based rehabilitation consisted of 9.5 sessions (8.0; 10.0).

The device used for rehabilitation was a brain-computer interface-controlled hand exoskeleton with kinesthetic and visual feedback (Exohand-2) developed at Pirogov Russian National Research Medical University, Moscow (Fig. 1)

BCI relies on the analysis of EEG patterns and recognition of sensorimotor μ-rhythm synchronization/desynchronization during hand motor imagery. EEG signals were bandpass-filtered at 5–30 Hz. The Bayesian classifier used in our study is described in [22]. Classification accuracy was measured using Cohen's kappa coefficient (perfect recognition accuracy: $\kappa = 1$, random chance: $\kappa = 0$ [23]) and the percentage of correct responses of the classifier (the recognition rate > 33% indicated above random recognition accuracy because the patients had a definite instruction to follow).

Recognition results were presented to the patient through visual and kinesthetic feedback: if the classifier recognized the motor imagery task given in the instruction, the cursor in the middle of the screen changed its color to green and the exoskeleton performed a hand opening movement. If other tasks were recognized, the cursor did not change its color and the exoskeleton did not produce any movement [4]. In essence, this type of therapy is controlled ideomotor training utilizing the principles of multichannel (visual, kinesthetic, EEG) biofeedback.

During the session, the patient was wearing a cap with EEG electrodes. Conductive gel was applied to the electrode surface. The electromechanically powered hand exoskeleton for hand opening was attached to both hands of the patient. The patient was sitting in the armchair in front of the computer screen. In the middle of the dark screen there was a circle for gaze fixation; three arrows outside the circle represented different instructions. A change of arrow color indicated task presentation. The patient performed one of 3 mental tasks: motor relaxation, kinesthetic imagery of slow right hand or left hand opening. Hand opening commands (the arrows in the right and left sections of the screen changed their colors accordingly) were presented in random order for 10 seconds. Mental imagery tasks were alternated with a task to relax indicated by a flash of the upper arrow; during the resting task, the patient had to sit for 10 s and look at the center of the screen. A session consisted of up to 3 trials, each lasting for 10 minutes. The patient rested for at least 3 min between the trials. The rehabilitation course lasted for 14–18 days; the interval between the sessions could extend up to 2 days.

RESULTS

The participants took the motor rehabilitation course consisting of standard physical therapy for post-stroke patients (kinesiotherapy, PNF, Motomed movement trainer) [24] and 9.5 sessions (8.0; 10.0) of BCI-controlled robotic hand -based training.

Motor activity of the upper limb was assessed using the following scales: the Fugl-Meyer Assessment (FMA) [25], the Medical Research Council Scale for Muscle Strength (MRCMS), the modified Ashworth scale (mAS) for spasticity. Functional activity of the upper limb was assessed using the Action Research Arm Test (ARAT) [26]. The Barhtel Index (BI) for Activities of Daily Living was applied to understand the level of patients' functional independence. Motor imagery performance was evaluated using the Movement Imagery Questionnaire (MIQ-RS) for clinical populations.

Statistical analysis was carried out in *Statistica* ver. 13.0 (StatSoft; USA) using the Mann-Whitney U and Wilcoxon tests and Spearman's correlation coefficient. In this article, the data are presented as medians and interquartile ranges (25; 75%) and differences are considered significant at $p < 0.05$.

The median efficacy of patient-BCI interaction (Cohen's kappa, the recognition rate) was 58.5% (45.7; 62.6) ($p < 0.05$), suggesting that such interaction was successful.

In order to study the ability of patients for kinesthetic motor imagery based on the MIQ-RS score, we divided them into two groups depending on stroke lateralization (Table 1).

The obtained differences were statistically significant. Patients with left-hemispheric lesions did better in generating kinesthetic motor images than patients with right-hemispheric lesions; these findings are consistent with the literature [27].

However, the attempt to establish a correlation between motor imagery performance in patients with different stroke localization and the efficacy of patient-BCI interaction using the classifier output was unsuccessful. So we distributed the patients' data into 2 groups depending on the quality of motor imagery inferred from the MIQ-RS total scores. The first group comprised patients who scored over 50% of the maximum score on the subscale representing the kinesthetic component; the second group consisted of patients who scored less than 50%. Thirteen patients perceived their ability

Fig. 1. The brain-computer interface-controlled hand exoskeleton with a kinesthetic and visual feedback (Exohand-2)

Table 1. Motor imagery performance in patients with different stroke lateralization

Parameter/the Mann–Whitney U test	Right hemisphere (n = 13)	Left hemisphere (n = 11)
MIQ-RS (p < 0.05)	29 (18.0; 35.0)	44.0 (25.0; 54.0)

Table 2. The efficacy of interaction between patients with different motor imagery performance and BCI (based on the MIQ-RS scale)

Parameter	Patients with MIQ-RS score > 50% (n = 13)	Patients with MIQ-RS score < 50% (n = 11)
Spearman's rank correlation coefficient	R = 0.67 (p < 0.05)	R = 0.43 (p < 0.05)
MIQ-RS	47.5 (32.0; 54.0)	27.0 (15.0; 29.0)
Classifier, p < 0.05	63.0 (54.0; 67.0)*	39.0 (32.0; 48.0)*

Note: * — p < 0,05.

Table 3. The relationship between motor recovery of the upper limb, functional independence of the patients and the efficacy of their interaction with BCI

Parameter/the Mann–Whitney U test	Patients with MIQ-RS score > 50% (n = 13)		Patients with MIQ-RS score < 50% (n = 11)	
Classifier, p < 0.05	63.0 (54.0; 67.0)		39.0 (32.5; 48.5)	
	Before	After	Before	After
FMA, total score	88.0 (62.0; 102.0)	102.0 (66.0; 112.0)*	95.5 (67.0; 109.0)	105.0 (69.0; 110.0)*
MRCWS	3.0 (2.0; 4.0)	3.0 (3.0; 4.0)	3.0 (2.0; 4.0)	3.0 (3.0; 4.0)
mAS	1.5 (3.0; 1.0)	1.0 (1.0; 1.0)*	2.0 (1.0; 2.0)	1.0 (1.0; 1.0)*
ARAT, total score	37.0 (4.0; 47.0)	42.0 (6.0; 53.0)*	35.0 (5.0; 43.0)	39.0 (4.0; 48.0)*
BI	90.0 (75.0; 95.0)	95.0 (80.0; 100.0)*	87.5 (75.0; 100.0)	92.5 (85.0; 100.0)*

for kinesthetic imagery as quite good: the median score was 47.5 (32.0; 54.0) points. For the rest 11 patients, the median score was 27.0 (15.0; 29.0) points. The difference between the groups was statistically significant (p < 0.05). In the next step, we investigated the association between the quality of motor imagery and the efficacy of patient-BCI interaction (Table 2).

The analysis of the obtained data revealed a significant moderate correlation between the quality of motor imagery (MIQ-RS) and the efficacy of patient-BCI interaction. In other words, the accuracy of the classifier was higher for patients with high MIQ-RS scores; patients with lower MIQ-RS scores interacted with the exoskeleton much less effectively.

The relationship between motor recovery/functional improvement of the upper limb and the efficacy of interaction with the exoskeleton is shown in Table 3.

In both groups, the dynamics were positive and statistically significant in terms of motor recovery and functional improvement of the upper limb. The dynamics were more pronounced in patients with a better ability for kinesthetic imagery; however, the difference between the groups was insignificant. Besides, we failed to establish a significant correlation between the efficacy of patient-BCI interaction (the classifier output) and the dynamics of motor recovery of the upper limb, which might be explained by the small sample size. Improved BI scores observed for both groups were due to the movements that involved both hands.

DISCUSSION

Noninvasive neurointerfaces decode brain activity in real time and thus allow users to manipulate external devices. In noninvasive approaches, the user performs a cognitive task while their brain signals are recorded by EEG and decoded in real time to execute control over the external device [28]. In spite of technical breakthroughs, the ability to effectively interact with BCI is limited for some healthy individuals. It has been shown that as many as 15 to 30% of users cannot execute effective control [29]. Studies carried out in larger populations demonstrate that up to 50% of individuals cannot achieve accuracy above 70% — the threshold indicating successful patient-BCI interaction [30]. Importantly, these parameters reflect the situation in the general population. Our study recruited neurology patients with moderate cognitive deficit. Of them, some patients performed better: Cohen's kappa and the recognition rate were 63.0% (54.0; 67.0) vs 39.0% (32.0; 48.0) in other patients. These data correlated with the MIQ-RS scores. Our findings have important theoretical and practical implications as they prove the unity of cognitive and motor components in the human body, demonstrates the need for a dualistic approach to the recovery of motor and cognitive functions in patients with brain injury, sets the goal of developing a personalized approach to applying the BCI technology for better clinical outcomes, which will result in a more rational use of rehabilitation resources.

CONCLUSION

This study has established a correlation between the ability of patients for motor imagery inferred from the MIQ-RS scale and the efficacy of patient-BCI interaction. A larger patient sample is needed to assess the effect of patient-BCI interaction on the dynamics of upper limb motor recovery dynamics.

References

1. Kutashov VA, Budnevskiy AV, Priputnevich DN, Surzhko GV. Psychological features of patients with consequences of acute disorders of cerebral circulation, hamper their social adaptation. Vestnik nevrologii, psihiatrii i nejrohirurgii. 2014; (8): 8–13.

2. Roman GC. Facts, myths, and controversies in vascular dementia. J Neurol Sci. 2004; 226: 49–52.

3. Ang KK, Phua KS, Wang C, Chin ZY, Kuah CW, Low W, et al. Randomized Controlled Trial of EEG-Based Motor Imagery Brain-

Computer Interface Robotic Rehabilitation for Stroke. Clinical EEG and neuroscience. 2015; 46 (4): 310–20. https://doi.org/10.1177/1550059414522229.

4. Frolov AA, Mokienko OA, Lyukmanov RKh, Chernikova LA, Kotov SV, et al. Preliminary results of a controlled study of the effectiveness of IMC-exoskeleton technology for post-stroke paresis of the arm. Vestnik RSMU. 2016; (2): 175.

5. Novak DA, Grefkes C, Arneli M, Fink GR. Interhemispheric competition after stroke: brain stimulation to enhance recovery of function of the affected hand. Neururehabil Neural Repair. 2009; (23): 641–57.

6. Sharma N, Simmons LH, Jones PS, Day DJ, Carpenter TA, Pomeroy VM, et al. Motor imagery after subcortical stroke: a functional magnetic resonance imaging study. Stroke. 2009; 40 (4): 315–24.

7. Johnson SH, Sprehn G, Saykin AJ. Intact motorimagery in chronic upper limb hemiplegics: evidence foractivity-independent action representations. Journal of Cognitive Neuroscience. 2002; 14 (6): 841–52.

8. Barclay-Goddard RE, Stevenson TJ, Poluha W, Thalman L. Mental practice for treating upper extremity deficits in individuals with hemiparesis after stroke. Cochrane Database Syst Rev. 2011; 11 (5): CD005950. DOI: 10.1002/14651858.CD005950.pub4.

9. Chholak P, Niso G, Maksimenko VA, Kurkin SA, Frolov NS, Pitsik EN et al. Visual and kinesthetic modes affect motor imagery classification in untrained subjects. 2019 Jul 8; 9 (1): 9838. DOI:10.1038/s41598-019-46310-9.

10. Schmidt R, Lee T. Motor Control and Learning: A Behavioral Emphasis. Champaign, IL: Human Kinetics, 1999; 592 p.

11. Bajaj S, Butler AJ, Drake D, Dhamala M. Brain effective connectivity during motor-imagery and execution following stroke and rehabilitation. Neuroimage Clin. 2015 (8): 572–82. https://doi.org/10.1016/j.nicl.2015.06.006.

12. Page SJ, Levine P, Leonard A. Mental practice in chronic stroke: results of a randomized, placebo-controlled trial. Stroke. 2007 Apr; 38 (4): 1293–7.

13. Braun SM, Beurskens AJ, Borm PJ, Schack T, Wade DT. The effects of mental practice in stroke rehabilitation: a systematic review. Arch Phys Med Rehabil. 2006 Jun; 87 (6): 842–52.

14. Román GC. Facts, myths, and controversies in vascular dementia. J Neurol Sci. 2004 Nov 15; 226 (1–2): 49–52.

15. Sauvage C, De Greef N, Manto M, Jissendi P, Nioche C, Habas C. Reorganization of large-scale cognitive networks during automation of imagination of a complex sequential movement // Journal of neuroradiology. 2015; 42 (2): 115–25.

16. Kaplan AYa. Neurophysiological foundations and practical implementation of the technology of the brain of machine

interfaces in neurological rehabilitation. Human Physiology. 2016; 42 (1): 118–27.

17. Hall CR, Martin KA. Measuring movement imagery abilities: A revision of the Movement Imagery Questionnaire. Journal of mental imagery. 1997.

18. Bocti C, Legault V, Leblanc N, Berger L, Nasreddine Z, BeaulieuBoire I, et al. Vascular cognitive impairment: most useful subtests of the Montreal Cognitive Assessment in minor stroke and transient ischemic attack. Dement Geriatr Cogn Disord. 2013; 36 (3–4): 154–62.

19. Compston A. Aids to the investigation of peripheral nerve injuries. Medical Research Council: Nerve Injuries Research Committee. His Majesty's Stationery Office: 1942; pp. 48 (iii) and 74 figures and 7 diagrams; with aids to the examination of the peripheral nervous system. By Michael O'Brien for the Guarantors of Brain. Saunders Elsevier: 2010; pp. 64.

20. Oldfield RC. The assessment and analysis of handedness: the Edinburgh inventory. Neuropsychologia. 1971 Mar; 9 (1): 97–113.

21. Bohannon RW, Smith MB. Interrater reliability of a modified Ashworth scale of muscle spasticity. Phys Ther. 1987 Feb; 67 (2): 206–7.

22. Bobrov PD, Korshakov AV, Roshchin VYu, Frolov AA. Bayesian approach to the implementation of the brain-computer interface based on the representation of movements. Journal of Higher Nervous Activities.2012; 62 (1): 89–99.

23. Jorgensen HS, Nakayama H, Raaschou HO, Olsen TS. Recovery of walking function in stroke patients: the Copenhagen Stroke Study. Archives of Physical Medicine and Rehabilitation. 1995. 76 (1): 27–32.

24. Stroke in adults: central paresis of the upper limb. Clinical recommendations ICD10: I60/I61/I62/I63/I64/I69.

25. Sanford J, Moreland J, Swanson LR, Stratford PW, Gowland C. Reliability of the Fugl–Meyer assessment for testing motor performance in patients following stroke. Phys Ther. 1993 Jul; 73 (7): 447–54.

26. Doussoulin SA, Rivas SR, Campos SV. Validation of «Action Research Arm Test» (ARAT) in Chilean patients with a paretic upper limb after a stroke. Rev Med Chil. 2012 Jan; 140 (1): 59– 65. Spanish.

27. Bogolyubov VM. Medicinskaja reabilitacija. M.: BINOM, 2010; s. 21.

28. Wolpaw JR, McFarland DJ. Control of a two-dimensional movement signal by a noninvasive brain-computer interface in humans. Proc Natl Acad Sci USA. 2004 (101): 17849–54.

29. Vidaurre C, Blankertz B. Towards a cure for BCI illiteracy. Brain Topogr. 2010; (23): 194–8.

30. Ahn M, Chan S. Performance variation in motor imagery brain – computer interface: A brief review. J Neurosci Methods. 2015; (243): 103–10.

Литература

1. Куташов В. А., Будневский А. В., Припутневич Д. Н., Суржко Г. В. Психологические особенности пациентов с последствиями кровообращения, затрудняющими социальную адаптацию. Вестник неврологии, психиатрии и нейрохирургии. 2014; (8): 8–13.

2. Roman GC. Facts, myths, and controversies in vascular dementia. J Neurol Sci. 2004; 226: 49–52.

3. Ang KK, Phua KS, Wang C, Chin ZY, Kuah CW, Low W, et al. Randomized Controlled Trial of EEG-Based Motor Imagery Brain-Computer Interface Robotic Rehabilitation for Stroke. Clinical EEG and neuroscience. 2015; 46 (4): 310–20. https://doi.org/10.1177/1550059414522229.

4. Фролов А. А., Мокиенко О. А., Люкманов Р. Х., Черникова Л. А., Котов С. В. и др., Предварительные результаты контролируемого исследования эффективности технологии ИМК-экзоскелет при постинсультном парезе руки. Вестник РГМУ. 2016; (2): 175.

5. Novak DA, Grefkes C, Arneli M, Fink GR. Interhemispheric competition after stroke: brain stimulation to enhance recovery of function of the affected hand. Neururehabil Neural Repair. 2009; (23): 641–57.

6. Sharma N, Simmons LH, Jones PS, Day DJ, Carpenter TA,

Pomeroy VM, et al. Motor imagery after subcortical stroke: a functional magnetic resonance imaging study. Stroke. 2009; 40 (4): 315–24.

7. Johnson SH, Sprehn G, Saykin AJ. Intact motorimagery in chronic upper limb hemiplegics: evidence foractivity-independent action representations. Journal of Cognitive Neuroscience. 2002; 14 (6): 841–52.

8. Barclay-Goddard RE, Stevenson TJ, Poluha W, Thalman L. Mental practice for treating upper extremity deficits in individuals with hemiparesis after stroke. Cochrane Database Syst Rev. 2011; 11 (5): CD005950. DOI: 10.1002/14651858.CD005950.pub4.

9. Chholak P, Niso G, Maksimenko VA, Kurkin SA, Frolov NS, Pitsik EN et al. Visual and kinesthetic modes affect motor imagery classification in untrained subjects. 2019 Jul 8; 9 (1): 9838. DOI:10.1038/s41598-019-46310-9.

10. Schmidt R, Lee T. Motor Control and Learning: A Behavioral Emphasis. Champaign, IL: Human Kinetics, 1999; 592 p.

11. Bajaj S, Butler AJ, Drake D, Dhamala M. Brain effective connectivity during motor-imagery and execution following stroke and rehabilitation. Neuroimage Clin. 2015 (8): 572–82. https://doi.org/10.1016/j.nicl.2015.06.006.

12. Page SJ, Levine P, Leonard A. Mental practice in chronic stroke: results of a randomized, placebo-controlled trial. Stroke. 2007 Apr; 38 (4): 1293–7.

13. Braun SM, Beurskens AJ, Borm PJ, Schack T, Wade DT. The effects of mental practice in stroke rehabilitation: a systematic review. Arch Phys Med Rehabil. 2006 Jun; 87 (6): 842–52.

14. Román GC. Facts, myths, and controversies in vascular dementia. J Neurol Sci. 2004 Nov 15; 226 (1–2): 49–52.

15. Sauvage C, De Greef N, Manto M, Jissendi P, Nioche C, Habas C. Reorganization of large-scale cognitive networks during automation of imagination of a complex sequential movement // Journal of neuroradiology. 2015; 42 (2): 115–25.

16. Каплан А. Я. Нейрофизиологические основания и практические реализации технологии мозг машинных интерфейсов в неврологической реабилитации. Физиология человека. 2016; 42 (1): 118–27.

17. Hall CR, Martin KA. Measuring movement imagery abilities: A revision of the Movement Imagery Questionnaire. Journal of mental imagery. 1997.

18. Bocti C, Legault V, Leblanc N, Berger L, Nasreddine Z, BeaulieuBoire I, et al. Vascular cognitive impairment: most useful subtests of the Montreal Cognitive Assessment in minor stroke and transient ischemic attack. Dement Geriatr Cogn Disord. 2013; 36 (3–4): 154–62.

19. Compston A. Aids to the investigation of peripheral nerve injuries. Medical Research Council: Nerve Injuries Research Committee. His Majesty's Stationery Office: 1942; pp. 48 (iii) and 74 figures and 7 diagrams; with aids to the examination of the peripheral nervous system. By Michael O'Brien for the Guarantors of Brain. Saunders Elsevier: 2010; pp. 64.

20. Oldfield RC. The assessment and analysis of handedness: the Edinburgh inventory. Neuropsychologia. 1971 Mar; 9 (1): 97–113.

21. Bohannon RW, Smith MB. Interrater reliability of a modified Ashworth scale of muscle spasticity. Phys Ther. 1987 Feb; 67 (2): 206–7.

22. Бобров П. Д., Коршаков А. В., Рощин В. Ю., Фролов А. А. Байесовский подход к реализации интерфейса мозг–компьютер, основанного на представлении движений. Журнал высшей нервной деятельности. 2012; 62 (1): 89–99.

23. Jorgensen HS, Nakayama H, Raaschou HO, Olsen TS. Recovery of walking function in stroke patients: the Copenhagen Stroke Study. Archives of Physical Medicine and Rehabilitation. 1995. 76 (1): 27–32.

24. Инсульт у взрослых: центральный парез верхней конечности. Клинические рекомендации МКБ10: I60/I61/I62/I63/I64/I69.

25. Sanford J, Moreland J, Swanson LR, Stratford PW, Gowland C. Reliability of the Fugl–Meyer assessment for testing motor performance in patients following stroke. Phys Ther. 1993 Jul; 73 (7): 447–54.

26. Doussoulin SA, Rivas SR, Campos SV. Validation of «Action Research Arm Test» (ARAT) in Chilean patients with a paretic upper limb after a stroke. Rev Med Chil. 2012 Jan; 140 (1): 59– 65. Spanish.

27. Боголюбов В. М. Медицинская реабилитация. М.: БИНОМ, 2010; с. 21.

28. Wolpaw JR, McFarland DJ. Control of a two-dimensional movement signal by a noninvasive brain-computer interface in humans. Proc Natl Acad Sci USA. 2004 (101): 17849–54.

29. Vidaurre C, Blankertz B. Towards a cure for BCI illiteracy. Brain Topogr. 2010; (23): 194–8.

30. Ahn M, Chan S. Performance variation in motor imagery brain – computer interface: A brief review. J Neurosci Methods. 2015; (243): 103–10.

CHANGES IN THE NOCICEPTIVE RESPONSE TO THERMAL STIMULATION IN RATS FOLLOWING ADMINISTRATION OF N-TERMINAL ANALOGS OF THE ADRENOCORTICOTROPIC HORMONE

Dodonova SA[1] ✉, Bobyntsev II[1], Belykh AE[1], Andreeva LA[2], Myasoedov NF[2]

[1] Kursk State Medical University, Kurks, Russia

[2] Institute of Molecular Genetics, Moscow, Russia

Melanocortins (MCs) are an increasingly studied class of regulatory peptides exerting a wide range of biological effects. All naturally occurring MCs share a His-Phe-Arg-Trp fragment (HFRW) corresponding to the sequence of amino acid residues 6–9 of the adrenocorticotropic hormone ($ACTH_{6-9}$), which is also a central active component of ACTH. Attaching the Pro-Gly-Pro (PGP) sequence to the C-end of the peptide extends the duration of the peptide's effect. The aim of this study was to investigate the effects of $ACTH_{6-9}$-PGP (HFRWPGP) on the spinal and supraspinal mechanisms involved in the nociceptive response in rats and to compare them to those of its structural analog $ACTH_{4-7}$-PGP (MEHFPGP). $ACTH_{6-9}$-PGP effects were studied following the intraperitoneal administration of the peptide at doses 0.5, 1.5, 5, 15, 50, 150, or 450 µg/kg 15 minutes before the hot plate and tail flick tests. $ACTH_{4-7}$-PGP effects were studied under the same conditions at the following doses: 50, 150 and 450 µg/kg. We found that $ACTH_{6-9}$-PGP administered intraperitoneally at 5 or 150 µg/kg induced a pronounced reduction in pain sensitivity 15 and 45 minutes after the injection ($p = 0.04$); this effect was implemented via supraspinal mechanisms. In the tail flick test, 150 µg/kg $ACTH_{6-9}$-PGP increased pain sensitivity, with the participation of segmental spinal mechanisms ($p = 0.04$). $ACTH_{4-7}$-PGP did not have any effect on the studied mechanisms of pain sensitivity. Thus, unlike $ACTH_{4-7}$-PGP, $ACTH_{6-9}$-PGP can both increase pain sensitivity and exert an analgesic effect.

Keywords: regulatory peptide, ACTH, pain, hot plate, tail flick

ИЗМЕНЕНИЕ ТЕМПЕРАТУРНОЙ БОЛЕВОЙ ЧУВСТВИТЕЛЬНОСТИ У КРЫС ПОСЛЕ ВВЕДЕНИЯ N-КОНЦЕВЫХ АНАЛОГОВ АДРЕНОКОРТИКОТРОПНОГО ГОРМОНА

С. А. Додонова[1] ✉, И. И. Бобынцев[1], А. Е. Белых[1], Л. А. Андреева[2], Н. Ф. Мясоедов[2]

[1] Курский государственный медицинский университет, Курск, Россия

[2] Институт молекулярной генетики, Москва, Россия

Меланокортины (МК) — один из активно исследуемых классов пептидных регуляторов с широким спектром биологических эффектов. В структуре всех природных МК присутствует общий фрагмент — His-Phe-Arg-Trp (HFRW), соответствующий последовательности с 6-го по 9-й аминокислотный остаток молекулы адренокортикотропного гормона ($AKTГ_{6-9}$) и являющийся ее активным центром. Показано, что присоединение к С-концу аминокислотной последовательности Pro-Gly-Pro (PGP) приводит к пролонгации действия пептидов. Целью работы было изучить влияние эффектов $AKTГ_{6-9}$-PGP (HFRWPGP) на спинальные и супраспинальные механизмы формирования болевой чувствительности у крыс, а также сравнить их с эффектами его структурного аналога — $AKTГ_{4-7}$-PGP (MEHFPGP). Эффекты $AKTГ_{6-9}$-PGP были исследованы при его внутрибрюшинном введении в дозах 0,5, 1,5, 5, 15, 50, 150 и 450 мкг/кг за 15 мин до начала опыта по изучению температурной болевой чувствительности у крыс с использованием тестов «горячая пластина» и «отдергивание хвоста». Эффекты $AKTГ_{4-7}$-PGP были исследованы в аналогичных условиях в дозах 50; 150 и 450 мкг/кг. Показано, что $AKTГ_{6-9}$-PGP в дозах 5 и 150 мкг/кг вызывал выраженное снижение температурной болевой чувствительности через 15 и 45 мин после его внутрибрюшинного введения ($p = 0,04$), реализованного на супраспинальном уровне. В тесте «отдергивание хвоста» $AKTГ_{6-9}$-PGP в дозе 150 мкг/кг повышал температурную болевую чувствительность с участием сегментарных спинальных механизмов ($p = 0,04$). $AKTГ_{4-7}$-PGP не оказывал влияния на исследованные механизмы болевой чувствительности. Таким образом, установлено, что $AKTГ_{6-9}$-PGP, в отличие от $AKTГ_{4-7}$-PGP, способен обладать как анальгетическими, так алгическими эффектами.

Ключевые слова: регуляторный пептид, АКТГ, боль, горячая пластина, отдергивание хвоста

Regulatory melanocortin peptides and their fragments exert a wide range of biological effects. This phenomenon has inspired the creation of synthetic melanocortin analogs for structure-function analysis and therapeutic applications [1, 2]. It is known that N-terminal regions of the adrenocorticotropic hormone (ACTH) have a neurotropic effect and affect the body's response to pain [3]. The His-Phe-Arg-Trp sequence found at $ACTH_{6-9}$ is required for the activation of all melanocortin receptor types [4]. Some of $ACTH_{6-9}$ effects are retained after the Pro-Gly-Pro (PGP) tripeptide is attached to its C-terminus so as to enhance resistance to carboxypeptidases [5]. However, the impact of the $ACTH_{6-9}$-PGP peptide on sensitivity to pain has not been studied so far. At the same time, a synthetic fragment $ACTH_{4-7}$-PGP, which is structurally close to $ACTH_{6-9}$-PGP and is also an active ingredient of a pharmaceutical drug Semax, has similar effects [3]. Therefore, it is important to investigate the neurotropic action of $ACTH_{6-9}$-PGP as part of the structure-function analysis of N-terminal ACTH fragments.

The aim of this work was to study the effect of the $ACTH_{6-9}$-PGP peptide on the spinal and supraspinal mechanisms of nociceptive response in rats and to compare them to the effects of $ACTH_{4-7}$-PGP.

METHODS

Our experiments were carried out in 121 male Wistar rats weighing 150–190 g. The animals were kept in cages (10 rats per cage) in standard housing conditions at a 12/12 light/dark cycle at controlled ambient temperature (22 ± 2 °C). The rats were fed a standard pellet diet and had free access to water. The experiments were carried out between 9 am and 15 pm.

Ten experimental and one control groups were formed consisting of 11 rats each. Each experimental group received a single dose of either $ACTH_{6-9}$-PGP or $ACTH_{4-7}$-PGP (Semax) from the dose range specified below. The peptides used in the experiment had been synthesized in advance at the Institute of Molecular Genetics (RAS). $ACTH_{6-9}$-PGP was dissolved in 0.9% normal saline. Fifteen minutes before the experiment, 7 experimental groups received a single intraperitoneal injection of $ACTH_{6-9}$-PGP at one of the following doses: 0.5, 1.5, 5, 15, 50, 150, or 450 µg/kg. $ACTH_{4-7}$-PGP was also dissolved in normal saline and administered intraperitoneally to the animals from the 3 remaining experimental groups at a single dose of 50, 150 or 450 µg/kg 15 min before the tests. The control group received equivalent amounts of normal saline (1 ml per 1 kg body weight).

Pain response to thermal stimulation was assessed using the hot plate and the tail flick tests [6] and the corresponding equipment: a hot plate (model LE7406) and a tail-flick meter (model LE7106) (PanLab Harvard Apparatus; Spain). The hot plate test consisted of 4 trials separated by 15-min breaks and conducted at 53 °C. In this test, the nociceptive threshold was measured once before the injection and 3 times after the injection. Each animal was placed on a hot plate and the latency to the first behavioral response (hind paw licking, jumping) to the nociceptive stimulus was measured. In the tail flick test, the middle section of the tail was exposed to the heat stimulus of fixed intensity (set to 50 units) and the latency to tail flicking was recorded. In this test, 5 measurements were taken at 15-min intervals: 2 pretreatment measurements of the baseline nociceptive threshold (averaged) and 3 measurements of the nociceptive threshold after the injection. The maximum possible effect (MPE) was calculated using the following formula: [6]:

$$MPE = \frac{LP_{ost} - LP_{re}}{CO_{time} - LP_{re}} \times 100\% ,$$

where LP_{ost} is posttreatment latency, LP_{re} is pretreatment latency, CO_{time} is cut-off time (45 s in the hot plate test and 9 s in the tail flick test).

Statistical analysis was carried out in MS Excel 2016 (Microsoft; USA), Statistica 13.3 (StatSoft; USA) and the R environment (The R Foundation for Statistical Computing; Austria). Normality of data distribution was assessed using the Shapiro Wilk test. The equality of variances was tested using Levene's test (lawstat). The obtained results were expressed as a median (Me), lower (25) and upper (75) quartiles (Q1 and Q3). Statistical significance was assessed using the nonparametric univariate Kruskal–Wallis test; post-hoc intergroup comparisons were done using the Mann–Whitney U test and the Benjamini–Hochberg procedure. The results were considered significant at $p < 0.05$

RESULTS

A single injection of the $ACTH_{6-9}$-PGP peptide produced a dose-dependent effect on the MPE value in the hot plate test (see Table). The analgesic effect was the most pronounced for the 5 µg/kg dose 15 and 45 min after the injection, with a significant 2.5-fold ($p = 0.04$) and 7-fold ($p = 0.02$) elevation of the nociceptive threshold, respectively. At a lower dose of 1.5 µg/kg, the peptide did not have any considerable impact on pain sensitivity. However, further dose reduction to 0.5 µg/kg changed the trend: 30 min after the $ACTH_{6-9}$-PGP injection, the MPE value dropped by 193% ($p = 0.15$) and remained at this low level for at least 45 min ($p = 0.07$).

Increasing the $ACTH_{6-9}$-PGP dose to 15 µg/kg did not have any significant effect. However, the peptide tended to increase sensitivity to pain 45 min after the injection when administered at 50 µg/kg ($p = 0.1$). Further dose increase to 150 µg/kg was accompanied by a significant elevation of the nociceptive threshold 15 min ($p = 0.04$) and 45 min ($p = 0.04$) after the injection. When administered at 450 µg/kg, $ACTH_{6-9}$-PGP did not have any significant effect on the studied parameters.

No statistically significant differences in the studied parameters were observed between the rats in the experimental groups following the injection of $ACTH_{4-7}$-PGP at all studied doses in comparison with the controls.

Based on the results of the tail flick test, no reliable changes in the nociceptive threshold were observed in the rats injected with 0.5, 1.5, 15, 50, and 450 µg/kg of $ACTH_{6-9}$-PGP (see Table).

Although no significant effect of $ACTH_{6-9}$-PGP administered at 5 and 150 µg/kg was observed in the hot plate test 30 min after the injection, the peptide did affect the rats' sensitivity to heat in the tail flick test 30 min after its administration: at 150 µg/kg the nociceptive threshold was significantly lower ($p = 0.04$) and at 5 µg/kg the peptide tended to increase pain sensitivity ($p = 0.1$).

The tail flick test did not reveal any significant changes in pain sensitivity in the animals treated with $ACTH_{4-7}$-PGP.

DISCUSSION

Biological effects of melanocortin peptides are implemented via a variety of melanocortin receptors (MCRs). Specifically, MCR1 is expressed in the neurons of the periaqueductal gray, MCR3 is expressed in the cortex and the thalamus, whereas MCR4, in the brain stem. The activation of these brain structures plays an important role in nociception by reducing pain progression [7, 8]. Considering that supraspinal structures are involved in the nociceptive response to thermal stimulation in the hot plate test [6], the interaction between $ACTH_{6-9}$-PGP and

Table 1. Effects of ACTH$_{6-9}$-PGP and ACTH$_{4-7}$-PGP on pain sensitivity in rats in the hot plate and tail flick tests, MPE (Me (Q1; Q3))

MPE, % / Group	15 min	30 min	45 min	15 min	30 min	45 min
	Hot plate test			Tail flick test		
Control	12.92 (−6.05; 26.83)	1.9 (−6.93; 5.84)	3.58 (−3.18; 9.53)	15.53 (−22.91; 29.78)	15.69 (−5.07; 28.69)	−17.81 (−46.16; 25.12)
ACTH$_{6-9}$-PGP 0.5 µg/kg (n = 11)	4.41 (−16.20; 7.73)	−18.11 (−38.62; −0.72)	−18.73 (−31.94; −7.92)	17.08 (6.06; 50.00)	0.05 (−30.59; 23.43)	−14.31 (−41.03; 5.79)
ACTH$_{6-9}$-PGP 1.5 µg/kg (n = 11)	8.98 (−0.59; 19.74)	16.28 (8.43; 23.68)	−9.05 (−26.00; 11.33)	11.68 (8.08; 38.79)	22.42 (−3.37; 54.11)	−5.95 (−7.98; 19.13)
ACTH$_{6-9}$-PGP 5 µg/kg (n = 11)	45.44* (23.88; 54.69)	28.05 (−1.46; 42.62)	31.11* (27.57; 36.58)	−7.73 (−28.83; 16.98)	−8.76 (−19.43; 12.29)	8.6 (−8.97; 41.44)
ACTH$_{6-9}$-PGP 15 µg/kg (n = 11)	16.48 (11.57; 48.20)	11.75 (−0.76; 29.79)	10.83 (−11.48; 46.64)	0.62 (−8.11; 22.87)	−6.11 (−17.38; 12.50)	1.96 (−3.77; 22.24)
ACTH$_{6-9}$-PGP 50 µg/kg (n = 11)	3.57 (−9.45; 23.48)	−4.09 (−32.97; 7.96)	−10.42 (−23.20; 2.20)	11.65 (−13.77; 40.37)	19.97 (9.45; 40.40)	15.73 (−5.16; 20.34)
ACTH$_{6-9}$-PGP 150 µg/kg (n = 11)	41.02* (16.37; 66.96)	10.06 (2.88; 29.73)	30.40* (19.13; 37.31)	−18.04 (−44.05; 6.37)	−31.67* (−36.45;−21.85)	−20.85 (−43.43; 8.58)
ACTH$_{6-9}$-PGP 450 µg/kg (n = 11)	24.15 (9.36; 26.39)	6.61 (−7.00; 17.15)	4.56 (−2.13; 6.92)	3.77 (−21.28; 23.96)	11.16 (−28.31; 40.84)	−5.78 (−22.03; 38.22)
ACTH$_{4-7}$-PGP 50 µg/kg (n = 11)	0.45 (−14.1; 37.27)	11.01 (−18.57; 23.17)	10.23 (−0.03; 42.15)	1.21 (−22.86; 38.97)	22.7 (−58.53; 32.46)	−4.63 (−47.24; 25.36)
ACTH$_{4-7}$-PGP 150 µg/kg (n = 11)	12.07 (−5.06; 34.59)	12.48 (0.64; 31.16)	1.52 (−5.75; 16.44)	10 (−43.69; 26.44)	0.1 (−44.11; 27.93)	−3.91 (−40.36; 21.57)
ACTH$_{4-7}$-PGP 450 µg/kg (n = 11)	20.37 (8.63; 27.69)	12.19 (−9.18; 32.12)	21.9 (−9.19; 35.83)	25.78 (1.54; 80.88)	−16.71 (−35.19; 25.67)	11.83 (−27.97; 26.38)

Note: * — differences are significant (*p* ≤ 0,05) in comparison with the control group at the same time points (according to the Mann-Whitney U test and the Benjamini–Hochberg procedure).

melanocortin receptors localized in the brain can affect pain sensitivity.

MCR4 is found in the spinal cord [3, 8]; a ACTH$_{6-9}$-PGP-induced change in their activity can affect the function of segmental mechanisms involved in nociception, which was observed in our flick tail test. It is still unclear how melanocortin receptors mediate the effect of ACTH analogs; it is hypothesized that there is at least one previously undescribed receptor subtype involved [9, 10].

The observed differences in the intensity and directionality of the effects induced by different peptide doses can be explained by the interaction of the peptide with various types of MCRs it encounters when travelling across the brain or by some aspects of intracellular mechanisms of its action. Specifically, transmembrane and subsequent intracellular signaling from an MCR can be implemented via different pathways depending on the concentration of the ligand: through cAMP activation, by inositol phosphates [1, 11], Ca^{2+} and protein kinases [1]. This is true for all types of melanocortin receptors [1]. The direction, intensity and duration of the nociceptive response to a stimulus are determined by the type of the activated signal transduction mechanism [1, 2]. These facts are consistent with our findings demonstrating the opposite dose-dependent trends in responding to the thermal stimulus following ACTH$_{6-9}$-PGP administration; these effects are typical of regulatory peptides as a separate class of bioactive substances [11, 12].

The opposite trends in the nociceptive response following ACTH$_{6-9}$-PGP administration observed in our study are also consistent with the literature reports on the effects of ACTH fragments and analogs on nociception [3, 13]. It could be

hypothesized that the mechanisms of the ACTH$_{6-9}$-PGP effect on the response to pain are similar to those of its structural analog ACTH$_{4-7}$-PGP (Semax), which reduces sensitivity to pain and exerts its effects via opioid and serotonin receptors [3].

Because the ACTH$_{6-9}$-PGP sequence is required for the activation of all types of melanocortin receptors [4], the effects of ACTH$_{6-9}$-PGP on pain sensitivity (compared to those of ACTH$_{4-7}$-PGP) observed in our study may result from the interaction of the peptide with all types of MCRs in CNS structures involved in nociception and antinociception. Interestingly, we did not observe the pain-reducing effect of ACTH$_{4-7}$-PGP described by other authors [3]. Considering that the character of pain response can be largely determined by the features of a specific animal breed or line [14, 15], the differences observed in our study may be to some extent explained by the use of Wistar rats vs outbred rodents exploited in the studies cited above.

CONCLUSIONS

In the hot plate test, a reduction in pain sensitivity was observed 15 and 45 minutes after the intraperitoneal injection of 5 and 150 µg/kg ACTH$_{6-9}$-PGP; this reduction was mediated by supraspinal mechanisms. Other studied doses of the peptide did not produce any effect on the nociceptive response. In the tail flick test, the injection of 150 µg/kg ACTH$_{6-9}$-PGP increased pain threshold, with the participation of segmental spinal mechanisms. No effect on pain response was observed for ACTH$_{4-7}$-PGP. Our findings broaden the knowledge of physiological effects of N-terminal ACTH analogs and can provide a theoretical rationale for developing neurotropic pharmaceutical agents based on these compounds.

References

1. Catania A, Lonati C, Sordi A, Carlin A, Leonardi P, Gatti S. The melanocortin system in control of inflammation. Scientific World Journal. 2010; (10): 1840–53.
2. Catania A. Neuroprotective actions of melanocortins: a therapeutic opportunity. Trends Neurosci. 2008. 31 (7): 353–60.
3. Koroleva SV, Myasoedov NF. Semax as a Universal Drug for Therapy and Research. Biology Bulletin. 2018; 45 (6): 589–600.
4. Clark AJ, Forfar R, Hussain M, Jerman J, McIver E, Taylor D, et al. ACTH Antagonists. Front Endocrinol (Lausanne). 2016; (7): 101.
5. Andreeva LA, Grivennikov IA, Gavrilova SA, Dolotov OV, Kamenskij AA, Koshelev VB, Levickaya NG, Myasoedov NF, avtory. Uchrezhdenie Rossijskoj akademii nauk Institut molekulyarnoj genetiki RAN, patentoobladatel'. Peptid, obladayushchij nejrotropnymi svojstvami. Patent RF № 2443711. 27.02.2012. Russian.
6. Mironov AN, redaktor. Rukovodstvo po provedeniyu doklinicheskih issledovanij lekarstvennyh sredstv. CHast' pervaya. M.: Grif i K, 2012; 944 s. Russian.
7. Kovalitskaya YuA, Funtikova AN, Sadovnikov VB, Navolotskaya EV. The influence of ACTH-like peptides on migration, adhesion and spreading of mouse peritoneal macrophages in vitro. Rossiyskiy immunologicheskiy zhurnal. 2011; 5 (1): 3–10. Russian.
8. Hill JW, Faulkner LD. The Role of the Melanocortin System in Metabolic Disease: New Developments and Advances.

Neuroendocrinology. 2017; 104 (4): 330–46.
9. Wikberg JE, Muceniece R, Mandrika I, Prusis P, Lindblom J, Post C, et al. New aspects on the melanocortins and their receptors. Pharmacol Res. 2000; 42 (5): 393–420.
10. Fridmanis D, Roga A, Klovins J. ACTH Receptor (MC2R) Specificity: What Do We Know About Underlying Molecular Mechanisms? Front Endocrinol (Lausanne). 2017; (8): 13.
11. Akmaev IG, Grinevich VV. Ot nejroendokrinologii k nejroimmunoendokrinologii. Byul eksperim biologii i mediciny. 2001; 131 (1): 22–32. Russian.
12. Ashmarin IP, Karazeeva EP, Lelekova TV. Effektivnost' ul'tramalyh doz endogennyh bioregulyatorov i immunoaktivnyh soedinenij. ZHurn mikrobiol. 2005; (3): 109–116. Russian.
13. Levitskaya NG, Kamensky AA. Melanocortin System. Uspekhi fiziologicheskikh nauk. 2009; 40 (1): 44–65. Russian.
14. Hestehave S, Abelson KSP, Pedersen TB, Munro G. The analgesic efficacy of morphine varies with rat strain and experimental pain model: implications for target validation efforts in pain drug discovery. Eur J Pain. 2019; 23 (3): 539–54. PubMed PMID: 30318662.
15. Hestehave S, Abelson KSP, Pedersen TB, Munro G. Stress sensitivity and cutaneous sensory thresholds before and after neuropathic injury in various inbred and outbred rat strains. Behavioural Brain Research. 2019; (375): 112149.

Литература

1. Catania A, Lonati C, Sordi A, Carlin A, Leonardi P, Gatti S. The melanocortin system in control of inflammation. Scientific World Journal. 2010; (10): 1840–53.
2. Catania A. Neuroprotective actions of melanocortins: a therapeutic opportunity. Trends Neurosci. 2008. 31 (7): 353–60.
3. Koroleva SV, Myasoedov NF. Semax as a Universal Drug for Therapy and Research. Biology Bulletin. 2018; 45 (6): 589–600.
4. Clark AJ, Forfar R, Hussain M, Jerman J, McIver E, Taylor D, et al. ACTH Antagonists. Front Endocrinol (Lausanne). 2016; (7): 101.
5. Андреева Л. А, Гривенников И. А., Гаврилова С. А., Долотов О. В., Каменский А. А., Кошелев В. Б., Левицкая Н. Г., Мясоедов Н. Ф., авторы. Учреждение Российской академии наук Институт молекулярной генетики РАН, патентообладатель. Пептид, обладающий нейротропными свойствами. Патент РФ № 2443711. 27.02.2012.
6. Миронов А. Н., редактор. Руководство по проведению доклинических исследований лекарственных средств. Часть первая. М.: Гриф и К, 2012; 944 с.
7. Ковалицкая А. Ю., Фунтикова А. Н., Садовников В. Б., Наволоцкая Е. В. Действие АКТГ-подобных пептидов на миграцию и расплавление перитонеальных макрофагов мыши in vitro. Российский иммунологический журнал. 2011; 5 (1): 3–10.
8. Hill JW, Faulkner LD. The Role of the Melanocortin System in Metabolic Disease: New Developments and Advances.

Neuroendocrinology. 2017; 104 (4): 330–46.
9. Wikberg JE, Muceniece R, Mandrika I, Prusis P, Lindblom J, Post C, et al. New aspects on the melanocortins and their receptors. Pharmacol Res. 2000; 42 (5): 393–420.
10. Fridmanis D, Roga A, Klovins J. ACTH Receptor (MC2R) Specificity: What Do We Know About Underlying Molecular Mechanisms? Front Endocrinol (Lausanne). 2017; (8): 13.
11. Акмаев И. Г., Гриневич В. В. От нейроэндокринологии к нейроиммуноэндокринологии. Бюллетень экспериментальной биологии и медицины. 2001; 131 (1): 22–32.
12. Ашмарин И. П., Каразеева Е. П., Лелекова Т. В. Эффективность ультрамалых доз эндогенных биорегуляторов и иммуноактивных соединений. Журнал микробиологии. 2005; (3): 109–16.
13. Левицкая Н. Г., Каменский А. А. Меланокортиновая система. Успехи физиол. наук. 2009; 40 (1): 44–65.
14. Hestehave S, Abelson KSP, Pedersen TB, Munro G. The analgesic efficacy of morphine varies with rat strain and experimental pain model: implications for target validation efforts in pain drug discovery. Eur J Pain. 2019; 23 (3): 539–54. PubMed PMID: 30318662.
15. Hestehave S, Abelson KSP, Pedersen TB, Munro G. Stress sensitivity and cutaneous sensory thresholds before and after neuropathic injury in various inbred and outbred rat strains. Behavioural Brain Research. 2019; (375): 112149.

ENGINEERING A RECOMBINANT HERPESVIRUS SAIMIRI STRAIN BY CO-CULTURING TRANSFECTED AND PERMISSIVE CELLS

Hamad A[1], Chumakov SP[2] ✉

[1] Moscow Institute of Physics and Technology, Moscow, Russia

[2] Shemyakin-Ovchinnikov Institute of Bioorganic Chemistry of the Russian Academy of Sciences, Moscow, Russia

Recombinant herpesviruses can be used as oncolytic therapeutic agents and high packaging capacity vectors for delivering expression cassettes into the cell. Herpesvirus saimiri is a gamma-herpesvirus that normally infects squirrel monkeys but also has a unique ability to infect and immortalize human lymphocytes while allowing them to retain their mature phenotype and functional activity. Recombination of the Herpesvirus saimiri genome in permissive cells is impeded by its resistance to chemical transfection and electroporation. The aim of this study was to develop an effective method for incorporating expression cassettes into the genome of Herpesvirus saimiri without having to transfect a permissive cell culture. Transfected HEK-293T cells expressing glycoproteins of the measles virus vaccine strain were co-cultured with permissive OMK cells infected with Herpesvirus saimiri. Cell fusion and formation of syncytia stimulated recombination between the viral genome and the expression cassette; this allowed us to obtain a recombinant Herpesvirus saimiri variant without chemical transfection in permissive cells. The genetically modified virus expressed a selectable marker and retained its ability to persist in the cell in the latent state; it also caused immortalization of primary lymphoid cells. The proposed approach allows engineering recombinant Herpesvirus saimiri strains carrying a variety of expression cassettes in its genome.

Keywords: herpesvirus, viral vector, recombinant strain, chimeric antigen receptor, CAR

ПОЛУЧЕНИЕ РЕКОМБИНАНТНОГО ШТАММА HERPESVIRUS SAIMIRI ПУТЕМ СОВМЕСТНОЙ КУЛЬТИВАЦИИ ТРАНСФИЦИРОВАННОЙ И ПЕРМИССИВНОЙ КЛЕТОЧНЫХ КУЛЬТУР

А. Хамад[1], С. П. Чумаков[2] ✉

[1] Московский физико-технический институт, Москва, Россия

[2] Институт биоорганической химии имени М. М. Шемякина и Ю. А. Овчинникова, Москва, Россия

Рекомбинантные герпесвирусы можно применять в качестве терапевтических агентов-онколитиков, а также в качестве векторов большой емкости для доставки протяженных экспрессионных конструкций в клетки. Гамма-герпесвирус беличьих обезьян Herpesvirus saimiri обладает уникальной способностью инфицировать человеческие лимфоциты и вызывать их иммортализацию при сохранении зрелого фенотипа и функциональной активности. Проведение рекомбинации генома Herpesvirus saimiri в пермиссивной клеточной культуре затруднено из-за ее устойчивости к химической трансфекции и электропорации. Целью работы являлась разработка эффективного способа введения экспрессионных кассет в геном Herpesvirus saimiri без проведения трансфекции пермиссивной клеточной культуры. Для этого мы использовали совместную культивацию трансфицированных клеток HEK-293T, экспрессирующих также гликопротеины вакцинного штамма вируса кори, и инфицированных Herpesvirus saimiri пермиссивных клеток линии OMK. Слияние клеток и образование синцитиев привели к запуску рекомбинации между вирусным геномом и экспрессионной кассетой, что позволило получить рекомбинантный вариант Herpesvirus saimiri без необходимости проведения химической трансфекции пермиссивных клеток. Трансгенный вариант вируса характеризовался стабильной экспрессией селективного маркера и сохранял способность персистировать в клеточной культуре в латентной форме, а также вызывать иммортализацию первичных лимфоидных клеток. Примененный метод позволяет в короткие сроки получать рекомбинантные варианты Herpesvirus saimiri с введенными в геном разнообразными экспрессионными кассетами.

Ключевые слова: герпесвирус, вирусный вектор, рекомбинантный штамм, химерный антигенный рецептор, ХАР

Herpesviridae are a large family of DNA viruses that infect humans and animals. These viruses have a lengthy genome of about 100 to 200 genes that replicate in the nucleus of the infected cell. The assembly of progeny virions and their release from the host cell cause its lysis. Herpesviruses can go into latency. In the latent phase, the full-sized episomal viral DNA is retained in the nucleus and replicates at the same rate as the host cell genome; by attaching to chromatid centromeres, the episomes can be distributed to daughter cells during cell division. Only a small number of specialized genes are expressed in latency, and the infection persists asymptomatically [1]. Members of the gamma-herpesvirus subfamily with tropism for lymphoid cells often have oncogenic potential: the Epstein–Barr virus (EBV) [2] and Kaposi's sarcoma-associated herpesvirus (KSHV) [3] are linked to lymphoproliferative disorders, specifically B-cell neoplasms. EBV is a common cause of spontaneous immortalization of B cells isolated from the blood of healthy donors [4].

The phylogenetic relative of KSHV, a rhadinovirus called Herpesvirus saimiri (HVS), infects New-World squirrel monkeys. This infection is usually asymptomatic and latent. However, it rapidly unfolds in other New-World monkey species, causing acute T-cell leukemias and death. HVS can induce spontaneous immortalization of animal T cells [5]. The same effect was observed when human lymphocytes and natural killer cells were infected with HVS group C strains [6]. In a similar experiment, infected cells acquired the ability for continuous IL2-dependent proliferation without losing their mature T-cell and natural killer cell phenotypes [7]. Three viral genes were reported to retain their expression, including *STP*, *TIP* (transforming genes) [8] and *ORF73* [9], a homologue of the latency-associated nuclear antigen (LANA) of KSHV required for segregating viral episomes to the host's daughter cells during mitosis [10]. In the daughter cells, the viral genome maintained its latent state; the attempts to induce lytic infection or otherwise track down formation of virions in the immortalized lymphoid cells of humans and New World monkeys ended up in failure. The experiments on macaques demonstrated that autologous reinfusion of T cells immortalized by the most aggressive HVS strain (C488) did not trigger neoplasms. The viral DNA persisted in the samples of peripheral mononuclear cells for at least 16 weeks, and the animals acquired immunity to HVS infection [11].

Homologous recombination of the viral genome inside permissive cells, as well as BAC (*bacterial artificial chromosome*)-based recombination, can be successfully used to engineer a herpesvirus vector for transgene expression [12]. For example, the genome of the HVS A11-S4 strain has been cloned into the bacterial chromosome. The HVS genome contains a few homologues of bacterial genes the majority of which can be found in other members of the HVS subfamily. The *vCD59* gene, however, does not occur in other gamma-herpesviruses; the receptor it codes for is responsible for inhibiting complement-mediated cytotoxicity [13]. This gene is expressed in the lytic phase and is not required for generating viral particles *in vitro*. In the studies of HVS-based vectors, the *vCD59* sequence has been successfully replaced by expression cassettes [14].

The accumulated body of data provides for a hypothesis that HVS can be exploited for the development of novel immunotherapy agents [15]. HVS-transformed T cells and NKs retain their effector function and can be directed against tumor antigens when equipped with chimeric antigen receptors. This approach allows generating an infinite number of effector cells from a relatively small volume of the patient's peripheral blood or through allogeneic cell transplantation. The length of the HVS genome and its good packaging capacity as a vector [14] means that cell immortalization and transduction of the expression cassette can be done in a single step. The aim of this study was to elaborate a fast method for engineering a recombinant HVS C488 strain that can carry a variety of transgenes in its genome.

METHODS

Cell culture and production of viral particles

The cell lines used in this study, including HEK-293T (transformed human embryonic kidney cells), OMK (Aotus trivirgatus kidney cells) and A549 (lung carcinoma cells), were provided by American Type Culture Collection (ATCC; USA). The cells were grown in the DMEM-F12 medium (PAA; Austria) supplemented with 10% fetal bovine serum, 2 mM alanyl glutamine (PanEco; Russia), 20 mM HEPES, 100 μg/ml penicillin, and 100 μg/ml streptomycin (PanEco; Russia).

Peripheral blood mononuclear cells (PBMC) were cultured in RPMI-1640 (PAA; Austria) supplemented with 10% fetal bovine serum, 2 mM alanyl glutamine (PanEco; Russia), 20 mM HEPES, 100 μg/ml penicillin, 100 μg/ml streptomycin, and 70 ng/ml IL2 (Peprotech; USA). All cells were cultured in a 5% CO_2 atmosphere at 37 °C.

HVS (strain C-488; ATCC VR-1414) was also provided by ATCC. Subconfluent OMK cells were infected with a small amount of the virus (MOI < 0.1) and grown in the culture medium for 5 to 15 days until complete cell lysis was achieved. Then, the virus-containing fluid was harvested and centrifuged at 5,000 g in the Eppendorf 5920R centrifuge (Eppendorf; Germany) for 15 min to separate cell debris. The supernatant was collected, aliquoted and stored at –20 °C.

Plasmid constructs

Plasmids pCG-4AHcΔ24 and pMD2-FΔ30 expressing surface glycoproteins of the measles virus had been synthesized previously. The design of the pUC-HVS-OFP vector is described below. Briefly, the vCD59-encoding region of the viral genome was chosen as a recombination site. Homology regions were represented by 600 bp-long sequences corresponding to the 3'- and 5'-end of vCD59. DNA isolated from the concentrated HVS stock was amplified by PCR. The promoter of the murine spleen focus-forming virus (SFFV), as well as sequences of a puromycin resistance gene (*pac*) and orange fluorescent protein (OFP), was inserted between the flanking regions of the expression cassette; the T2A signal peptide sequence was inserted between *pac* and OFP sequences to allow their polycistronic expression. The sequence consisting of two 600 bp-long flanking regions homologous to the *vCD59* region of the HVS genome and the expression cassette was cloned into the pUC18 plasmid carrier (Fig. 1) at NotI and BamHI restriction sites. Three components of the cloning fragment were assembled using overlap extension PCR [16]. Primers used for the amplification of HVS regions and the expression cassette are described in Table 1. The sequences of the assembled constructs and recombinant HVS DNA were validated by Sanger sequencing (Eurogen; Russia).

Transfection

In order to determine the most effective transfection technique for OMK cells, 3 techniques were assessed for efficacy, including transfection by 25 kDa cationic linear polyethyleneimine (PEI-25) (Polysciences; USA), cationic Lipofectamine 2000 (Invitrogen; USA) and electroporation. Twenty-four hours before transfection, the cells were plated onto 10 cm-sized culture dishes (SPL; Korea) in the amount of 2×10^6 cells per dish. The cells were transfected with either circular or linearized pUC-HVS-OFP plasmid (the plasmid was linearized with NotI and BamHI restriction enzymes immediately before transfection). PEI-25-assisted transfection was performed using previously described buffers and conditions [17]. Briefly, plasmid DNA was combined with PEI-25 (5 μg/μl) at a 6 : 1 ratio in the lactate buffer (pH 4) and incubated for 15 min. Then, the OptiMEM reduced serum medium (Invitrogen; USA) was added, and the resulting mixture was introduced into the dishes with growing cell cultures. To determine optimal transfection conditions, transfection was performed with 3, 5, 10, 15, and 20 μg of the circular plasmid and with 1, 3, 5, 10, and 15 μg of the linearized plasmid. Lipofectamine 2000-based transfection was carried out following the manufacturer's protocol. We used 7, 10 and 15 μg of circular or linearized plasmid DNA and 17.5, 25 and 37.5 μl of the reagent, respectively. Three hours after
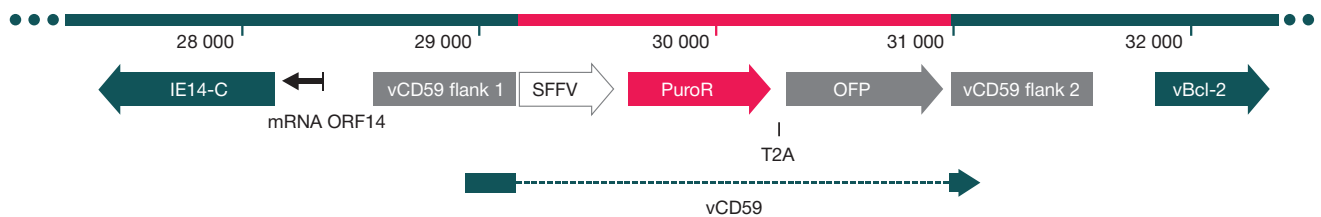
Fig. 1. A schematic representation of the HVS vCD59 region after insertion of the expression cassette. vCD59 flank 1 and vCD59 flank 2 represent recombination homology regions

transfection the medium was replaced with the fresh growth medium used to culture OMK cells. For electroporation, the cells were dissociated from the adherent surfaces using TrypLE (Gibco; USA) and centrifuged in the Eppendorf 5702 centrifuge (Eppendorf; Germany) at 1,100 rpm for 5 min. The cell pellet was resuspended in 500 µl of phosphate buffered saline. Electroporation was carried out in electroporation cuvettes with 0.4 cm interelectrode distance in a GenePulser pulse generator (Bio-Rad; USA) operated at 300 v / 500 uF or 200 v / 250 uF. Prior to electroporation, 5 or 10 µg of circular or linearized plasmid DNA were added to the cells. After electroporation, the cells were immediately plated onto 10 cm-sized culture dishes containing 10 ml of full growth medium. Forty-eight hours after transfection, the proportion of the transfected cells was estimated in a FacsVantage SE flow cytometer (Beckton-Dickinson; USA). Cell viability was assessed using a Cytosmart Cell Counter (Corning; USA) after the cells were dissociated from the adherent surfaces with TrypLE and stained with trypan blue (Paneco; Russia).

Overnight cultures of HEK-293T cells (40 to 60% confluence) were transfected in the presence of PEI-25 in 6-well plates coated with the OptiMEM culture medium. The cells were transfected with the pUC-HVS-OFP construct containing the expression cassette flanked by homologous regions from the HVS genome and with the plasmids expressing surface glycoproteins F (*fusion protein*) and H (*haemagglutinin*) of the measles vaccine strain. The F glycoprotein was expressed by

the pMD2-FΔ30 plasmid, whereas H, by the pCG-4AHcΔ24 plasmid. The pMD2-FΔ30 plasmid encoded the F protein with a shortened (minus 30 amino acid residues) C-terminal cytoplasmic domain. The pCG-4AHcΔ24 plasmid encoded the H protein sequence in which the first 24 amino acids of the N-terminal cytoplasmic domain were substituted with 4 alanine residues. Protein expression was driven by the cytomegalovirus promoter. During transfection, plasmids pUC-HVS-OFP, pMD2-FΔ30 and pCG-4AHcΔ24 were combined in the ratio 8 : 7 : 1. After HEK-293T cells were incubated with the transfection mix for 3 h, they were dissociated from the dishes using trypsin solution (Paneco; Russia) and co-cultured with OMK cells infected with HVS-C488. The ratios are provided in Table 2.

Virus titration and cloning

OMK cells were infected with a serial 5-fold dilution of the viral stock; the procedure was performed in 96-well plates (Greiner; Austria) in 4 replicates. After the cytopathic effect was achieved, the virus was titrated using the Reed–Muench method. Twenty-four hours before the cloning procedure, fresh subconfluent OMK cells were seeded in the 96-well plate. A culture medium containing infected fluorescent OMK cells sorted in a FacsVantage SE flow cytometer (Beckton-Dickinson; USA) was introduced into the wells immediately before HSV-OFP cloning. The concentration of the infected cells per well was 10, 1, 0.1

Table 1. Primers used for the assembly of the expression cassette

Name	Nucleotide sequence
vCD59 F1 dir	AGAGAGGCGGCCGCACAGGCTGCTCTTCAGGAGCACCAG
vCD59 F1 rev	CAATTGATTTGAGATGCGTTTGAAGC
vCD59 F1 bridge	GCAAAATGGCGTTACCTCGAGCAATTGATTTGAGATGCGTTTGAAGC
SFFV dir	CTCGAGGTAACGCCATTTTGC
OFP rev	CCTGCAGGTCAAGCTTCGAA
vCD59 F2 bridge	TTCGAAGCTTGACCTGCAGGTCTGAAACACAGTTAAAGTATCATTGTTG
vCD59 F2 dir	TCTGAAACACAGTTAAAGTATCATTGTTG
vCD59 F2 BamHI rev	TCTCTCGGATCCGCTGGCAGATATTTCTTTTTATAAACAGG
vCD59 F1 diag dir	GCACAGGCTGCTCTTCAGGAGCACCAG
vCD59 F2 diag rev	GCTGGCAGATATTTCTTTTTATAAACAGG

Table 2. The number and ratios of co-cultured cells and the viral titer in the supernatants

№	OMK (thous)	HEK-293T (thous)	Ratio	Virus titer
1	450	1333	0.34	1.60E + 03
2	100	1333	0.08	8.00E + 02
3	23	1333	0.02	0
4	68	200	0.34	2.56E + 04
5	27	200	0.14	1.28E + 04
6	10	200	0.05	0
7	450	133	3.38	2.56E + 04
8	225	266	0.85	2.56E + 04

and 0.01. Five to seven days later, the wells were checked for the presence of single fluorescent foci indicating cytotoxicity.

Detecting recombination

To confirm recombination, the cloned HVS-OFP samples were concentrated using 3kDA Amicon Ultra centrifugal filters (Merck; Germany). The target insertion in the HVS genome was detected by PCR with the vCD59 F1 diag dir and vCD59 F2 diag rev primers. The reaction product of ~3000 bp suggested the presence of the target insertion; the length of ~1200 bp indicated the wild type virus.

Statistical analysis

Statistical analysis was carried out in Prism 6.0 (GraphPad Software; USA).

RESULTS

In order to achieve viral genome recombination and engineer a transgenic HVS-C488 variant, we designed an expression cassette containing 2 selectable markers: the orange fluorescent protein (OFP) gene and the puromycin resistance gene coding for puromycin-N-acetyltransferase (Pac). Transfection of permissive OMK cells was the most effective with PEI-25 and the linearized expression cassette (the PEI to DNA ratio was 6 : 1; 10 µg DNA per 2×10^6 cells; Table 3). However, the proportion of transfected cells did not exceed 50 % of the total cell population (Fig. 2). Using more DNA and more transfection reagent caused a significant reduction in cell viability. Electroporation did not have a negative effect on cell viability, but the proportion of cells successfully transfected by

electroporation was very low. In order to find out if the most effective transfection technique could produce recombinant viral particles capable of inducing expression of selectable markers in the infected cells, we collected clarified virus-containing culture fluid from OMK cells infected with HVS-C488 and transfected by PEI-25 and the linearized fragment of the expression cassette. Culture fluids were used to infect fresh OMK cells. Subsequent observation of OMK culture did not reveal any presence of cells expressing the fluorescent marker.

An alternative technique for delivering modified DNA into permissive cells was developed to increase the odds of recombination between HSV and the expression cassette. We hypothesized that the ability of OMK cells to maintain the lytic cycle of the virus would be retained after fusion with nonpermissive HEK-293T cells transfected with the expression cassette immediately before fusion. For recombination in the mixed cell system, HEK-293T cells were transfected with the linearized expression cassette or the nonlinearized plasmid containing the cassette and the plasmids coding for the surface glycoproteins of the measles vaccine strain (proteins F and H with shortened cytoplasmic domains). The presence of these glycoproteins in the cell membrane induces fusion of contacting cells into syncytia via CD46 binding (Fig. 3E, F). Three hours after transfection, the cells were suspended and seeded into the wells containing OMK cells infected with HVS-C488 (MOI = 4) two days before transfection. Cell ratios and densities are provided in Table 2.

Four days into culture, the supernatant was collected and the virus was titrated. After viral concentrations were compared, sample 5 was chosen for further selection of the monoclonal recombinant virus because it contained the highest viral titer relative to the total number of permissive cells and their ratio to the HEK-293T cells.

Table 3. Conditions for permissive OMK cell line transduction with the expression cassette for HVS recombination and transduction efficacy

Transfection technique	Conditions	Percentage of transfected cells	Reduction in viability
PEI-25	3 µg of circular DNA	0.7% ± 0.15%	–
	5 µg of circular DNA	1.82% ± 0.15%	–
	10 µg of circular DNA	3.73% ± 0.15%	+/–
	15 µg of circular DNA	3.13% ± 0.15%	+
	20 µg of circular DNA	1.77% ± 0.15%	+
	1 µg of linear DNA	< 0.15% ± 0.15%	–
	3 µg of linear DNA	0.85% ± 0.15%	–
	5 µg of linear DNA	1.91% ± 0.15%	–
	10 µg of linear DNA	4.76% ± 0.15%	+/–
	15 µg of linear DNA	3.2% ± 0.15%	+
Lipofectamine 2000	7 µg of circular DNA	3.11% ± 0.15%	–
	10 µg of circular DNA	4.11% ± 0.15%	–
	15 µg of circular DNA	4.09% ± 0.15%	+
	7 µg of linear DNA	3.18% ± 0.15%	–
	10 µg of linear DNA	4.63% ± 0.15%	–
	15 µg of linear DNA	4.54% ± 0.15%	+
Electroporation	5 µg of circular DNA, 200V/250uF	< 0.15% ± 0.15%	–
	10 µg of circular DNA, 200V/250uF	< 0.15% ± 0.15%	–
	5 µg of linear DNA, 200V/250uF	< 0.15% ± 0.15%	–
	10 µg of linear DNA, 200V/250uF	< 0.15% ± 0.15%	–
	5 µg of circular DNA, 300V/500uF	< 0.15% ± 0.15%	–
	10 µg of circular DNA, 300V/500uF	< 0.15% ± 0.15%	–
	5 µg of linear DNA, 300V/500uF	< 0.15% ± 0.15%	–
	10 µg of linear DNA, 300V/500uF	< 0.15% ± 0.15%	–

The medium with the viral particles collected from sample 5 was used to infect OMK cells (MOI = 0.01). Seven days after infection, foci of lytic infection started to form in the confluent culture. Some of the foci contained single plaques constituted primarily by fluorescent cells (Fig. 3B). The population of fluorescent cells was sorted and used to infect permissive cells in a 96-well plate at a concentration of 10, 1, 0.1, and 0.01 infected cells per well. Ten days after infection, 3 (out of 96) single fluorescent plaques appeared in the samples infected at a concentration of 0.1 cells per well; the plaques were most likely formed by individual recombinant viral particles. The virus-containing culture fluid from well 2, where the lytic infection was the most aggressive, was used to produce preparative amounts of the recombinant virus for further analysis.

Sequencing of the vCD59 region of the recombinant HVS-OFP revealed the presence of the target expression cassette. Transduction of peripheral blood mononuclear cells and A549 cells with the HVS-OFP virus (MOI = 5) yielded a fraction of fluorescent cells (Fig. 3C, D); in the A549 culture, their proportion was constant for 5 weeks after infection; for PBMC, this proportion was continuously growing (Fig. 3A). This leads us to conclude that our recombinant herpesvirus HVS-OFP
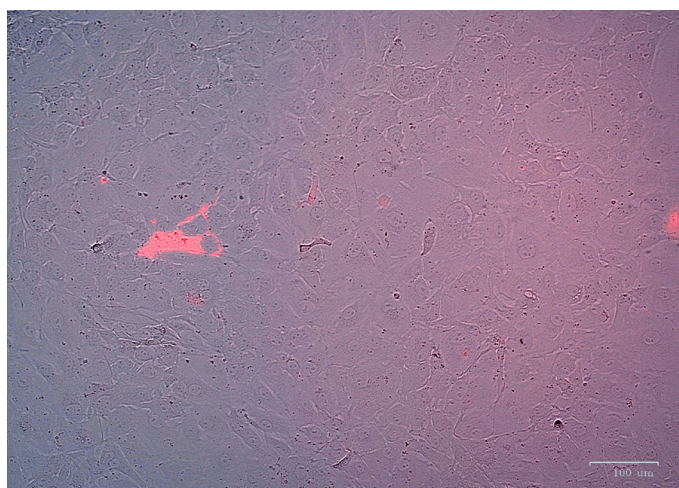
Fig. 2. A population of permissive OMK cells transduced with the expression cassette SFFV-PURO-OFP
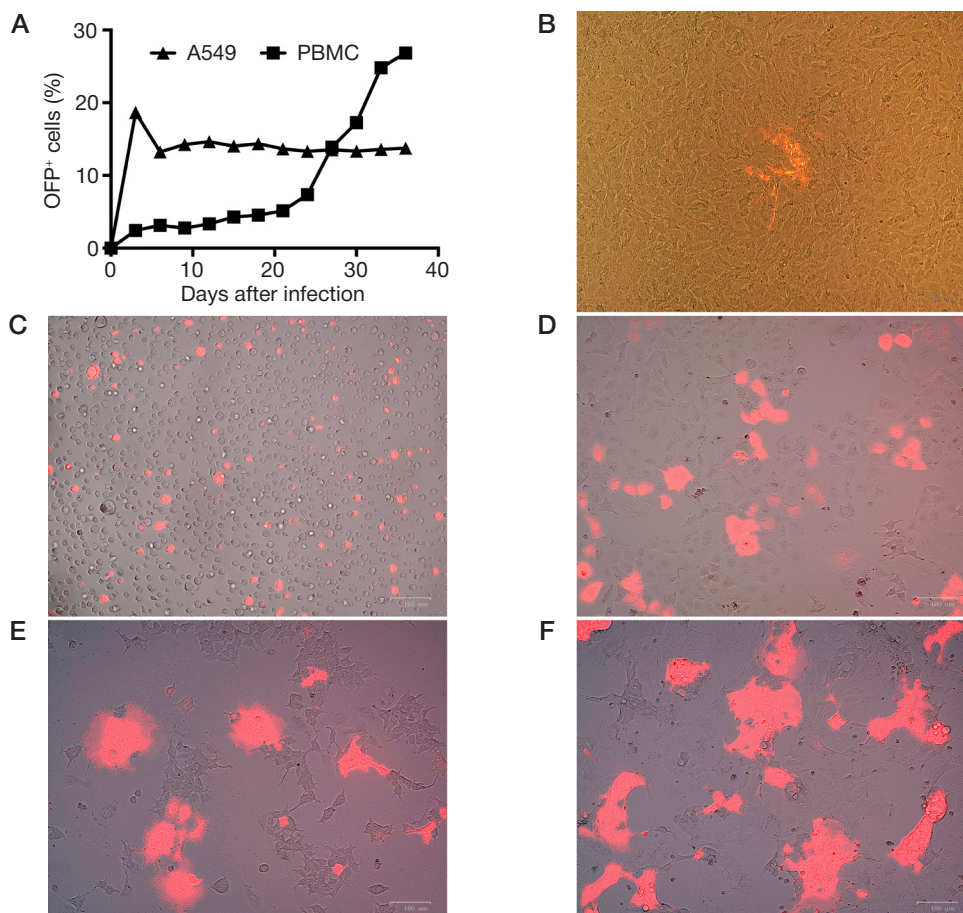
Fig. 3. A. Dynamics of fluorescent populations after HVS-OFP infection. **B**. A fluorescent plaque formed after OMK cells were infected with the recombinant HVS-OFP. **C**, **D**. PBMC (**C**) and A549 cells (**D**) transduced with HVS-OFP. **E**, **F**. Co-culturing of HEK-293T cells transfected with the recombination cassette and the expressers of the measles virus strain glycoproteins with OMK cells infected with HVS at low (**E**) and high (**F**) confluence

did not lose its ability for latency and immortalization of healthy lymphoid cells. The cassette retained its expression both in the lytic and latent cycles of herpesvirus infection.

DISCUSSION

We have developed and tested a new approach to the recombination-based genetic engineering of herpesviruses. We tested a few different techniques for increasing the odds of recombination and found that it was necessary to use an expression cassette with two selectable markers. Before the tests, we had hypothesized that puromycin-based artificial selection or sorting of fluorescent OMK cells immediately after transfection would allow us to eliminate nontransfected cells from the population. However, the period between the delivery of the expression cassette and the onset of the cytopathic effect/the release of the virus into the environment was too short for puromycin-based selection, while the stress accompanying fluorescence-based sorting of transduced cells inhibited production of virions. The use of two selectable markers made it more convenient to sort and monitor the proportion of cells successfully transduced with recombinant HVS. Speaking of the HVS-C488 strain, our approach helps to overcome the major obstacle associated with transfection of permissive cells with a transgenic cassette: its low efficacy [18]. Transfection is a key step in all HVS recombination methods described so far [15, 19]. The efficacy of recombination depends on the length of a recombined fragment, meaning that insertion of larger cassettes expressing several genes will either result in more recombination steps or necessitate the use of larger cell populations for transfection and artificial selection. Our approach is not as effective as BAC-based recombination that has proved its efficacy in the experiments on the HVS genome [20, 21]. Although recombination in eukaryotes is more laborious than BAC-based recombination, it might still be preferred when a single transgene expressor is introduced or when a viral genome is being prepared for cloning into a BAC and a selectable cassette should be inserted for easier recombineering. This application is particularly interesting because the genome of the C488 strain, which is highly effective in transforming human T cells and natural killers [22], has not been cloned into a BAC yet.

Our method has the potential to be applied to the engineering of chimeric viral particles devoid of genes involved in establishing lytic infection and suitable for producing immortalized lymphoid cells for immunotherapy. Notably, the high cloning capacity of the herpesvirus vector [23] allows using it for simultaneous delivery of almost all components of CAR-T cell therapy: mono- and bispecific chimeric antigen receptors or even their full-sized pairs that target a specific cancer cell phenotype; immune checkpoint inhibitors that reduce sensitivity to immunosuppressive signals; inducible expression cassettes for secretion of cytokines that stimulate tumor microenvironment and defense mechanisms that induce suicide of modified lymphocytes and rapidly eliminate them from the patient's organism in case of adverse events or after successful treatment. Given the ability to immortalize peripheral T cells and natural killers, such vector can be used to produce unlimited quantities of agents for allogeneic cell-mediated immunotherapy *ex vivo*.

CONCLUSIONS

Co-culturing of HEK-293T cells transfected with an expression cassette and the plasmids encoding surface glycoproteins Fd30 and Hd24 of the measles virus in the ratio 8 : 1 : 7 and permissive OMK cells (MOI = 4) infected with a wild type HVS-C488 in the ratio 27 : 200 48 hours before the experiment produced recombinant viral particles (~3%) and allowed us to obtain a viral preparation with the integrated expression cassette in only 3 passages. The obtained recombinant herpesvirus HVS-OFP retained its ability to cause lytic infection in permissive OMK cells only and went into latency in A549 cells. The virus immortalized human peripheral blood mononuclear cells, where it persisted in the latent state. The expression cassette was functional during both lytic and latent cycles of the herpesvirus.

References

1. Davison AJ. Overview of classification. In: Arvin A, Campadelli-Fiume G, Mocarski E, Moore PS, Roizman B, Whitley R, et al., editors. Human Herpesviruses: Biology, Therapy and Immunoprophylaxis. Cambridge, 2007.
2. Javier RT, Butel JS. The history of tumor virology. Cancer Res. 2008; 68 (19): 7693–706. DOI: 10.1158/0008-5472.CAN-08-3301. PubMed PMID: 18829521.
3. Chang Y, Cesarman E, Pessin MS, Lee F, Culpepper J, Knowles DM, et al. Identification of herpesvirus-like DNA sequences in AIDS-associated Kaposi's sarcoma. Science. 1994; 266 (5192): 1865–9. DOI: 10.1126/science.7997879. PubMed PMID: 7997879.
4. Fu Z, Cannon MJ. Functional analysis of the CD4(+) T-cell response to Epstein-Barr virus: T-cell-mediated activation of resting B cells and induction of viral BZLF1 expression. J Virol. 2000; 74 (14): 6675–9. DOI: 10.1128/jvi.74.14.6675-6679.2000. PubMed PMID: 10864684.
5. Fickenscher H, Fleckenstein B. Herpesvirus saimiri. Philos Trans R Soc Lond B Biol Sci. 2001; 356 (1408): 545–67. DOI: 10.1098/rstb.2000.0780. PubMed PMID: 11313011.
6. Biesinger B, Muller-Fleckenstein I, Simmer B, Lang G, Wittmann S, Platzer E, et al. Stable growth transformation of human T lymphocytes by herpesvirus saimiri. Proc Natl Acad Sci USA. 1992; 89 (7): 3116–9. DOI: 10.1073/pnas.89.7.3116. PubMed PMID: 1313581.
7. Vogel B, Tennert K, Full F, Ensser A. Efficient generation of human natural killer cell lines by viral transformation. Leukemia. 2014; 28 (1): 192–5. DOI: 10.1038/leu.2013.188. PubMed PMID: 23787393.
8. Duboise SM, Guo J, Czajak S, Desrosiers RC, Jung JU. STP and Tip are essential for herpesvirus saimiri oncogenicity. J Virol. 1998; 72 (2): 1308–13. PubMed PMID: 9445031.
9. Griffiths R, Whitehouse A. Herpesvirus saimiri episomal persistence is maintained via interaction between open reading frame 73 and the cellular chromosome-associated protein MeCP2. J Virol. 2007; 81 (8): 4021–32. DOI: 10.1128/JVI.02171-06. PubMed PMID: 17267510.
10. Verma SC, Robertson ES. ORF73 of herpesvirus Saimiri strain C488 tethers the viral genome to metaphase chromosomes and binds to cis-acting DNA sequences in the terminal repeats. J Virol. 2003; 77 (23): 12494–506. DOI: 10.1128/jvi.77.23.12494-12506.2003. PubMed PMID: 14610173.
11. Knappe A, Feldmann G, Dittmer U, Meinl E, Nisslein T, Wittmann S, et al. Herpesvirus saimiri-transformed macaque T cells are tolerated and do not cause lymphoma after autologous reinfusion. Blood. 2000; 95 (10): 3256–61. PubMed PMID: 10807797.
12. Menotti L, Avitabile E, Gatta V, Malatesta P, Petrovic B, Campadelli-Fiume G. HSV as A Platform for the Generation of Retargeted, Armed, and Reporter-Expressing Oncolytic Viruses. Viruses. 2018; 10 (7). DOI: 10.3390/v10070352. PubMed

PMID: 29966356.

13. Albrecht JC, Nicholas J, Biller D, Cameron KR, Biesinger B, Newman C, et al. Primary structure of the herpesvirus saimiri genome. J Virol. 1992; 66 (8): 5047–58. PubMed PMID: 1321287.

14. White RE, Calderwood MA, Whitehouse A. Generation and precise modification of a herpesvirus saimiri bacterial artificial chromosome demonstrates that the terminal repeats are required for both virus production and episomal persistence. J Gen Virol. 2003; 84 (Pt 12): 3393–403. DOI: 10.1099/vir.0.19387-0. PubMed PMID: 14645920.

15. Hiller C, Wittmann S, Slavin S, Fickenscher H. Functional long-term thymidine kinase suicide gene expression in human T cells using a herpesvirus saimiri vector. Gene Ther. 2000; 7 (8): 664–74. DOI: 10.1038/sj.gt.3301158. PubMed PMID: 10800089.

16. Horton RM, Hunt HD, Ho SN, Pullen JK, Pease LR. Engineering hybrid genes without the use of restriction enzymes: gene splicing by overlap extension. Gene. 1989; 77 (1): 61–8. DOI: 10.1016/0378-1119(89)90359-4. PubMed PMID: 2744488.

17. Fukumoto Y, Obata Y, Ishibashi K, Tamura N, Kikuchi I, Aoyama K, et al. Cost-effective gene transfection by DNA compaction at pH 4.0 using acidified, long shelf-life polyethylenimine. Cytotechnology. 2010; 62 (1): 73–82. DOI: 10.1007/s10616-010-9259-z. PubMed PMID: 20309632.

18. Turrell SJ, Whitehouse A. Mutation of herpesvirus Saimiri ORF51 glycoprotein specifically targets infectivity to hepatocellular carcinoma cell lines. J Biomed Biotechnol. 2011; 2011: 785158. DOI: 10.1155/2011/785158. PubMed PMID: 21197456.

19. Duboise SM, Guo J, Desrosiers RC, Jung JU. Use of virion DNA as a cloning vector for the construction of mutant and recombinant herpesviruses. Proc Natl Acad Sci USA. 1996; 93 (21): 11389–94. DOI: 10.1073/pnas.93.21.11389. PubMed PMID: 8876145.

20. White RE, Calderwood MA, Whitehouse A. Generation and precise modification of a herpesvirus saimiri bacterial artificial chromosome demonstrates that the terminal repeats are required for both virus production and episomal persistence. J Gen Virol. 2003; 84 (Pt 12): 3393–403. DOI: 10.1099/vir.0.19387-0. PubMed PMID: 14645920.

21. Collins CM, Medveczky MM, Lund T, Medveczky PG. The terminal repeats and latency-associated nuclear antigen of herpesvirus saimiri are essential for episomal persistence of the viral genome. J Gen Virol. 2002; 83 (Pt 9): 2269–78. DOI: 10.1099/0022-1317-83-9-2269. PubMed PMID: 12185282.

22. Ensser A, Thurau M, Wittmann S, Fickenscher H. The genome of herpesvirus saimiri C488 which is capable of transforming human T cells. Virology. 2003; 314 (2): 471–87. DOI: 10.1016/s0042-6822(03)00449-5. PubMed PMID: 14554077.

23. Macnab S, White R, Hiscox J, Whitehouse A. Production of an infectious Herpesvirus saimiri-based episomally maintained amplicon system. J Biotechnol. 2008; 134 (3–4): 287–96. DOI: 10.1016/j.jbiotec.2008.01.012. PubMed PMID: 18328588.

Литература

1. Davison AJ. Overview of classification. In: Arvin A, Campadelli-Fiume G, Mocarski E, Moore PS, Roizman B, Whitley R, et al., editors. Human Herpesviruses: Biology, Therapy and Immunoprophylaxis. Cambridge, 2007.

2. Javier RT, Butel JS. The history of tumor virology. Cancer Res. 2008; 68 (19): 7693–706. DOI: 10.1158/0008-5472.CAN-08-3301. PubMed PMID: 18829521.

3. Chang Y, Cesarman E, Pessin MS, Lee F, Culpepper J, Knowles DM, et al. Identification of herpesvirus-like DNA sequences in AIDS-associated Kaposi's sarcoma. Science. 1994; 266 (5192): 1865–9. DOI: 10.1126/science.7997879. PubMed PMID: 7997879.

4. Fu Z, Cannon MJ. Functional analysis of the CD4(+) T-cell response to Epstein-Barr virus: T-cell-mediated activation of resting B cells and induction of viral BZLF1 expression. J Virol. 2000; 74 (14): 6675–9. DOI: 10.1128/jvi.74.14.6675-6679.2000. PubMed PMID: 10864684.

5. Fickenscher H, Fleckenstein B. Herpesvirus saimiri. Philos Trans R Soc Lond B Biol Sci. 2001; 356 (1408): 545–67. DOI: 10.1098/rstb.2000.0780. PubMed PMID: 11313011.

6. Biesinger B, Muller-Fleckenstein I, Simmer B, Lang G, Wittmann S, Platzer E, et al. Stable growth transformation of human T lymphocytes by herpesvirus saimiri. Proc Natl Acad Sci USA. 1992; 89 (7): 3116–9. DOI: 10.1073/pnas.89.7.3116. PubMed PMID: 1313581.

7. Vogel B, Tennert K, Full F, Ensser A. Efficient generation of human natural killer cell lines by viral transformation. Leukemia. 2014; 28 (1): 192–5. DOI: 10.1038/leu.2013.188. PubMed PMID: 23787393.

8. Duboise SM, Guo J, Czajak S, Desrosiers RC, Jung JU. STP and Tip are essential for herpesvirus saimiri oncogenicity. J Virol. 1998; 72 (2): 1308–13. PubMed PMID: 9445031.

9. Griffiths R, Whitehouse A. Herpesvirus saimiri episomal persistence is maintained via interaction between open reading frame 73 and the cellular chromosome-associated protein MeCP2. J Virol. 2007; 81 (8): 4021–32. DOI: 10.1128/JVI.02171-06. PubMed PMID: 17267510.

10. Verma SC, Robertson ES. ORF73 of herpesvirus Saimiri strain C488 tethers the viral genome to metaphase chromosomes and binds to cis-acting DNA sequences in the terminal repeats. J Virol. 2003; 77 (23): 12494–506. DOI: 10.1128/jvi.77.23.12494-12506.2003. PubMed PMID: 14610173.

11. Knappe A, Feldmann G, Dittmer U, Meinl E, Nisslein T, Wittmann S, et al. Herpesvirus saimiri-transformed macaque T cells are tolerated and do not cause lymphoma after autologous reinfusion. Blood. 2000; 95 (10): 3256–61. PubMed PMID: 10807797.

12. Menotti L, Avitabile E, Gatta V, Malatesta P, Petrovic B, Campadelli-Fiume G. HSV as A Platform for the Generation of Retargeted, Armed, and Reporter-Expressing Oncolytic Viruses. Viruses. 2018; 10 (7). DOI: 10.3390/v10070352. PubMed PMID: 29966356.

13. Albrecht JC, Nicholas J, Biller D, Cameron KR, Biesinger B, Newman C, et al. Primary structure of the herpesvirus saimiri genome. J Virol. 1992; 66 (8): 5047–58. PubMed PMID: 1321287.

14. White RE, Calderwood MA, Whitehouse A. Generation and precise modification of a herpesvirus saimiri bacterial artificial chromosome demonstrates that the terminal repeats are required for both virus production and episomal persistence. J Gen Virol. 2003; 84 (Pt 12): 3393–403. DOI: 10.1099/vir.0.19387-0. PubMed PMID: 14645920.

15. Hiller C, Wittmann S, Slavin S, Fickenscher H. Functional long-term thymidine kinase suicide gene expression in human T cells using a herpesvirus saimiri vector. Gene Ther. 2000; 7 (8): 664–74. DOI: 10.1038/sj.gt.3301158. PubMed PMID: 10800089.

16. Horton RM, Hunt HD, Ho SN, Pullen JK, Pease LR. Engineering hybrid genes without the use of restriction enzymes: gene splicing by overlap extension. Gene. 1989; 77 (1): 61–8. DOI: 10.1016/0378-1119(89)90359-4. PubMed PMID: 2744488.

17. Fukumoto Y, Obata Y, Ishibashi K, Tamura N, Kikuchi I, Aoyama K, et al. Cost-effective gene transfection by DNA compaction at pH 4.0 using acidified, long shelf-life polyethylenimine. Cytotechnology. 2010; 62 (1): 73–82. DOI: 10.1007/s10616-010-9259-z. PubMed PMID: 20309632.

18. Turrell SJ, Whitehouse A. Mutation of herpesvirus Saimiri ORF51 glycoprotein specifically targets infectivity to hepatocellular carcinoma cell lines. J Biomed Biotechnol. 2011; 2011: 785158. DOI: 10.1155/2011/785158. PubMed PMID: 21197456.

19. Duboise SM, Guo J, Desrosiers RC, Jung JU. Use of virion DNA as a cloning vector for the construction of mutant and recombinant herpesviruses. Proc Natl Acad Sci USA. 1996; 93 (21): 11389–94. DOI: 10.1073/pnas.93.21.11389. PubMed PMID: 8876145.

20. White RE, Calderwood MA, Whitehouse A. Generation and precise modification of a herpesvirus saimiri bacterial artificial chromosome demonstrates that the terminal repeats are required for both virus production and episomal persistence. J Gen Virol. 2003; 84 (Pt 12): 3393–403. DOI: 10.1099/vir.0.19387-0. PubMed PMID: 14645920.

21. Collins CM, Medveczky MM, Lund T, Medveczky PG. The terminal

repeats and latency-associated nuclear antigen of herpesvirus saimiri are essential for episomal persistence of the viral genome. J Gen Virol. 2002; 83 (Pt 9): 2269–78. DOI: 10.1099/0022-1317-83-9-2269. PubMed PMID: 12185282.

22. Ensser A, Thurau M, Wittmann S, Fickenscher H. The genome of herpesvirus saimiri C488 which is capable of transforming human

T cells. Virology. 2003; 314 (2): 471–87. DOI: 10.1016/s0042-6822(03)00449-5. PubMed PMID: 14554077.

23. Macnab S, White R, Hiscox J, Whitehouse A. Production of an infectious Herpesvirus saimiri-based episomally maintained amplicon system. J Biotechnol. 2008; 134 (3–4): 287–96. DOI: 10.1016/j.jbiotec.2008.01.012. PubMed PMID: 18328588.

A MUTANT OF THE PHOTOTOXIC PROTEIN KILLERRED THAT DOES NOT FORM DSRED-LIKE CHROMOPHORE

Gorbachev DA, Sarkisyan KS ✉

Shemyakin-Ovchinnikov Institute of Bioorganic Chemistry, Moscow, Russia

Genetically encodable photosensitizers based on fluorescent proteins produce reactive oxygen species when illuminated with light. Although widely used as optogenetic tools, existing photosensitizers with green fluorescence possess suboptimal properties motivating for a search of new protein variants with efficient chromophore maturation and high phototoxicity. Here we report a mutant of the phototoxic fluorescent protein KillerRed protein with fluorescence in the green part of the spectrum. The mutant variant carries mutations I64L, D114G, and T115S and does not form a DsRed-like chromophore. The protein can be used as a template to create new genetically encodable photosensitizers that are spectrally different from KillerRed.

✉ **Correspondence should be addressed:** Karen S. Sarkisyan
Miklukho-Maklaya, 16/10, of. 34/632, Moscow, 117997; karen.s.sarkisyan@gmail.com

МУТАНТ ФОТОТОКСИЧНОГО БЕЛКА KILLERRED, НЕ ФОРМИРУЮЩИЙ DSRED-ПОДОБНОГО ХРОМОФОРА

Д. А. Горбачев, К. С. Саркисян ✉

Институт биоорганической химии имени М. М. Шемякина и Ю. А. Овчинникова, Москва, Россия

Генетически кодируемые фотосенсибилизаторы на основе флуоресцентных белков способны производить активные формы кислорода при облучении светом, и потому их широко используют в качестве оптогенетических инструментов. Разработанные на сегодняшний день фотосенсибилизаторы с зеленой флуоресценцией обладают неоптимальными свойствами. Целью настоящей работы был поиск новых вариантов флуоресцентных белков с эффективным созреванием хромофора и высокой фототоксичностью. С помощью случайного мутагенеза фототоксичного флуоресцентного белка KillerRed и направленной эволюции в *E. coli* получен белок с хромофором на основе тирозина, флуоресцирующий в зеленой области спектра. Новый белок, несущий мутации I64L, D114G и T115S, не формирует DsRed-подобного хромофора и может быть использован как базовый генотип для разработки новых спектрально отличных от KillerRed генетически кодируемых фотосенсибилизаторов.

✉ **Для корреспонденции:** Карен Сергеевич Саркисян
ул. Миклухо-Маклая, 16/10, оф. 34/632, г. Москва, 117997; karen.s.sarkisyan@gmail.com

Fluorescent proteins are widely used as genetically encodable tags for optical labeling of living systems [1]. Their chromophores are located inside the protein structure and are protected from the surrounding solvent; therefore, most of the existing fluorescent proteins are passive reporter molecules: irradiation with light does not significantly affect cells expressing these markers.

At the same time, a unique family of genetically encoded photosensitizers has been developed based on the fluorescent protein anm2CP. Upon light illumination, members of the family produce reactive oxygen species that can damage the cell [2]. Structural studies of these proteins have identified a water-filled channel that connects the chromophore to the solvent. This structural feature of phototoxic fluorescent proteins is thought to be responsible for the efficient diffusion of reactive oxygen species into the environment [3, 4].

KillerRed was the first protein engineered to produce reactive oxygen species demonstrating phototoxicity levels exceeding other fluorescent proteins more than thousand-fold [2]. Depending on the cellular localization and the excitation light dose, reactive oxygen species generated by KillerRed can lead to various physiological consequences — from inactivation of fusion proteins [2], to cell division arrest [5, 6] or cellular death through necrosis or apoptosis [2, 7]. Due to these capabilities, KillerRed is used as an optogenetic tool in cell biology to inactivate proteins with light, to study intracellular oxidative stress or to ablate specific cell populations. KillerRed

has also been used as a photosensitizer for treatment of tumors in model systems [7–9].

Other genetically encoded photosensitizers have been created based on KillerRed, including SuperNova, a monomeric KillerRed variant with similar spectral characteristics [10], as well as orange fluorescent protein KillerOrange [11] and green fluorescent protein SuperNova Green [12]. Besides that, non-fluorescent protein-based photosensitizers miniSOG, Pp2FbFP and others that generate singlet oxygen have been developed [13, 14].

None of the existing photosensitizers with green fluorescence can be universally used in relevant applications. Some proteins demonstrate incomplete or slow chromophore maturation rate; others may not generate the type of reactive oxygen species suitable for a particular application, or their phototoxicity may depend on the availability of external chromophore [15]. In this work, we aimed to find a mutant version of KillerRed that did not form a DsRed-like "red" chromophore and, therefore, could serve as a basis for the development of the new generation of efficient photosensitizers with green fluorescence.

METHODS

DNA amplification and analysis of amplification products

DNA amplification was performed using the Encyclo PCR Kit (Evrogen; Russia) on a PTC-200 Thermal Cycler (MJ Research; USA). The analysis of amplification products was carried out in 1–2% agarose gel. Ethidium bromide was used at a concentration of 0.5 µg/ml.

Generation of the mutant library for directed evolution

Mutagenesis was performed by error-prone PCR. We added manganese ions and a skewed ratio of nucleotide triphosphates (50x mix: 0.2 мМ dGTP, 0.2 мМ dATP, 1 мМ dCTP, 1 мМ dTTP) into the PCR reaction mixture leading errors in Taq-polymerase-based DNA amplification. The average mutation rate was 8 nucleotide substitutions per 1000 amplified nucleotides after 25 cycles of PCR.

For electroporation, the ligation mixture was purified on Cleanup Mini DNA purification columns (Evrogen; Russia). 40 µl of electrocompetent cells were thawed on ice, and up to 5 µl of purified ligation mixture was added to thawed cells. Cells were then transferred into a pre-cooled electroporation cuvette (Bio-Rad; USA) and electroporated on the MicroPulser device (Bio-Rad; USA). Immediately after electroporation, 3 ml of SOB medium was added to the cuvette, and the bacterial suspension was transferred into 1.5 ml plastic tubes. The tubes were incubated for one hour in an incubator at 37 °C and then plated on LB agar. The plates were incubated at 37 °C for 18 hours. The average density of *E. coli* colonies was 5,000 per plate and the total diversity of genotypes in the library was estimated to be around 100,000 clones. The number of fluorescent colonies was 22%.

Expression and purification of recombinant proteins

E. coli XL1 Blue was grown in 800 ml flasks in LB medium with ampicillin (100 mg/ml), induced with isopropyl-β-D-1-thiogalactopyranoside to the final concentration 0.5 mM and incubated for 3 hours. All further operations were performed on ice. The culture was centrifuged, the supernatant was discarded, the pellet was resuspended in 4 ml of phosphate buffer (pH 7.4), the suspension was lysed in Sonics Vibra Cell sonicator (Sonics & Materials; USA) and centrifuged again. The supernatant was transferred into a new tube with 400 µl of Talon metal-affinity resin (Clontech; USA), equilibrated with phosphate buffer. The tube was placed in a shaker for one hour at 200 rpm at room temperature. Then, the resin with the protein was washed several times with phosphate buffer and eluted with phosphate buffer containing imidazole (250 mM).

RESULTS

We relied on random mutagenesis to find KillerRed mutant with green fluorescence. The mutant library was cloned into pQE-30 vector, transformed into *E. coli* cells and grown on agar plates without induction. We visually screened bacterial colonies exposed by 400 nm and 480 nm light to identify mutants with significant green fluorescence and identified the KillerRed I64L/D114G/T115S mutant (see Table, the numbering of positions in the protein is indicated according to the established notation so that the chromophore-forming residues are in positions 65–67 [1]). This mutant had very dim fluorescence in the red part of the spectrum while being noticeably fluorescent in green under when illuminated with 480 nm light. Observed spectral properties indicated that the protein formed the "classical" GFP-like chromophore instead of the DsRed-like chromophore found in the parental KillerRed.

Since proteins with GFP-like chromophores and DsRed-like chromophores have specific absorption spectra that are easily distinguishable from each other, we isolated and purified KillerRed protein and it's mutant KillerRed I64L/D114G/T115S (Fig. 1). The absorption spectrum of purified KillerRed I64L D114G T115S was significantly different from the absorption spectrum of KillerRed and had a pick with the maximum at 514 nm and a blue-shifted shoulder characteristic of GFP-like chromophores.

DISCUSSION

The lack of absorbance at 550–600 nm in KillerRed I64L/D114G/T115S indicated that introduced mutations almost entirely prevented formation of DsRed-like chromophore. The peak with a maximum at 514 nm and a characteristic shoulder at 480–485 nm suggested that chromophore catalysis stopped at a "classical" GFP-like chromophore [1].

Mutations found in the KillerRed variant we identified are interesting in the context of existing literature on fluorescent proteins mutagenesis. In particular, mutations at position 64

Table. Amino acid sequences of proteins described in this study. Chromophore-forming residues are highlighted in purple, positions containing mutations are highlighted in orange

Amino acid sequence of KillerRed I64L D114G T115S (identified in this study)	MRGSHHHHHHGSEGGPALFQSDMTFKIFIDGEVNGQKFTIVADGSSKFPHGDFNVHAVCETGK LPMSWKPICHLLQYGEPFFARYPDGISHFAQECFPEGLSIDRTVRFENDGTMTSHHTYELDGSC VVSRITVNCDGFQPDGPIMRDQLVDILPNETHMFPHGPNAVRQLAFIGFTTADGGLMMGHFDS KMTFNGSRAIEIPGPHFVTIITKQMRDTSDKRDHVCQREVAYAHSVPRITSAIGSDED
Amino acid sequence of KillerRed	MRGSHHHHHHGSEGGPALFQSDMTFKIFIDGEVNGQKFTIVADGSSKFPHGDFNVHAVCETGK LPMSWKPICHLIQYGEPFFARYPDGISHFAQECFPEGLSIDRTVRFENDGTMTSHHTYELDDTCV VSRITVNCDGFQPDGPIMRDQLVDILPNETHMFPHGPNAVRQLAFIGFTTADGGLMMGHFDSK MTFNGSRAIEIPGPHFVTIITKQMRDTSDKRDHVCQREVAYAHSVPRITSAIGSDED
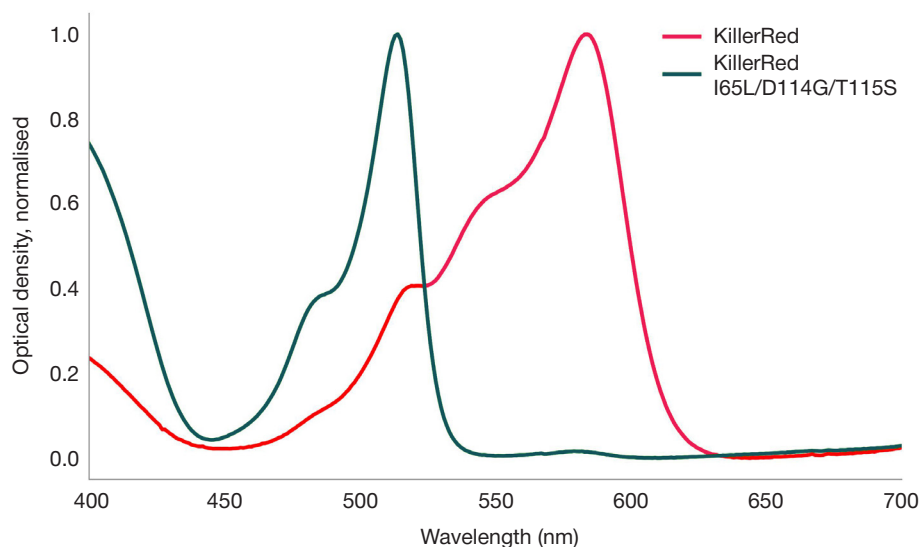
Fig. 1. Absorption spectra of purified proteins KillerRed and KillerRed I64L/D114G/T115S
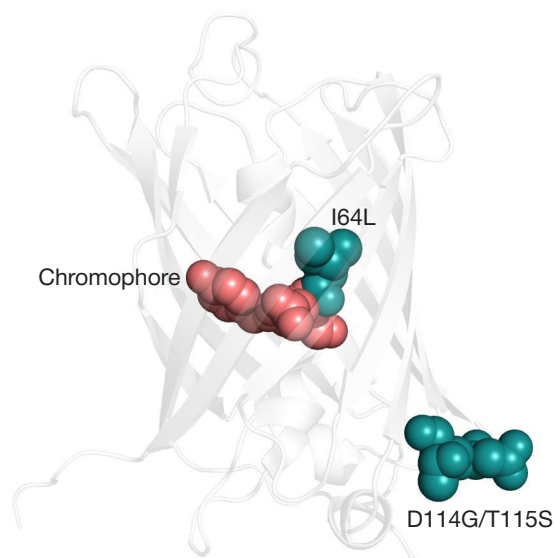
Fig. 2. Location of the chromophore and mutations I64L, D114G and T115S in the structure of KillerRed.

were previously described as affecting chromophore maturation: for instance, in *Aequorea victoria* GFP, the F64L mutation improves maturation of the chromophore when expressed at 37 °C [1], while in the chromoprotein from *Acropora millepora* the S64C mutation changes the color of the protein [16]. Mutations D114G and T115S are located in the neighboring positions on the loop connecting the beta-strands 5 and 6 (Fig. 2) and may contribute to the adaptation of the beta-barrel to the replacement of isoleucine with leucine at position 64.

CONCLUSION

The KillerRed variant described in this work is a promising template for further directed evolution to create a new generation of genetically encodable photosensitizers with green fluorescence. Unlike other KillerRed spectral variants developed to date, the KillerRed I64L/D114G/T115S mutant forms a tyrosine-based chromophore and exhibits fluorescence in the green region of the spectrum.

References

1. Chudakov DM, Matz MV, Lukyanov S, Lukyanov KA. Fluorescent proteins and their applications in imaging living cells and tissues. Physiol Rev. 2010; (9)0: 1103–63. DOI:10.1152/physrev.00038.2009/=.
2. Bulina ME, Chudakov DM, Britanova OV, Yanushevich YG, Staroverov DB, Chepurnykh TV, et al. A genetically encoded photosensitizer. Nat Biotechnol. 2006; (24): 95–9. DOI:10.1038/nbt1175.
3. Pletneva NV, Pletnev VZ, Sarkisyan KS, Gorbachev DA, Egorov ES, Mishin AS, et al. Crystal Structure of Phototoxic Orange Fluorescent Proteins with a Tryptophan-Based Chromophore. PLoS One. 2015; (10): e0145740. DOI:10.1371/journal.pone.0145740.
4. Pletnev S, Gurskaya NG, Pletneva NV, Lukyanov KA, Chudakov DM, Martynov VI, et al. Structural basis for phototoxicity of the genetically encoded photosensitizer KillerRed. J Biol Chem. 2009; (284): 32028–39. DOI:10.1074/jbc.M109.054973.
5. Serebrovskaya EO, Gorodnicheva TV, Ermakova GV, Solovieva EA, Sharonov GV, Zagaynova EV, et al. Light-induced blockage of cell division with a chromatin-targeted phototoxic fluorescent protein. Biochem J. 2011; (435): 65–71. DOI:10.1042/BJ20101217.

6. Lan L, Nakajima S, Wei L, Sun L, Hsieh C-L, Sobol RW, et al. Novel method for site-specific induction of oxidative DNA damage reveals differences in recruitment of repair proteins to heterochromatin and euchromatin. Nucleic Acids Res. 2014; (42): 2330–45. DOI:10.1093/nar/gkt1233.

7. Shirmanova MV, Serebrovskaya EO, Lukyanov KA, Snopova LB, Sirotkina MA, Prodanetz NN, et al. Phototoxic effects of fluorescent protein KillerRed on tumor cells in mice. J Biophotonics. 2013; (6): 283–90. DOI:10.1002/jbio.201200056.

8. Kuznetsova DS, Shirmanova MV, Dudenkova VV, Subochev PV, Turchin IV, Zagaynova EV, et al. Photobleaching and phototoxicity of KillerRed in tumor spheroids induced by continuous wave and pulsed laser illumination. J Biophotonics. 2015; 9999. DOI:10.1002/jbio.201400130.

9. Yan L, Kanada M, Zhang J, Okazaki S, Terakawa S. Photodynamic Treatment of Tumor with Bacteria Expressing KillerRed. PLoS One. 2015; (10): e0131518. DOI:10.1371/journal.pone.0131518.

10. Takemoto K, Matsuda T, Sakai N, Fu D, Noda M, Uchiyama S, et al. SuperNova, a monomeric photosensitizing fluorescent protein for chromophore-assisted light inactivation. Sci Rep. 2013; (3): 2629. DOI:10.1038/srep02629.

11. Sarkisyan KS, Zlobovskaya OA, Gorbachev DA, Bozhanova NG, Sharonov GV, Staroverov DB, et al. KillerOrange, a Genetically Encoded Photosensitizer Activated by Blue and Green Light. PLoS One. 2015; (10): e0145287. DOI:10.1371/journal.pone.0145287.

12. Riani YD, Matsuda T, Takemoto K, Nagai T. Green monomeric photosensitizing fluorescent protein for photo-inducible protein inactivation and cell ablation. BMC Biol. 2018; (16): 50. DOI:10.1186/s12915-018-0514-7.

13. Shu X, Lev-Ram V, Deerinck TJ, Qi Y, Ramko EB, Davidson MW, et al. A genetically encoded tag for correlated light and electron microscopy of intact cells, tissues, and organisms. PLoS Biol. 2011; (9): e1001041. DOI:10.1371/journal.pbio.1001041.

14. Torra J, Burgos-Caminal A, Endres S, Wingen M, Drepper T, Gensch T, et al. Singlet oxygen photosensitisation by the fluorescent protein Pp2FbFP L30M, a novel derivative of Pseudomonas putida flavin-binding Pp2FbFP. Photochem Photobiol Sci. 2015; (14): 280–7. DOI:10.1039/c4pp00338a.

15. Acharya A, Bogdanov AM, Grigorenko BL, Bravaya KB, Nemukhin AV, Lukyanov KA, et al. Photoinduced Chemistry in Fluorescent Proteins: Curse or Blessing? Chem Rev. 2017; (117): 758–95. DOI:10.1021/acs.chemrev.6b00238.

16. Alieva NO, Konzen KA, Field SF, Meleshkevitch EA, Hunt ME, Beltran-Ramirez V, et al. Diversity and evolution of coral fluorescent proteins. PLoS One. 2008; (3): e2680. DOI:10.1371/journal.pone.0002680.

Литература

1. Chudakov DM, Matz MV, Lukyanov S, Lukyanov KA. Fluorescent proteins and their applications in imaging living cells and tissues. Physiol Rev. 2010; (9)0: 1103–63. DOI:10.1152/physrev.00038.2009/=.

2. Bulina ME, Chudakov DM, Britanova OV, Yanushevich YG, Staroverov DB, Chepurnykh TV, et al. A genetically encoded photosensitizer. Nat Biotechnol. 2006; (24): 95–9. DOI:10.1038/nbt1175.

3. Pletneva NV, Pletnev VZ, Sarkisyan KS, Gorbachev DA, Egorov ES, Mishin AS, et al. Crystal Structure of Phototoxic Orange Fluorescent Proteins with a Tryptophan-Based Chromophore. PLoS One. 2015; (10): e0145740. DOI:10.1371/journal.pone.0145740.

4. Pletnev S, Gurskaya NG, Pletneva NV, Lukyanov KA, Chudakov DM, Martynov VI, et al. Structural basis for phototoxicity of the genetically encoded photosensitizer KillerRed. J Biol Chem. 2009; (284): 32028–39. DOI:10.1074/jbc.M109.054973.

5. Serebrovskaya EO, Gorodnicheva TV, Ermakova GV, Solovieva EA, Sharonov GV, Zagaynova EV, et al. Light-induced blockage of cell division with a chromatin-targeted phototoxic fluorescent protein. Biochem J. 2011; (435): 65–71. DOI:10.1042/BJ20101217.

6. Lan L, Nakajima S, Wei L, Sun L, Hsieh C-L, Sobol RW, et al. Novel method for site-specific induction of oxidative DNA damage reveals differences in recruitment of repair proteins to heterochromatin and euchromatin. Nucleic Acids Res. 2014; (42): 2330–45. DOI:10.1093/nar/gkt1233.

7. Shirmanova MV, Serebrovskaya EO, Lukyanov KA, Snopova LB, Sirotkina MA, Prodanetz NN, et al. Phototoxic effects of fluorescent protein KillerRed on tumor cells in mice. J Biophotonics. 2013; (6): 283–90. DOI:10.1002/jbio.201200056.

8. Kuznetsova DS, Shirmanova MV, Dudenkova VV, Subochev PV, Turchin IV, Zagaynova EV, et al. Photobleaching and phototoxicity of KillerRed in tumor spheroids induced by continuous wave and pulsed laser illumination. J Biophotonics. 2015; 9999. DOI:10.1002/jbio.201400130.

9. Yan L, Kanada M, Zhang J, Okazaki S, Terakawa S. Photodynamic Treatment of Tumor with Bacteria Expressing KillerRed. PLoS One. 2015; (10): e0131518. DOI:10.1371/journal.pone.0131518.

10. Takemoto K, Matsuda T, Sakai N, Fu D, Noda M, Uchiyama S, et al. SuperNova, a monomeric photosensitizing fluorescent protein for chromophore-assisted light inactivation. Sci Rep. 2013; (3): 2629. DOI:10.1038/srep02629.

11. Sarkisyan KS, Zlobovskaya OA, Gorbachev DA, Bozhanova NG, Sharonov GV, Staroverov DB, et al. KillerOrange, a Genetically Encoded Photosensitizer Activated by Blue and Green Light. PLoS One. 2015; (10): e0145287. DOI:10.1371/journal.pone.0145287.

12. Riani YD, Matsuda T, Takemoto K, Nagai T. Green monomeric photosensitizing fluorescent protein for photo-inducible protein inactivation and cell ablation. BMC Biol. 2018; (16): 50. DOI:10.1186/s12915-018-0514-7.

13. Shu X, Lev-Ram V, Deerinck TJ, Qi Y, Ramko EB, Davidson MW, et al. A genetically encoded tag for correlated light and electron microscopy of intact cells, tissues, and organisms. PLoS Biol. 2011; (9): e1001041. DOI:10.1371/journal.pbio.1001041.

14. Torra J, Burgos-Caminal A, Endres S, Wingen M, Drepper T, Gensch T, et al. Singlet oxygen photosensitisation by the fluorescent protein Pp2FbFP L30M, a novel derivative of Pseudomonas putida flavin-binding Pp2FbFP. Photochem Photobiol Sci. 2015; (14): 280–7. DOI:10.1039/c4pp00338a.

15. Acharya A, Bogdanov AM, Grigorenko BL, Bravaya KB, Nemukhin AV, Lukyanov KA, et al. Photoinduced Chemistry in Fluorescent Proteins: Curse or Blessing? Chem Rev. 2017; (117): 758–95. DOI:10.1021/acs.chemrev.6b00238.

16. Alieva NO, Konzen KA, Field SF, Meleshkevitch EA, Hunt ME, Beltran-Ramirez V, et al. Diversity and evolution of coral fluorescent proteins. PLoS One. 2008; (3): e2680. DOI:10.1371/journal.pone.0002680.

ASSOCIATIONS BETWEEN SNPS IN THE GENES ENCODING UROKINASE SYSTEM PROTEINS AND THE RISK OF PLACENTAL INSUFFICIENCY

Revina DB[1] ✉, Balatskiy AV[1,2], Larina EB[3], Oleynikova NA[1], Mishurovsky GA[1], Malkov PG[1], Samokhodskaya LM[1], Panina OB[1], Tkachuk VA[1,2]

[1] Lomonosov Moscow State University, Moscow, Russia
[2] National Medical Research Center of Cardiology, Moscow, Russia
[3] Lapino Clinical Hospital "Mother and Child", Moscow, Russia

Placental insufficiency (PI) and its complications are multifactorial conditions that cause perinatal morbidity and mortality. Since the urokinase system is involved in placentation, it should have a role in PI pathogenesis. The aim of this work was to study the associations between single nucleotide polymorphisms (SNPs) of genes coding for protein components of the urokinase system and PI, as well as investigate their effect on the expression of these proteins in the placenta and placental structure. We examined 114 women with uncomplicated pregnancy and delivery, 48 female patients with pre-eclampsia and/or intrauterine growth restriction (IUGR), and 95 newborns, (pre-eclampsia and/or IUGR: $n = 60$; uncomplicated pregnancy and delivery: $n = 35$). Maternal and fetal DNAs were genotyped using real-time PCR. Placenta fragments were subjected to morphometry and immunohistochemistry. We discovered the associations between PI and the maternal C allele of rs4065 (PI group: CC-CT 64.1%, TT 35.9%; controls: CC-CT 25.6%, TT 74.49%; OR (95%CI): 6.83 (2.63–17.79)), the maternal A allele of rs2302524 (GG-GA 20.5%, AA 79.5% vs. GG-GA 48.1%, AA 51.9%, OR (95%CI): 0.27 (0.1–0.71)), the fetal C allele of rs4065 (CC-CT 76.4 %, TT 23.6% vs. CC-CT 69.6%, TT 30.4%, OR (95%CI): 1.37 (0.45–4.17)), and the fetal C allele of rs344781 (TT-TC 69.1%, CC 30.9% vs. TT-TC 95.7%, CC 4.3%, OR (95% CI): 5.02 (1.07–23.6)). The multivariate analysis confirmed the significance of the fetal rs4065 genotype. In patients with PI, uPA expression was lower (ME (95%CI): 116.45 (100.5; 128.74) vs. 126.09 (113.76; 139.19); $p < 0.05$. No associations were established between SNPs and protein expression. The degree of vascularization depended on the maternal rs4065 genotype (the stroma-to-vessel ratio for the CC genotype was 0.17 (0.15; 0.19); for the CT genotype, 0.18 (0.15; 0.21) and for the TT genotype, 0.23 (0.2; 0.27); $p < 0.05$). We conclude that high placental uPA and the presence of the fetal TT rs4065 genotype are protective against the risk of PI.

Keywords: pre-eclampsia, intrauterine growth restriction, placental insufficiency, urokinase-type plasminogen activator, urokinase-type plasminogen activator receptor, single nucleotide polymorphism, angiogenesis

АССОЦИАЦИЯ SNP ГЕНОВ БЕЛКОВ УРОКИНАЗНОЙ СИСТЕМЫ С РАЗВИТИЕМ ПЛАЦЕНТАРНОЙ НЕДОСТАТОЧНОСТИ

Д. Б. Ревина[1] ✉, А. В. Балацкий[1,2], Е. Б. Ларина[3], Н. А. Олейникова[1], Г. А. Мишуровский[1], П. Г. Мальков[1], Л. М. Самоходская[1], О. Б. Панина[1], В. А. Ткачук[1,2]

[1] Московский государственный университет имени М. В. Ломоносова, Москва, Россия
[2] Национальный медицинский исследоваельский центр кардиологии, Москва, Россия
[3] Клинический госпиталь Лапино «Мать и дитя», Москва, Россия

Плацентарная недостаточность (ПН) и ее осложнения — многофакторные заболевания, ведущие к перинатальной заболеваемости и смертности. Урокиназная система задействована в формировании плаценты и может быть рассмотрена как участник патогенеза ПН. Целью работы было исследовать ассоциацию однонуклеотидных полиморфизмов (SNP) генов белков урокиназной системы с развитием ПН, их влияние на экспрессию соответствующих белков в плаценте и ее строение. Обследованы 114 женщин с физиологическим течением беременности и родов и 48 пациенток с преэклампсией и/или задержкой роста плода (ЗРП), 95 новорожденных детей (беременность с преэклампсией и/или ЗРП — 60, физиологическое течение беременности и родов — 35). Проведено генотипирование при помощи ПЦР в реальном времени, морфометрическое и иммуногистохимическое исследования фрагментов плацент. Выявлены ассоциации между развитием ПН и наличием у матери — аллеля С rs4065 (в группе ПН — СС-СТ 64,1%, ТТ 35,9%, в контрольной группе — СС-СТ 25,6%, ТТ 74,49%, ОШ (95% ДИ) — 6,83 (2,63–17,79)), аллеля А rs2302524 (GG-GA 20,5%, АА 79,5% против GG-GA 48,1%, АА 51,9%, ОШ (95% ДИ) — 0,27 (0,1–0,71)), у плода — аллеля С rs4065 (СС-СТ 76,4 %, ТТ 23,6% против СС-СТ 69,6%, ТТ 30,4%, ОШ (95% ДИ) — 1,37 (0,45–4,17)), аллеля С rs344781 (ТТ-ТС 69,1%, СС 30,9% против ТТ-ТС 95,7%, СС 4,3%, ОШ (95% ДИ) — 5,02 (1,07–23,6)). Многофакторный анализ подтвердил значимость генотипа плода по rs4065. Экспрессия uPA была ниже при ПН (медиана (95% ДИ) — 116,45 (100,5; 128,74) против 126,09 (113,76; 139,19); $p < 0,05$). Ассоциации SNP с экспрессией белков выявлено не было. Васкуляризация зависела от генотипа матери по rs4065 (стромально-сосудистое соотношение при генотипе СС — 0,17 (0,15; 0,19), СТ — 0,18 (0,15; 0,21), ТТ — 0,23 (0,2; 0,27); $p < 0,05$). Таким образом, высокий уровень uPA в плаценте и наличие генотипа rs4065 ТТ у плода носят протективный характер в отношении развития ПН.

Ключевые слова: преэклампсия, задержка роста плода, плацентарная недостаточность, активатор плазминогена урокиназного типа, рецептор активатора плазминогена урокиназного типа, однонуклеотидный полиморфизм, ангиогенез

Placental insufficiency (PI) and the ensuing pregnancy complications, including intrauterine growth restriction (IUGR) and pre-eclampsia, are clinical manifestations of impaired placental perfusion. The mechanisms implicated in PI involve abnormal placental angiogenesis and villous maldevelopment caused by: 1) insufficient trophoblast invasion; 2) incomplete remodeling of spiral arteries; 3) imbalance between pro- and antiangiogenic factors; 4) maternal coagulation defects [1]. Therefore, research into PI etiology should be focused on the potential role of multifunctional regulatory systems, including the urokinase system, as contributors to the defects described above. The urokinase system consists of the urokinase-type plasminogen activator (uPA), its main substrate (plasminogen), plasminogen activator inhibitors (PAI-1, PAI-2), and the uPA receptor (uPAR); the latter regulates and improves the efficacy of urokinase-mediated proteolysis by binding to uPA [2]. The urokinase system can trigger a variety of signaling cascades and thereby transform the cellular environment through proteolysis of the extracellular matrix, as well as induce cell migration and proliferation in response to such transformations [3].

Almost all components of the urokinase system have genetic polymorphisms that affect uPA activity or the level of its expression. Today, there is sufficient evidence confirming the role of some of those genetic variants in promoting pregnancy complications. So far, associations between such polymorphisms and PI have been best studied for PAI-1. For example, the indel mutation in the *SERPINE1* promoter (–675 5G/4G) has been reliably linked to early pregnancy loss/pre-eclampsia [4, 5].

Polymorphisms of the urokinase and urokinase receptor genes are less studied. In this article, we investigate possible associations between PI and 4 SNPs: 2 of the *PLAU* gene (rs4065, rs2227564) and another 2 of the *PLAUR* gene (rs344781, rs2302524). PLAU rs4065 C/T 3′-UTR is a C/T substitution in the noncoding gene region resulting in enhanced mRNA stability and hence aberrant uPA levels [6]. *PLAU* Pro141Leu (rs2227564) results in the increased hydrophobicity of the kringle domain, which reduces uPA affinity to fibrin and possibly the components of the extracellular matrix [7]. Although the role of the urokinase kringle domain is not fully clear, this polymorphism can alter urokinase activity. *PLAUR* rs2302524 (A659G) is another missense mutation that presumably affects the activity of the urokinase system [8]. *PLAUR* rs344781 affects the activity of the *PLAUR* promoter; the T allele enhances transcription [9]. Considering the significance of assessing both maternal and fetal components of the mother-placenta-fetus system, we analyzed the genotypes of the mother and the fetus. Genotyping data were compared to the results of a histopathological examination of placental specimens so as to determine the effect of gene polymorphisms on placental tissue morphology and the expression of urokinase system proteins. The aim of this work was to study the associations between PI and SNPs in the genes coding for the components of the uPA–uPAR-system, as well as their effects on the intensity of protein expression in placental tissue and placental morphology.

METHODS

The study was conducted at the Medical Research and Educational Center of Lomonosov Moscow State University in 2018. Samples of venous blood, placental tissue and umbilical cords, as well as clinical data, were obtained from the Center's Biobank. Originally, the samples had been collected from 162 female patients aged 20 to 49 years and 95 newborns immediately after delivery.

The control group consisted of 114 healthy women with uncomplicated pregnancy and delivery. The PI group included 48 patients with early pre-eclampsia (< 34 weeks into gestation) and/or early grade II-III IUGR (< 32 gestational weeks). IUGR was diagnosed based on a biometric lag of 2 weeks; the actual gestational age was inferred from the first day of the last menstrual period and from the findings of the early ultrasound scan. Pre-eclampsia was defined as elevated systolic BP ≥ 140 mmHg and diastolic BP ≥ 90 mmHg on at least two occasions after week 20 into gestation in the presence of at least one of the following signs: proteinuria ≥ 300 mg/day, renal failure (hypercreatininemia ≥ 90 μmol/L), liver dysfunction (ALT or AST > 40 IU/L), impaired blood flow in the mother-placenta-fetus system on the Doppler scan, thrombocytopenia < 150,000/μL, and neurological symptoms. The exclusion criteria were as follows: multifetal pregnancy, Rh-sensitization, gestational diabetes mellitus, severe extragenital pathology, drug abuse, smoking, fetal abnormalities or genetic disorders. All pregnancies were spontaneous. In order to exclude "small for gestational age" fetuses from the study, a Doppler scan of the umbilical artery was performed. Women with normal blood flow parameters were excluded.

Umbilical cord samples were collected from 60 newborns in the PI group (pregnancies complicated by pre-eclampsia and/ or IUGR) and 35 newborns in the control group (uncomplicated pregnancies and delivery). For the analysis, we selected umbilical cord fragments located 8–10 cm away from the placenta. The samples were fixed in 10% formalin or frozen at –80 °C. In 53 cases (25 patients with PI and 28 controls), we collected samples of maternal blood, umbilical cord fragments and placental tissue. For each mother-newborn pair, 3 fragments of seemingly healthy tissue sized 1 × 0.5 × 0.5 cm were collected from the peripheral, paracentral and central areas of the placenta; the fragments were fixed in 10% buffered formalin for 12 h; then the samples were dehydrated and embedded in paraffin. All placenta donors in the PI group gave birth by Caesarian section at >28 weeks gestation (2 patients before gestational week 34; 6 patients after week 34); in the control group, the babies were delivered at term.

Genotyping

DNA was isolated from K_2 EDTA-containing peripheral maternal blood using a QIAmp DNA Blood Mini Kit and from umbilical cord fragments using a DNeasy Blood and Tissue Kit (QIAGEN; Germany) following the manufacturer's protocol. (the minimum sample weight of 25 mg and prolonged overnight lysis).

PLAU C/T 3′-UTR (rs4065) and *PLAUR* T(-516)C (rs344781) polymorphisms were detected by real-time PCR. Amplification was performed in a RotorGene Q thermocycler (QIAGEN; Germany). Allele-specific hydrolyzed probes were used. The following primers and probes were used:
rs4065_F: 5'-TGGTTGTCATTTTTGCAGTAGAGTC-3';
rs4065_R: 5'-GGCCTATGCCTGAGGGTAAAG-3';
rs4065_prC:FAM-5'-AAGCTATTGTCGTTCGCCCTGGTGG-3'-BHQ1;
rs4065_prT: HEX-5'-AAGCTATTGTCGTTCACCCTGGTGGG-3'-BHQ1;
rs344781_F: 5'-ATCCTGAAATATGCATCTCTTAAACACT-3';
rs344781_R: 5'-TTAACATTTACCAAGGACCTACTTCG-3';
rs344781_prC:FAM-5'-CACAGCGGGAAGCAAAGCAAGGGT-3'-BHQ1;
rs344781_prT: HEX-5'-CACAGCAGGAAGCAAAGCAAGGGT-3'-BHQ1).

PLAU C/T 7240 (rs2227564), *PLAUR* A659G (rs2302524) and SERPINE1 -675 5G/4G polymorphisms were detected by real-time PCR using commercial kits for SNP detection (DNA-Technology; Russia).

Morphometry and immunohistochemistry

Four-µm thick sections were prepared from paraffin blocks and mounted on Polysine Slides (Menzel GmbH & Co KG; Germany). Dewaxing, rehydrating and epitope retrieval were performed using Dewax and HIER BufferM (pH 8.0) (Thermo; UK) at 95–98 °C for 20 min in the pre-treatment PT-Module (Thermo; UK). Immunohistochemistry reactions were carried out in a Thermo Scientific LabVision Autostainer 480S (Thermo; UK). The sections were incubated with 1 : 150 monoclonal rabbit anti-uPA antibodies (ab133563) and 1 : 100 polyclonal rabbit anti-uPAR antibodies (ab103791) (Abcam; UK) for 30 min. A chromogenic (DAB) Ultra Vision Quanto Detection System (Thermo; UK) was used to detect staining. Then, the sections were treated with hematoxylin (1–3 min) and covered with a cover-glass. The slides were examined under a Leica DM 1000 microscope equipped with an HI PLAN 40×/0.65 ∞/0.17/0FN25 lens and a digital high-resolution camera Leica DMC 2900; the images were processed in Leica Application Suite 8.0 (Leica; Germany). A total of 1,060 microphotographs were taken: 530 for uPAR-treated and 530 for uPA-treated slides.

Image processing

On each image, an area of 7 × 7 pixels was selected in the background outside the specimen; this area was assigned an average color value of all the pixels it contained. This average value was used to white-balance the image, so that the corrected color would be white. As a result, the background on all images appeared very close to white and all microphotographs did not differ in color tones. After color normalization, large clusters of red blood cells and artifacts were manually selected and removed on each photograph. All images were resized to 1024 × 768 pixels.

Measured parameters

Using ImageJ, v1.51s (National Institutes of Health; USA), we calculated the villi surface area (mm^2) and the area occupied by the intervillous space (mm^2) for each image. To estimate the vessel surface area (% of the villi surface area), the stroma-to-vessel ratio and the intensity of uPA/uPAR expression in the villi, blood vessels were highlighted manually. The stroma-to-vessel ratio was determined by the formula: vessel surface area / (villi surface area — vessel surface area). All parameters were calculated as a geometric mean from 10 processed images per section.

Measurement of marker expression intensity

To estimate the intensity of uPA and uPAR expression, the ImageJ color threshold function was applied to the areas representing villi on the images. The following parameters were used: hue [0;37], saturation [46;255] and brightness [62;251], as they allow detecting a vast variety of brown tones. The selected areas were converted into black and white to evaluate pixel color intensity. Purely black pixels were assigned the value of 255, whereas purely white pixels, 0. All pixels outside the villi or those outside the specified color range were assigned a 0 value. The mean color value was calculated for each image

based on non-white pixels (color≠0). Expression intensity was calculated by the formula: ,

$$INT = \frac{\Sigma_{c=0}^{255} c \times N_c}{V_i \times 1024 \times 768} \ ,$$

where INT is intensity; c is the mean color value for non-white pixels; N is the number of pixels with the specific c; V is the area of the image occupied by the villi expressed in the range from 0 to 1. The yielded values can be interpreted as uPA/uPAR expression intensity in the range from 0 (no expression) to 255 (maximum expression) providing that staining of the villi is uniform.

Statistical analysis

Statistical analysis was conducted in RStudio v1.1.453 and the SNP Stats web tool [10] developed for the analysis of genetic polymorphism data. The Akaike information criterion was used to choose the type of inheritance model (codominant, dominant, recessive, overdominant, or log-additive). We selected models with the lowest AIC indicating better goodness of fit in the presence of fewer parameters. Continuous variables were tested for normality using the Shapiro-Wilk test. Differences between the groups were assessed using Student's *t*-test, one-way ANOVA for parametric data, the Wilcoxon rank-sum test, or the Tukey test for nonparametric data depending on the number of groups, the Kruskal–Wallis test. Categorical variables were assessed using the χ^2 test. Odds ratios for the risk of PI were also calculated. Univariate binary logistic regression models were used to construct 95% CI and estimate OR pointwise. Statistical weight and significance of individual genotypes were analyzed using logistic regression. Differences were considered significant at $p < 0.05$.

RESULTS

Table 1 shows frequencies of maternal and fetal SNPs significantly associated with the risk of PI (corrected to maternal age). Associations have been established between PI and the following alleles: the maternal C allele *PLAU* rs4065, the maternal A allele *PLAUR* rs2302524, the fetal C allele *PLAU* rs4065, and the fetal C allele *PLAUR* rs344781. To study the effects of both maternal and fetal genotypes, we built a model in which PI was the dependent variable and maternal and fetal genotypes were predictors (the presence of 2 mutant alleles scored 2 points, heterozygous variants scored 1 point, and the presence of 2 referent alleles scored 0). Then, we estimated the statistical significance of the predictors, their weight and effect (positive or negative). Characteristics of the model are provided in Table 2; a statistically significant effect was demonstrated for the fetal *PLAU* rs4065 polymorphism: the C to T substitution was protective against PI, i.e. reduced its probability; TT was the most prognostically favorable genotype.

In the control group samples, villous tree architecture was normal, dominated by terminal villi with sinusoidally dilated capillaries and showing an intimate contact between the trophoblastic surface and the vascular wall underneath. In the PI group, a variety of histopathologic phenomena were observed. In some cases, nonbranching angiogenesis prevailed presenting as the lack of terminal villi, small villous diameter and the absence of syncytial knotting. In 16 cases, an excessive compensatory placental response was observed, including angiomatosis of the villi, extensive syncytial knotting in the aggregated terminal villi and the narrowing of the intervillous space. These findings were fortified by the estimates of

the villi surface area and the intervillous space (Table 3). No differences were found between the PI and control groups in the vessel surface area and the stroma-to-vessel ratio (Table 3), which may be explained by the morphological heterogeneity observed in patients with preeclampsia and IUGR, as well as by the difference in gestational age at delivery.

The data yielded by genotyping of maternal and fetal specimens were compared to the results of the microscopic examination of the placenta (morphometric parameters and the immunohistochemical expression of uPA and uPAR). The intensity of uPA/uPAR expression in syncytiotrophoblasts exceeded that in the stromal cells and the endothelium of villous vessels (Fig. 1 A–D). The intensity of uPA expression was reliably lower in the placental tissue of patients with PI ($p = 0.033$) (Table 3; Fig. 1A–B); no difference in uPAR expression was observed between the groups (Table 3; Fig. 1C–D).

Table 1. Genotype frequencies for urokinase system SNPs associated with the risk of PI

	Inheritance model	Genotype	PI, % (*n*)	Control % (*n*)	OR (CI 95%)*	*p*	AIC
			maternal SNP				
PLAU rs4065	Codominant	C/C	23.1 (9)	3.8 (3)	12.90 (2.68–51.68)	0.0001	120.9
		C/T	41 (16)	21.8 (17)	5.46 (1.94–15.37)		
		T/T	35.9 (14)	74.4 (58)	1		
	Dominant	C/T–C/C	64.1 (25)	25.6 (20)	6.83 (2.63–17.79)	<0.0001	120.1
		T/T	35.9 (14)	74.4 (58)	1		
	Recessive	C/C	23.1 (9)	3.8 (3)	6.97 (1.58–30.68)	0.006	130
		T/T–C/T	76.9 (30)	96.2 (75)	1		
	Overdominant	C/C–T/T	59 (23)	78.2 (61)	1	0.01	131
		C/T	41 (16)	21.8 (17)	3.46 (1.33–9.03)		
	Additive	–	–	–	4.14 (2.02–8.51)	<0.0001	119.5
PLAUR rs2302524	Codominant	A/A	79.5 (31)	51.9 (42)	1	0.02	133.7
		A/G	15.4 (6)	38.3 (31)	0.27 (0.09–0.77)		
		G/G	5.1 (2)	9.9 (8)	0.30 (0.05–0.68)		
	Dominant	A/A	79.5 (31)	51.9 (42)	1	0.005	131.8
		A/G–G/G	20.5 (8)	48.1 (39)	0.27 (0.1–0.71)		
	Recessive	A/A–A/G	94.9 (37)	90.1 (73)	1	0.31	138.5
		G/G	5.1 (2)	9.9 (8)	0.43 (0.08–2.41)		
	Overdominant	A/A–G/G	84.6 (33)	61.7 (50)	1	0.018	134
		A/G	15.4 (6)	38.3 (31)	0.31 (0.11–0.87)		
	Additive	–	–	–	0.39 (0.18–0.85)	0.01	132.9
			fetal SNP				
PLAU rs4065	Codominant	C/C	30.9 (17)	4.3 (1)	8.25 (0.88–77.21)	0.031	92.8
		C/T	45.5 (25)	65.2 (15)	0.91 (0.29–2.87)		
		T/T	23.6 (13)	30.4 (7)	1		
	Dominant	C/T–C/C	76.4 (42)	69.6 (16)	1.37 (0.45–4.17)	0.58	97.4
		T/T	23.6 (13)	30.4 (7)	1		
	Recessive	C/C	30.9 (17)	4.3 (1)	8.82 (1.09–71.67)	0.009	90.8
		T/T–C/T	69.1 (38)	95.7 (22)	1		
	Overdominant	C/T	45.5 (25)	65.2 (15)	0.47 (0.17–1.31)	0.14	95.5
		C/C–T/T	54.5 (30)	34.8 (8)	1		
	Additive	–	–	–	1.99 (0.92–4.29)	0.073	94.5
PLAUR rs344781	Codominant	T/T	23.6 (13)	30.4 (7)	1	0.014	117.9
		T/C	45.5 (25)	65.2 (15)	0.28 (0.11–0.71)		
		C/C	30.9 (17)	4.3 (1)	2.71 (0.53–13.76)		
	Dominant	T/T	23.6 (13)	30.4 (7)	1	0.098	131.4
		T/C –C/C	76.4 (42)	69.6 (16)	0.49 (0.21–1.16)		
	Recessive	T/T– T/C	69.1 (38)	95.7 (22)	1	0.018	128.5
		C/C	30.9 (17)	4.3 (1)	5.02 (1.07–23.6)		
	Overdominant	C/C–T/T	54.5 (30)	34.8 (8)	1	7e–4	122.7
		T/C	45.5 (25)	65.2 (15)	0.22 (0.09–0.54)		
	Additive	–	–	–	1.00 (0.57–1.77)	0.99	134.1

Note: * — OR (95% CI) adjusted for maternal age.

No associations were established between the studied SNPs in *PLAU* and *PLAUR* and the intensity of protein expression in placental tissue.

The protective effect of the C to T substitution in maternal *PLAU* rs4065 was confirmed by its relationship with the degree of villous vascularization: the vessel surface area (% of the villi surface area) and the stroma-to-vessel ratio varied depending on the genotype (Fig. 2). The maximum vasculature corresponded to the TT genotype (Table 4).

DISCUSSION

The uRA–uPAR system is multifunctional. It exerts fibrinolytic activity, participates in degrading the extracellular matrix, affects the bioavailability of growth factors, and regulates cell migration and proliferation. Once the embryo has been implanted, trophoblast cells start to express urokinase [11], and uPAR expression increases at the cell pole involved in trophoblast invasion; throughout the process, uPA activity is regulated by PAI-1,2. Thus, the urokinase system takes an active part in the modulated trophoblast invasion. Natural killers and macrophages are another source of uPA in the placenta. They ensure remodeling of spiral arteries in the endometrium at trophoblast-independent stages; by interacting with NK and macrophages, uPAR-positive smooth muscle cells and endothelial cells acquire their migration phenotype [12, 13]. The urokinase system (specifically, the cells expressing its protein components) "supervises" formation and degradation of fibrin-type fibrinoid [14]. Proteolysis of the extracellular matrix by serine proteases leads to the release of angiogenic factors from its scaffold, including vascular endothelial growth factor (VEGF). The interaction between VEGF and its class 2 receptor results in the exposure of the proteolytic uPA–uPAR complex to integrins [15], confirming the role of the urokinase system as a mediator of angiogenic factors and an active participant of angiogenesis in the placenta.

In this study, we attempted to assess the risk of placenta-associated pregnancy complications based on the presence of SNPs in maternal and fetal genes. We were able to demonstrate that the TT genotype of *PLAU* rs4065 was associated with the lowest risk for PI. Considering that in the majority of cases the placental and the fetal genotypes are the same, the fetal T allele should be regarded as more significant. Unfortunately, we could not prove that abnormal uPA levels in the placenta are determined by the SNPs in the corresponding gene, which might be explained by the small sample size. However, the association between the TT genotype and the greater vessel surface area in the villi confirms the observed phenomenon.

Previously uPAR expression in chorionic villi was demonstrated to be higher in females with uncomplicated pregnancies than in those at risk of pregnancy loss [16]. The immunohistochemistry analysis conducted as part of our study revealed that uPAR levels in the placenta did not differ between healthy females and patients with placenta-related pregnancy complications. However, the groups did differ in terms of urokinase expression intensity.

There was no previous solid evidence of the direct effect of rs4065 on the level of uPA expression. Our findings suggest that the TT genotype stimulates cell migration and proliferation, is proangiogenic and reduces the risk of PI. Our observation is confirmed by the fact that this polymorphism increases the risk of tumor growth and enhances tumor angiogenesis. There

Table 2. Parameters of the regression model showing the relationship between the risk of PI and SNPs in the genes encoding urokinase system proteins

	Coefficients of factors	Standard error	*z*-score	*p*
Free coefficient	−0.6347	1.4248	−0.445	0.656
Fetal SNP				
PLAU rs2227564	4.0476	2.4788	1.778	0.075
SERPINE-1 rs1799889	0.1157	1.2417	0.093	0.926
PLAU rs4065	−3.3538	1.3791	−2.432	0.015
PLAUR rs344781	2.7448	1.5893	1.727	0.084
PLAUR rs2302524	0.3755	1.4117	0.266	0.79
Maternal SNP				
PLAU rs2227564	−1.9485	1.3233	−1.472	0.141
SERPINE-1 rs1799889	−2.276	1.387	−1.641	0.101
PLAU rs4065	1.8566	0.985	1.885	0.059
PLAUR rs344781	−0.7773	1.3769	−0.564	0.572
PLAUR rs2302524	2.0156	1.3489	1.494	0.135

Table 3. Morphological characteristics and immunohistochemical expression of uPA/uPAR in placental tissue

	Median (95% CI)		*p*
	PI	Control	
Villi surface area (mm^2)	7.445 (6.852; 7.863)	6.464 (6.213; 7.157)	0.005
Intervillous space (mm^2)	6.621 (6.22; 7.17)	7.611 (6.887; 7.84)	0.007
Vessel surface area (% of villi surface area)	19.55 (16.45; 24.85)	18.2 (14.2; 22.6)	0.326
Stroma-to-vessel ratio	0.206 (0.166; 0.26)	0.178 (0.147; 0.253)	0.462
uPA expression	116.449 (100.496; 128.74)	126.087 (113.761; 139.191)	0.033
uPAR expression	117.59 (96.24; 138.94)	130.42 (107.93; 152.91)	0.351
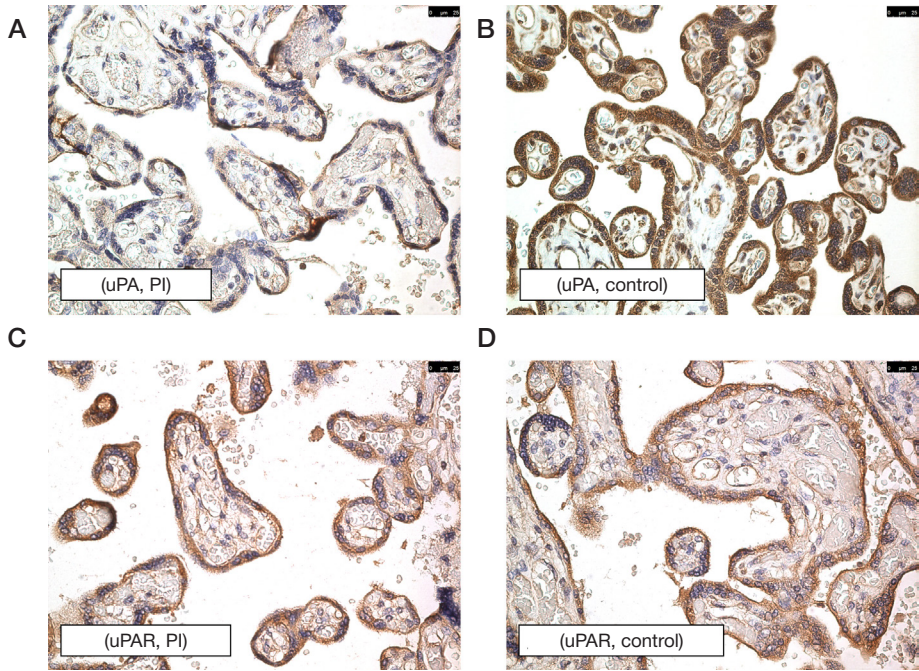
Fig. 1. Immunohistochemical expression of uPA (**A**, **B**) and uPAR (**C**, **D**) in the chorionic villi in the controls (**A**, **C**) and the PI group (**B**, **D**). Staining of syncytiotrophoblast cells with anti- uPA and anti- uPAR antibodies produces intense coloration in healthy tissue and samples of PI patients (**A–D**). Placental tissue of patients with PI (**A**) shows less intense coloration of ssyncytiotrophoblast cells after uPA staining in comparison with the control group (**B**). No difference was observed in immunohistochemical uPAR expression between the groups (**C**, **D**). Scale bar: 25 µm
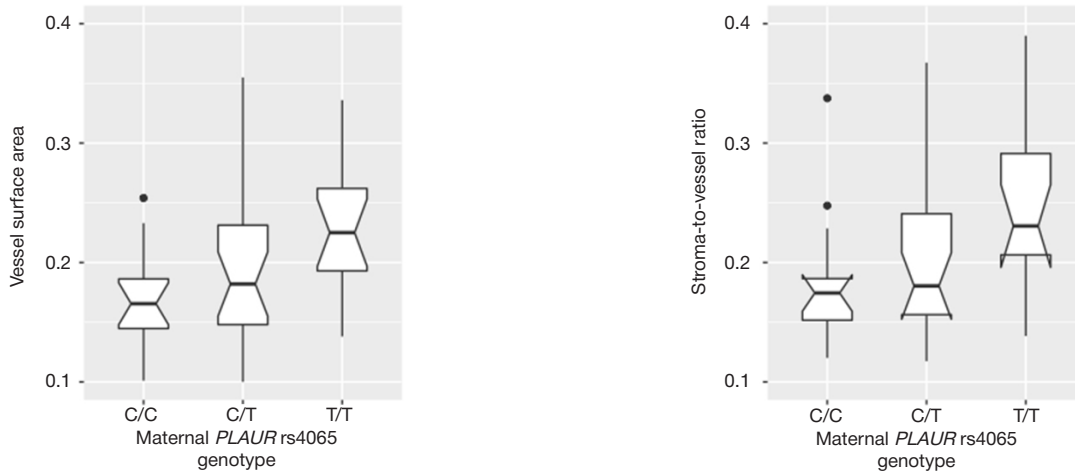
Fig. 2. The vessel surface area and the stroma-to-vessel ratio for different maternal *PLAU* rs4065 genotypes. The ends of the box are Q1 and Q3; the vertical line inside the box is the median. The ends of the whiskers: Q1 minus 1.5 IQR; Q3 plus 1.5 IQR. Outliers are represented by dots. Confidence intervals are represented by notches

Table 4. The vessel surface area and the stroma-to-vessel ratio for different maternal *PLAU* rs4065 genotypes

rs4065 genotype	Vessel surface area, mm²			Stroma-to-vessel ratio		
	Median	95% CI	p^{**}	Median	95% CI	p^{**}
CC	0.1655	[0.1461; 0.1849]		0.1715	[0.1524; 0.1907]	
CT	0.182	[0.1528; 0.2112]	0.0305	0.1804	[0.1485; 0.2123]	0.0265
TT	0.225	[0.1969; 0.2531]		0.2306	[0.1959; 0.2652]	

Note: ** — the Kruskal–Wallis test applied.

are reports of the significantly increased risk for cancer in the presence of the T allele and the TT genotype [17–19]. At the same time, it is known that high uPA levels in some tumors predict a poor outcome [20]. Besides, the T allele of rs4065 has been linked to Quebec platelet disorder caused by excess fibrinolysis due to elevated uPA content in platelets [21].

CONCLUSIONS

High placental uPA and the fetal TT genotype (*PLAU* rs4065) are protective against the risk of PI. We hope that our findings will expand the potential of noninvasive prenatal screening and predict PI by genotyping fetal DNA for rs4065 *PLAU*.

References

1. Benirschke K, Burton GJ, Baergen RN. Pathology of the Human Placenta, 6th ed. Springer, 2012; p. 411.
2. Poettler M, Unseld M, Mihaly-Bison J, Uhrin P, Koban F. Binder BR, et al. The urokinase receptor (CD87) represents a central mediator of growth factor-induced endothelial cell migration. Thromb Haemost. 2012; 108 (8): 357–66.
3. Tkachuk VA, Plekhanova OS, Parfyonova YV. Regulation of arterial remodeling and angiogenesis by urokinase-type plasminogen activator. Can J Physiol Pharmacol. 2009; 87 (4): 231–51.
4. Khosravi F, Zarei S, Ahmadvand N, Akbarzadeh-Pasha Z, Savadi E, Zarnani A, et al. Association between plasminogen activator inhibitor 1 gene mutation and different subgroups of recurrent miscarriage and implantation failure. J Assist Reprod Genet. 2014; 31 (1): 121–4.
5. Zhao L, Bracken MB, DeWan AT, Chen S. Association between the SERPINE1 (PAI-1) 4G/5G insertion/deletion promoter polymorphism (rs1799889) and pre-eclampsia: A systematic review and meta-analysis. Molecular Human Reproduction. 2013; 19 (3): 136–43.
6. Tran H, Maurer F, Nagamine Y. Stabilization of urokinase and urokinase receptor mRNAs by HuR is linked to its cytoplasmic accumulation induced by activated mitogen-activated protein kinase-activated protein kinase 2. Mol Cell Biol. 2003; 23 (20): 7177–88.
7. Xu J, Li W, Bao X, Ding H, Chen J, Zhang W, et al. Association of putative functional variants in the PLAU gene and the PLAUR gene with myocardial infarction. Clin Sci (Lond). 2010; 119 (8): 353–9.
8. Yosrlimoto M, Youichi, Ushiyama Y, Sakaia M, Tamakia S, Hara H, et al. Characterization of single chain urokinase-type plasminogen activator with a novel amino-acid substitution in the kringle structure. Biochimica et Biophysica Acta (BBA)-Protein Structure and Molecular Enzymology. 1996; 1293 (1): 83–9.
9. Campbell DB, Li C, Sutcliffe JS, Persico AM, Levitt P. Genetic evidence implicating multiple genes in the met receptor tyrosine kinase pathway in autism spectrum disorder. Autism Res. 2008; 1 (3): 159–68.
10. Solé X, Guinó E, Valls J, Iniesta R, Moreno V. SNPStats: a web tool for the analysis of association studies. Bioinformatics. 2006; 22 (15): 1928–29.
11. Martínez-Hernández MG, Baiza-Gutman LA, Castillo-Trápala A,

Armant DR. Regulation of proteinases during mouse peri-implantation development: Urokinase-type plasminogen activator expression and cross talk with matrix metalloproteinase 9. Reproduction. 2011; 141 (2): 227.
12. Lash GE, Otun HA, Innes BA, Percival K, Searle RF, Robson SC, et al. Regulation of extravillous trophoblast invasion by uterine natural killer cells is dependent on gestational age. Hum Reprod. 2010; 25 (5): 1137–45.
13. Naruse K, Lash GE, Bulmer JN, Innes BA, Otun HA, Searle RF, et al. The Urokinase Plasminogen Activator (uPA) System in Uterine Natural Killer Cells in the Placental Bed During Early Pregnancy. Placenta. 2009; 30 (5): 398–404.
14. Pierleoni C, Castellucci M, Kaufmann P, Lund LR, Schnack Nielsen B, Urokinase receptor is up-regulated in endothelial cells and macrophages associated with fibrinoid deposits in the human placenta. Placenta. 2003; 24 (6): 677–85.
15. Breuss JM, Uhrin P. VEGF-initiated angiogenesis and the uPA/uPAR system. Cell adhesion & migration. 2012; 6 (6): 535–40.
16. Liu S, Zheng Q, Cui XY, Dai KX, Yang XS, Li FS, et al. Expression of uPAR in human trophoblast and its role in trophoblast invasion. Int J Clin Exp Pathol [Internet]. e-Century Publishing Corporation; 2015; 8 (11): 14325–34. Available from: https://www.ncbi.nlm.nih.gov/pmc/articles/PMC4713534/.
17. Xu Z, Meng L-L, Lin J, Ling Y, Chen S, Lin N. Association between the polymorphisms of urokinase plasminogen activation system and cancer risk: a meta-analysis. Onco Targets Ther [Internet]. Dove Medical Press. 2015; 9 (8): 2493–502. Available from: http://www.ncbi.nlm.nih.gov/pmc/articles/PMC4574847/.
18. Andreasen P, Kjøller L, Christensen L, Duffy MJ. The urokinase-type plasminogen activator system in cancer metastasis: a review. Int J Cancer. 1997; 72 (1): 1–22.
19. Duffy MJ, Maguire TM, McDermott EW, O'Higgins N. Urokinase plasminogen activator: a prognostic marker in multiple types of cancer. J Surg Oncol. 1999; 71 (2): 130–5.
20. Fuhrman B. The urokinase system in the pathogenesis of atherosclerosis. Atherosclerosis. Ireland; 2012 May; 222 (1): 8–14.
21. Diamandis M, Paterson AD, Rommens JM, Veljkovic DK, Blavignac J, Bulman DE, et al. Quebec platelet disorder is linked to the urokinase plasminogen activator gene (PLAU) and increases expression of the linked allele in megakaryocytes. Blood. 2009; 113 (7): 1543–6.

Литература

1. Benirschke K, Burton GJ, Baergen RN. Pathology of the Human Placenta, 6th ed. Springer, 2012; p. 411.
2. Poettler M, Unseld M, Mihaly-Bison J, Uhrin P, Koban F. Binder BR, et al. The urokinase receptor (CD87) represents a central mediator of growth factor-induced endothelial cell migration. Thromb Haemost. 2012; 108 (8): 357–66.
3. Tkachuk VA, Plekhanova OS, Parfyonova YV. Regulation of arterial remodeling and angiogenesis by urokinase-type plasminogen activator. Can J Physiol Pharmacol. 2009; 87 (4): 231–51.
4. Khosravi F, Zarei S, Ahmadvand N, Akbarzadeh-Pasha Z, Savadi E, Zarnani A, et al. Association between plasminogen activator inhibitor 1 gene mutation and different subgroups of recurrent miscarriage and implantation failure. J Assist Reprod Genet. 2014; 31 (1): 121–4.
5. Zhao L, Bracken MB, DeWan AT, Chen S. Association between the SERPINE1 (PAI-1) 4G/5G insertion/deletion promoter polymorphism (rs1799889) and pre-eclampsia: A systematic review and meta-analysis. Molecular Human Reproduction. 2013; 19 (3): 136–43.
6. Tran H, Maurer F, Nagamine Y. Stabilization of urokinase and urokinase receptor mRNAs by HuR is linked to its cytoplasmic accumulation induced by activated mitogen-activated protein kinase-activated protein kinase 2. Mol Cell Biol. 2003; 23 (20): 7177–88.
7. Xu J, Li W, Bao X, Ding H, Chen J, Zhang W, et al. Association

of putative functional variants in the PLAU gene and the PLAUR gene with myocardial infarction. Clin Sci (Lond). 2010; 119 (8): 353–9.
8. Yosrlimoto M, Youichi, Ushiyama Y, Sakaia M, Tamakia S, Hara H, et al. Characterization of single chain urokinase-type plasminogen activator with a novel amino-acid substitution in the kringle structure. Biochimica et Biophysica Acta (BBA)-Protein Structure and Molecular Enzymology. 1996; 1293 (1): 83–9.
9. Campbell DB, Li C, Sutcliffe JS, Persico AM, Levitt P. Genetic evidence implicating multiple genes in the met receptor tyrosine kinase pathway in autism spectrum disorder. Autism Res. 2008; 1 (3): 159–68.
10. Solé X, Guinó E, Valls J, Iniesta R, Moreno V. SNPStats: a web tool for the analysis of association studies. Bioinformatics. 2006; 22 (15): 1928–29.
11. Martínez-Hernández MG, Baiza-Gutman LA, Castillo-Trápala A, Armant DR. Regulation of proteinases during mouse peri-implantation development: Urokinase-type plasminogen activator expression and cross talk with matrix metalloproteinase 9. Reproduction. 2011; 141 (2): 227.
12. Lash GE, Otun HA, Innes BA, Percival K, Searle RF, Robson SC, et al. Regulation of extravillous trophoblast invasion by uterine natural killer cells is dependent on gestational age. Hum Reprod. 2010; 25 (5): 1137–45.
13. Naruse K, Lash GE, Bulmer JN, Innes BA, Otun HA, Searle RF, et

al. The Urokinase Plasminogen Activator (uPA) System in Uterine Natural Killer Cells in the Placental Bed During Early Pregnancy. Placenta. 2009; 30 (5): 398–404.

14. Pierleoni C, Castellucci M, Kaufmann P, Lund LR, Schnack Nielsen B, Urokinase receptor is up-regulated in endothelial cells and macrophages associated with fibrinoid deposits in the human placenta. Placenta. 2003; 24 (6): 677–85.

15. Breuss JM, Uhrin P. VEGF-initiated angiogenesis and the uPA/uPAR system. Cell adhesion & migration. 2012; 6 (6): 535–40.

16. Liu S, Zheng Q, Cui XY, Dai KX, Yang XS, Li FS, et al. Expression of uPAR in human trophoblast and its role in trophoblast invasion. Int J Clin Exp Pathol [Internet]. e-Century Publishing Corporation; 2015; 8 (11): 14325–34. Available from: https://www.ncbi.nlm.nih.gov/pmc/articles/PMC4713534/.

17. Xu Z, Meng L-L, Lin J, Ling Y, Chen S, Lin N. Association between the polymorphisms of urokinase plasminogen activation system and cancer risk: a meta-analysis. Onco Targets Ther [Internet]. Dove Medical Press. 2015; 9 (8): 2493–502. Available from: http://www.ncbi.nlm.nih.gov/pmc/articles/PMC4574847/.

18. Andreasen P, Kjøller L, Christensen L, Duffy MJ. The urokinase-type plasminogen activator system in cancer metastasis: a review. Int J Cancer. 1997; 72 (1): 1–22.

19. Duffy MJ, Maguire TM, McDermott EW, O'Higgins N. Urokinase plasminogen activator: a prognostic marker in multiple types of cancer. J Surg Oncol. 1999; 71 (2): 130–5.

20. Fuhrman B. The urokinase system in the pathogenesis of atherosclerosis. Atherosclerosis. Ireland; 2012 May; 222 (1): 8–14.

21. Diamandis M, Paterson AD, Rommens JM, Veljkovic DK, Blavignac J, Bulman DE, et al. Quebec platelet disorder is linked to the urokinase plasminogen activator gene (PLAU) and increases expression of the linked allele in megakaryocytes. Blood. 2009; 113 (7): 1543–6.

POLYMORPHISM OF PROINFLAMMATORY CYTOKINE GENES IN GIRLS PREDISPOSED TO RECURRENT RESPIRATORY INFECTIONS

Kazakova AV[1], Uvarova EV[2], Limareva LV[1] ✉, Lineva OI[1], Svetlova GN[1], Trupakova AA[1]

[1] Samara State Medical University, Samara

[2] Kulakov National Medical Research Center for Obstetrics, Gynecology, and Perinatology, Moscow

Acute respiratory infections (ARI) are very common in children and often prompt parents to seek medical advice. Increased susceptibility to ARI is caused by a number of factors, including genetically determined imbalances in cytokine production. The aim of this study was to analyze the frequency of 6 clinically relevant polymorphisms of proinflammatory cytokine genes in girls predisposed to recurrent respiratory infections. The study was conducted in girls aged 7–17 years who were undergoing a routine medical checkup. A group of children with frequent respiratory infections was identified. The following polymorphisms were analyzed for possible associations with predisposition to frequent respiratory infections: *IL1β T-31C* (rs1143627), *IL1β T-511C* (rs16944), *IL1β C-3953T* (rs1143634), *IL1β G-1473C* (rs1143623); *IL6 C-174G* (rs1800795), and *TNFα G-308A* (rs1800629). For polymorphism detection, PCR and gel electrophoresis were used. The following alleles were found to be associated with an increased risk for recurrent respiratory infections in girls aged 7–17 years: *C-31* (rs1143627) (OR = 2.05; CI: 1.16–3.64; p = 0.013) and *C-511* (rs16944) (OR = 3.11; CI: 1.25–7.76; p = 0.013) of the *IL-1β* gene.

Keywords: recurrent respiratory infections in children, pro-inflammatory cytokines, gene polymorphism

ОСОБЕННОСТИ ПОЛИМОРФИЗМА ГЕНОВ ПРОВОСПАЛИТЕЛЬНЫХ ЦИТОКИНОВ У ДЕВОЧЕК, ПРЕДРАСПОЛОЖЕННЫХ К ЧАСТЫМ РЕСПИРАТОРНЫМ ЗАБОЛЕВАНИЯМ

А. В. Казакова[1], Е. В. Уварова[2], Л. В. Лимарева[1] ✉, О. И. Линева[1], Г. Н. Светлова[1], А. А. Трупакова[1]

[1] Самарский государственный медицинский университет, Самара, Россия

[2] Национальный медицинский исследовательский центр акушерства, гинекологии и перинатологии имени академика В. И. Кулакова, Москва, Россия

Респираторные заболевания (ОРЗ) относят к числу наиболее распространенных заболеваний детского возраста и служат поводом частого обращения за медицинской помощью. Повышенная заболеваемость детей определяется целым рядом факторов, в том числе наличием дисбаланса в системе цитокинов, уровень синтеза которых генетически детерминирован. Целью работы было проанализировать особенности распределения шести клинически значимых полиморфных локусов в генах провоспалительных цитокинов у девочек с частыми респираторными заболеваниями. Среди девочек 7–17 лет, проходящих плановый профилактический осмотр, на основании анамнеза была выделена группа часто болеющих детей. Проведен анализ ассоциации полиморфных вариантов генов провоспалительных цитокинов *IL1β T-31C* (rs1143627), *IL1β T-511C* (rs16944), *IL1β C-3953T* (rs1143634), *IL1β G-1473C* (rs1143623) в гене интерлейкина-1β; *IL6 C-174G* (rs1800795) — в гене интерлейкина-6 и *TNFα G-308A* (rs1800629) — в гене фактора некроза опухоли альфа с предрасположенностью к частым респираторным заболеваниям. Полиморфные варианты генов выявляли методом ПЦР с электрофоретической детекцией. Показано, что с повышенным риском рецидивирующих респираторных заболеваний у девочек 7–17 лет ассоциированы аллели *С-31* (rs1143627) (ОШ = 2,05; ДИ: 1,16–3,64; p = 0,013) и *С-511* гена *IL-1β* (rs16944) (ОШ = 3,11; ДИ: 1,25–7,76; p = 0,013).

Ключевые слова: часто болеющие дети, провоспалительные цитокины, полиморфизм генов

To date, it has been convincingly demonstrated that the immune system plays a critical role in disease progression. In both health and pathology, immune response is regulated by cytokines, the key mediators of cell-cell interactions in the immune system [1, 2]. An imbalance between pro- and anti-inflammatory cytokines compromises immune defense against infection and leads to chronicity [3]. The intensity of cytokine secretion depends on the expression of cytokine-encoding genes, which, in turn, is determined by the presence of persistent microorganisms and genetic features of the host [4]. Single nucleotide polymorphisms (SNPs) of human genes coding for immunocompetent molecules determine the level of cytokine production in response to infection, affecting the clinical course of the disease [5–7]. So far, a number of polymorphic loci have been identified in promotor regions of the genes involved in the production of proinflammatory cytokines (IL1β, IL6, TNFα, etc.) [8–12].

Acute respiratory infections (ARI) are very common in childhood. A child falls in the "frequently ill" category if he/she

has more than 6 episodes of ARI a year; this definition refers to repeated or recurrent viral, bacterial or mixed infections of ear, nose and throat (adenoiditis, tonsillitis, otitis), upper (laryngitis) or lower respiratory tract (tracheitis, bronchitis, pneumonia) developing as a result of compromised immunity or inadequate therapy for ARI [13–15]. Increased susceptibility to ARI is determined by a few factors, including genetic ones. There is an ongoing search for possible immunogenetic markers of such predisposition.

The aim of our study was to explore possible associations between the polymorphisms of genes coding for key proinflammatory cytokines and predisposition to frequent respiratory infections in girls aged 7 to 17 years.

METHODS

We examined 116 girls aged 7 to 17 years residing in Samara who visited a pediatric/adolescent gynecologist for a routine checkup in 2014–2016. The following inclusion criteria were applied: age between 7 and 17 years; the absence of severe organic pathology; normal physical, sexual and cognitive development. Exclusion criteria: age outside the specified range; severe organic pathology; developmental abnormalities. We analyzed the medical history of the patients (frequency of respiratory infections and their course) and allele and genotype frequencies for proinflammatory cytokine genes using PCR with gel electrophoresis (SNP-EXPRESS assay; Litech; Russia). We searched for the following SNPs: *IL1β T-31C* (rs1143627), *IL1β T-511C* (rs16944), *IL1β C-3953T* (rs1143634), *IL1β G-1473C* (rs1143623); *IL6 C-174G* (rs1800795), and *TNFα G-308A* (rs1800629). DNA was isolated from the buccal mucosa using an express DNA isolation kit (Litech; Russia). SNPs selected for our study are associated with human immune status and were proposed as clinically and diagnostically relevant at the 15th International Histocompatibility and Immunogenetics Workshop in Brazil in 2008 [16].

DNA was amplified in a DTlite-4S1 thermocycler (DNA-Technology; Russia). The observed genotype frequencies were tested for conformity to Hardy-Weinberg expectations using Pearson's χ^2. We measured possible associations and assessed the significance of differences in the distribution of categorical variables (odds ratios and 95% confidence intervals). Statistical analysis was performed online on the website of the Institute of Human Genetics (Munich, Germany) using DeFinetti software [17]. The minor alleles were hypothesized to be risk alleles and were analyzed in all combinations.

RESULTS

The analysis of clinical data and medical histories revealed that 56.9% of the participants had ARI 6 to 10 times a year. Of them, 10.6% had a chronic ENT pathology (tonsillitis, pharyngolaryngitis) with frequent relapses (4 to 6 times a year) in the setting of acute viral and/or bacterial infection. The girls were divided into 2 groups: 65 girls constituted the group of children with recurrent respiratory infections and 51 girls made up the group without recurrent ARI.

The genotype frequency of 5 out of 6 analyzed SNPs conformed to the Hardy-Weinberg equilibrium. The only exception was *TNFα (G-308A)*; therefore, this polymorphism was excluded from further analysis (see Table).

The analysis of allele/genotype frequencies of the genes encoding proinflammatory cytokines demonstrated that the general sample was dominated by the carriers of the alleles *T-31*, *G-1473* and *C-3953* in the *IL1β* gene ($p < 0.05$) determining

the high levels of the encoded cytokines. In the case of *IL1β (T-511C)* and IL6 (C-174G), the alleles associated with high and low levels of *IL1β* and *IL6* were distributed in our sample relatively equally.

Comparison of individual polymorphisms occurring at the clinically relevant loci of the studied cytokine genes and associated with high/low levels of their expression revealed that homozygous and heterozygous *C* alleles at positions *31* and *511* of the *IL1β* gene were significantly more frequent in the group of girls suffering from recurrent infections. The presence of the *C-31* allele increased the risk of frequent respiratory infections twofold (OR = 2.05; CI: 1.16–3.64) in comparison with the *T-31* allele. The highest risk of recurrent infections was detected in the carriers of the *CC* genotype in comparison with heterozygous *CT* carriers (OR = 2.58; CI: 1.14–5.85) and the pooled *CT* and *TT* genotypes (OR = 2.65; CI: 1.25–5.63). The presence of any *C-511* allele variant also indicated a high risk of recurrent respiratory infections (OR = 1.68; CI: 0.99–2.83; $p = 0.053$). The risk of frequent respiratory infections increased more than threefold in the carriers homozygous for *CC* in comparison with heterozygous *CT* (OR= 3.28; CI: 1.22–8.79), homozygous *TT* (OR = 2.9; CI: 1.03–8.17) and the pool of children with *CT* or *TT* (OR = 3.11; CI: 1.25–7/76) at -511C/T of the *IL1β* gene.

We failed to establish a statistically significant association between recurrent respiratory infections and the *IL6 (C-174G)* polymorphism, but the girls suffering from recurrent infections were homozygous for the *G* allele associated with high levels of IL6 1.5 times as rare as the girls without recurrent respiratory infections (OR = 0.57; CI: 0.20–1.59; $p = 0.77$).

DISCUSSION

Long-lasting and frequent respiratory infections, especially at early age, present a medical challenge yet unsolved, creating a serious social and economic burden for the family and the society in general. The contemporary view on the problem is that the primary causes of high susceptibility to infection in children are the immaturity of the immune system and genetic predisposition [18, 19]. Cytokines play an important role in defense against pathogens: they regulate response to infection not only at the immune system level but also at the level of the whole organism. So far, extensive evidence has been accumulated suggesting that SNPs of cytokine genes can be functional and alter expression of the latter. Such functional polymorphisms hereditarily determine the levels of cytokine production in an individual, affecting the progression and outcome of infectious diseases and immunopathological processes [20]. Anti-inflammatory cytokines play a central role in the formation and regulation of inflammatory response in both innate and adaptive immunities. Therefore, research into the polymorphisms of genes coding for key proinflammatory cytokines can result in the emergence of new diagnostic and therapeutic approaches [21, 22].

In this study, we analyzed associations between polymorphisms of genes coding for key proinflammatory cytokines and predisposition to recurrent respiratory infections in 7 to 17-year old girls. Clinically relevant functional polymorphisms were assessed, including *IL1β (T-31C)*, *IL1β (T-511C)*, *IL1β (C-3953T)*, *IL1β (G-1473C)*, *IL6 (C-174G)*, and *TNFα (G-308A)*.

In the first stage of the study, we analyzed allele/genotype frequencies of polymorphic variants of the genes encoding proinflammatory cytokines in all study participants regardless of their predisposition to frequent ARI and tested the conformity of the observed data to the Hardy-Weinberg equilibrium. This is an

Table. Polymorphic allele and genotype frequencies for the genes encoding proinflammatory cytokines in girls aged 7 to 17 years

Gene polymorphism	Allele, genotype	Frequency, abs / %			
		All girls $n = 116$	Without recurrent ARI $n = 51$	With recurrent ARI OP3 $n = 65$	Odds ratio (Confidence interval) (minor allele dominating)
IL1B (T-31C)	T	100/67.0 ± 3.3*	46/75.0 ± 4.7	54/60.0 ± 4.4	[1]<->[2]**: 2.05 (1.16–3.64), χ^2 = 6.18. p = 0.013 [11]<->[12]**: 2.58 (1.14–5.85), χ^2 = 5.28. p = 0.022[11]<->[22]: 2.84 (0.87–9.28), χ^2 = 5.28, p = 0.077 [11]<->[12 + 22]**: 2.65 (1.25–5.63), χ^2 = 6.53, p = 0.011
	C	61/33.0 ± 3.3	20/25.0 ± 4.7	41/40.0 ± 4.4	
	TT	55/47.4	31/60.8	24/36.9	
	CT	45/38.8	15/29.4	30/46.2	
	CC	16/13.8	5/9.8	11/16.9	
IL1B (T-511C)	T	78/45.0 ± 3.4	36/52 ± 5.5	42/39 ± 4.1	[1]<->[2]: 1.68 (0.99–2.83), χ^2 = 3.74, p = 0.053 [11]<->[12]**: 3.28 (1.22–8.79), χ^2 = 5.80, p = 0.016 [11]<->[22]**: 2.90 (1.03–8.17), χ^2 = 3.13, p = 0.042 [11]<->[12+22]**: 3.11(1.25–7.76), χ^2 = 6.24, p = 0.013
	C	90 /55.0 ± 3.4	34/48 ± 5.5	56/61 ± 4.1	
	TT	26 / 22.4	17/33.3	9/13.8	
	CT	52 / 44.8	19/37.3	33/50.8	
	CC	38 / 32.8	15/29.4	23/35.4	
IL1B (G-1473C)	G	94 / 57.0 ± 3.3*	40/59.0 ± 5.3	54/55 ± 4.1	[1]<->[2]: 1.15 (0.68–1.94), χ^2 = 0.28, p = 0.600 [11]<->[12]: 2.00 (0.86–4.63), χ^2 = 2.65, p = 0.104 [11]<->[22]: 1.11 (0.39–3.18), χ^2 = 0.04, p = 0.844 [11]<->[12 + 22]: 1.69(0.77–3.68), χ^2 = 1.72, p = 0.189
	C	78 / 43.0 ± 3.3	31/41±5.3	47/45 ± 4.1	
	GG	38 / 32.7	20/39.2	18/27.7	
	GC	56 / 48.3	20/39.2	36/55.4	
	CC	22 / 19.0	11/21.6	11/16.9	
IL1β (C-3953T)	C	109/78.0 ± 2.8*	48/80 ± 4.2	51/77.0 ± 3.8	[1]<->[2]: 0.28 (0.65–2.33), χ^2 = 0.41, p = 0.524 [11]<->[12]: 1.37 (0.61–3.09), χ^2 = 0.58, p = 0.447 [11]<->[22]: 1.16 (0.24–5.57), χ^2 = 0.04, p = 0.851 [11]<->[12 + 22]: 1.33 (0.62–2.87), χ^2 = 0.54, p = 0.461
	T	43 / 22.0 ± 2.8	17/20.0 ± 4.2	26/23.0 ± 3.8	
	CC	73 / 62.9	34/66.7	39/60.0	
	TC	36 / 31.0	14/27.5	22/33.9	
	TT	7 / 6.0	3/5.9	4/6.2	
IL6 (C −174G)	C	79 / 45.0 ± 3.4	31/40.0 ± 5.2	48/48.0 ± 4.3	[1]<->[2]: 0.72 (0.42–1.21), χ^2 = 1.58, p = 0.209 [11]<->[12]: 1.05 (0.40–2.76), χ^2 = 0.01 p = 0.925 [11]<->[22]: 0.57 (0.20–1.59), χ^2 = 1.18, p = 0.277 [11]<->[12 + 22]: 0.81 (0.33–2.00), χ^2 = 0.20, p = 0.652
	G	91 / 55.0 ± 3.4	41/60.0 ± 5.2	50/52.0 ± 4.3	
	CC	25 / 21.5	10/19.6	15/23.1	
	CG	54 / 46.5	21/41.2	33/50.8	
	GG	37 / 31.9	20/39.2	17/26.2	
TNFα (G-308A)	G	32 / 18.0 ± 2.9			
	A	106/92.0 ± 2.9	Does not conform to the Hardy–Weinberg equilibrium (p = 0.0001)		
	GG	10 / 8.6			
	GA	22 / 19.0			
	AA	84 / 72.4			

Note: ARI — acute respiratory infections; * — statistically significant differences in the allele frequency at the given locus (p < 0.05); ** — statistically significant associations with increased risk of respiratory infections.

important stage because if observed frequencies are consistent with those predicted by the Hardy–Weinberg equation, it means that patient selection for a genetic study is adequate. The frequencies of 5 out of 6 analyzed polymorphisms was consistent with the Hardy–Weinberg equilibrium, except for *TNFα (G-308A)*. For the *G-308A* polymorphism of the *TNFα* gene, the frequency of the heterozygous genotype observed in the general sample was different from the predicted frequency. This could be explained by the insufficient number of observations and the character of allele distribution for this locus in the studied group. Therefore, *TNFα (G-308A)* was excluded from further analysis.

The analysis of allele and genotype frequencies of *IL1β* and *IL6* revealed that the general sample was dominated by the carriers of the *T-31*, *G-1473* and *C-3953* polymorphisms of the *IL1β* gene and the *G-174* polymorphism of the *IL6* genes. The distribution of *IL1β (T-511C)* alleles was relatively even. The pattern of allele/genotype distribution for this polymorphism was similar to that observed in the European female population

[23] and Russian females residing in Moscow [24], which may indicate the evolutionary advantage of the alleles that determine high levels of proinflammatory cytokines in the Caucasian population.

The subsequent analysis of the associations between predisposition to frequent ARI and the carriership of the studied alleles at the polymorphic loci of the genes encoding proinflammatory cytokines demonstrated that the presence of the *C-31* and *C-511* alleles in the *IL1β* gene significantly increased the risk of recurrent respiratory infections (2- to 3-fold), especially in the homozygous patients. In the girls with recurrent respiratory tract infections, the *G* allele in locus 174 of the *IL-6* gene was 1.5 times rarer (p > 0.05). The discovered association between the polymorphic *C-31* and *C-511* alleles of the *IL1β* gene and frequent respiratory infections is consistent with the literature: *IL-1β* plays a central role in the generation and regulation of immune response against infection; carriership of polymorphic variants at positions *31T* and *511T* in most cases leads to an increase in the production of this cytokine *in vivo*

and *in vitro* in comparison with *C* alleles, whose carriership increases the severity and frequency of respiratory infections in children and adults [25–27].

For some European populations, *IL1β (T-31C)* is in 100% linkage disequilibrium with *IL1β (T-511C)* [28], which seems to explain similar risks associated with this pair of SNPs.

The fact that only 2 SNPs of the *IL1β* gene were significantly associated with frequent respiratory infections suggests the need for identifying the subgroups with high prevalence of bacterial/viral infections, the presence/absence of allergies, etc. in the general sample of children predisposed to recurrent ARI, as well as the need for a larger patient sample. At the same time, the cytokine system is a polymorphic, highly reliable pleiotropic regulatory network of mediators whose biological effects are exerted in a cascade manner, are very diverse and sometimes excessive [29]. Therefore, a decrease in the expression of one or several cytokine genes and the resulting low production of the peptide mediator will not always be accompanied by a pronounced pathology. This means that research into the effects of polymorphisms in the cytokine genes should not be limited to the analysis of carriership of individual polymorphic variants occurring in a few cytokine genes. It is important to consider linked inheritance, mutual effects, interactions with

receptors and other factors affecting the cytokine status in health and pathology.

CONCLUSIONS

1. The studied group of 7 to 17-year old girls residing in Samara was dominated by the carriers of the alleles *T-31*, *G-1473*, *C-3953* in the *IL1β* gene and the *G-174* allele in the *IL6* gene. 2. The presence of the alleles *C-31* and *C-511* in the *IL1β* gene was associated with the increased risk of recurrent respiratory infections. 3. The established association between the studied gene variants and respiratory infections dictates the need for further research into the functional polymorphisms of cytokine genes aiming at developing new diagnostic approaches, prevention measures and personalized therapies. 4. The analysis of carriership of individual polymorphic gene variants in the cytokine system is not enough for the comprehensive assessment of individual immunogenetic features and the search for genetic markers for prediction, prevention and personalized treatment; it is important to account for linked inheritance, mutual effects, interactions with receptors and other factors affecting the cytokine status in health and pathology.

References

1. Sepiashvili RI, Slavyanskaya TA. Strategiya i taktika kompleksnoy immunoreabilitatsii bol'nykh s zabolevaniyami immunnoy sistemy. Allergologiya i immunologiya. 2015; 16 (1): 51–7. Russian.
2. Ketlinskiy SA, Simbirtsev AS. TSitokiny. SPb.: Foliant, 2008; 552 s. Russian.
3. Gulomov ZS, Simbirtsev AS, Yanov YuK, Varyushina EA, Tyrnova EV. Rol' tsitokinov pri lechenii ostrykh i khronicheskikh zabolevaniy verkhnikh dykhatel'nykh putey (Obzor literatury). Rossiyskaya otorinolaringologiya. 2008; 37 (6): 200–5. Russian.
4. Prilepskaya VN, Letunovskaya AB, Donnikov AE. Mikrobiotsenoz vlagalishcha i polimorfizm genov tsitokinov kak marker zdorov'ya zhenshchiny (obzor literatury). Ginekologiya. 2015; 17 (2): 4–13. Russian.
5. Bodiyenkova GM, Titova ZhV. Rol' polimorfizma i ekspressii otdel'nykh genov tsitokinov v formirovanii patologii (Obzor). Uspekhi sovremennogo estestvoznaniya. 2015; (1): 616–20. Russian.
6. Nesterova IV, Kovaleva SV, Kleshchenko EI, Shinkareva ON, Malinovskaya VV, Vyzhlova EN. Retrospektivnyy analiz klinicheskoy effektivnosti korotkikh kursov interferonov v lechenii ORVI u immunokomprometirovannykh chasto i dlitel'no boleyushchikh detey. Pediatriya. ZHurnal imeni G.N. Speranskogo. 2014; 93 (2): 62–7. DOI:10.24110/0031-403X-2014-93-2-62-67. Russian.
7. Shevchenko AV, Golovanova OV, Konenkov VI. Osobennosti polimorfizma promotornykh regionov genov tsitokinov IL1, IL4, IL5, IL6, IL10 i TNF-α u evropeoidnogo naseleniya Zapadnoy Sibiri. Immunologiya. 2010; (4): 176–81. Russian.
8. Abramov DD, Kofiadi IA, Khaitov MR, Sergeyev IV, Trofimov DYu, Gudima GO, i dr. Osobennosti polimorfizma genov, reguliruyushchikh razlichnyye komponenty immunnogo otveta, v russkoy populyatsii. Rossiyskiy allergologicheskiy zhurnal. 2012; (6): 72–5. Russian.
9. Prokofyev VF, Shevchenko AV, Golovanova OV, Zonova EV, Korolev MA, Leonova YuB. Kompleksnyy analiz polimorfizma v promotornykh uchastkakh genov tsitokinov IL-1B T-31C, IL-6 G-174C, TNFA G-238A, TNFA G-308A, TNFA C-863A, IL-4 C-590T i IL-10 C-592α v prognoze effekta ot lecheniya revmatoidnogo artrita. Meditsinskaya immunologiya. 2010; (4): 361–74. Russian.
10. Smolnikova MV, Smirnova SV, Tyutina OS. Polimorfizm genov tsitokinov pri atopicheskoy bronkhial'noy astme. Sibirskoye meditsinskoye obozreniye. 2013; (2): 63–69. Russian.

11. Kutikhin AG, Brusina EB, Volkov AN, Yuzhalin AE, Zhivotovskiy AS. Correlation between genetic polymorphisms within IL-1B and TLR4 genes and cancer risk in a Russian population: a case-control study. Tumor Biol. 2014; 35 (5): 4821–30.
12. Zhu Q, Sun J, Chen Y. Preterm birth and single nucleotide polymorphisms in cytokine genes. Transl Pediatr. 2014; 3 (2): 120–134. DOI: 10.3978/j.issn.2224-4336.2014.03.02.
13. Abramova NA, Savenkova MS. Rol' sotsial'nykh i ekologicheskikh faktorov v formirovanii gruppy chasto boleyushchikh detey v sotsial'no blagopoluchnykh sem'yakh g. Moskvy. Detskiye infektsii. 2013; (4): 52–7. Russian.
14. Yulish EI, Yaroshenko SyA. Chasto boleyushchiye deti i taktika pediatra. Zdorov'ye rebenka. 2013; 49 (6): 70–6. Russian.
15. Khlynina YuO, Kramar LV. Sovremennyye podkhody k profilaktike i lecheniyu ORZ u chasto boleyushchikh detey. Lekarstvennyy vestnik. 2015; 59 (4): 40–5. Russian.
16. Marsh SG, Albert ED, Bodmer WF, Bontrop RE, Dupont B, Erlich HA, et al. An update to HLA nomenclature, 2010. 2010; 45 (5): 846–8.
17. Available from: http://ihg.gsf.de/cgi-bin/hw/hwa1.pl.
18. Levina AS, Babachenko IV, Skripchenko NV, Imyanitov EN. Etiologicheskaya struktura zabolevaniy u chasto boleyushchikh detey v zavisimosti ot vozrasta. Rossiyskiy vestnik perinatologii i pediatrii. 2017; 62 (2): 72–7. Russian.
19. Esposito S, Bianchini S, Bosis S, Tagliabue C, Coro I, Argentiero A, Principi N. A randomized, placebo-controlled, double-blinded, single-centre, phase IV trial to assess the efficacy and safety of OM-85 in children suffering from recurrent respiratory tract infections. J Transl Med. 2019 Aug 23; 17 (1): 284. DOI: 10.1186/s12967-019-2040-y. PMID: 31443716 Free PMC Article.
20. Simbirtsev AS, Totolyan AA. Tsitokiny v laboratornoy diagnostike. Infektsionnyye bolezni: novosti, mneniya, obucheniye. 2015; (2): 82–98. Russian.
21. Kazakova AV, Uvarova EV, Limareva LV, Trupakova AA, Mishina AI. Sposob prognozirovaniya bakterial'nogo vul'vovaginita u devochek v zavisimosti ot stadii polovogo razvitiya soglasno shkale Tannera. Vestnik RGMU. 2019; (5): 116–22. DOI: 10.24075/vrgmu.2019.070. Russian.
22. Khazim K, Azulay EE, Kristal B, Cohen I. Interleukin 1 gene polymorphism and susceptibility to disease. Immunol Rev. 2018 Jan; 281 (1): 40–56. DOI: 10.1111/imr.12620.
23. Available from: http://www.ensembl.org/index.html.

24. Kofiadi IA, Kadochnikova VV, Abramov DD, Goncharova EV, Donnikov AE, Trofimov DYu, i dr. Chastota vstrechayemosti 100 klinicheski znachimykh odnonukleotidnykh polimorfizmov u zdorovykh predstaviteley russkoy populyatsii. Fiziologiya i patologiya immunnoy sistemy. 2011; (2): 3–10. Russian.

25. Terskova NV, Shnayder NA, Vakhrushev SG, Ikonnikova EV, Pilyugina MS. Rol' polimorfizma gena interleykina-1β v razvitii vospaleniya glotochnoy mindaliny. Ros. otorinolaringologiya. 2010; (6): 87–93. Russian.

26. Chen H, Wilkins LM, Aziz N. Single nucleotide polymorphisms in the human interleukin-1B gene affect transcription according to haplotype context. Hum Mol Genet. 2006; (15): 519–29.

27. Todorović MM, Zvrko EZ. Immunoregulatory cytokines and chronic tonsillitis. Bosn J Basic Med Sci. 2013; 13 (4): 230–6. PMID: 24289758.

28. Gromova AYu, Simbirtseva AS. Polimorfizm genov semeystva IL-1 cheloveka. Tsitokiny i vospaleniye. 2005; (2): 3–12. Russian.

29. Tsygan VN, Ivanov AM, Kamilova TA, Protasov OV, Artyushkin SA. Geneticheskiy polimorfizm tsitokinov. Vestnik Rossiyskoy voyenno-meditsinskoy akademii. 2010; 30 (2): 211–9. Russian.

Литература

1. Сепиашвили Р. И., Славянская Т. А. Стратегия и тактика комплексной иммунореабилитации больных с заболеваниями иммунной системы. Аллергология и иммунология. 2015; 16 (1): 51–7.

2. Кетлинский С. А., Симбирцев А. С. Цитокины. СПб.: Фолиант, 2008; 552 с.

3. Гуломов З. С., Симбирцев А. С., Янов Ю. К., Варюшина Е. А., Тырнова Е. В. Роль цитокинов при лечении острых и хронических заболеваний верхних дыхательных путей (Обзор литературы). Российская оториноларингология. 2008; 37 (6): 200–05.

4. Прилепская В. Н., Летуновская А. Б., Донников А. Е. Микробиоценоз влагалища и полиморфизм генов цитокинов как маркер здоровья женщины (обзор литературы). Гинекология. 2015; 17 (2): 4–13.

5. Бодиенкова Г. М., Титова Ж. В. Роль полиморфизма и экспрессии отдельных генов цитокинов в формировании патологии (Обзор). Успехи современного естествознания. 2015; (1): 616–20.

6. Нестерова И. В., Ковалева С. В., Клещенко Е. И., Шинкарева О. Н., Малиновская В. В., Выжлова Е. Н. Ретроспективный анализ клинической эффективности коротких курсов интерферонов в лечении ОРВИ у иммунокомпрометированных часто и длительно болеющих детей. Педиатрия. Журнал имени Г. Н. Сперанского. 2014; 93 (2): 62–7. DOI:10.24110/0031-403X-2014-93-2-62-67

7. Шевченко А. В., Голованова О. В., Коненков В. И. Особенности полиморфизма промоторных регионов генов цитокинов IL1, IL4, IL5, IL6, IL10 и TNF-α у европеоидного населения Западной Сибири. Иммунология. 2010; (4): 176–81.

8. Абрамов Д. Д., Кофиади И. А., Хаитов М. Р., Сергеев И. В., Трофимов Д. Ю., Гудима Г. О. и др. Особенности полиморфизма генов, регулирующих различные компоненты иммунного ответа, в русской популяции. Российский аллергологический журнал. 2012; (6): 72–5.

9. Прокофьев В. Ф., Шевченко А. В., Голованова О. В., Зонова Е. В., Королев М. А., Леонова Ю. Б. Комплексный анализ полиморфизма в промоторных участках генов цитокинов IL-1B T-31C, IL-6 G-174C, TNFA G-238A, TNFA G-308A, TNFA C-863A, IL-4 C-590T и IL-10 C-592α в прогнозе эффекта от лечения ревматоидного артрита. Медицинская иммунология. 2010; (4): 361–74.

10. Смольникова М. В., Смирнова С. В., Тютина О. С. Полиморфизм генов цитокинов при атопической бронхиальной астме. Сибирское медицинское обозрение. 2013; (2) 63–9.

11. Kutikhin AG, Brusina EB, Volkov AN, Yuzhalin AE, Zhivotovskiy AS. Correlation between genetic polymorphisms within IL-1B and TLR4 genes and cancer risk in a Russian population: a case-control study. Tumor Biol. 2014; 35 (5): 4821–30.

12. Zhu Q, Sun J, Chen Y. Preterm birth and single nucleotide polymorphisms in cytokine genes. Transl Pediatr. 2014; 3 (2): 120–34. DOI: 10.3978/j.issn.2224-4336.2014.03.02.

13. Абрамова Н. А., Савенкова М. С. Роль социальных и экологических факторов в формировании группы часто болеющих детей в социально благополучных семьях г. Москвы. Детские инфекции. 2013; (4): 52–7.

14. Юлиш Е. И., Ярошенко С. Я. Часто болеющие дети и тактика педиатра. Здоровье ребенка. 2013; 49 (6): 70–6.

15. Хлынина Ю. О., Крамарь Л. В. Современные подходы к профилактике и лечению ОРЗ у часто болеющих детей. Лекарственный вестник. 2015; 59 (4): 40–5.

16. Marsh SG, Albert ED, Bodmer WF, Bontrop RE, Dupont B, Erlich HA, et al. An update to HLA nomenclature, 2010. 2010; 45 (5): 846–8.

17. Доступно по ссылке: http://ihg.gsf.de/cgi-bin/hw/hwa1.pl.

18. Левина А. С., Бабаченко И. В., Скрипченко Н. В., Имянитов Е. Н. Этиологическая структура заболеваний у часто болеющих детей в зависимости от возраста. Российский вестник перинатологии и педиатрии. 2017; 62 (2): 72–7.

19. Esposito S, Bianchini S, Bosis S, Tagliabue C, Coro I, Argentiero A. et al. A randomized, placebo-controlled, double-blinded, single-centre, phase IV trial to assess the efficacy and safety of OM-85 in children suffering from recurrent respiratory tract infections. J Transl Med. 2019 Aug 23; 17 (1): 284. DOI: 10.1186/s12967-019-2040-y. PMID: 31443716 Free PMC Article.

20. Симбирцев А. С., Тотолян А. А. Цитокины в лабораторной диагностике. Инфекционные болезни: новости, мнения, обучение. 2015; (2): 82–98.

21. Казакова А. В., Уварова Е. В., Лимарева Л. В., Трупакова А. А., Мишина А. И. Способ прогнозирования бактериального вульвовагинита у девочек в зависимости от стадии полового развития согласно шкале Таннера. Вестник РГМУ. 2019; (5): 116–22. DOI: 10.24075/vrgmu.2019.070.

22. Khazim K, Azulay EE, Kristal B, Cohen I. Interleukin 1 gene polymorphism and susceptibility to disease. Immunol Rev. 2018 Jan; 281 (1): 40–56. DOI: 10.1111/imr.12620.

23. Доступно по ссылке: http://www.ensembl.org/index.html.

24. Кофиади И. А., Кадочникова В. В., Абрамов Д. Д., Гончарова Е. В., Донников А. Е., Трофимов Д. Ю. Частота встречаемости 100 клинически значимых однонуклеотидных полиморфизмов у здоровых представителей русской популяции. Физиология и патология иммунной системы. 2011; (2): 3–10.

25. Терскова Н. В., Шнайдер Н. А., Вахрушев С. Г., Иконникова Е. В., Пилюгина М. С. Роль полиморфизма гена интерлейкина-1β в развитии воспаления глоточной миндалины. Рос. оториноларингология. 2010; (6): 87–93.

26. Chen H, Wilkins LM, Aziz N. Single nucleotide polymorphisms in the human interleukin-1B gene affect transcription according to haplotype context. Hum Mol. Genet. 2006; (15): 519–29.

27. Todorović MM, Zvrko EZ. Immunoregulatory cytokines and chronic tonsillitis. Bosn J Basic Med Sci. 2013; 13 (4): 230–6. PMID: 24289758.

28. Громова А. Ю., Симбирцева А. С. Полиморфизм генов семейства IL1 человека. Цитокины и воспаление. 2005; (2): 3–12.

29. Цыган В. Н., Иванов А. М., Камилова Т. А., Протасов О. В., Артюшкин С. А. Генетический полиморфизм цитокинов. Вестник Российской военно-медицинской академии. 2010; 30 (2): 211–9.

AUTONOMOUS BIOLUMINESCENT SYSTEMS: PROSPECTS FOR USE IN THE IMAGING OF LIVING ORGANISMS

Osipova ZM[1,2], Shcheglov AS[1,2] ✉, Yampolsky IV[1,2]

[1] Shemyakin–Ovchinnikov Institute of Bioorganic Chemistry, Moscow, Russia

[2] Pirogov Russian National Research Medical University, Moscow, Russia

Bioluminescent systems are increasingly being used for the development of highly sensitive optical imaging techniques *in vivo*. However, it is necessary to inject expensive and unstable synthetic substrates (luciferins) before each analysis for most of the systems applied. Autonomous bacterial and fungal bioluminescent systems, that recently have become available for implementation in eukaryotic cells, in our opinion, may be developed into an effective tool in new technologies of bioluminescent imaging.

✉ Correspondence should be addressed: Alexander S. Shcheglov
Miklukho-Maklaya, 16/10, Moscow, 117997; jukart@mail.ru

АВТОНОМНЫЕ БИОЛЮМИНЕСЦЕНТНЫЕ СИСТЕМЫ: ПЕРСПЕКТИВЫ ИСПОЛЬЗОВАНИЯ В ИМИДЖИНГЕ ЖИВЫХ ОРГАНИЗМОВ

З. М. Осипова[1,2], А. С. Щеглов[1,2] ✉, И. В. Ямпольский[1,2]

[1] Институт биоорганической химии имени М. М. Шемякина и Ю. А. Овчинникова РАН, Москва, Россия

[2] Российский национальный исследовательский медицинский университет имени Н. И. Пирогова, Москва, Россия

Биолюминесцентные системы все чаще применяют для разработки высокочувствительных оптических методов имиджинга *in vivo*. Однако при использовании популярных систем необходимо инъекционно вводить дорогие и малостабильные синтетические субстраты (люциферины) перед каждым анализом. Автономные системы бактерий и грибов, которые недавно стали доступны для работы с эукариотическими клетками, по нашему мнению, могут развиться в полноценный инструмент для создания новых технологий биолюминесцентного имиджинга.

✉ Для корреспонденции: Александр Сергеевич Щеглов
ул. Миклухо-Маклая, д. 16/10, г. Москва, 117997; jukart@mail.ru

The use of *in vivo* optical imaging as a visualization method is growing in modern biomedical research [1, 2]. A non-invasive investigation of animal objects takes place during bioimaging, in which light is emitted as a result of the oxidation of a luciferin molecule (a chemical reaction catalyzed by the protein luciferase), or in response to the excitation of a fluorescent protein by light from an external source. To date the most popular optical reporter proteins are fluorescent (GFP and its homologs of different colors) as well as bioluminescent proteins from insects (FLuc) and marine organisms (RLuc, GLuc). The scope of bioluminescent and fluorescent imaging in medicine based on these proteins is very wide and includes (but is not limited to) the study of gene functions, protein-protein interactions, pathological processes and oncogenesis, drug development, etc. both in cells and tissues, as well as in lab animals real-time assays [3].

A huge variety of fluorescent proteins with different spectral properties available and a large functional toolset based on them (photoactivated, photoswitchable proteins and sensors) are the indisputable benefits of the existing fluorescence imaging technologies [4]. However, the use of fluorescent proteins requires the external source of light, resulting in the sharp decrease of sensitivity due to autofluorescence, phototoxicity and background noise. High-resolution imaging *in vivo* is usually accompanied by a complex invasive procedure [5]. Bioluminescent systems are free from such flaws and therefore successfully compete with fluorescent proteins. The resolution up to a single cell inside a living organism recently became available for bioluminescent imaging. Meanwhile, possible toxicity, low stability and high cost of synthetic luciferins (bioluminescent substrates), which have to be injected into the studied organism prior to every analysis, complicate bioluminescent imaging procedures.

The use of autonomously luminescent systems, for which the biosynthesis of luciferin can be reproduced by genetic engineering in the cells of the studied organism, can become an effective alternative to the existing *in vivo* bioimaging technologies. Unfortunately, among thousands (~10^3) of

glowing species and around 40 (~10^2) different bioluminescence mechanisms, only 10 luciferins' (glowing substrates) structures and 7 luciferases' gene families (~10^1) [6, 7] are discovered to date, and the complete pathway of luciferin biosynthesis is determined only for bacterial [3] and, more recently, for fungal [8] bioluminescent systems. There is some evidence that firefly D-luciferin in insects is synthesized from *p*-benzoquinone and *L*-cysteine [9], but proteins responsible for these processes have not yet been isolated. LRE protein, regenerating D-luciferin from oxyluciferin [10, 11], cannot become an only substitute for the complete biosynthesis pathway of a luminescent substrate from common metabolites. Thus only two luminescent systems are real candidates for the development of new autonomous imaging technologies for now.

Bacterial bioluminescence: from prokaryotes to eukaryotes

Luminescent bacteria are the most widespread glowing organisms, being represented by both marine and terrestrial species. Bacterial bioluminescence is well studied: the cassette of five genes *luxCDABE* is responsible for the generation of light. *LuxAB* gene encodes a heterodimeric bacterial luciferase, *luxC*, *luxD* and *luxE* encode three proteins (reductase, transferase and synthase) which perform biosynthesis of the substrate (dodecanal) for bioluminescence reaction (Fig. 1A). Also, the *frp* gene encoding flavin reductase, responsible for the synthesis of flavin mononucleotide $FMNH_2$, an essential component for the luminescence reaction, can also be included in the cassette [12]. Thus, bacterial bioluminescence could be completely transferred to a new organism and make it glow without the addition of luciferin from the outside. The dependence on the presence of $FMNH_2$ and fatty aldehydes, low brightness and, most importantly, the blue color of luminescence (490 nm), which is inconvenient for *in vivo* deep tissue imaging, are the main disadvantages of this system.

Heterologous gene expression of an autonomous bacterial luminescent system was quickly and successfully implemented in prokaryotic cells [13], however, the large size of the operon, its multigenic organization and the toxicity of the system to the host organism (due to the cytotoxicity of dodecanal) became a fundamental difficulty for its transfer to eukaryotic cells. To solve this problem a large-scale structural rearrangement of the operon was necessary.

The first success in transferring autonomous bacterial luminescence to eukaryotes came with the transgenic luminous yeast *Saccharomyces cerevisiae* [14]. Efficient expression of genes was achieved by codon optimization and addition of linker regions. The choice of a thermostable luciferase of terrestrial species *Photorhabdus luminescens*, which remains active at 37 °C, instead of a marine one from *Vibrio harveyi*, was also important. Nevertheless, the glow was dim and unstable. The first successful adaptation and optimization of genes *luxAB* of bacterial luciferase for HEK293 cells was made after 2 years [15]. And finally, the first application of autonomous bacterial luminescence in mammalian cells for *in vivo* bioimaging with a sensitivity of about 20,000 cells was described in 2010 [16]. In parallel, first autonomously luminescent plants were obtained [17].

However, despite all the work done to further optimize and reduce the operon for its application in mammalian cells (for example, [18]), there is a limited number of examples of the use of bacterial bioluminescence for eukaryotic bioimaging [19–21] due to its low brightness in comparison with non-autonomous systems, for example, D-luciferin-dependent. Recently, after additional changes in the operon and the use of individual plasmids for optimized gene expression a new bacterial system "*co Lux*" was developed with the brightness sufficient for single-cell imaging of HEK293 cells and comparable to that of FLuc luciferase [22, 23]. Low concentration of long chain aldehyde does not lead to adverse toxic effects. The only noticeable effect was a decrease in NADPH concentration in luminous cells (due to its increased consumption during the bioluminescence reaction). The first example of autonomous bioimaging based on a fuse between LuxAB and yellow fluorescent protein YPET was also described [24].

Autonomous luminescence from fungi: an alternative to bacteria

The study of luminous fungi has a long history. For the first time, the structure of fungal luciferin (3-hydroxyhispidin) was established in 2015 [25]. In 2018 fungal luciferase and the complete cycle of luciferin biosynthesis from a widespread secondary plant metabolite caffeic acid were described, followed by the application of this system to developing autonomously luminescent yeast [8] (Fig. 1B).

The luminescence of fungi is based on the genes *hisps*, *h3h*, *luz* (luciferase) and *cph*. *His*ps and *h3h* encode the proteins that
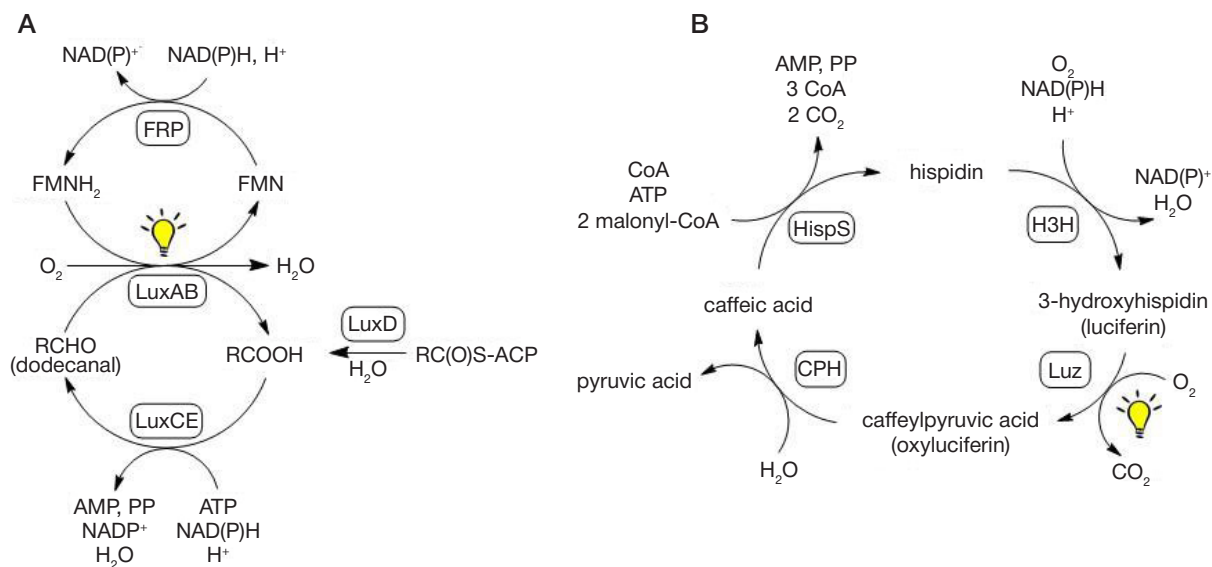

Fig. 1. Biochemical cycles of autonomous bioluminescence in bacteria (**A**) and fungi (**B**)

sequentially assemble hispidin from "caffeic acid" and luciferin (3-hydroxyhyspidin), respectively. *Luz* encodes luciferase, and *cph* is responsible for the protein which converts the product of luciferin oxidation (oxyluciferin) back into caffeic acid. It was shown recently that the expression of only three genes *hisps*, *h3h* and *luz* in *Nicotiana tabacum* plants is sufficient for the creation of bright, autonomously luminescent plants [26, 27]. Unlike the bacterial luminescent system, thorough codon optimization is not necessary to obtain transgenic plants, since the genetic material is originally taken from eukaryotes and the new biosynthetic cycle fits into the metabolism of the host organism.

The first example of autonomously glowing mammalian HEK293T cells based on fungal bioluminescence genes required the use of a mixture of eight plasmids [26]. The resulting low brightness and instability of the glow indicates the necessity to further optimize the genetic constructs to achieve maximum light emission. The total length of the currently used coding sequences of the bacterial bioluminescence system is 6.2 thousand base pairs (kb), whereas for the fungal system this value is about 12.8 kb, but it can be reduced to 9.6 kb in case of utilization of alternative enzymes. Meanwhile, a significant advantage of autonomous fungal bioluminescence is the maximum of luminescence at 540 nm (yellow), which makes this system more promising for *in vivo* bioimaging.

CONCLUSION

The number of instruments for optical imaging in medical research is constantly increasing. In our opinion, more sensitive in vivo bioluminescent imaging in the future may compete with established fluorescence technologies. Actively studied at the moment, autonomous genetically encoded bioluminescent systems based on bacterial or fungal gene cassettes are able to be on a par with existing imaging methods.

References

1. Kiessling F, Pichler BJ, Hauff P, editors. Small animal imaging: Basics and practical guide. 2nd ed. Cham: Springer International Publishing AG, 2017.
2. Kubala E, Menzel MI, Feuerecker B, Glaser SJ, Schwaiger M. Molecular Imaging. In: Canales A, editor. Biophysical techniques in drug discovery. London: Royal Society of Chemistry, 2017; p. 277–306.
3. Kaskova ZM, Tsarkova AS, Yampolsky IV. 1001 lights: luciferins, luciferases, their mechanisms of action and applications in chemical analysis, biology and medicine. Chem Soc Rev. 2016; 45 (21): 6048–77.
4. Specht EA, Braselmann E, Palmer AE. A critical and comparative review of fluorescent tools for live-cell imaging. Annu Rev Physiol. 2017; (79): 93–117.
5. Yeh HW, Ai HW. Development and applications of bioluminescent and chemiluminescent reporters and biosensors. Annu Rev Anal Chem. 2019; (12): 129–50.
6. Shimomura O, Yampolsky I. Back matter. In: Shimomura O, Yampolsky I, editors. Bioluminescence: Chemical principles and methods. 3rd ed. Singapore: World Scientific Co. Pte. Ltd., 2019; p. 381–522.
7. Kotlobay AA, Dubinnyi MA, Purtov KV, Guglya EB, Rodionova NS, et al. Bioluminescence chemistry of fireworm Odontosyllis. Proc Natl Acad Sci USA. 2019; 116 (38): 18911–6.
8. Kotlobay AA, Sarkisyan KS, Mokrushina YA, Marcet-Houben M, Serebrovskaya EO, et al. Genetically encodable bioluminescent system from fungi. Proc Natl Acad Sci USA. 2018; 115 (50): 12728–32.
9. Kanie S, Nakai R, Ojika M, Oba Y. 2-S-cysteinylhydroquinone is an intermediate for the firefly luciferin biosynthesis that occurs in the pupal stage of the japanese firefly, Luciola lateralis. Bioorg Chem. 2018; (80): 223–9.
10. Gomi K, Kajiyama N. Oxyluciferin, a luminescence product of firefly luciferase, is enzymatically regenerated into luciferin. J Biol Chem. 2001; 276 (39): 36508–13.
11. Cheng YY, Liu YJ. Luciferin regeneration in firefly bioluminescence via proton transfer facilitated hydrolysis, condensation and chiral inversion. Chem Phys Chem. 2019; (20): 1719–27.
12. Tu SC. Activity coupling and complex formation between bacterial luciferase and flavin reductases. Photochem Photobiol Sci. 2008; 7 (2): 183–8.
13. Close DM, Xu T, Sayler GS, Ripp S. In vivo bioluminescent imaging (BLI): noninvasive visualization and interrogation of biological processes in living animals. Sensors. 2011; 11 (1): 180–206.
14. Gupta RK, Patterson SS, Ripp S, Simpson ML, Sayler GS. Expression of the Photorhabdus luminescens lux genes (luxA, B, C, D, and E) in Saccharomyces cerevisiae. FEMS Yeast Res. 2003; 4 (3): 305–13.
15. Patterson SS, Dionisi HM, Gupta RK, Sayler GS. Codon optimization of bacterial luciferase (lux) for expression in mammalian cells. J Ind Microbiol Biotechnol. 2005; 32 (3): 115–23.
16. Close DM, Patterson SS, Ripp S, Baek SJ, Sanseverino J, et al. Autonomous bioluminescent expression of the bacterial luciferase gene cassette (lux) in a mammalian cell line. PloS one. 2010; 5 (8): e12441.
17. Krichevsky A, Meyers B, Vainstein A, Maliga P, Citovsky V. Autoluminescent plants. PloS one. 2010; 5 (11): e15461.
18. Xu T, Ripp S, Sayler GS, Close DM. Expression of a humanized viral 2A-mediated lux operon efficiently generates autonomous bioluminescence in human cells. PLoS One. 2014; 9 (5): e96347.
19. Class B, Thorne N, Aguisanda F, Southall N, McKew JC, et al. High-throughput viability assay using an autonomously bioluminescent cell line with a bacterial lux reporter. J Lab Autom. 2015; 20 (2): 164–74.
20. Xu T, Young A, Marr E, Sayler G, Ripp S, et al. A rapid and reagent-free bioassay for the detection of dioxin-like compounds and other aryl hydrocarbon receptor (AhR) agonists using autobioluminescent yeast. Anal Bioanal Chem. 2018; 410 (4): 1247–56.
21. Xu T, Kirkpatrick A, Toperzer J, Ripp S, Close D. Improving estrogenic compound screening efficiency by using self-modulating, continuously bioluminescent human cell bioreporters expressing a synthetic luciferase. Toxicol Sci. 2019; 168 (2): 551–60.
22. Gregor C, Gwosch KC, Sahl SJ, Hell SW. Strongly enhanced bacterial bioluminescence with the ilux operon for single-cell imaging. Proc Natl Acad Sci USA. 2018; 115 (5): 962–7.
23. Gregor C, Pape JK, Gwosch KC, Gilat T, Sahl SJ, et al. Autonomous bioluminescence imaging of single mammalian cells with the bacterial bioluminescence system. bioRxiv. 2019: 798108.
24. Srinivasan P, Griffin NM, Joshi P, Thakur DP, Nguyen-Le A, et al. An Autonomous Molecular Bioluminescent Reporter (AMBER) for voltage imaging in freely moving animals. bioRxiv. 2019: 845198.
25. Purtov KV, Petushkov VN, Baranov MS, Mineev KS, Rodionova NS, et al. The chemical basis of fungal bioluminescence. Angew Chem Int Ed. 2015; 54 (28): 8124–8.
26. Mitiouchkina T, Mishin AS, Somermeyer LG, Markina NM, Chepurnyh TV, et al. Plants with self-sustained luminescence. bioRxiv. 2019: 809376.
27. Khakhar A, Starker C, Chamness J, Lee N, Stokke S. Building customizable auto-luminescent luciferase-based reporters in plants. bioRxiv. 2019: 809533.

Литература

1. Kiessling F, Pichler BJ, Hauff P, editors. Small animal imaging: Basics and practical guide. 2nd ed. Cham: Springer International Publishing AG, 2017.
2. Kubala E, Menzel MI, Feuerecker B, Glaser SJ, Schwaiger M. Molecular Imaging. In: Canales A, editor. Biophysical techniques in drug discovery. London: Royal Society of Chemistry, 2017; p. 277–306.
3. Kaskova ZM, Tsarkova AS, Yampolsky IV. 1001 lights: luciferins, luciferases, their mechanisms of action and applications in chemical analysis, biology and medicine. Chem Soc Rev. 2016; 45 (21): 6048–77.
4. Specht EA, Braselmann E, Palmer AE. A critical and comparative review of fluorescent tools for live-cell imaging. Annu Rev Physiol. 2017; (79): 93–117.
5. Yeh HW, Ai HW. Development and applications of bioluminescent and chemiluminescent reporters and biosensors. Annu Rev Anal Chem. 2019; (12): 129–50.
6. Shimomura O, Yampolsky I. Back matter. In: Shimomura O, Yampolsky I, editors. Bioluminescence: Chemical principles and methods. 3rd ed. Singapore: World Scientific Co. Pte. Ltd., 2019; p. 381–522.
7. Kotlobay AA, Dubinnyi MA, Purtov KV, Guglya EB, Rodionova NS, et al. Bioluminescence chemistry of fireworm Odontosyllis. Proc Natl Acad Sci USA. 2019; 116 (38): 18911–6.
8. Kotlobay AA, Sarkisyan KS, Mokrushina YA, Marcet-Houben M, Serebrovskaya EO, et al. Genetically encodable bioluminescent system from fungi. Proc Natl Acad Sci USA. 2018; 115 (50): 12728–32.
9. Kanie S, Nakai R, Ojika M, Oba Y. 2-S-cysteinylhydroquinone is an intermediate for the firefly luciferin biosynthesis that occurs in the pupal stage of the japanese firefly, Luciola lateralis. Bioorg Chem. 2018; (80): 223–9.
10. Gomi K, Kajiyama N. Oxyluciferin, a luminescence product of firefly luciferase, is enzymatically regenerated into luciferin. J Biol Chem. 2001; 276 (39): 36508–13.
11. Cheng YY, Liu YJ. Luciferin regeneration in firefly bioluminescence via proton transfer facilitated hydrolysis, condensation and chiral inversion. Chem Phys Chem. 2019; (20): 1719–27.
12. Tu SC. Activity coupling and complex formation between bacterial luciferase and flavin reductases. Photochem Photobiol Sci. 2008; 7 (2): 183–8.
13. Close DM, Xu T, Sayler GS, Ripp S. In vivo bioluminescent imaging (BLI): noninvasive visualization and interrogation of biological processes in living animals. Sensors. 2011; 11 (1): 180–206.
14. Gupta RK, Patterson SS, Ripp S, Simpson ML, Sayler GS. Expression of the Photorhabdus luminescens lux genes (luxA, B, C, D, and E) in Saccharomyces cerevisiae. FEMS Yeast Res. 2003; 4 (3): 305–13.
15. Patterson SS, Dionisi HM, Gupta RK, Sayler GS. Codon optimization of bacterial luciferase (lux) for expression in mammalian cells. J Ind Microbiol Biotechnol. 2005; 32 (3): 115–23.
16. Close DM, Patterson SS, Ripp S, Baek SJ, Sanseverino J, et al. Autonomous bioluminescent expression of the bacterial luciferase gene cassette (lux) in a mammalian cell line. PloS one. 2010; 5 (8): e12441.
17. Krichevsky A, Meyers B, Vainstein A, Maliga P, Citovsky V. Autoluminescent plants. PloS one. 2010; 5 (11): e15461.
18. Xu T, Ripp S, Sayler GS, Close DM. Expression of a humanized viral 2A-mediated lux operon efficiently generates autonomous bioluminescence in human cells. PLoS One. 2014; 9 (5): e96347.
19. Class B, Thorne N, Aguisanda F, Southall N, McKew JC, et al. High-throughput viability assay using an autonomously bioluminescent cell line with a bacterial lux reporter. J Lab Autom. 2015; 20 (2): 164–74.
20. Xu T, Young A, Marr E, Sayler G, Ripp S, et al. A rapid and reagent-free bioassay for the detection of dioxin-like compounds and other aryl hydrocarbon receptor (AhR) agonists using autobioluminescent yeast. Anal Bioanal Chem. 2018; 410 (4): 1247–56.
21. Xu T, Kirkpatrick A, Toperzer J, Ripp S, Close D. Improving estrogenic compound screening efficiency by using self-modulating, continuously bioluminescent human cell bioreporters expressing a synthetic luciferase. Toxicol Sci. 2019; 168 (2): 551–60.
22. Gregor C, Gwosch KC, Sahl SJ, Hell SW. Strongly enhanced bacterial bioluminescence with the ilux operon for single-cell imaging. Proc Natl Acad Sci USA. 2018; 115 (5): 962–7.
23. Gregor C, Pape JK, Gwosch KC, Gilat T, Sahl SJ, et al. Autonomous bioluminescence imaging of single mammalian cells with the bacterial bioluminescence system. bioRxiv. 2019: 798108.
24. Srinivasan P, Griffin NM, Joshi P, Thakur DP, Nguyen-Le A, et al. An Autonomous Molecular Bioluminescent Reporter (AMBER) for voltage imaging in freely moving animals. bioRxiv. 2019: 845198.
25. Purtov KV, Petushkov VN, Baranov MS, Mineev KS, Rodionova NS, et al. The chemical basis of fungal bioluminescence. Angew Chem Int Ed. 2015; 54 (28): 8124–8.
26. Mitiouchkina T, Mishin AS, Somermeyer LG, Markina NM, Chepurnyh TV, et al. Plants with self-sustained luminescence. bioRxiv. 2019: 809376.
27. Khakhar A, Starker C, Chamness J, Lee N, Stokke S. Building customizable auto-luminescent luciferase-based reporters in plants. bioRxiv. 2019: 809533.

THE POTENTIAL OF CD4+ REGULATORY T CELLS FOR THE THERAPY OF AUTOIMMUNE DISEASES

Churov AV[1] ✉, Siutkina AI[2], Mamashov KY[3], Oleinik EK[1]

[1] Karelian Research Centre of the Russian Academy of Sciences, Petrozavodsk, Russia

[2] Perm State Pharmaceutical Academy, Perm, Russia

[3] Kemerovo State Medical University, Kemerovo, Russia

Despite the considerable progress in the therapy of autoimmune pathologies, the existing methods are associated with the risk of serious adverse events. We think that regulatory T cells hold great promise for the therapy of disorders caused by a breakdown in immunological self-tolerance. This article aims at estimating the possible challenges facing Treg-based clinical approaches and offers solutions to the technical issues associated with the use of these cells in the therapy of autoimmune diseases.

Keywords: regulatory T cells, FOXP3, autoimmune disease, immunotherapy, cell therapy, CAR-Treg therapy, CRISPR/Cas9

✉ Correspondence should be addressed: Alexey V. Churov
Pushkinskaya, 11, Petrozavodsk, 186910; achurou@yandex.ru

ВОЗМОЖНОСТИ ПРИМЕНЕНИЯ CD4+-РЕГУЛЯТОРНЫХ Т-КЛЕТОК В ТЕРАПИИ АУТОИММУННЫХ ЗАБОЛЕВАНИЙ

А. В. Чуров[1] ✉, А. И. Сюткина[2], К. Ы. Мамашов[3], Е. К. Олейник[1]

[1] Федеральный исследовательский центр «Карельский научный центр Российской академии наук», Петрозаводск, Россия

[2] Пермская государственная фармацевтическая академия, Пермь, Россия

[3] Кемеровский государственный медицинский университет, Кемерово, Россия

На сегодняшний день достигнуты значительные успехи в терапии аутоиммунных патологий, однако существующие методы сопряжены с риском возникновения тяжелых побочных эффектов. Применение Treg-клеток, на наш взгляд, представляет значительную перспективу в терапии состояний, связанных с нарушением аутотолерантности. В работе дана оценка возможных трудностей использования клинического подхода на основе Treg-клеток и предложены пути решения научно-технических задач, возникающих при применении Treg в терапии аутоиммунных заболеваний.

Ключевые слова: регуляторные Т-клетки, FOXP3, аутоиммунное заболевание, иммунотерапия, клеточная терапия, CAR-Treg-терапия, CRISPR/Cas9

✉ Для корреспонденции: Алексей Викторович Чуров
ул. Пушкинская, д. 11, г. Петрозаводск, 186910; achurou@yandex.ru

Autoimmune diseases constitute a group of disorders arising from an imbalance in the immune system and a breakdown of self-tolerance mechanisms; these defects trigger a cascade of immune reactions against the body's own tissues.

At present, the treatment of choice for autoimmune disorders includes immunosuppressants, disease modifying antirheumatic drugs (DMARD) or genetically engineered therapeutics. However, these drugs are associated with the risk of serious adverse events. Regulatory T cells (Tregs) prevent immune responses to self-antigens, keep inflammation in check and thus block the development of autoimmune disorders by inducing and maintaining peripheral tolerance. Tregs constitute 3–5% of the peripheral CD4+ T-cell population and can inhibit activation, proliferation and effector functions of CD4+ and CD8+ T cells, natural killer cells, B lymphocytes, and antigen presenting cells (APCs) [1]. In patients with autoimmune disorders, Treg levels are aberrant and Treg function is often weakened or impaired [2, 3]. Experiments conducted in the mouse models of autoimmune diseases have demonstrated that adoptive transfer of Treg cells isolated from healthy mice has a good therapeutic effect [4]. The positive outcomes of preclinical trials have raised hopes for Treg-based approaches to the therapy of autoimmune diseases.

The current state of research in the field and the limitations of the existing treatments for autoimmune disorders dictate the need for novel, highly specific, safe and effective approaches. We believe that Tregs can become the key component in the combination therapy of autoimmune disorders once the existing technical hurdles are overcome.

Based on the results of research and clinical trials, we offer our opinion on the prospects of harnessing Tregs for treating autoimmune diseases, assess challenges facing this approach and offer potential solutions.

Regulatory T cells and suppressive mechanisms

The key Treg markers are CD25 (a membrane antigen) and FOXP3 (an intracellular transcription factor). *FOXP3* expression enables Tregs to exert their suppressive function [5], whereas CD25 is an IL2 receptor α-chain, whose expression is correlated with proliferation and differentiation of Tregs [6].

Treg differentiation occurs in the thymus and peripheral tissues. After leaving the thymus, Tregs migrate into the blood stream and to peripheral lymphoid organs during the first 2 or 3 days of their life [7], where those with the CD4+FOXP3– phenotype can further differentiate into induced Tregs that actively express FOXP3 (CD4+CD25+FOXP3+).

Tregs exert their suppressive activity against immunocytes either via direct contact with the latter or by secreting bioactive molecules. There are 4 major mechanisms involved: a direct cytotoxic effect mediated by PD-1/PD-L1, OX40/OX40L and granzyme B; induction of metabolic changes in the target cells (CD25, CD39, tryptophan); secretion of inhibiting cytokines (IL10, TGFβ and IL35); suppression of APCs (CD80 and CD86/CTLA-4) [8].

Clinical trials of Treg immunotherapies

Clinical trials of Treg immunotherapies for autoimmune diseases began less than a decade ago. They sought to investigate technical challenges associated with Treg infusion, as well as to assess its safety and efficacy. In these clinical trials, a general approach is used: sorting of Treg cells, polyclonal expansion of Treg cells, Treg dose selection and infusion into patients. However, this approach does not account for the functional state of the used cells. The lack of stable FOXP3 expression and sustained suppressive activity are the common problems facing this approach to cell therapy and often the root cause of its low efficacy.

Published in 2012, a phase I/IIa open-label multicenter clinical study known as CATS1 conducted in 4 groups of 20 patients with symptomatic refractory Crohn's disease has demonstrated the safety of Treg infusions [9] In February 2018, a double-blind placebo-controlled trial (TRIBUTE; NCT03185000) was started to assess the effect of CD4+CD25+CD127lowCD45RA+ Treg immunotherapy in patients with Crohn's disease resistant to at least two standard regimens.

Trials of Treg immunotherapy for type 1 diabetes mellitus (DM1) have produced favorable results. They began in 2014; the first trial was a phase I randomized study aimed at assessing the safety and feasibility of autologous Tregs isolated *ex vivo* from patients aged 7 to 18 years with a recently diagnosed DM1 [10]. This one-year-long trial did not reveal any serious adverse effects of Treg infusions and confirmed their safety. Besides, 8 of 12 patients participating in the trial showed signs of remission.

Another study carried out at the University of California and Yale University also investigated the efficacy and safety of Treg-based immunotherapy in adult patients with DM1; its results were published in 2015 [11]. Fourteen patients recruited for the study (6 females and 8 males aged 18–43 years) were distributed into 4 groups depending on the Treg dose. The participants received infusions of polyclonal Treg cells with the CD4+CD127lo/–CD25+ phenotype in the amount of 0.05×10^8 to 26×10^8 cells. Up to 25% of the cells (from their peak amount) were retained in the peripheral blood of the recipients for the entire year following the adoptive transfer. No infusion-related or adverse effects were observed [11]. However, the optimal number of cells for infusion was not determined in the study and the effect of Treg therapy on the function of pancreatic β-cells was not established. A new phase II multicenter randomized double-blind placebo-controlled ongoing clinical trial (NCT02691247) is now attempting to fil this knowledge gap. The use of umbilical cord Treg cells with liraglutide and insulin therapies in adult/elderly patients with autoimmune diabetes is now being assessed in two phase I/II randomized open-label trials NCT03011021 and NCT02932826 (Central South University, Changsha).

In addition, two trials of immunotherapies with autologous polyclonal Treg cell infusions have already been initiated to test its efficacy and safety in patients with active pemphigus (NCT03239470) and autoimmune hepatitis (NCT02704338).

Prospects and challenges of Treg immunotherapy

The feasibility of Treg immunotherapy in patients with autoimmune pathology and the relative safety of this approach have been demonstrated in a few pilot clinical trials. Further research should focus on how immunosuppressive therapies can be combined with Treg infusions as some immunosuppressants affect Treg properties in a dose-dependent manner and can reduce the efficacy of these cells [12]. The use of Treg cells in combination with other therapies tailored to an individual patient holds the greatest promise for the future.

One of the major challenges impeding successful translation of Tregs into the clinic is production of stable Treg populations with sustained immunosuppressive activity. Currently, Tregs are isolated from peripheral blood cells and expanded *ex vivo*. Peripheral blood cells are heterogeneous and largely represented by the cells with induced FOXP3 expression.

Improving the specificity of Treg therapy is another important task. Treg functional activity is essentially antigen-specific. Antigen presentation leads to Treg activation and enhances the expression of membrane-bound inhibitory molecules that exert a suppressive effect on the target cell.

This phenomenon has been demonstrated *in vivo* for CTLA-4, the key inhibiting molecule of Treg cells. CTLA-4 is constitutively expressed by Tregs and T-effector cells [13]. Tregs control activation of T effectors by blocking their access to the co-stimulating molecules CD80/86 on the APC membrane. CTLA-4 competitively blocks CD80/86 on the APC surface, binds and transports CD80/86 into the cell in the process of trans-endocytosis. Thus, Tregs can regulate the APC phenotype and effectively restrain the CD28-dependent activation of T effectors. The competitive effect is achieved due to the fact that CTLA-4 expression on antigen-specific Treg cells is significantly higher than on T cells. The capture of CD80/86 by Treg is triggered by self-antigen presentation [13].

Clinical trials of Treg immunotherapy typically assess the effect of infusions of polyclonally expanded Treg cells with unknown antigen specificity. The majority of fused clones cannot effectively inhibit effector cells and suppress immune response. Besides, with polyclonal lymphocytes there is a high

risk of adverse events, such as systemic immune suppression and reactivation of latent infection. Thus, clinical approaches based on polyclonal Treg cells are inevitably weak.

The past decade has seen the emergence of new highly effective therapeutic approaches based on adoptive cell transfer that can overcome the barriers preventing the use of Treg cells in the treatment of autoimmune diseases. Such approaches include genetically engineered effector T cells expressing highly specific chimeric antigen receptors (CARs), as well as genome editing techniques, such as CRISPR/Cas9.

T cells modified with CARs are successfully used in the therapy of some cancers. Such modification can also be effectively applied to Treg cells. CAR-Tregs have enormous potential: due to their antigen specificity, they can significantly improve the efficacy of treatment while causing very mild side effects [14]. In comparison with polyclonal Tregs, CAR-Tregs can bind to a specific protein on the membrane of the target cell. However, the manufacturing of CAR-Treg cells with sustained suppressive activity is technologically demanding. Besides, similarly to CAR-T cells, there is a risk of inducing the so-called cytokine storm and neurotoxicity. This is a very serious obstacle preventing the use of CAR-Tregs in the clinical setting. Moreover, identification and selection of targets for targeted therapy also pose a difficulty, especially in autoimmune diseases due to some aspects of their pathogenesis and the lack of knowledge of their etiology.

Previously, we mentioned that it is hard to produce a stable fraction of Treg cells. CRISPR/Cas9 (clustered, regularly interspaced, short palindromic repeats / CRISPR-associated protein) technologies or their advanced counterparts can offer a solution. The first preclinical studies of using CRISPR/Cas9 for immunotherapy have yielded encouraging results. Attempts are being made to stabilize and enhance the functional activity of Treg cells. It is known that one of the major challenges is maintaining Treg viability *ex vivo*, which directly depends on the stability of *FOXP3* expression. Here, the CRISPR/Cas9 technology can be recommended for the editing of genes participating in the regulation of transcription programs controlling Treg differentiation and the level of *FOXP3* expression. A CRISPR/Cas9 system is highly specific due to small RNAs that guide Cas9 precisely into the target genome fragment [15]. In the case of Tregs and *FOXP3*, the CRISPR/Cas9 technology can also be employed for editing the epigenome. An experiment in the primary T cells of mice has shown that a modification of a baseline technology, specifically the use of a mutant Cas9 without endonuclease activity (dead Cas9; CRISPR/dCas9), can induce the desired epigenetic changes promoting stabilization of *Foxp3* expression [16].

CONCLUSIONS

The first results of clinical trials have demonstrated the relative safety of Treg-based therapy for autoimmune diseases. Research studies of the efficacy of polyclonally expanded Treg cells in patients with Crohn's disease, type 1 diabetes mellitus and some other autoimmune disorders have yielded inspiring results. However, the majority of clinical studies of Treg safety were conducted on small groups of patients and the approach itself has a few serious drawbacks, including its low antigen specificity in the first place. Further research should focus on the unsolved problems of adoptive Treg transfer, such as the search for the effective Treg dose, the improvement of the method's specificity by identification of novel molecular targets and the use of antigen-specific Treg infusions, stabilization of Treg immunosuppressive activity and achieving a sustained response to cell therapy in patients with autoimmune diseases.

References

1. Sakaguchi S, Miyara M, Costantino CM, Hafler DA. FOXP3+ regulatory T cells in the human immune system. Nat Rev Immunol. 2010; 10 (7): 490–500. DOI:10.1038/nri2785.

2. Venken K, Hellings N, Liblau R, Stinissen P. Disturbed regulatory T cell homeostasis in multiple sclerosis. Trends Mol Med. 2010; 16 (2): 58–68. DOI: 10.1016/j.molmed.2009.12.003.

3. Kravchenko PN, Zhulai GA, Churov AV, Oleinik EK, Oleinik VM, Barysheva OY, et al. Subpopulations of regulatory T-lymphocytes in the peripheral blood of patients with rheumatoid arthritis. Vestnik Rossiiskoi Akademii Meditsinskikh Nauk. 2016; 71 (2): 148–153. DOI: 10.15690/vramn656.

4. Miyara M, Gorochov G, Ehrenstein M, Musset L, Sakaguchi S, Amoura Z. Human FoxP3+ regulatory T cells in systemic autoimmune diseases. Autoimmunity Reviews. 2011; 10 (12): 744–55. DOI:10.1016/j.autrev.2011.05.004.

5. Fontenot J, Gavin M, Rudensky A. Foxp3 programs the development and function of CD4+CD25+ regulatory T cells. Nature Immunology. 2003; 4 (4): 330–36. DOI: 10.1038/ni904.

6. Nazzal, Gradolatto, Truffault, Bismuth, Berrih-Aknin. Human thymus medullary epithelial cells promote regulatory T-cell generation by stimulating interleukin-2 production via ICOS ligand. Cell Death Dis. 2014; (5): e1420. DOI:10.1038/cddis.2014.37.

7. Famili F, Wiekmeijer A-S, Staal F. The development 719 of T cells from stem cells in mice and humans. Future Science OA. 2017; (3): FSO186. DOI:10.4155/fsoa-2016-0095.

8. Christoffersson G, von Herrath M. Regulatory Immune Mechanisms beyond Regulatory T Cells. Trends in Immunology. 2019; 40 (6): 482–91. DOI:10.1016/j.it.2019.04.005.

9. Desreumaux P, Foussat A, Allez M, Beaugerie L, Hébuterne X, Bouhnik Y, et al. Safety and efficacy of antigen-specific regulatory T-cell therapy for patients with refractory Crohn's disease. Gastroenterology. 2012; (143): 1207–17. DOI:10.1053/j.gastro.2012.07.116.

10. Marek-Trzonkowska N, Myśliwiec M, Dobyszuk A, Grabowska M, Derkowska I, et al. Therapy of type 1 diabetes with CD4(+)CD25(high)CD127-regulatory T cells prolongs survival of pancreatic islets — results of one year follow-up. Clinical immunology (Orlando, Fla). 2014; (153): 23–30. DOI:10.1016/j.clim.2014.03.016.

11. Bluestone JA, Buckner JH, Fitch M, Gitelman SE, Gupta S, Hellerstein MK, et al. Type 1 diabetes immunotherapy using polyclonal regulatory T cells. Science translational medicine. 2016; (7): 315ra189. DOI:10.1126/scitranslmed.aad4134.

12. Scottà C, Fanelli G, Hoong SJ, Romano M, Lamperti EN, Sukthankar M, et al. Impact of immunosuppressive drugs on the therapeutic efficacy of ex vivo expanded human regulatory T cells. Haematologica. 2016; (101): 91–100. DOI:10.3324/haematol.2015.128934.

13. Ovcinnikovs V, Ross EM, Petersone L, Edner NM, Heuts F, Ntavli E. CTLA-4–mediated transendocytosis of costimulatory molecules primarily targets migratory dendritic cells. Science Immunology. 2019; 4 (35): eaaw0902. DOI:10.1126/sciimmunol.aaw0902.

14. Arpaia N, Campbell C, Fan X, Dikiy S, Veeken J van der, deRoos P, et al. Metabolites produced by commensal bacteria promote peripheral regulatory T-cell generation. Nature. 2013; (504): 451–5. DOI:10.1038/nature12726.

15. Jinek M, Chylinski K, Fonfara I, Hauer M, Doudna JA, Charpentier E. A Programmable Dual-RNA-Guided DNA Endonuclease in Adaptive Bacterial Immunity. Science. 2012; 337 (6096): 816–21. DOI:10.1126/science.1225829.

16. Okada M, Kanamori M, Someya K, Nakatsukasa H, Yoshimura A. Stabilization of Foxp3 expression by CRISPR-dCas9-based epigenome editing in mouse primary T cells. Epigenetics Chromatin. 2017; (10): 24. DOI: 10.1186/s13072-017-0129-1.

Литература

1. Sakaguchi S, Miyara M, Costantino CM, Hafler DA. FOXP3⁺ regulatory T cells in the human immune system. Nat Rev Immunol. 2010; 10 (7): 490–500. DOI:10.1038/nri2785.
2. Venken K, Hellings N, Liblau R, Stinissen P. Disturbed regulatory T cell homeostasis in multiple sclerosis. Trends Mol Med. 2010; 16 (2): 58–68. DOI: 10.1016/j.molmed.2009.12.003.
3. Кравченко П. Н., Жулай Г. Ф., Чуров А. В., Олейник Е. К., Олейник В. М., Барышева О. Ю. и др. Субпопуляции регуляторных Т-лимфоцитов в периферической крови больных ревматоидным артритом. Вестник РАМН. 2016; 71 (2): 148–53. DOI: 10.15690/vramn656.
4. Miyara M, Gorochov G, Ehrenstein M, Musset L, Sakaguchi S, Amoura Z. Human FoxP3⁺ regulatory T cells in systemic autoimmune diseases. Autoimmunity Reviews. 2011; 10 (12): 744–55. DOI:10.1016/j.autrev.2011.05.004.
5. Fontenot J, Gavin M, Rudensky A. Foxp3 programs the development and function of CD4⁺CD25⁺ regulatory T cells. Nature Immunology. 2003; 4 (4): 330–36. DOI: 10.1038/ni904.
6. Nazzal, Gradolatto, Truffault, Bismuth, Berrih-Aknin. Human thymus medullary epithelial cells promote regulatory T-cell generation by stimulating interleukin-2 production via ICOS ligand. Cell Death Dis. 2014; (5): e1420. DOI:10.1038/cddis.2014.37.
7. Famili F, Wiekmeijer A-S, Staal F. The development 719 of T cells from stem cells in mice and humans. Future Science OA. 2017; (3): FSO186. DOI:10.4155/fsoa-2016-0095.
8. Christoffersson G, von Herrath M. Regulatory Immune Mechanisms beyond Regulatory T Cells. Trends in Immunology. 2019; 40 (6): 482–91. DOI:10.1016/j.it.2019.04.005.
9. Desreumaux P, Foussat A, Allez M, Beaugerie L, Hébuterne X, Bouhnik Y, et al. Safety and efficacy of antigen-specific regulatory T-cell therapy for patients with refractory Crohn's disease. Gastroenterology. 2012; (143): 1207–17. DOI:10.1053/j.gastro.2012.07.116.
10. Marek-Trzonkowska N, Myśliwiec M, Dobyszuk A, Grabowska M, Derkowska I, et al. Therapy of type 1 diabetes with CD4(+)CD25(high)CD127-regulatory T cells prolongs survival of pancreatic islets — results of one year follow-up. Clinical immunology (Orlando, Fla). 2014; (153): 23–30. DOI:10.1016/j.clim.2014.03.016.
11. Bluestone JA, Buckner JH, Fitch M, Gitelman SE, Gupta S, Hellerstein MK, et al. Type 1 diabetes immunotherapy using polyclonal regulatory T cells. Science translational medicine. 2016; (7): 315ra189. DOI:10.1126/scitranslmed.aad4134.
12. Scottà C, Fanelli G, Hoong SJ, Romano M, Lamperti EN, Sukthankar M, et al. Impact of immunosuppressive drugs on the therapeutic efficacy of ex vivo expanded human regulatory T cells. Haematologica. 2016; (101): 91–100. DOI:10.3324/haematol.2015.128934.
13. Ovcinnikovs V, Ross EM, Petersone L, Edner NM, Heuts F, Ntavli E. CTLA-4–mediated transendocytosis of costimulatory molecules primarily targets migratory dendritic cells. Science Immunology. 2019; 4 (35): eaaw0902. DOI:10.1126/sciimmunol.aaw0902.
14. Arpaia N, Campbell C, Fan X, Dikiy S, Veeken J van der, deRoos P, et al. Metabolites produced by commensal bacteria promote peripheral regulatory T-cell generation. Nature. 2013; (504): 451–5. DOI:10.1038/nature12726.
15. Jinek M, Chylinski K, Fonfara I, Hauer M, Doudna JA, Charpentier E. A Programmable Dual-RNA-Guided DNA Endonuclease in Adaptive Bacterial Immunity. Science. 2012; 337 (6096): 816–21. DOI:10.1126/science.1225829.
16. Okada M, Kanamori M, Someya K, Nakatsukasa H, Yoshimura A. Stabilization of Foxp3 expression by CRISPR-dCas9-based epigenome editing in mouse primary T cells. Epigenetics Chromatin. 2017; (10): 24. DOI: 10.1186/s13072-017-0129-1.

HEPATOPROTECTIVE EFFECT OF POLYPHENOLS IN RATS WITH EXPERIMENTAL THIOACETAMIDE-INDUCED TOXIC LIVER PATHOLOGY

Dergachova DI[1], Klein OI[1], Marinichev AA[1,2], Gessler NN[1], Bogdanova ES[3], Smirnova MS[3] ✉, Isakova EP[1], Deryabina YI[1]

[1] Bach Institute of Biochemistry, Federal Research Centre "Fundamentals of Biotechnology" RAS, Moscow, Russia

[2] Dmitry Mendeleev University of Chemical Technology, Moscow, Russia

[3] Vavilov Institute of General Genetics, Moscow, Russia

Non-alcoholic fatty liver disease is associated with a number of disorders (diabetes, obesity, cardiovascular diseases), and can also be induced by drugs or toxic compounds. Recently the important branch of medicine is the search for effective means of prevention and treatment of fatty hepatosis. Our work was aimed to study the effect of some biologically active natural polyphenols (resveratrol and pinosylvin stilbenes as well as dihydromyricetin dihydroflavonol) on the function and histologic features of the liver. In the experimental model of thioacetamide-induced toxic hepapitis, the male rats of the *Wistar* line daily received the effective doses of polyphenols intragastically by gavage together with 0.05% thioacetamide added to drinking water. All studied polyphenols contributed to stabilization of rat weight and a two-fold significant ($p < 0.05$) decrease in the level of direct bilirubin in the blood serum of animals treated with thioacetamide. Histological analysis of the liver confirmed a decrease in inflammation and hemorrhage in animals treated with polyphenols amid continued administration of thioacetamide for 30 days. Based on the data obtained, it can be concluded that the natural polyphenols which belong to the classes of dihydroflavonols (dihydromyricetin) and stilbenes (resveratrol and pinosylvin) have a positive effect on liver function in the experimental model of toxic hepatosis. The studied polyphenols can be considered as potential hepatoprotective drugs used as a part of the liver diseases complex therapy.

Keywords: polyphenol, resveratrol, dihydromyricetin, pinosylvin, thioacetamide, steatosis, hepatitis, rat

ГЕПАТОПРОТЕКТОРНОЕ ДЕЙСТВИЕ ПОЛИФЕНОЛОВ ПРИ ЭКСПЕРИМЕНТАЛЬНОЙ ТОКСИЧЕСКОЙ ПАТОЛОГИИ ПЕЧЕНИ, ВЫЗВАННОЙ ТИОАЦЕТАМИДОМ

Д. И. Дергачева[1], О. И. Кляйн[1], А. А. Мариничев[1,2], Н. Н. Гесслер[1], Е. С. Богданова[3], М. С. Смирнова[3] ✉, Е. П. Исакова[1], Ю. И. Дерябина[1]

[1] Институт биохимии имени А. Н. Баха, Федеральный исследовательский центр «Фундаментальные основы биотехнологии» РАН, Москва, Россия

[2] Московский химико-технологический университет имени Д. И. Менделеева, Москва, Россия

[3] Институт общей генетики имени Н. И. Вавилова, Москва, Россия

Неалкогольная жировая дисфункция печени сопровождает целый ряд заболеваний (диабет, ожирение, кардиоваскулярные болезни), а также может развиваться под действием лекарственных препаратов или токсических соединений. Актуальным направлением современной медицины является поиск эффективных средств профилактики и лечения жирового гепатоза. Целью работы было исследовать действие некоторых биологически активных природных полифенолов — стильбенов ресвератрола и пиносильвина, а также дигидрофлавонола дигидромирицетина — на функциональное состояние и гистологическую картину печени. В модели токсического гепатита, вызываемого введением гепатотоксиканта тиоацетамида, самцам крыс линии *Wistar* внутрижелудочно ежедневно вводили зондом эффективные дозы полифенолов на фоне добавления тиоацетамида к питьевой воде в концентрации 0,05%. Все исследованные полифенолы способствовали стабилизации веса крыс и двухкратному достоверному ($p < 0,05$) снижению уровня прямого билирубина в сыворотке крови животных, получавших тиоацетамид. Гистологическое исследование печени подтвердило замедление воспалительных процессов и уменьшение кровоизлияний у животных, получавших полифенолы на фоне продолжающегося введения тиоацетамида в течение 30 дней. На основании полученных данных можно сделать выводы, что природные полифенолы класса дигидрофлавонолов (дигидромирицетин) и стильбенов (ресвератрол и пиносильвин) оказывают положительное воздействие на функции печени в модели экспериментального токсического гепатоза; исследованные полифенолы можно рассматривать в качестве потенциальных гепатопротекторов в составе комплексной терапии при заболеваниях печени.

Ключевые слова: полифенол, ресвератрол, дигидромирицетин, пиносильвин, тиоацетамид, стеатоз, гепатит, крыса

Liver diseases include a wide range of pathologies, from fatty hepatosis (steatosis) and hepatitis to liver cirrhosis and hepatocellular carcinoma. These disorders are common all over the world and have high social significance [1]. Hepatic failure, especially its severe form caused by liver cirrhosis, is on the 12th place among the causes of deaths in the world [2]. The cirrhosis not only leads to impaired liver function, but also causes the hepatic encephalopathy syndrome which is associated with cognitive function and psychomotor impairment. Hepatic syndrome can be a cause of disability [3]. Over the past 10 years, non-alcoholic fatty liver dysfunction has become the main type of the liver chronic lesions. It has been revealed in more than 30% of population [4]. Fatty hepatosis is statistically associated with diabetes mellitus, cardiovascular diseases and obesity. The occurrence of fatty hepatosis is provoked by the use of drugs and exposure to toxicants. Association of steatosis with other chronic diseases, such as sleep apnea, colorectal cancer, osteoporosis, psoriasis and endocrine disorders, has been revealed [5]. Non-alcoholic fatty liver disease is a non-specific response of hepatocytes to toxic effects. It is characterized by an abnormal fat accumulation in the liver. In patients with severe fatty liver dystrophy, steatomas and proliferation of connective tissue can be observed, which lead to functional disorders of the liver and associated systemic pathologies.

Multiple signaling and metabolic pathways involved in the regulation of liver function make it possible to select therapeutic targets [6]. Various agents are used as hepatoprotective compounds as part of complex therapy: antibiotics (neomycin, paromycin, metronidazole, vancomycin, rifaximin) [7] and poorly digested disaccharides (lactulose, lactitol) [8], natural amino acids and nitrogen metabolites (ornithine aspartate, branched chain amino acids) [9], modulators of gut microbiota (probiotics, synbiotics) [10], bile acids derivatives and thyroid hormone receptors β-agonists [11]. However, the currently existing means for the liver pathologies of varying severity and etiology prevention and treatment include mainly symptomatic drugs of a rather wide range of effects. A significant amount of these drugs is either not recommended for prolonged use or is not approved in a number of countries. Essential phospholipids (EPL), ursodeoxycholic acid (UDCA), milk thistle extract based drugs, ademethionine can be distinguished as long-term use hepatoprotective drugs with high proven efficacy and safety [12].

Natural polyphenols are now widely used as antioxidant pharmacological substances that have a general anti-inflammatory, neuro- and cardioprotective effect simulate autophagy and protect mitochondria from pathological events inducing the cell survival signaling pathways [13]. The success of the use of polyphenols for the treatment of complex etiology diseases (neurodegenerative disorders of various origins, autoimmune, allergic, oncological and prion diseases) is associated with the direct effect on the cells of the body defense systems and the main tissues cells apoptosis induction [14]. Plant polyphenols affect oxidative stress, lipid metabolism, insulin resistance and inflammation, which are the most important pathological processes in the etiology of the liver diseases [1]. The positive effect of some polyphenols on the liver functional state in a model of toxic hepatitis induced by various hepatotoxicants was demonstrated. This, quercetin natural flavonoid protected the liver from carbon tetrachloride-induced dysfunction (CCl_4). The authors associated its action mechanism with antioxidant effect, as well as with the suppression of a number of reactions with NF-κB, which led to a decrease in the level of inflammatory liver cytokines [15]. Another flavonoid, puerarin, also significantly attenuated

the effects of CCl_4- induced hepatotoxicity by reducing the production of reactive oxygen species (ROS), activating the antioxidant enzyme system, and regulating the expression of genes responsible for liver lipid biosynthesis and metabolism [16]. The isolated from skullcap (*Scutellaria radix* Georgi) baikalin flavonoid was effective in protecting the liver from acetaminophen-induced toxic damage due to suppression of the extracellular signal-regulated kinase pathway signaling [17].

Administration of thioacetamide (TAA) leads to the liver fibrosis and cirrhosis induction in rats and mice. In a number of studies, 2 weeks after the start of TAA administration a significant increase in the activity of hepatic aminotransferases (alanine aminotransferase (ALT) and aspartate aminotransferase (AST)) was observed, indicating the development of a pathological process. By the end of the 4th week, the activity of AST and ALT was back to normal, while the level of collagen in the liver tissue increased [18]. Oxidative stress is considered the main factor of TAA-induced liver fibrous degeneration caused by the thioacetamide-S-oxide toxic metabolite formed during the transformation of TAA by cytochrome P450 family enzymes (CYP1A2, CYP2C6, CYP2E1, CYP3A2) and microsomal FAD-containing monooxygenases [19, 20]. According to the published data, resveratrol significantly reduced the TAA-induced liver damage. The mechanism of its action is due to a decrease in the intensity of oxidative stress, the suppression of the NF-κB- dependent cascade and apoptosis [21].

Our work was aimed to investigate the potential hepatoprotective effect of stilbene-type polyphenols (resveratrol (RSV) and pinosilvin (PS)) and dihydromyricetin (DHM) dihydroflavonol on the functional state and histological picture of the liver in a rat model of TAA-induced toxic hepatitis.

METHODS

Experiments were conducted on the male white rats of the *Wistar* line (initial weight of the rats was 190–230 g) obtained from Stolbovaya breeding nursery (Moscow Region). The animals' care in the breeding nursery complied with the GLP requirements. During the experiment the animals were kept in vivarium with natural light (day 12 hours, night 12 hours), the nutritionally balanced laboratory animal diet was used in accordance with GOST Standard P502580092. The study was carried in accordance with the Guidelines for Preclinical Trials of Medicinal Products (2 parts, editor Mironov AN (latest version)) and corresponding regulatory documents.

To induce toxic liver damage and the development of liver pathology, 0.05% TAA aqueous solution was administered to animals with food daily, which demonstrated a high efficiency in developing a liver pathology model [18, 20]. The TAA administration led to liver fibrosis and cirrhosis induction in rats and mice.

The rats were divided into groups of 10 animals:

1 — group of intact animals which were kept on a normal diet;

2 — group of control animals which received 0.05% TAA in drinking water;

3 — treatment group which received 0.05% TAA in drinking water together with RSV (15 mg/kg orally);

4 — treatment group which received 0.05% TAA in drinking water together with DHM (10 mg/kg orally);

5 — treatment group which received 0.05% TAA in drinking water together with PS (5 g/kg orally).

TAA was administered to animals during 30 days. Examination of animals was carried out daily, weighing was carried out every 3 days. Polyphenols were isolated and purified from plant raw materials (coniferous biomaterials available in

Russian Federation). Polyphenols were administered as a solution in an aqueous 2% starch gel intragastically by gavage daily after feeding at a dose of not more than 0.4 ml for each animal. Animals' blood and liver samples for biochemical and histological studies were collected on the 10th, 20th, and 30th days of the experiment. Liver tissue and blood samples were collected immediately after autopsy. The direct bilirubin and enzyme activity (AST and ALT aminotransferases) in the blood serum samples were assayed using the AU 480 Chemistry Analyzer (Beckman Coulter; USA). Blood chemistry tests for the laboratory animals were carried out in the Bio Chance Independent Veterinary Laboratory (participant of the Federal System of External Quality Assessment of Clinical Laboratory Testing, ID 10705) using the AU Chemistry Analyzer 480 (Beckman Coulter; USA), BA 400 analyzer (BioSystems; Spain) and Abacus Vet 4 analyzer (Diatron; Austria). The fatty liver index was determined as the ratio of the weight of organ to body weight (%). For histological studies, liver fragments were taken from the lower part of the right lobe. Histological preparations (thin sections) were obtained by making paraffin microsections according to the method described in [22]. Sample preparation included the following stages:

1. Preparation of organs for placement into the 4% paraformaldehyde (PFA) solution in phosphate-buffered saline (PBS). The collected during autopsy rat organs were kept in the plates with 4% PFA for 30 minutes. Every 30 min, a 4% PFA was changed thrice, after which the organs were left for 24 hours at a temperature of +4 °C.

2. Preparation of organs for placement in the sealing media was carried out according to the following procedure: a) washing 3 times with PBS for 30 min at +4 °C; b) incubation in 70% ethanol, 3 turns 30 min each; c) incubation in 80% ethanol for 40 minutes; d) incubation in the 82% ethanol–butanol mixture (3 : 1) for 40 minutes; e) incubation in the 96% ethanol–butanol mixture (1 : 1) for 50 minutes; f) incubation in the 100% ethanol (absolute) — butanol mixture (1 : 3) for 50 minutes; g) incubation in butanol I for 1 hour; h) incubation in butanol II for 1 hour.

3. Organs embedding in paraffin wax. Paraffin wax heated to +60 °C was poured in the prepared and heated foil mold, after that the sample was placed in paraffin wax. Paraffin wax blocks had been dried for 10–12 hours.

4. Sections preparation for staining. Cooled paraffin blocks were fixed on a wooden block with melted paraffin. Sections (slices) were obtained using the MC-2 sliding microtome (Tochmedpribor; Russia). Then the slices were mounted on the glass slides and placed in a dryer for 30 min at a temperature of +40 °C.

5. Staining of sections. Before staining, paraffin wax was removed from slices using toluene or xylene. Sections were stained using the hematoxylin–eosin staining system. After staining, Immuno Mount with DABCO™ (Genetex; Canada) was applied to sections and a glass cover was placed on top.

Statistical analysis was performed using STATISTICA 6.0 software for personal computer (Dell; USA). Data were presented as arithmetic mean and standard error of the mean (M ± m). Student t-test was used for evaluation of the differences between groups of animals. The differences were considered significant when $p < 0.05$.

RESULTS

The animals' weight dynamics assessment demonstrated that the body weight of intact animals increased throughout the entire period of the experiment (Fig. 1, curve 1). Against the background of the TAA introduction, regardless of the administration of polyphenols, the weight of the animals decreased significantly during the first week of the experiment. The polyphenols administration provided a positive trend in increasing the animals' weight compared with the control group, starting from the third week, which could indicate a positive effect of polyphenols on the liver function. By the end of the experiment, the liver index (the ratio of organ mass to animal body weight) increased from 3.65 ± 0.2 in intact animals to 5.1 ± 0.3 in treated with TAA animals of the control group. In the groups treated with polyphenols together with TAA, the liver index was 4.5 ± 0.19, 4.6 ± 0.23 and 4.4 ± 0.16 for animals treated with RSV, DHM and PS respectively. A decrease in the liver index in animals treated with polyphenols indicated a decrease in pathological changes caused by the TAA administration.

Analysis of the biochemical blood parameters dynamics of laboratory animals treated with TAA demonstrated that the level of bilirubin in the blood increased by almost 10 times, while the administration of polyphenols decreased that indicator by 2–4 times (Table 1). It should be noted that the effect of lowering serum bilirubin level was observed throughout the entire period of the polyphenols administration. The total protein and glucose level decreased slightly in all treated with TAA groups, regardless of the administration of polyphenols (no significant differences, data not shown).

AST activity significantly increased ($p < 0.05$) in the blood serum of animals in all treated with TAA groups compared to control (Fig. 2A). An almost twofold AST increase in animals of the control group by the 20th day and then a slight decrease
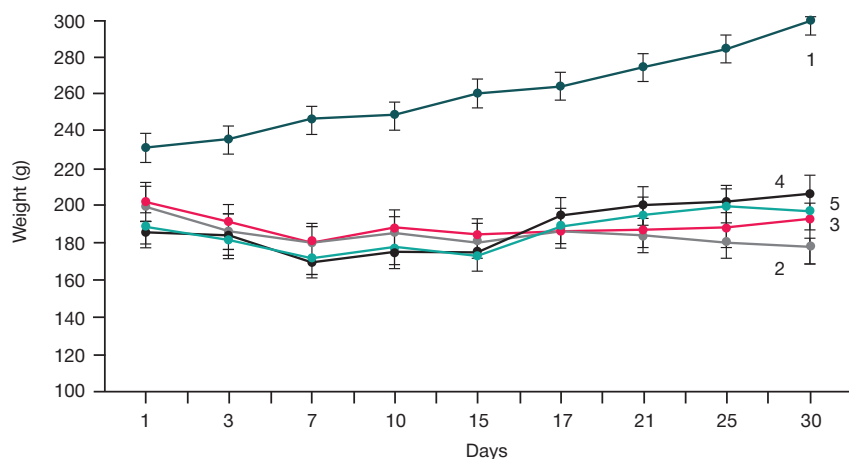

Fig. 1. Dynamics of animals' weight changes during the experiment: 1 — intact animals group; 2 — control group treated with TAA; 3–5 — groups of animals treated with TAA together with polyphenols (RSV, DHM and PS respectively)

Table 1. Bilirubin level change in the blood serum of rats during the experiment

Period	Direct bilirubin, μmol/l				
	Intact	Control	RSV	DHM	PS
10 days	0.4 ± 0.1	4.9 ± 0.5*	1.1 ± 0.2*,**	1.5 ± 0.6*,**	1.2 ± 0.6*,**
20 days	0.4 ± 0.2	4.4 ± 0.5*	2.0 ± 0.8*,**	1.3 ± 0.5*,**	2.5 ± 0.2*,**
30 days	0.45 ± 0.2	4.2 ± 1.1*	1.1 ± 0.1*,**	2.4 ± 0.6*,**	1.5 ± 0.7*,**

Note: * — $p < 0.05$ in relation to corresponding indicators of intact animals group; ** — $p < 0.05$ in relation to corresponding indicators of control group.

by the 30th day of the experiment is characteristic of this hepatotoxicity model, it is in line with the data of other authors [18, 21]. In rats receiving polyphenols, AST was lower. By the end of the experiment, in the groups receiving resveratrol and pinosylvin, a significant decrease in this indicator was observed compared to the control group (Fig. 2A).

ALT activity in the control group receiving TAA significantly increased ($p < 0.05$) by 40% only after the 20th day of the experiment (Fig. 2B). An increase in ALT activity in the middle of the experiment was also noted in animals which received RSV together with TAA (about 30%), as well as slight increase (20%) in animals which received PS by the 30th day of the experiment. In the group treated with DHM, ALT values did not differ from those in intact animals throughout the observation period. By the end of the experiment, ALT values were back to normal in animals of the RSV-treated group (Fig. 2B).

At the next stage, histological sections of the liver of all the studied treatment groups of animals were analyzed. Hepatocytes of intact animals were characterized by normal cytomorphology with well-defined nuclei and moderate tissue polymorphism (Fig. 3A). TAA hepatotoxicant intoxication led to diapedetic hemorrhage (Fig. 3B) and small-droplet (microvesicular) steatosis. The obtained histological picture corresponded to the known symptoms of liver pathology arising due to the action of xenobiotics (TAA and CCl_4) [23]. Administration of polyphenols (Fig. 3D–F) prevented significant

degradation of liver tissue: hepatocytes structure violation, the development of hematomas and inflammation foci containing small cell formations (Fig. 3D–F).

DISCUSSION

The positive effect of a number of natural polyphenols on hepatotoxicant-induced liver pathologies is well known. The quercetin flavonoid exhibited a protective effect on the CCl4-induced toxic hepatitis in mice [15]. *Eisenia bicyclis* (Kjellman) Setchell brown algae polyphenol dieckol protected the liver of mice from CCl_4-induced destruction through regulation of genes responsible for the expression of apoptotic proteins Bax and Bcl-xl [24]. In the other work, isorhamnetin 3-O-galactoside polyphenol isolated from *Artemisia capillaris* Thunberg also had a positive effect on CCl_4-induced liver pathology by decreasing the level of phosphorylated c-JNK, extracellular signal–regulated kinase (ERK) and p38 MAPK [25]. The baikalin flavonoid had a significant protective effect in mice with acetaminophen-induced hepatitis [17]. In the model of TAA-induced toxic liver damage used in our work, the protective effect of polyphenols was studied only on the example of the RSV stilbene polyphenol. In the recent work [21], RSV-induced inflammation and oxidative stress inhibition in rat liver tissues due to reduction of the expression level of NF-κB and CYP2E1 as well as necrotic hepatocytes apoptosis
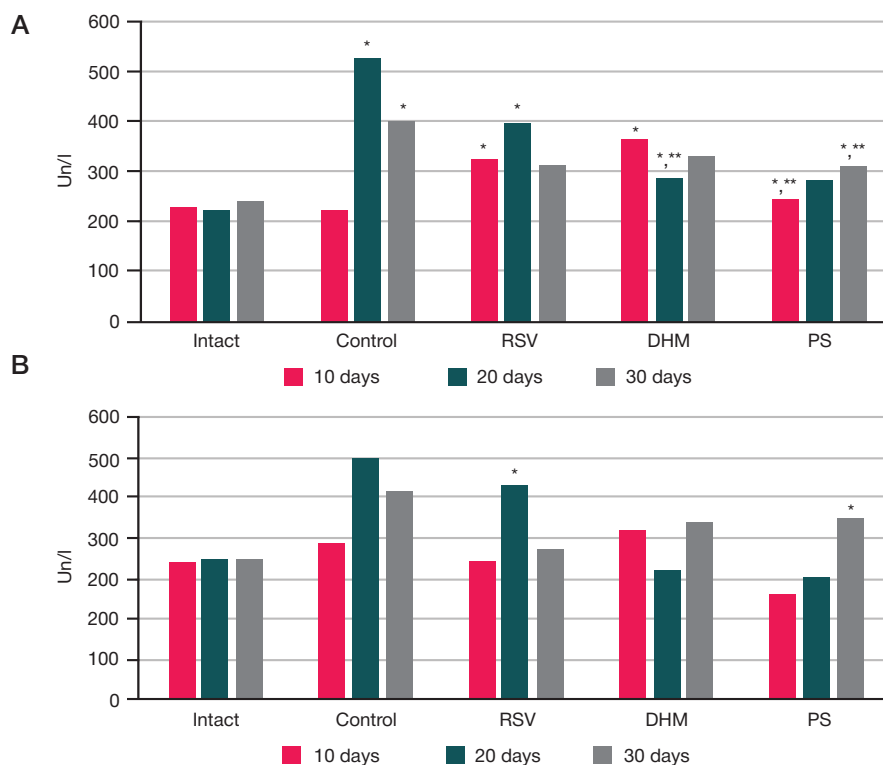
Fig. 2. AST (**A**) and ALT (**B**) change in the blood serum of rats during the experiment. * — $p < 0.05$ in relation to corresponding indicators of intact animals group; ** — $p < 0.05$ in relation to corresponding indicators of control group
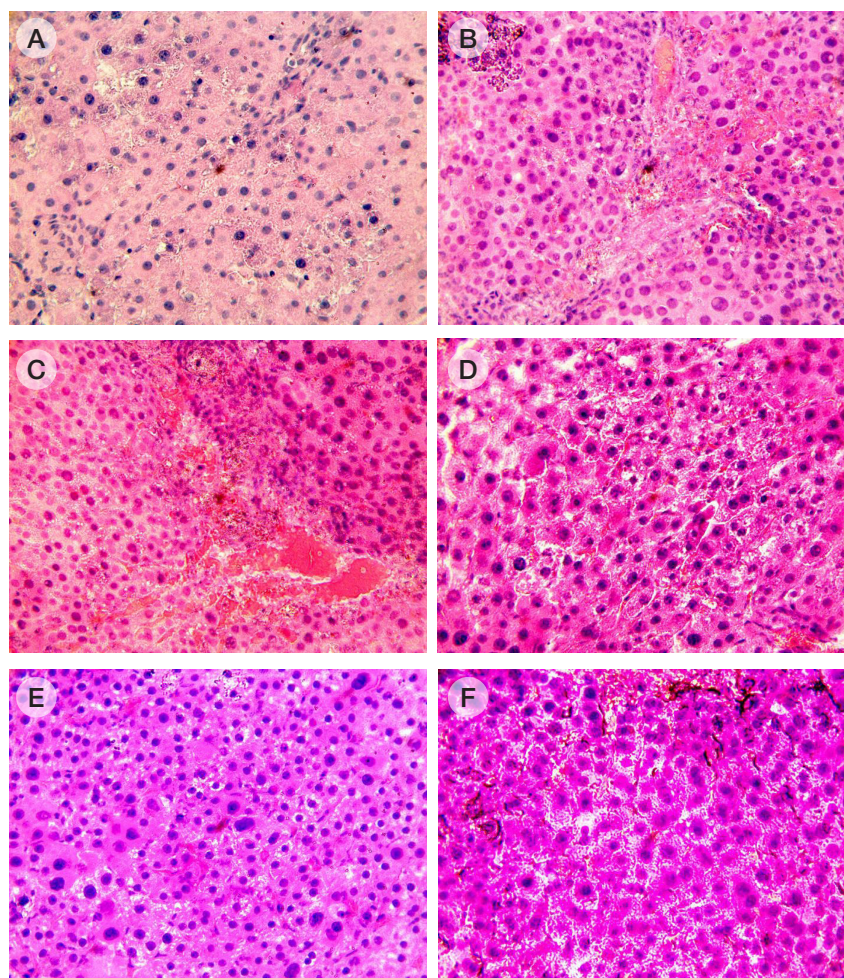
Fig. 3. Micrographs of treatment groups animals' liver sections stained with hematoxylin-eosin. **A**. Intact animals group (1). **B**, **C**. Control group (2). **D**. Treatment group (3). **E**. Treatment group (4). **F**. Treatment group (5). Magnification ×400

increase was demonstrated. In addition, stabilization of blood biochemical parameters (ALT and AST) was shown as well as normalization of tissue architecture of the liver in laboratory animals receiving RSV (10 mg/kg per animal). Given these data, we can assume that in our studies there is a similar mechanism of RSV action, based on its powerful antioxidant effect. There are no literature data on the effects of DHM and PS in the model of toxic hepatitis induction in laboratory animals. There is only evidence of a pro-apoptotic effect of DHM on HepG2 cells of hepatocellular carcinoma [26]. Given the high biological activity of these polyphenols in various disorder models, it can be assumed that the protective effect of DHM and PS studied by us in rats with TAA-induced hepatopathology can also be associated with powerful antioxidant potential.

Some authors [27] demonstrated, that dioscin (saponin isolated from *Dioscorea nipponica* Makino), like the studied by us polyphenols, decreased the TAA hepatotoxicity, increasing the level of glutathione in the liver cells and the activity of the glutathione peroxidase and superoxid dismutase antioxidant enzymes, decreasing the content of malondialdehyde. Treatment of animals by dioscin increased the expression of FXR and p-AMPKα, as well as Nrf2, HO-1, NQO-1 and GCLM. On the contrary, the level of proinflammatory factors NF-κB (p65), ICAM 1, HMGB1, COX-2, TNFα, IL1β and IL6 in the liver cells decreased due to dioscin administration, which, according to the authors, was evidence of the ability of said natural compound to suppress TAA hepatotoxicity due to the FXR/AMPK signaling pathway weakening in hepatocytes.

CONCLUSION

The study has shown that the natural polyphenols which belong to the class of dihydroflavonols (DHM) and stilbenes (RSV and PS) have a positive effect on liver function in the experimental model of toxic hepatosis and can be considered as potential hepatoprotectors.

References

1. Li S, Tan HY, Wang N, Cheung F, Hong M, Feng Y. The potential and action mechanism of polyphenols in the treatment of liver diseases. Oxid Med Cell Longev. 2018; 8394818. DOI: 10.1155/2018/8394818.
2. Raff E, Singal AK. Optimal management of alcoholic hepatitis. Minerva Gastroenterol Dietol. 2014; 60 (1): 25–38.
3. Riggio O, Ridola L, Pasquale C. World J Gastrointest Pharmacol Ther Hepatic encephalopathy therapy: An overview. 2010; 1 (2): 54–63.
4. Neuschwander-Tetri BA. Non-alcoholic fatty liver disease. BMC Med. 2017; 15 (1): 45.
5. Popov VB, Lim JK. Treatment of nonalcoholic fatty liver disease:

The role of medical, surgical, and endoscopic weight loss. J Clin Transl Hepatol. 2015; 3 (3): 230–38.

6. Hong M, Li S, Tan H, Wang N, Tsao SW, Feng Y. Current status of herbal medicines in chronic liver disease therapy: the biological effects, molecular targets and future prospects. Int J Mol Sci. 2015; 16 (12): 28705–45.

7. Festi D, Vestito A, Mazzella G, Roda E, Colecchia A. Management of hepatic encephalopathy: focus on antibiotic therapy. Digestion. 2006; 73 (Suppl. 1): 94–101.

8. Malaguarnera M, Gargante MP, Malaguarnera G, Salmeri M, Mastrojeni S, Rampello L, et al. Bifidobacterium combined with fructo-oligosaccharide versus lactulose in the treatment of patients with hepatic encephalopathy. Eur J Gastroenterol Hepatol. 2010; 22 (2): 199–206.

9. Efrati C, Masini A, Merli M, Valeriano V, Riggio O. Effect of sodium benzoate on blood ammonia response to oral glutamine challenge in cirrhotic patients: a note of caution. Am J Gastroenterol. 2000; 95 (12): 3574–78.

10. Plauth M, Cabre E, Riggio O, Assis-Camilo M, Pirlich M, Kondrup J, et al. ESPEN guidelines on enteral nutrition: liver disease. Clin Nutr. 2006; 25 (2): 285–94.

11. Wong VW, Singal AK. Emerging medical therapies for non-alcoholic fatty liver disease and for alcoholic hepatitis. Transl Gastroenterol Hepatol. 2019; (4): 53.

12. Minushkin ON, Maslovsky LV, Bukshuk AA. The use of hepatic protectors in clinical practice. Zh Nevrol Psikhiatr Im SS Korsakova. 2012; 10 (2): 67–72.

13. Teplova VV, Isakova EP, Klein OI, Dergacheva DI, Gessler NN, Deryabina YI. Natural Polyphenols: Biological Activity, Pharmacological Potential, Means of Metabolic Engineering (Review). Applied Biochemistry and Microbiology. 2018; 54 (3): 221–37.

14. Quideau S, Deffieux D, Douat-Casassus C, Pouysegu L. Plant polyphenols: chemical properties, biological activities, and synthesis. Angewandte Chemie Intern Edition. 2011; 50 (3): 586–621.

15. Ma JQ, Li Z, Xie WR, Liu CM, Liu SS. Quercetin protects mouse liver against CCl4-induced inflammation by the TLR2/4 and MAPK/NF-κB pathway. Intern Immunopharm. 2014; 28 (1): 531–39.

16. Ma JQ, Ding J, Zhao H, Liu CM. Puerarin attenuates carbon tetrachloride-induced liver oxidative stress and hyperlipidaemia in mouse by JNK/c-Jun/CYP7A1 pathway. Basic Clin Pharmacol Toxicol. 2014; 115 (5): 389–95.

17. Liao CC, Day YJ, Lee HC, Liou JT, Chou AH, Liu FC. ERK signaling pathway plays a key role in baicalin protection against acetaminophen-induced liver injury. Am J Chinese Med. 2017; 45 (1): 105–21.

18. Wallace MC, Hamesch K, Lunova M, Kim Y, Weiskirchen R, Strnad P, et al. Standard operating procedures in experimental liver research: thioacetamide model in mice and rats. Laboratory Animals. 2015; 49 (S1): 21–9.

19. Xie Y, Wang G, Wang H, Yao X, Jiang S, Kang A, et al. Cytochrome P450 dysregulations in thioacetamide-induced liver cirrhosis in rats and the counteracting effects of hepatoprotective agents. Drug Metabolism and Disposition. 2012; 40 (4): 796–802.

20. Ingawale DK, Mandlik SK, Naik SR. Models of hepatotoxicity and the underlying cellular, biochemical and immunological mechanism(s): a critical discussion. Environ Toxicol Pharmacol. 2014; 37 (1): 118–33.

21. Seif El-Din SH, El-Lakkany NM, Salem MB, Hammam OA, Saleh S, Botros SS. Resveratrol mitigates hepatic injury in rats by regulating oxidative stress, nuclear factorkappa B, and apoptosis. J Advanc Pharmaceut Technol Res. 2016; 7 (3): 99–104.

22. Frank GA, Malkov PG, редакторы. 101 shag na puti k uspekhu v gistologii. Leica Microsystems Vetzlar, Germany, 2012; 136 с. Russisn.

23. Kang MC, Kang SM, Ahn G, Kim KN, Kang N, Samarakoon KW, et al. Protective effect of a marine polyphenol, dieckol against carbon tetrachlorideinduced acute liver damage in mouse. Environ Toxicol Pharmacol. 2013; 35 (3): 517–23.

24. Kang MC, Kang SM, Ahn G, Kim KN, Kang N, Samarakoon KW, et al. Protective effect of a marine polyphenol, dieckol against carbon tetrachlorideinduced acute liver damage in mouse. Environ Toxicol Pharmacol. 2013; 35 (3): 517–23.

25. Kim DW, Cho HI, Kim KM, Kim YS. Isorhamnetin-3-O-galactoside protects against CCl4-induced hepatic injury in mice. Biomolecules Therapeutics. 2012; 20 (4): 406–12.

26. Huang X, Lian T, Guan X, Liu B, Hao S, Zhang J, et al. Dihydromyricetin reduces TGF-β via P53 activation-dependent mechanism in hepatocellular carcinoma HepG2 cells. Protein Pept Lett. 2017; 24 (5): 419–24.

27. Zheng L, Yin L, Xu L, Qi Y, Li H, Xu Y, et al. Protective effect of dioscin against thioacetamide-induced acute liver injury via FXR/AMPK signaling pathway in vivo. Biomed Pharmacother. 2018; (97): 481–8. DOI: 10.1016/j.biopha.2017.10.153.

Литература

1. Li S, Tan HY, Wang N, Cheung F, Hong M, Feng Y. The potential and action mechanism of polyphenols in the treatment of liver diseases. Oxid Med Cell Longev. 2018; 8394818. DOI: 10.1155/2018/8394818.

2. Raff E, Singal AK. Optimal management of alcoholic hepatitis. Minerva Gastroenterol Dietol. 2014; 60 (1): 25–38.

3. Riggio O, Ridola L, Pasquale C. World J Gastrointest Pharmacol Ther Hepatic encephalopathy therapy: An overview. 2010; 1 (2): 54–63.

4. Neuschwander-Tetri BA. Non-alcoholic fatty liver disease. BMC Med. 2017; 15 (1): 45.

5. Popov VB, Lim JK. Treatment of nonalcoholic fatty liver disease: The role of medical, surgical, and endoscopic weight loss. J Clin Transl Hepatol. 2015; 3 (3): 230–38.

6. Hong M, Li S, Tan H, Wang N, Tsao SW, Feng Y. Current status of herbal medicines in chronic liver disease therapy: the biological effects, molecular targets and future prospects. Int J Mol Sci. 2015; 16 (12): 28705–45.

7. Festi D, Vestito A, Mazzella G, Roda E, Colecchia A. Management of hepatic encephalopathy: focus on antibiotic therapy. Digestion. 2006; 73 (Suppl. 1): 94–101.

8. Malaguarnera M, Gargante MP, Malaguarnera G, Salmeri M, Mastrojeni S, Rampello L, et al. Bifidobacterium combined with fructo-oligosaccharide versus lactulose in the treatment of patients with hepatic encephalopathy. Eur J Gastroenterol Hepatol. 2010; 22 (2): 199–206.

9. Efrati C, Masini A, Merli M, Valeriano V, Riggio O. Effect of sodium benzoate on blood ammonia response to oral glutamine challenge in cirrhotic patients: a note of caution. Am J Gastroenterol. 2000; 95 (12): 3574–78.

10. Plauth M, Cabre E, Riggio O, Assis-Camilo M, Pirlich M, Kondrup J, et al. ESPEN guidelines on enteral nutrition: liver disease. Clin Nutr. 2006; 25 (2): 285–94.

11. Wong VW, Singal AK. Emerging medical therapies for non-alcoholic fatty liver disease and for alcoholic hepatitis. Transl Gastroenterol Hepatol. 2019; (4): 53.

12. Минушкин О. Н., Масловский Л. В., Букшук А. А. Применение гепатопротекторов в клинической практике. Журнал неврологии и психиатрии им. С. С. Корсакова. 2012; 10 (2): 67–72.

13. Теплова В. В., Исакова Е. П., Кляйн О. И., Дергачева Д. И., Гесслер Н. Н., Дерябина Ю. И. Природные полифенолы: биологическая активность, фармакологический потенциал, пути метаболической инженерии (Обзор). Прикладная биохимия и микробиология. 2018; 54 (3): 215–35.

14. Quideau S, Deffieux D, Douat-Casassus C, Pouysegu L. Plant polyphenols: chemical properties, biological activities, and synthesis. Angewandte Chemie Intern Edition. 2011; 50 (3): 586–621.

15. Ma JQ, Li Z, Xie WR, Liu CM, Liu SS. Quercetin protects mouse liver against CCl4-induced inflammation by the TLR2/4 and MAPK/NF-κB pathway. Intern Immunopharm. 2014; 28 (1): 531–39.

16. Ma JQ, Ding J, Zhao H, Liu CM. Puerarin attenuates carbon tetrachloride-induced liver oxidative stress and hyperlipidaemia

in mouse by JNK/c-Jun/CYP7A1 pathway. Basic Clin Pharmacol Toxicol. 2014; 115 (5): 389–95.

17. Liao CC, Day YJ, Lee HC, Liou JT, Chou AH, Liu FC. ERK signaling pathway plays a key role in baicalin protection against acetaminophen-induced liver injury. Am J Chinese Med. 2017; 45 (1): 105–21.

18. Wallace MC, Hamesch K, Lunova M, Kim Y, Weiskirchen R, Strnad P, et al. Standard operating procedures in experimental liver research: thioacetamide model in mice and rats. Laboratory Animals. 2015; 49 (S1): 21–9.

19. Xie Y, Wang G, Wang H, Yao X, Jiang S, Kang A, et al. Cytochrome P450 dysregulations in thioacetamide-induced liver cirrhosis in rats and the counteracting effects of hepatoprotective agents. Drug Metabolism and Disposition. 2012; 40 (4): 796–802.

20. Ingawale DK, Mandlik SK, Naik SR. Models of hepatotoxicity and the underlying cellular, biochemical and immunological mechanism(s): a critical discussion. Environ Toxicol Pharmacol. 2014; 37 (1): 118–33.

21. Seif El-Din SH, El-Lakkany NM, Salem MB, Hammam OA, Saleh S, Botros SS. Resveratrol mitigates hepatic injury in rats by regulating oxidative stress, nuclear factorkappa B, and apoptosis. J Advanc

Pharmaceut Technol Res. 2016; 7 (3): 99–104.

22. Франк Г. А., Мальков П. Г., редакторы. 101 шаг на пути к успеху в гистологии. Leica Microsystems Vetzlar, Germany, 2012; 136 с.

23. Манских В. Н. Патоморфология лабораторной мыши. М.: ВАКО, 2018; 224 с.

24. Kang MC, Kang SM, Ahn G, Kim KN, Kang N, Samarakoon KW, et al. Protective effect of a marine polyphenol, dieckol against carbon tetrachlorideinduced acute liver damage in mouse. Environ Toxicol Pharmacol. 2013; 35 (3): 517–23.

25. Kim DW, Cho HI, Kim KM, Kim YS. Isorhamnetin-3-O-galactoside protects against CCl4-induced hepatic injury in mice. Biomolecules Therapeutics. 2012; 20 (4): 406–12.

26. Huang X, Lian T, Guan X, Liu B, Hao S, Zhang J, et al. Dihydromyricetin reduces TGF-β via P53 activation-dependent mechanism in hepatocellular carcinoma HepG2 cells. Protein Pept Lett. 2017; 24 (5): 419–24.

27. Zheng L, Yin L, Xu L, Qi Y, Li H, Xu Y, et al. Protective effect of dioscin against thioacetamide-induced acute liver injury via FXR/AMPK signaling pathway in vivo. Biomed Pharmacother. 2018; (97): 481–8. DOI: 10.1016/j.biopha.2017.10.153.

COLUMNAR METAPLASIA AND BARRETT'S ESOPHAGUS: MORPHOLOGICAL HETEROGENEITY AND IMMUNOHISTOCHEMICAL PHENOTYPE

Mikhaleva LM[1,2] ✉, Voytkovskaya KS[2], Fedorov ED[2,3], Gracheva NA[2], Birukov AE[1,2], Shidiy-Zakrua AV[3], Guschin MY[1]

[1] Research Institute of Human Morphology, Moscow, Russia

[2] City Clinical Hospital № 31, Moscow, Russia

[3] Pirogov Russian National Research Medical University, Moscow, Russia

Barrett's esophagus (BE) is a pathologically confirmed intestinal metaplasia (CM) of the distal esophagus. BE is recognized as a potential complication of gastroesophageal reflux disease (GERD) and a premalignant condition with a high risk of neoplastic progression. The aim of this study was to compare the morphology of biopsied BE segments and CM segments extending < 1 cm and > 1 cm above the gastroesophageal junction (GEJ), as well as to perform the immunohistochemical analysis of biopsies with BE and CM > 1 cm above GEJ with or without dysplasia. The study recruited 92 patients with GERD: 42 patients with BE, 24 patients with CM > 1 cm above GEJ (C0M1.5–C13M14) and 26 patients with CM < 1 cm above GEJ (C0M0.3–0.8). Comparative analysis of tissue morphology revealed an association between the reactive changes in the epithelium and the severity of esophagitis in all groups. Reactive changes were detected significantly more often in BE segments than in CM segments > 1 cm (Mann-Whitney U, $p < 0.05$). Eight patients with BE (19.05%) were found to have low-grade dysplasia. One patient with CM > 1 cm above GEJ (4.2%) had high-grade dysplasia with cardiac-type metaplasia and immunohistochemical features of submorphological enteralization. Immunohistochemical testing for the intestinal and gastric markers of cell differentiation revealed the signs of submorphological enteralisation in all esophageal specimens with cardiac and fundic type metaplasia and in the specimens with BE in the areas lacking goblet cells.

Keywords: columnar metaplasia, Barrett's esophagus, low-grade dysplasia, high-grade dysplasia, carcinogenesis

ЦИЛИНДРОКЛЕТОЧНАЯ МЕТАПЛАЗИЯ И ПИЩЕВОД БАРРЕТТА: МОРФОЛОГИЧЕСКАЯ НЕОДНОРОДНОСТЬ И ИММУНОГИСТОХИМИЧЕСКИЙ ФЕНОТИП

Л. М. Михалева[1,2] ✉, К. С. Войтковская[2], Е. Д. Федоров[2,3], Н. А. Грачева[2], А. Е. Бирюков[1,2], А. В. Шидии-Закруа[3], М. Ю. Гущин[1]

[1] Научно-исследовательский институт морфологии человека, Москва, Россия

[2] Городская клиническая больница № 31, Москва, Россия

[3] Российский национальный исследовательский медицинский университет имени Н. И. Пирогова, Москва, Россия

Пищевод Барретта (ПБ), или доказанная морфологически кишечная метаплазия слизистой оболочки дистального отдела пищевода, является облигатным предраковым заболеванием, которое развивается как осложнение гастроэзофагеальной рефлюксной болезни (ГЭРБ). Цель исследования — выполнить сравнительный морфологический анализ биопсированных фрагментов ПБ, ЦМ на расстоянии < 1 см и > 1 см от гастроэзофагеального перехода (ГЭП), а также провести иммуногистохимическое исследование фрагментов с ПБ и ЦМ > 1 см от ГЭП при наличии и отсутствии дисплазии. В исследование вошли 92 пациента с ГЭРБ: 42 пациента с ПБ, 24 пациента с ЦМ > 1 см от ГЭП (C0M1,5 до C13M14) и 26 пациентов с ЦМ < 1 см от ГЭП (C0M0,3–0,8). При сравнительном морфологическом анализе наличие реактивных изменений эпителия было связано с тяжестью эзофагита во всех группах. Реактивные изменения эпителия выявляли достоверно чаще при ПБ по сравнению с ЦМ > 1 см от ГЭП ($p < 0,05$ при использовании критерия Манна–Уитни). При ПБ в восьми наблюдениях (19,05%) выявлена low-grade дисплазия. В одном наблюдении ЦМ > 1 см от ГЭП (4,2%) выявлена high-grade дисплазия на фоне кардиальной метаплазии с иммуногистохимическими признаками субморфологической энтерализации. При иммуногистохимическом исследовании с маркерами желудочной и кишечной дифференцировки признаки субморфологической энтерализации выявлены во всех фрагментах пищевода с кардиальной метаплазией и у пациентов с ПБ в зонах с отсутствием бокаловидных клеток.

Ключевые слова: цилиндроклеточная метаплазия пищевода, пищевод Барретта, low-grade и high-grade дисплазия, канцерогенез

Barrett's esophagus (BE) refers to intestinal metaplasia (CM) of the distal esophagus confirmed by endoscopy and histological examination. BE is recognized as a potential complication of gastroesophageal reflux disease (GERD) and a premalignant condition with a high risk of neoplastic progression. At present, there is no universally accepted definition of BE because the affected tissue is very heterogeneous and can present as a mosaic of various metaplastic phenotypes within one biopsied fragment of the distal esophageal mucosa. The American Gastroenterological Association maintains that BE should be diagnosed only in the presence of intestinal metaplasia in the biopsies collected from the sites of the columnar-lined esophagus [1]. The British Society of Gastroenterology (BSG) defines BE as any type of columnar metaplasia (CM) extending ≥1 cm above the gastroesophageal junction (GEJ) [2]. The International Consensus BOB CAT group (2015) recognizes BE as any type of CM of the distal esophagus but emphasizes that the type of metaplasia should be clearly specified in the pathology report [3].

Embraced by many clinicians, the definition formulated by BSG has become fairly popular. But of course, it did not make the underlying biology of the disease any different. Therefore, for the sake of diagnostic accuracy, it is essential to meticulously compare endoscopy and pathology findings, especially for biopsies collected <1 cm above GEJ [4].

In the distal esophagus, 3 types of metaplasia can be distinguished, including cardiac, fundic and intestinal. The first is often seen in short-segment BE and is the earliest metaplastic transformation of the esophagus in patients with GERD. In cardiac-type metaplasia, squamous epithelium is replaced with foveolar cells. Fundic-type metaplasia is characterized by the presence of chief and parietal cells as normally in the gastric corpus mucosa. Intestinal metaplasia usually presents as a patchwork of goblet and foveolar cells and sometimes Paneth cells [5].

Biopsies of one and the same patient can contain different types of columnar-lined epithelium. As a rule, intestinal metaplasia affects the proximal side of columnar-lined esophagus, whereas cardiac and fundic types usually occur more distally, close to GEJ. Intestinal metaplasia is reported to be twice as prevalent in the biopsies from the proximal side of columnar-lined esophagus than in the fragments close to GEJ [6].

Today, the pathogenesis of esophageal CM is linked to the transdifferentiation of the stratified squamous epithelium or to the transcommitment of progenitor cells involved in the repair of reflux-induced damage [7].

The prevalence of goblet cells is associated with the pH gradient along the BE segment: the lower the pH value (i.e. the closer to GEJ), the fewer and more scattered the goblet cells. This phenomenon might be tied to the solubility gradient of bile acids determined by pH levels: at more acidic pH (closer to GEJ) the solubility of bile acids is the lowest; at neutral pH typical of the proximal BE, the solubility of bile acids increases [8]. A study conducted in mice has shown the role of bile acids in the pathogenesis of BE with intestinal metaplasia and CDX2/MUC2 expression [9].

Another study has demonstrated that cardiac CM can undergo early enteralization, i.e. retain morphological features of cardiac-type cells but start expressing markers of intestinal differentiation, such as Villin and CDX2 [10].

There is ongoing debate about whether goblet cells play an exclusive role in carcinogenesis in the distal esophagus or other CM types can also contribute to dysplasia and development of esophageal adenocarcinoma. In one of epidemiological studies, the incidence of progression to malignancy in patients

with intestinal metaplasia was higher (0.38% per year) than in patients without this condition (0.07% per year) [11]. However, this trend was not corroborated by another long-term observation (8–20 years) [12]. In over 70% of patients with small (<2 cm) esophageal adenocarcinomas, cancer was preceded by columnar metaplasia of the esophagus, but the metaplastic transformation of mucosa adjacent to the tumor was not intestinal but cardiac [13]. These findings were confirmed by other researchers [14] who reported expression of gastric markers (MUC5A and MUC6) in minute Barrett's tumors (< 5 mm). Non-goblet cardiac-type CM epithelium without CDX2 expression can also undergo malignant transformation [15]. At the same time, high density of goblet cells can reduce the risk of adenocarcinoma [16, 17]. Perhaps, there are two independent carcinogenesis pathways in the distal esophagus: foveolar and intestinal, i.e. involving both gastric-type and specialized intestinal metaplasia [18–20]. The implicated type of carcinogenesis can be identified by immunohistochemistry from the expression of gastric (MUC1, MUC5A, MUC6) and intestinal (MUC2, CD10, CDX2, Villin, etc.) markers.

According to the definition proposed by BSG, BE should be diagnosed if the metaplastic epithelium extends ≥1 cm above GEJ. Although this criterion is increasingly applied, it is still arbitrary. So far, research into the contribution of ultra-short BE (<1 cm) to esophageal carcinogenesis has produced conflicting evidence.

The aim of this study was to compare the morphology of columnar-lined esophagus segments extending < 1 cm above GEJ (ultra-short BE), classic goblet BE and CM extending > 1 cm above GEJ, to identify the relative prevalence of different metaplasia types, the frequency of reactive changes in the epithelium (indefinite for metaplasia) and dysplasia of the metaplastic esophageal epithelium, as well as to carry out the immunohistochemical analysis of BE specimens with different types of metaplastic transformations with or without dysplasia.

METHODS

The study was carried out at the City Clinical Hospital № 31 between January 1, 2018 and September 1, 2019. The study recruited patients with GERD who were undergoing medical examination at the Hospital at that time. The following inclusion criterion was applied: the presence of columnar-lined esophageal segments of any length detected on endoscopy and subsequently confirmed by histological examination. Mucosal biopsies were taken from the distal esophagus of 92 patients with GERD during upper endoscopy (EGD) and then examined by the pathologists. Of all the examined patients, 42 had BE, 24 had CM extending > 1 cm above GEJ (C0M1.5 to C13M14) and 26 patients had endoscopic features of CM < 1 cm above GEJ (C0M0.3–0.8). Exclusion criteria were as follows: the absence of columnar metaplasia in the biopsy histological examination; the absence of esophageal mucosa components in the biopsied specimens (stratified squamous epithelium, glands of the esophageal lamina propria and their ducts), especially in ultra-short BE, which prevented us from drawing a firm conclusion that the biopsies had been collected from the esophagus but not from the stomach. In the group of patients with CM < 1 cm above GEJ, the mean age was 55.50 ± 1.10 years (range 22–82 years); of them 11 were men (mean age 50.09 ± 18.03) and 15 women (mean age 59.47 ± 14.57); the male to female ratio was 1 : 1.36. The group of patients with CM segment length > 1 cm consisted of 24 individuals aged 19–94 years (mean age 52.21 ± 18.00); of them 7 were male (mean age 47 ± 20.05) and 17 were female (mean age 53.5 ± 17.47); the male to

female ratio was 1 : 2.4. The group of patients with BE was represented by 42 patients aged 19–93 years (mean age 61.80 ± 16.33); of them 29 were men (mean age 54.47 ± 21.79) and 13 women (69.23 ± 13.57); the male to female ratio was 2.23 : 1. The patients with CM length < 1 cm and > 1 cm tended to be younger than those with BE, but the difference between the groups was insignificant. In the group with CM < 1 cm and CM > 1 cm above GEJ, as well as in the BE group, the mean age of male participants was lower than that of women, because the male sex is one of the risk factors for GERD.

Pre-existing conditions predisposing our patients to the CM of the distal esophagus and BE included sliding hiatal hernia and cardiac sphincter incompetence. Endoscopy was suggestive of sliding hiatal hernia in 14 of 26 (53.8%) patients who had endoscopic evidence of CM < 1 cm; another 3 (11.5%) patients with CM < 1 cm had signs of cardiac sphincter incompetence in the absence of hiatal hernia. In the group with CM extending > 1 cm above GEJ, hiatal hernia was detected by EGD in 11 (45.83%) patients and cardiac sphincter incompetence, in 3 (12.5%) individuals. Of all study participants with BE, endoscopy was suggestive of hiatal hernia in 18 (42.86%) patients and of cardiac sphincter incompetence, in 6 (14.29%) participants.

Biopsied esophageal specimens were processed following the standard protocol. The slides were stained with hematoxylin-eosin and Schiff reagent-Alcian blue. The latter helps to identify goblet cells and discriminate between goblet and dystrophic pseudogoblet cells. Pseudogoblet cells were detected in 88.04% of all examined specimens.

Biopsies with intestinal metaplasia were evaluated for the density of goblet cells in the glands. If goblet cells made less than 5% of all epithelial cells in the glands, the sample was categorized as containing few goblet cells; if these cells amounted to 5-50% of all epithelial cells, the sample was categorized as containing low-density goblet cells; if the proportion of goblet cells exceeded 50%, the sample was regarded as containing high-density goblet cells.

All biopsies collected from the patients with CM < 1 cm were analyzed for the presence of esophageal mucosa components, including stratified squamous epithelium (20 patients, 76.92%), esophageal glands (19 patients, 73.07%) and their excretory ducts (5 patients, 19.23%). This helped us to determine whether the studied specimens had been collected from the distal esophagus vs the stomach. The fragments that lacked the aforementioned components of the esophageal mucosa were excluded from the final analysis.

In 24 cases of BE and CM > 1 cm above GEJ, immunohistochemistry was performed using the following

antibodies: anti-MUC1 (1 : 100, Ventana; Roche), anti-MUC2 (1 : 125, Ventana; Roche), anti-MUC5A (1 : 250, Ventana; Roche), anti-MUC6 (ready to use, Ventana; Roche), anti-CDX2 (1 : 125, Ventana; Roche), and anti-Villin (ready to use, Leica).

RESULTS

Three metaplasia types were identified in the patients with CM < 1 cm above GEJ: cardiac, fundic and intestinal. In the absence of other metaplastic changes, cardiac-type metaplasia was present in 7 (26.92%) patients and fundic-type, in 4 patients (15.38%) in the group with CM < 1 cm (Fig.1). Intestinal metaplasia with different relative goblet cell density was observed in 15 patients (57.69%) (Fig. 2). In 5 patients (33.33%), goblet cells were few. Low-density goblet cells (10 to 49%) were observed in 8 patients (53.33%); high-density goblet cells (50 and 70%), in 2 patients (13.33%). Biopsies of 6 patients (23.07%) contained a mosaic of 3 metaplasia types. Esophagitis was a pre-existing condition in all study participants. Inflammatory cell infiltration was moderate in 69.23% of specimens and pronounced in 30.77% of cases. Erosions of esophageal mucosa were observed in 8 patients (30.77%); ulceration was detected in 1 patient. Biopsies of 9 patients (34.62%) were described as indefinite for dysplasia (reactive changes of the epithelium characterized by the irregular arrangement and crowding of the glands, their angulated shape, slightly enlarged and hyperchromic nuclei, and single mitotic cells). In 2 specimens, reactive changes of the epithelium were observed in the presence of cardiac-type metaplasia; in 6 cases, in the presence of intestinal metaplasia with low density of goblet cells; in 1 case, in the presence of intestinal metaplasia with high density of goblet cells. Low-grade or high-grade dysplasia was not detected in any of the esophageal specimens with CM < 1 cm.

In the group with CM > 1 cm above GEJ, cardiac-type metaplasia was detected in 14 of 24 patients (58.33%), whereas fundic, in 10 individuals (41.67%). The group of patients with BE included 42 individuals with intestinal metaplasia. If we merge these two groups into one, the ratio of metaplasia types will be as follows (Fig. 3): cardiac type, 14 of 66 patients (21.21%), fundic type, 10 (15.15%), intestinal type, 42 (63.64%). The mosaic of all 3 types was observed in 8 patients with BE (12.12%). In the BE group (42 patients with intestinal metaplasia; Fig. 4), few goblet cells were detected in 8 participants (18.18%); low-density goblet cells, in 15 individuals (43.09%); high-density goblet cells, in 21 patients (47.73%).
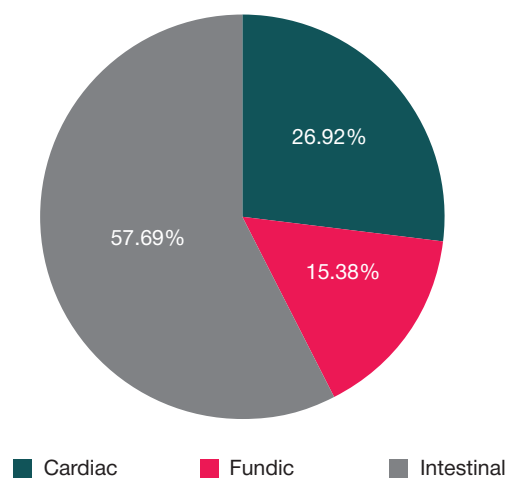

Fig. 1. Prevalence of different metaplasia types in CM segments extending < 1 cm above GEJ
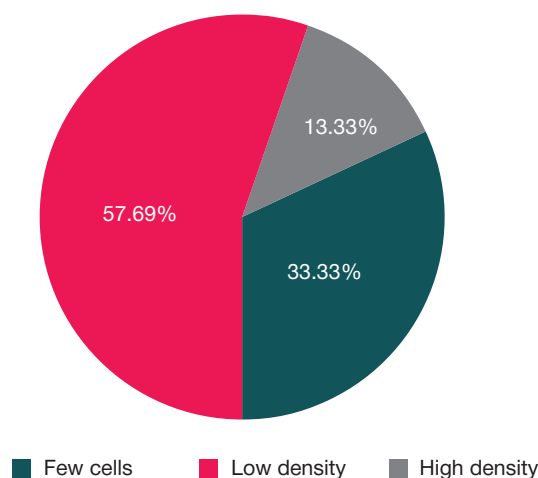

Fig. 2. The relative number of goblet cells in CM segments extending < 1 cm above GEJ

Thus, intestinal metaplasia was more prevalent in the biopsies of patients with CM > 1 cm above GEJ and BE than in the group with CM < 1 cm above GEJ (63.64 and 57.69% respectively; Fig. 5). High-density goblet cells occurred in the patients with BE 3.5 times more often than in those with CM < 1 cm (Fig. 6).

Signs of esophagitis with moderate inflammatory lymphocyte/plasma cell infiltration were detected in 16 patients with CM > 1 cm above GEJ (66.67%), whereas signs of pronounced inflammation, in 8 patients (33.33%). Erosions of the metaplastic mucosa were present in 11 patients (45.83%); of them 1 patient had areas of ulceration. Reactive changes of the epithelium were observed in 5 patients with columnar metaplasia (20.83%); of them 3 had cardiac type and 2, fundic type. One patient was found to have high-grade dysplasia of the metaplastic segment in the presence of cardiac-type metaplasia (4.2%).

Signs of esophagitis with moderate inflammatory lymphocyte/plasma cell infiltration were detected in 18 patients with BE (42.86%), whereas signs of pronounced inflammation, in 26 patients (57.14%); 27 patients had erosions of metaplastic esophageal segments (64.29%), of them 4 individuals had areas of ulceration. Erosions were detected 2.1 times more often in the patients with BE than in those with CM < 1 cm above GEJ and 1.4 times more often than in the patients with CM > 1 cm above GEJ. Reactive changes of the epithelium were observed in 15 patients (35.71%). Thus, reactive changes of the epithelium occurred with the same frequency in the patients with BE and CM < 1 cm above GEJ and were 1.7 more rare in the patients with CM > 1 cm without intestinal metaplasia. Reactive changes of the epithelium were significantly more frequent in the patients with BE than in those with CM > 1 cm above GEJ (Mann–Whitney U test; $p < 0.05$). Such changes were equally prevalent in the samples differing in the density of goblet cells (few goblet cells, low density of goblet cells and high density of goblet). In all cases, the changes were associated with the severity of inflammation (Mann–Whitney U, $p < 0.05$).

Low- or high-grade dysplasia was absent in the patients with CM < 1 cm. Low-grade dysplasia (Fig. 7A) was diagnosed in 8 patients with BE (19.05%); of them 6 patients had high-density goblet cells and 2, single goblet cells. One patient with CM > 1 cm was found to have high-grade dysplasia (4.2%; Fig. 7B).

Eight specimens of CM > 1 cm and 16 specimens of BE were tested for the markers of intestinal (MUC2, CDX2, Villin) and gastric (MUC1, MUC5A, MUC6) differentiation using immunohistochemistry assays. Samples with cardiac and fundic-type metaplasia were characterized by strong diffuse expression of MUC5A in the cytoplasm of the surface epithelial layer, weak diffuse expression of MUC1 in the cytoplasm of the surface epithelial layer, diffuse expression of MUC1, MUC5A and MUC6 in the cytoplasm of glandular epithelium. MUC2 was not expressed in the samples with cardiac or fundic-type metaplasia. CDX2 was expressed in 5 patients with cardiac and fundic-type metaplasia (in up to 30% of the cells in the biopsied fragment); Villin expression was noted in 8 cases (in 15–20 to 80% of glandular epithelial cells). Expression of intestinal markers (CDX2 and Villin) in the samples with cardiac and fundic-type metaplasia is a sign of submorphological enteralization. In our study, intestinal markers (MUC2, CDX2, Villin) were expressed in all 16 patients with BE and intestinal metaplasia. Their expression depended on the density of goblet cells: cytoplasmic expression of MUC2 was observed in 10 to 50% of the cells; nuclear expression of CDX2 was discovered in 10 to 90% of epithelial cells, including cells of the columnar glandular epithelium with the cardiac phenotype; cytoplasmic expression of Villin was detected in 70–100% of epithelial cells. Because goblet cells in the metaplastic BE epithelium are interspersed with foveolar cells, intestinal metaplasia is also characterized by the expression of gastric markers: MUC1, MUC5A and MUC6, which seems to be weaker than in cardiac-type metaplasia and not so spread out.

The immunohistochemical analysis of BE fragments with low-grade dysplasia revealed pronounced expression of MUC2, CDX2 and Villlin and weak expression of MUC1, MUC5A and MUC6. MUC1, MUC5A, MUC6, and Villin were also expressed in one sample with high-grade dysplasia and cardiac-type metaplasia negative for MUC2 and CDX2 expression.

DISCUSSION

This study compares morphological phenotypes of columnar-lined epithelium segments extending < 1 cm above GEJ, > 1 cm above GEJ, and BE segments. Interestingly, our groups of patients with CM > 1 cm and BE were almost mirror-symmetrical in terms of male to female ratio: for the patients with CM > 1 cm, the male to female ratio was 1 : 2.4, whereas for the patients with BE, it was 2.23 : 1. In all groups, the mean age of male participants was a bit lower than the mean age of women because the male sex is one of the risk factors for GERD. It is believed that cardiac-type metaplasia is the earliest type of CM in patients with GERD. In our study, in the

63.64%   21.21%   15.15%

■ Cardiac   ■ Fundic   ■ Intestinal
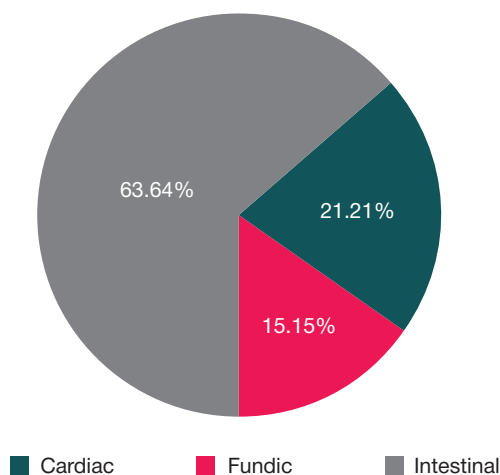
**Fig. 3.** Prevalence of different types of columnar metaplasia in different parts of the biopsied segment > 1 cm above GEJ, including BE

18.18%   47.73%   43.09%

■ Few cells   ■ Low density   ■ High density
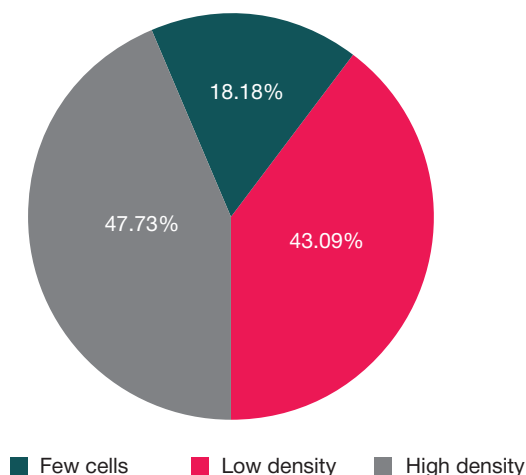
Fig. 4. The relative number of goblet cells in BE segments.

absence of other metaplastic changes cardiac-type metaplasia was detected more frequently in the patients with CM < 1 cm (26.92%) than in C0M1.5–C13M14 biopsies (21.21%). Goblet cells occurred more frequently in the metaplastic segments > 1 cm in length; high-density goblet cells were seen 3.5 times more often in the patients with CM < 1 cm than in those with CM < 1 cm. According to the literature, the frequency of goblet cell occurrence increases with the length of the metaplastic esophageal segment [6]. In our next study, we will be attempting to establish a correlation between the length of the BE segment, the frequency of goblet cell occurrence and their density.

Reactive changes of the epithelium were observed significantly more often in the group of patients with BE vs the group with CM > 1 cm above GEJ and were associated with the severity of inflammation (Mann-Whitney U, p < 0.05). In the patients with BE, dysplasia was detected more often (19.05%) than in the patients with CM > 1 cm (4.2%). Biopsies characterized by low-grade dysplasia in the presence of BE showed pronounced expression of intestinal (MUC2, CDX2, Villin) and weaker expression of gastric (MUC1, MUC5A, MUC6) markers, which is consistent with the mixed metaplastic phenotype dominated by intestinal metaplasia [13, 14, 18–20]. The only case of high-grade dysplasia with CM > 1 cm was characterized by bright expression of MUC1, MUC5A, MUC6, and Villin and was negative for MUC2 and CDX2 expression, suggesting the cardiac phenotype. Thus, we

observed both intestinal (BE) and foveolar (CM >1 cm above GEJ) carcinogenesis pathways, but the intestinal one prevailed in our sample, in spite of the miniature size of the dysplastic focus (≥ 2 mm).

It is hypothesized that high density of goblet cells can be protective against dysplasia [16, 17]. In our sample, low-grade dysplasia was detected in 6 of 8 biopsies (75%) characterized by high density of goblet cells in the adjacent esophageal mucosa. This can be explained by a small number of low-grade dysplasia cases in our patient sample. Further research is needed to provide a more objective morphological profile for patients with BE in the early stage of dysplasia and to identify the group at risk for this condition.

CONCLUSIONS

The accuracy of ultra-short BE diagnosis largely depends on precise targeting during biopsy sampling. This diagnosis can be established only if the biopsied specimen contains esophageal components (stratified squamous cell epithelium, excretory ducts and glands of the mucosa) and shows distinct metaplastic changes in the esophageal epithelium. Our comparative analysis of biopsy samples revealed that reactive changes in the epithelium were more frequent in the BE segments than in the specimens with CM > 1 cm above GEJ (Mann-Whitney U, $p < 0.05$); in the group with CM < 1 cm, these

Columnar metaplasia < 1 cm above GEJ
Columnar metaplasia > 1 cm above GEJ
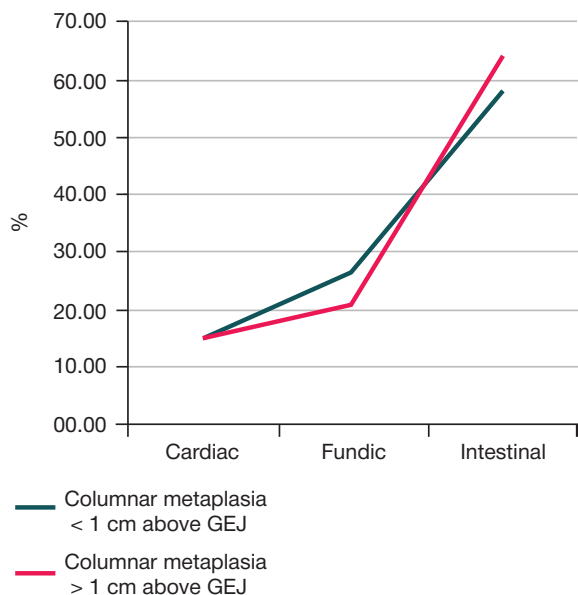
Fig. 5. The relative number of different metaplasia types in CM segments < 1 cm and > 1 cm above GEJ

The relative number of goblet cells in CM segments extending < 1 cm above GEJ
The relative number of goblet cells in BE segments
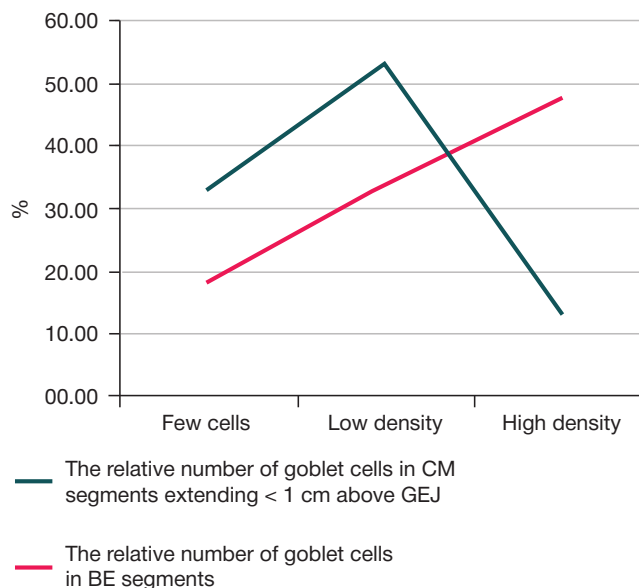
Fig. 6. The relative number of goblet cells in CM segments < 1 cm above GEJ and in BE segments

Low-grade dysplasia


Mitosis
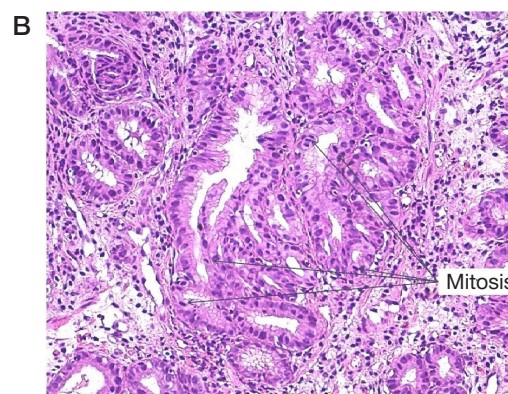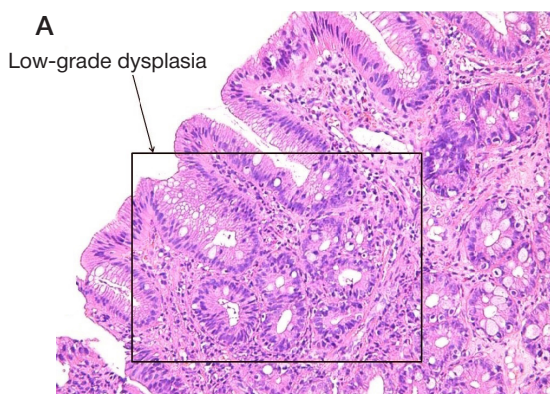
Fig. 7. A. Low-grade esophageal dysplasia in patients with BE. **B**. High-grade esophageal dysplasia in patients with CM > 1 cm above GEJ. Staining: hematoxylin-eosin; magnification ×200

changes were observed more often in the presence of goblet cells. Reactive changes in the epithelium were associated with the severity of esophagitis. Genuine dysplasia was detected in 8 patients with BE (low-grade dysplasia, 19.05%) and in 1 patient with CM > 1 cm above GEJ (high-grade dysplasia,

4.2%). Immunohistochemical testing for the intestinal and gastric markers of cell differentiation revealed the signs of submorphological enteralization in all esophageal specimens with cardiac and fundic type metaplasia and in the specimens with BE in the areas lacking goblet cells.

References

1. Shaheen NJ, Falk GW, Iyer PG, Gerson LB. ACG clinical guideline: diagnosis and management of Barrett's esophagus. Am J Gastroenterol. 2016; 111 (1): 30–50. PubMed PMID: 26526079.
2. Fitzgerald RC, di Pietro M, Ragunath K, Ang Y, et al. British Society of Gastroenterology guidelines on the diagnosis and management of Barrett's oesophagus. Gut. 2014; (63): 7–42. PubMed PMID: 24165758.
3. Bennett C, Moayyedi P, Corley DA, DeCaestecker J et al. BOB CAT: A Large-Scale Review and Delphi Consensus for Management of Barrett's Esophagus With No Dysplasia, Indefinite for, or Low-Grade Dysplasia. Am J Gastroenterol. 2015; (110): 662–82. PubMed PMID: 25869390.
4. Montgomery EA, Canto MI, Srivastava A. Evaluation and reporting of biopsies from the columnar-lined esophagus and gastro-esophageal junction (GEJ). Ann Diagn Pathol. 2019; (39): 111–7. PubMed PMID: 30802810.
5. Biswas S, Quante M, Leedham S, Jansen M. The metaplastic mosaic of Barrett's oesophagus Virchows Archiv. 2018; (472): 43–54. PubMed PMID: 29500519
6. Harrison R, Perry I, Haddadin W, McDonald S, et al. Detection of intestinal metaplasia in Barrett's esophagus: an observational comparator study suggests the need for a minimum of eight biopsies. Am J Gastroenterol. 2007; (102): 1154–61. PubMed PMID: 17433019.
7. Que J, Garman KS, Souza RF, Spechler SJ. Pathogenesis and Cells of Origin of Barrett's Esophagus. Gastroenterology. 2019; 157 (2): 349–64. PubMed PMID: 31082367.
8. Theodorou D, Ayazi S, DeMeester SR, Zehetner J, et al. Intraluminal pH and goblet cell density in Barrett's esophagus. J Gastrointest Surg. 2012; (16): 469–74. PubMed PMID: 22095525.
9. Sun D, Wang X, Gai Z, Song X, Jia X, Tian H. Bile acids but not acidic acids induce Barrett's esophagus. Int J Clin Exp Pathol. 2015; 8 (2): 1384–92. PMID: 25973022.
10. Hahn HP, Blount PL, Ayub K, Das KM, et al. Intestinal differentiation in metaplastic, nongoblet columnar epithelium in the esophagus. Am J Surg Pathol. 2009; (33): 1006–15. PubMed PMID: 19363439.
11. Bhat S, Coleman HG, Yousef F, Johnston BT, et al. Risk of malignant progression in Barrett's esophagus patients: results from a large population-based study. 2011; J Natl Cancer Inst. 103 (13): 1049–57. PubMed PMID: 21680910.
12. Kelty CJ, Gough MD, Van Wyk Q, Stephenson TJ, Ackroyd R. Barrett's oesophagus: intestinal metaplasia is not essential for cancer risk. Scand J Gastroenterol. 2007; 42 (11): 1271–4. PubMed PMID: 17852872.
13. Takubo K, Aida J, Naomoto Y, et al. Cardiac rather than intestinal type background in endoscopic resection specimens of minute Barrett adenocarcinoma. Hum Pathol. 2009; 40 (1): 65–74. PubMed PMID: 18755496.
14. Watanabe G, Ajioka Y, Takeuchi M, Annenkov A, Kato T, et al. Intestinal metaplasia in Barrett's oesophagus may be an epiphenomenon rather than a preneoplastic condition, and CDX2-positive cardiac-type epithelium is associated with minute Barrett's tumour. Histopathology. 2015; 66 (2): 201–14. PubMed PMID: 25040564.
15. Lavery DL, Martinez P, Gay LJ, Cereser B, et al. Evolution of oesophageal adenocarcinoma from metaplastic columnar epithelium without goblet cells in Barrett's oesophagus. Gut. 2016; 65 (6): 907–13. PubMed PMID: 26701877.
16. Schellnegger R, Quante A, Rospleszcz S, Schernhammer M, et al. Goblet cell ratio in combination with differentiation and stem cell markers in Barrett esophagus allow distinction of patients with and without esophageal adenocarcinoma. Cancer Prev Res. (Phila). 2017; 10 (1): 55–66. PubMed PMID: 27807078.
17. Srivastava A, Golden KL, Sanchez CA, Liu K, et al. High goblet cell count is inversely associated with ploidy abnormalities and risk of adenocarcinoma in Barrett's esophagus. PLoS One. 2015; 10 (7): e0133403. PubMed PMID: 26230607.
18. Agoston AT, Srivastava A, Zheng Y, et al. Prevalence and concordance of subtypes of dysplasia in patients with Barrett's esophagus-associated adenocarcinoma. Mod Pathol. 2014; (27): 162a–162a.
19. Demicco EG, Farris AB, Baba Y, Agbor-Etang B, et al. The dichotomy in carcinogenesis of the distal esophagus and esophagogastric junction: intestinal-type vs cardiac-type mucosa-associated adenocarcinoma. Mod Pathol. 2011; (24): 1177–90. PubMed PMID: 21572404.
20. Khor TS, Alfaro EE, Ooi EM, Li Y, et al. Divergent expression of MUC5AC, MUC6, MUC2, CD10, and CDX-2 in dysplasia and intramucosal adenocarcinomas with intestinal and foveolar morphology: Is this evidence of distinct gastric and intestinal pathways to carcinogenesis in Barrett esophagus? Am J Surg Pathol. 2012; (36): 331–42. PubMed PMID: 22261707.

Литература

1. Shaheen NJ, Falk GW, Iyer PG, Gerson LB. ACG clinical guideline: diagnosis and management of Barrett's esophagus. Am J Gastroenterol. 2016; 111 (1): 30–50. PubMed PMID: 26526079.
2. Fitzgerald RC, di Pietro M, Ragunath K, Ang Y, et al. British Society of Gastroenterology guidelines on the diagnosis and management of Barrett's oesophagus. Gut. 2014; (63): 7–42. PubMed PMID: 24165758.
3. Bennett C, Moayyedi P, Corley DA, DeCaestecker J et al. BOB CAT: A Large-Scale Review and Delphi Consensus for Management of Barrett's Esophagus With No Dysplasia, Indefinite for, or Low-Grade Dysplasia. Am J Gastroenterol. 2015; (110): 662–82. PubMed PMID: 25869390.
4. Montgomery EA, Canto MI, Srivastava A. Evaluation and reporting of biopsies from the columnar-lined esophagus and gastro-esophageal junction (GEJ). Ann Diagn Pathol. 2019; (39): 111–7. PubMed PMID: 30802810.
5. Biswas S, Quante M, Leedham S, Jansen M. The metaplastic mosaic of Barrett's oesophagus Virchows Archiv. 2018; (472): 43–54. PubMed PMID: 29500519
6. Harrison R, Perry I, Haddadin W, McDonald S, et al. Detection of intestinal metaplasia in Barrett's esophagus: an observational comparator study suggests the need for a minimum of eight biopsies. Am J Gastroenterol. 2007; (102): 1154–61. PubMed PMID: 17433019.
7. Que J, Garman KS, Souza RF, Spechler SJ. Pathogenesis and Cells of Origin of Barrett's Esophagus. Gastroenterology. 2019; 157 (2): 349–64. PubMed PMID: 31082367.
8. Theodorou D, Ayazi S, DeMeester SR, Zehetner J, et al. Intraluminal pH and goblet cell density in Barrett's esophagus. J Gastrointest Surg. 2012; (16): 469–74. PubMed PMID:

22095525.

9. Sun D, Wang X, Gai Z, Song X, Jia X, Tian H. Bile acids but not acidic acids induce Barrett's esophagus. Int J Clin Exp Pathol. 2015; 8 (2): 1384–92. PMID: 25973022.

10. Hahn HP, Blount PL, Ayub K, Das KM, et al. Intestinal differentiation in metaplastic, nongoblet columnar epithelium in the esophagus. Am J Surg Pathol. 2009; (33): 1006–15. PubMed PMID: 19363439.

11. Bhat S, Coleman HG, Yousef F, Johnston BT, et al. Risk of malignant progression in Barrett's esophagus patients: results from a large population-based study. 2011; J Natl Cancer Inst. 103 (13): 1049–57. PubMed PMID: 21680910.

12. Kelty CJ, Gough MD, Van Wyk Q, Stephenson TJ, Ackroyd R. Barrett's oesophagus: intestinal metaplasia is not essential for cancer risk. Scand J Gastroenterol. 2007; 42 (11): 1271–4. PubMed PMID: 17852872.

13. Takubo K, Aida J, Naomoto Y, et al. Cardiac rather than intestinal type background in endoscopic resection specimens of minute Barrett adenocarcinoma. Hum Pathol. 2009; 40 (1): 65–74. PubMed PMID: 18755496.

14. Watanabe G, Ajioka Y, Takeuchi M, Annenkov A, Kato T, et al. Intestinal metaplasia in Barrett's oesophagus may be an epiphenomenon rather than a preneoplastic condition, and CDX2-positive cardiac-type epithelium is associated with minute Barrett's tumour. Histopathology. 2015; 66 (2): 201–14. PubMed PMID: 25040564.

15. Lavery DL, Martinez P, Gay LJ, Cereser B, et al. Evolution of oesophageal adenocarcinoma from metaplastic columnar epithelium without goblet cells in Barrett's oesophagus. Gut. 2016; 65 (6): 907–13. PubMed PMID: 26701877.

16. Schellnegger R, Quante A, Rospleszcz S, Schernhammer M, et al. Goblet cell ratio in combination with differentiation and stem cell markers in Barrett esophagus allow distinction of patients with and without esophageal adenocarcinoma. Cancer Prev Res. (Phila). 2017; 10 (1): 55–66. PubMed PMID: 27807078.

17. Srivastava A, Golden KL, Sanchez CA, Liu K, et al. High goblet cell count is inversely associated with ploidy abnormalities and risk of adenocarcinoma in Barrett's esophagus. PLoS One. 2015; 10 (7): e0133403. PubMed PMID: 26230607.

18. Agoston AT, Srivastava A, Zheng Y, et al. Prevalence and concordance of subtypes of dysplasia in patients with Barrett's esophagus-associated adenocarcinoma. Mod Pathol. 2014; (27): 162a–162a.

19. Demicco EG, Farris AB, Baba Y, Agbor-Etang B, et al. The dichotomy in carcinogenesis of the distal esophagus and esophagogastric junction: intestinal-type vs cardiac-type mucosa-associated adenocarcinoma. Mod Pathol. 2011; (24): 1177–90. PubMed PMID: 21572404.

20. Khor TS, Alfaro EE, Ooi EM, Li Y, et al. Divergent expression of MUC5AC, MUC6, MUC2, CD10, and CDX-2 in dysplasia and intramucosal adenocarcinomas with intestinal and foveolar morphology: Is this evidence of distinct gastric and intestinal pathways to carcinogenesis in Barrett esophagus? Am J Surg Pathol. 2012; (36): 331–42. PubMed PMID: 22261707.

LIPIDOME FEATURES IN PATIENTS WITH DIFFERENT PROBABILITY OF FAMILY HYPERCHOLESTEROLEMIA

Rogozhina AA[1,2], Minushkina LO[1] ✉, Alessenko AV[3], Gutner UA[3], Shupik MA[3], Kurochkin IN[3], Maloshitskaya OA[4], Sokolov SA[4], Zateyshchikov DA[1,2]

[1] Central State Medical Academy under the Administrative Department of the President of the Russian Federation, Moscow, Russia

[2] City Clinical Hospital № 51, Moscow, Russia

[3] Institute for Biochemical Physics, Moscow, Russia

[4] Lomonosov Moscow State University, Moscow, Russia

Development of modern methods for metabolome assessment, such as gas chromatography–mass spectrometry, allows one to expand the knowledge about the features of lipid metabolism in various clinical conditions. The study was aimed to investigate lipidome features in patients with different probability of family hypercholesterolemia (FH). The study involved 35 patients: 15 men (42.9%) and 20 women (57.1%) with dislipidemia or early cardiovascular diseases which manifested below 55 in men and 60 in women (average age of patients was 49.8 ± 9.96). The family dislipidemia probability was evaluated using the Dutch Lipid Clinic Network Score. In 10 patients the probability of FH was low (score 1–2), 22 patients had possible FH (score 3–5). Three patients had probable or definite FH (score 6 in 2 patients, score 9 in one patient). Determination of molecular species of sphingomyelins, ceramides and sphingoid bases (sphingosine, sphinganine) as well as galactosylceramide was carried out using gas chromatography–mass spectrometry. In patients with definite/probable FH the sphingosine level was significantly higher compared with patients having low probability of FH (144.36 ± 107.863 and 50.14 ± 62.409 ng/ml; $p = 0.01$). In patients with FH, an increase in the proportion of long chain sphingomyelin SM 18 : 1/22 : 0 as well as a significant increase in the level of long chain ceramides with C 20 : 1 and C 22 : 1 was determined. Positive correlation of low-density lipoproteins and sphingosine level ($r = 0.344$; $p = 0.047$) together with negative correlation of high-density lipoproteins (HDL), sphinganine ($r = -0.52$; $p = 0.002$), and galactosylceramide level ($r = -0.56$; $p = 0.001$) were detected. Thus, in patients with high probability of FH the lipidome changes were observed, which could be considered the cardiovascular risk markers.

Keywords: atherosclerosis, family hyperlipidemia, sphingomyelins, sphingosine, ceramides, risk marker

✉ **Correspondence should be addressed:** Larisa O. Minushkina
Filevsky Boulevard, 36–19, Moscow, 121601; minushkina@mail.ru

ОСОБЕННОСТИ ЛИПИДОМА У БОЛЬНЫХ С РАЗЛИЧНОЙ КЛИНИЧЕСКОЙ ВЕРОЯТНОСТЬЮ СЕМЕЙНОЙ ГИПЕРЛИПИДЕМИИ

А. А. Рогожина[1,2], Л. О. Минушкина[1] ✉, А. В. Алесенко[3], У. А. Гутнер[3], М. А. Шупик[3], И. Н. Курочкин[3], О. А. Малошицкая[4], С. А. Соколов[4], Д. А. Затейщиков[1,2]

[1] Центральная государственная медицинская академия Управления делами Президента Российской Федерации, Москва, Россия

[2] Городская клиническая больница № 51, Москва, Россия

[3] Институт биохимической физики имени Н. М. Эмануэля РАН, Москва, Россия

[4] Московский государственный университет имени М. В. Ломоносова, Москва, Россия

Разработка современных методов оценки метаболома, таких как хромато-масс-спектрометрия, позволяет существенно расширить представления о липидном обмене в конкретных клинических ситуациях. Целью исследования было изучить особенности липидома у больных с различной вероятностью семейной гиперхолестеринемии (СГХС). В исследовании приняли участие 35 пациентов — 15 мужчин (42,9%) и 20 женщин (57,1%) с дислипидемией или ранними сердечно-сосудистыми заболеваниями, развившимися в возрасте до 55 лет у мужчин и до 60 лет у женщин. Средний возраст пациентов составил 49,8 ± 9,96 лет. Вероятность семейной дислипидемии оценивали по критериям сети голландских липидных клиник. У 10 пациентов вероятность СГХС оценивали как низкую (1–2 балла), у 22 пациентов диагноз расценивали как вероятную СГХС (3–5 баллов). У 3 пациентов присутствовала возможная или определенная СГХС (2 пациента — 6 баллов, один пациент — 9 баллов). Определение молекулярных видов сфингомиелинов, церамидов и сфингоидных оснований (сфингозина, сфинганина), а также галактозоцерамида проводили методом хромато-масс-спектрометрии. Пациенты с определенной/вероятной СГХС имели достоверно более высокий уровень сфингозина по сравнению с пациентами с низкой клинической вероятностью СГХС ($144,36 \pm 107,863$ и $50,14 \pm 62,409$ нг/мл; $p = 0,01$). В случае семейной СГХС отмечали увеличение доли длинноцепочечного сфингомиелина SM 18 : 1/22 : 0 и существенное увеличение уровня церамидов с длинной углеродной цепью C 20 : 1 и C 22 : 1. Была выявлена значимая прямая корреляция уровня липопротеинов низкой плотности (ЛНП) и сфингозина ($r = 0,344$; $p = 0,047$) наряду с обратными корреляциями уровня липопротеинов высокой плотности (ЛВП), сфинганина ($r = -0,52$; $p = 0,002$) и галактозилцерамида ($r = -0,56$; $p = 0,001$). Таким образом, у пациентов с высокой клинической вероятностью СГХС были выявлены изменения липидома, являющиеся маркерами риска сердечно-сосудистых осложнений.

Ключевые слова: атеросклероз, семейная гиперлипидемия, сфингомиелины, сфингозин, церамиды, маркеры риска

✉ **Для корреспонденции:** Минушкина Лариса Олеговна
Филевский б-р, 36–19, г. Москва, 121601; minushkina@mail.ru

Lipid metabolism disorders, including the hereditary ones, are a key risk factor for atherosclerosis and its complications. The development of newest metabolome investigation methods, such as gas chromatography-mass spectrometry, allows one to expand the knowlege about the features of lipid metabolism in various clinical situations.

It was found that sphingolipids (sphingomyelins, ceramides, sphingosine, sphinganine sphingosine-1-phosphate (S1P) etc.) can play a significant role [1]. A change in the ratio of various sphingolipids is detected in patients affected with certain metabolic, genetic and autoimmune diseases (Fabry disease, Niemann–Pick diseases, Gaucher disease etc., some types of epilepsy, migraine, Alzheimer's disease).

An active study of the lipidome features associated with cardiovascular diseases is currently carried out. The prognostic value of some lipid fractions, mainly ceramides, in acute coronary syndrome has been revealed. The ratios of ceramides C 16 : 0, C 20 : 0, C 24 : 1 and their relationship к C 24 : 0 are considered as possible risk markers.

The prognostic value of ceramides was evaluated in prospective studies. The ceramides' level was determined in patients with acute coronary syndrome [2]. It was found that the level of sphingomyelins, sphingosine, sphingazine-1-

phosphate and ceramides can differ significantly in patients with acute and chronic forms of coronary heart disease [3].

At the same time, the lipidome features in patients with hereditary dislipidemia have not been studied. There are still no convincing data on the dynamics of the level of sphingolipids and ceramides against the background of lipid-lowering therapy. There are only single cases of comparison of the level of sphingolipids in patients without therapy and in patients receiving the lipid-lowering therapy [4, 5].

The study was aimed to investigate the features of sphingolipids in patients with different probability of family hypercholesterolemia.

METHODS

The study was carried out at the City Clinical Hospital № 51 in March-October 2019. Thirty five patients were surveyed. In the group of patients under study there were 15 men (42.9%) and 20 women (57.1%), average age was 49.8 ± 9.96. Inclusion criteria: early manifestations of atherosclerosis (coronary heart disease, peripheral artery disease or cerebrovascular disease with the age of onset below 55 in men and 60 in women, and/or dislipidemia (LDL > 4,9 mmol/l). Exclusion criteria:

Table 1. Lipids and sphingolipids level in patiens with different probability of family hyperlipidemia

Parameters	Unlikely FH (n = 10)	Probable FH (n = 22)	Possible/definite FH (n = 3)	p
	1	2	3	
TC, µmol/l	6.79 ± 0.627	8.04 ± 1.746	12.00 ± 5.344	0.006
LDL, µmol/l	4.32 ± 0.45435	5.40 ± 0.973	7.24 ± 1.447	0.001
HDL, µmol/l	1.52 ± 0.431	1.45 ± 0.457	1.15 ± 0.578	0.713
TG, µmol/l	1.81 ± 1.123	2.46 ± 3.245	5.80 ± 6.141	0.240
Sphingosine, ng/ml	50.14 ± 62.409	83.59 ± 70.774	144.36 ± 107.863	0.051 *0.010 (groups 1 and 3)
Sphinganine, ng/ml	0.752 ± 0.3713	0.895 ± 0.5841	1.663 ± 1.4619	0.142
Galactosylceramide, ng/ml	55.48 ± 29.867	66.60 ± 43.291	76.95 ± 25.626	0.473
Sphingomyelines				
SM 18 : 1/16 : 0, µg/ml	18997.6 ± 13203.93	15407.2 ± 7769.07	9557.6 ± 2435.11	0.274
SM 18 : 1/16 : 1, µg/ml	1893.9 ± 714.16	1861.1 ± 1642.95	2208.3 ± 1071.19	0.432
SM 18 : 1/18 : 0, µg/ml	3646.2 ± 2447.91	3322.6 ± 1981.05	2392.6 ± 1758.81	0.629
SM 18 : 1/18 : 1, µg/ml	6138.8 ± 4915.11	5605.4 ± 2747.14	7240.6 ± 3716.52	0.806
SM 18 : 1/20 : 0, µg/ml	19573.6 ± 9198.49	22693.9 ± 15985.31	24874.3 ± 6191.24	0.525
SM 18 : 1/20 : 1, µg/ml	55331.1 ± 34643.17	55612.7 ± 32720.49	45554.0 ± 17549.55	0.924
SM 18 : 1/22 : 0, µg/ml	6484.3 ± 3692.833	7141.1 ± 2842.95	10927.6 ± 4151.37	0.028
SM 18 : 1/22 : 1, µg/ml	407.4 ± 191.59	416.9 ± 211.78	478.6 ± 143.01	0.721
SM 18 : 1/24 : 0, µg/ml	1759.7 ± 1613.16	2155.4 ± 1063.40	1728.0 ± 337.634	0.328
SM 18 : 1/24 : 1, µg/ml	6095.1 ± 3364.35	4835.2 ± 2611.45	4711.3 ± 1018.43	0.569
Ceramides				
C 18 : 0, µg/ml	3.70 ± 8.820	6.04 ± 9.740	0.018 ± 0.186	0.513
C 20 : 0, µg/ml	224.70 ± 655.577	240.60 ± 431.668	367.67 ± 144.417	0.075
C 20 : 1, µg/ml	85.10 ± 124.969	98.00 ± 229.133	698.67 ± 1138.155	0.019
C 22 : 0, µg/ml	149.60 ± 347.728	75.96 ± 71.642	221.33 ± 170.365	0.100
C 22 : 1, µg/ml	77.00 ± 82.254	60.80 ± 111.859	714.67 ± 1118.787	0.003
C 24 : 0, µg/ml	587.80 ± 200.069	737.96 ± 354.259	782.00 ± 357.669	0.598
C 24 : 1, µg/ml	206.20 ± 77.150	313.08 ± 254.952	465.67 ± 457.362	0.546
C 18 : 0/C 24 : 0, µg/ml	0.0043 ± 0.00938	0.0079 ± 0.01275	0.0000 ± 0.00000	0.963
C 24 : 1/C 24 : 0, µg/ml	0.3678 ± 0.13805	0.4600 ± 0.35776	0.5124 ± 0.29631	0.675

Note: Kruskal–Wallis test.

acute myocardial infarction, acute stroke, diabetes mellitus, secondary dislipidemia. The study did not include patients who received lipid-lowering therapy at the time of the examination.

In the beginning of the study 16 patients had arterial hypertension (45.7%), 10 patients had coronary heart disease (28.6%) and one patient had peripheral artery disease (2.9%). Nineteen patients (54.3%) had significant family history of cardiovascular diseases. Nine patients (25.7%) smoked in their past but stopped smoking before inclusion in the study, 8 patients smoked at the moment of inclusion in the study (22.9%)

The familial hypercholesterolemia (FH) probability was evaluated using the Dutch Lipid Clinic Network Score. In 10 patients the probability of FH was low (score 1–2), 22 patients had possible FH (score 3–5). Three patients had probable or definite FH (score 6 in 2 patients, score 9 in one patient).

Blood sampling for biochemical analysis and mass spectrometry was performed on the day the patients were included in the study (in the morning on an empty stomach, after a 12-hour fast). Blood was taken from the cubital vein into sterile

Vakutainer tubes. Serum was obtained by blood centrifuging at a speed of 3000 rpm for 15 minutes. Parameters with the following reference values were defined: total cholesterol (TC, 2.0–5.2 mmol/l), low-density lipoprotein cholesterol (LDL-C, up to 3.3 mmol/l), high-density lipoprotein cholesterol (HDL-C, 0.91–1.56 mmol/l), blood serum triglycerides (TG, 0.50–1.70 mmol/l). To determine the parameters of serum, the CLIMA MC-15 biochemical analyzer was used (RAL; Spain).

Lipids were extracted from plasma in accordance with Bligh and Dyer Procedure [6]. Mass-spectrometry of molecular species of sphingomyelins, ceramides and sphingoid bases (sphingosine and sphinganine), as well as galactosylceramides, was performed using the TSQ Endura Triple Quadrupole Mass Spectrometer (Thermo Fisher Scientific; Germany) working in the MMP mode. The pressure at the collision cell was 1.5 mTorr. The resolution on Q1 and Q3 was 1.2 Da.

Ceramides: fragmentation of the protonated and dehydrated molecules was carried out at the energy of 25 eV down to ion with m/z 264.4 Da, the dwell time was 25 ms.

Table 2. Blood lipids and sphingolipids in patients with family history and in patients without family history

Parameters	No family history (n = 16)	Family history (n = 19)	p
TC, µmol/l	8.11 ± 1.142	7.35 ± 1.881	0.026
LDL, µmol/l	5.49 ± 1.063	4.75 ± 0.820	0.039
HDL, µmol/l	1.63 ± 0.352	1.32 ± 0.479	0.034
TG, µmol/l	1.91 ± 1.119	2.57 ± 3.712	0.845
Sphingosine, ng/ml	65.31 ± 55.298	82.37 ± 84.841	0.021
Sphinganine, ng/ml	0.25 ± 0.447	0.47 ±0.612	0.062
Galactosylceramide, ng/ml	59.38 ± 46.989	67.00 ± 33.579	0.123
Sphingomyelines			
SM 18 : 1/16 : 0, µg/ml	15812.5 ± 8874.74	16142.37 ± 10210.772	0.678
SM 18 : 1/16 : 1,µg/ml	1703.38 ± 1153.149	2079.74 ± 1637.244	0.635
SM 18 : 1/18 : 0, µg/ml	3446.00 ± 2012.195	3115.37 ± 1651.906	0.942
SM 18 : 1/18 : 1, µg/ml	6066.06 ± 4210.684	5388.68 ± 2755.342	0.862
SM 18 : 1/20 : 0, µg/ml	21605.00 ± 6986.063	22197.89 ± 18558.786	0.756
SM 18 : 1/20 : 1, µg/ml	57836.31 ± 37448.414	51584.74 ± 29461.884	0.684
SM 18 : 1/22 : 0, µg/ml	8366.13 ± 3752.568	8090.74 ± 2977.416	0.862
SM 18 : 1/22 : 1, µg/ml	387.56 ± 224.592	441.26 ± 183.190	0.672
SM 18 : 1/24 : 0, µg/ml	1809.31 ± 983.979	2218.1 ± 1409.971	0.584
SM 18 : 1/24 : 1, µg/ml	5398.19 ± 2713.511	5094.32 ± 2995.497	0.682
Ceramides			
C 18 : 0, µg/ml	6.31 ± 10.163	4.58 ± 8.946	0.213
C 20 : 0, µg/ml	78.56 ± 150.510	391.21 ± 629.556	0.021
C 20 : 1, µg/ml	57.38 ± 108.836	121.32 ± 257.882	0.010
C 22 : 0, µg/ml	60.19 ± 64.744	130.21 ± 252.256	0.040
C 22 : 1, µg/ml	47.75 ± 52.003	77.16 ± 133.153	0.252
C 24 : 0, µg/ml	726.69 ± 334.931	622.16 ± 255.175	0.572
C 24 : 1, µg/ml	324.25 ± 264.550	247.05 ± 181.903	0.457
C 18 : 0/C 24 : 0, µg/ml	0.0072 ± 0.01166	0.0067 ± 0.01235	0.323
C 24 : 1/C 24 : 0, µg/ml	0.4730 ± 0.37832	0.4078 ± 0.24104	0.872

Note: Mann–Whitney test.

Sphingomyelines: fragmentation of the protonated molecules was performed at the energy of 25 eV down to ion with m/z 184.1 Да, the dwell time was 25 ms.

Sphingosine and its deuterated standard (d7, Avanti; USA): fragmentation of the protonated molecules was carried out at the energy of 12.5 eV down to ions with m/z 264.4 and 259.3 Da respectively. The dwell time was 25 ms.

Sphinganine: fragmentation of the protonated molecule was performed at the energy of 12.5 eV down to ion with m/z 266.4 Да, the dwell time was 50 ms.

Galactosylceramide d18 : 1/18 : 0: $[M + H]^+$ ion with a mass of 728.5 Da.

The following parameters of the ionization source were used: heater temperature 300 °C, capillary temperature 340 °C, sheath gas flow 45 arb, auxiliary gas flow 13 arb, sweep gas flow 1 arb.

Sphingosine d7, sphinganine, sphingomyelin d18 : 1/16 : 0, sphingomyelin d18 : 1/18 : 0, ceramide d18 : 1/16 : 0, ceramide d18 : 1/18 : 1, ceramide d18 : 1/18 : 0, ceramide d18 : 1/24 : 1, ceramide d18 : 1/24 : 0 and galactosylceramide d18 : 1/18 : 0 (Avanti; USA) were used as standards.

Chromatography

Chromatography was performed using the Ultimate 3000 system (Thermo Fisher Scientific; Germany) and Eclipse Plus C8 column 3.0 × 150 mm (Agilent; USA), the particle size was 3.5 μm. The temperature was 50 °C, and the flow rate was 400 μl/min.

When determining sphingosine, ceramides and sphingomyelin, the following mobile phases were used: phase A, water + 0.1% (v.v.) formic acid, phase B, methanol + 0.1% (v.v.) formic acid (0.7 minutes 55% of phase B, 100 % of phase B up to 6.7 minutes, 100% of phase B up to 12th minute, 55% of phase B up to 1 –17th minute, 55% of phase B up to 13th minute).

When determining sphinganine, the following mobile phases were used: фаза A, water + 0.1% (v.v.) formic acid, phase B, 50% methanol + 50% acetonitrile + 0.1% (v.v.) formic acid (1.5 minutes 20% of phase B, 100 % of phase B up to 3.2 minutes, 100% of phase B up to 6.7 minutes, 20% of phase B up to 7.7 minutes, 20% of phase B up to 10th minute).

Data processing

The relative content of ceramides was evaluated using external calibration (method of standard addition). The Ceramide Porcine Brain 860052P ceramide mixture (Avanti; USA) was
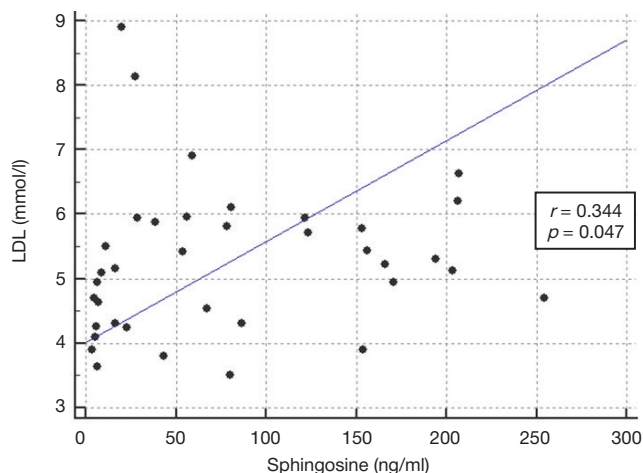
used for calibration with 50% of Cer d18 : 1/18 : 0 and 20% of Cer d18 : 1/24 : 1. The calculation was based on the sum of peak areas of the MMP transitions $MH^{+\cdot} \rightarrow$ m/z 264.4 Da and $(MH-H_2O)^{+\cdot} \rightarrow$ m/z 264.4 Da.

When determining sphingomyelines, the Sphingomielin Porcine Brain 860062P mixture (Avanti; USA) and sphingomyelines d18 : 1/16 : 0, d18 : 1/18 : 0 (Avanti; USA) were used for calibration. The sum of peak areas of the MRM transitions $MH^{+\cdot} \rightarrow$ m/z 184.1 Da was used for calculation.

The sphingosine d18 : 1 content was determined by internal calibration (internal standard method, the standard was D-erythro-sphingosine d7, Sigma; USA) using the sum of peak areas of the MMP transitions (m/z $300^{+\cdot} \rightarrow$ m/z 264.4 Da for non-deuterated and m/z $307^{+\cdot} \rightarrow$ m/z 259.3 Da for deuterated sphingosine).

The sphinganine d18 : 0 content was determined by external calibration (the standard was DL-erythro-dihidrosphingosine, Sigma; USA) using the sum of peak areas of the MMP transitions (m/z $302^{+\cdot} \rightarrow$ m/z 266 Da).

Statistical analysis

Statistical analysis was carried out using the SPSS software, version 23.0 (IBM; USA). Quantitative variables were presented as mean with standard deviation. All variables were checked for compliance with normal distribution using the Shapiro–Wilk test. The distribution of all quantitative variables was different from normal. The significance of differences for two independent samples was evaluated using the Mann–Whitney test, and for three of more samples using the Kruskal–Wallis test. The significance of correlations was determined using the Sperman rank correlation test. The differences were considered significant when $p < 0.05$.

RESULTS

Comparison of blood lipids and sphingolipids was carried out in groups of patients with different probability of family hyperlipidemia (Table 1).

Higher level of TC and LDL was observed in patients with FH. In addition, in patients with FH, a tendency was observed to sphingosine level increase compared with a group of patients having a low probability of FH ($p < 0.05$).

In patients with FH, an increase in the proportion of long-chain sphingomyelin SM 18 : 1/22 : 0 was noted, as well as a significant increase in the level of long chain ceramides, C 20 : 1 and C 22 : 1. No significant differences of C 18 : 0/C 24 : 0 and C 24 : 1/C 24 : 0 ratios were revealed.

Fig. 1. Correlation of LDL and blood sphingosine level
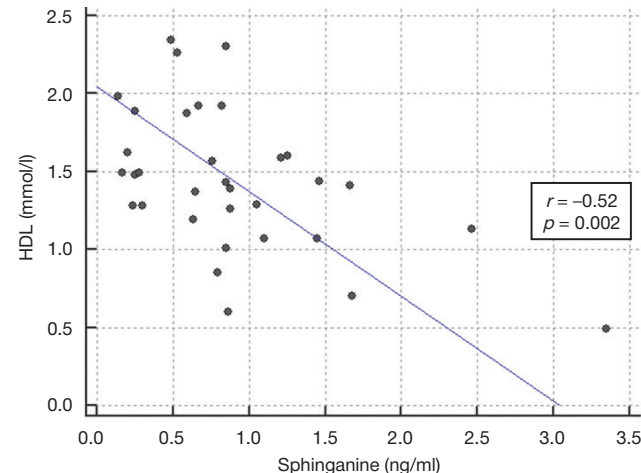
Fig. 2. Correlation of HDL and blood sphinganine level

Table 3. Correlation of blood lipids, sphingomyeline and ceramide levels

		TC, µmol/l	TG, µmol/l	LDL-C, µmol/l	HDL-C, µmol/l
SM 18 : 1/16 : 0, µg/ml	r	0.178	−0.104	0.084	0.162
	p	0.307	0.564	0.636	0.391
SM 18 : 1/16 : 1, µg/ml	r	0.260	−0.171	0.093	0.045
	p	0.132	0.341	0.602	0.813
SM 18 : 1/18 : 0, µg/ml	r	0.257	−0.140	0.278	0.236
	p	0.135	0.439	0.111	0.210
SM 18 : 1/18 : 1, µg/ml	r	−0.139	−0.095	−0.202	0.077
	p	0.426	0.597	0.251	0.686
SM 18 : 1/20 : 0, µg/ml	r	0.363*	−0.015	0.184	−0.110
	p	0.032	0.934	0.297	0.561
SM 18 : 1/20 : 1, µg/ml	r	−0.101	0.111	−0.098	0.334
	p	0.562	0.540	0.581	0.072
SM 18 : 1/22 : 0, µg/ml	r	−0.017	−0.313	−0.155	0.165
	p	0.924	0.076	0.383	0.382
SM 18 : 1/22 : 1, µg/ml	r	0.082	0.146	0.125	−0.187
	p	0.642	0.419	0.481	0.321
SM 18 : 1/24 : 0, µg/ml	r	0.048	−0.183	0.100	−0.254
	p	0.782	0.307	0.572	0.175
SM 18 : 1/24 : 1 µg/ml	r	0.217	−0.297	0.148	0.046
	p	0.210	0.094	0.403	0.809
C 18 : 0, µg/ml	r	0.104	−0.041	0.105	−0.104
	p	0.552	0.820	0.556	0.584
C 20 : 0, µg/ml	r	0.055	0.141	−0.003	−0.420*
	p	0.752	0.433	0.987	0.021
C 20 : 1, µg/ml	r	−0.177	0.447**	−0.425*	0.525**
	p	0.310	0.009	0.012	0.003
C 22 : 0, µg/ml	r	0.015	0.342	0.049	−0.429*
	p	0.932	0.052	0.783	0.018
C 22 : 1, µg/ml	r	0.070	0.051	−0.094	−0.168
	p	0.689	0.776	0.598	0.374
C 24 : 0, µg/ml	r	0.475**	0.100	0.334	0.008
	p	0.004	0.579	0.054	0.965
C 24 : 1, µg/ml	r	0.558**	0.005	0.471**	0.296
	p	0.000	0.976	0.005	0.112

Note: r — Spearman rank correlation; * — $p < 0.005$; ** — $p < 0.001$.
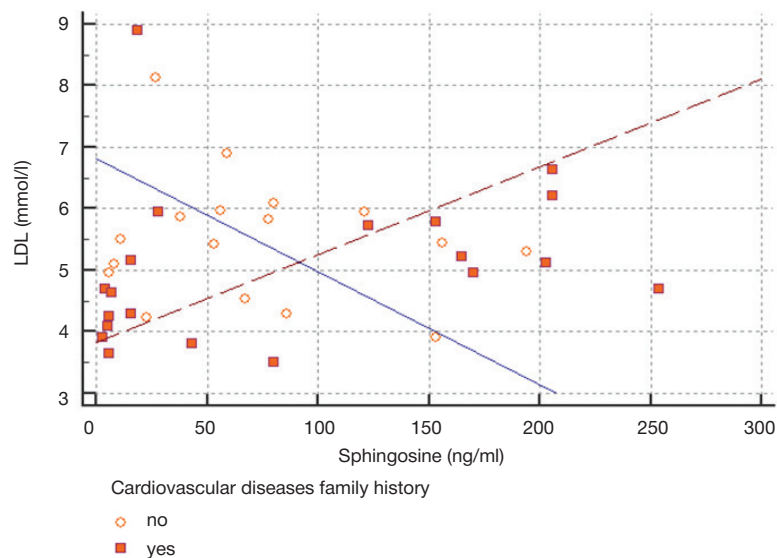
Fig. 3. Correlation of LDL and blood sphingosine level

We analyzed the relationship between the level of various lipids and sphingolipids and the presence of a significant family history in patients (Table 2). In patients with significant family history, the higher level of sphingosine and significantly higher level of ceramides C 20 : 0, C 20 : 1, C 22 : 0 were observed.

Positive correlation of LDL and sphingosine level was revealed (Fig. 1). In addition, it was possible to identify negative correlation of HDL and sphinganin (Fig. 2) and galactosylceramide levels (r = –0.56; p = 0.001). Correlation analysis of sphingomyelin fractions level and ceramides with classical lipid fractions is presented in Table 3. A positive correlation of the level of ceramides C 24 : 0 and C 24 : 1 with the TC and LDL level is noteworthy. For C 20 : 0 ceramide, a positive correlation with the HDL and TG level and a negative correlation with LDL level were revealed. Negative correlation of the C22 : 0 ceramide level with the HDL level was determined.

We analyzed correlations between the level of classical lipids and sphingolipids in patients having a significant family history and in patients with no sifnificant family history. It is noteworthy, that a positive correlation between the level of LDL-C and sphingosine, revealed in the whole group, was of greater strength in patients with a significant family history (r = 0.536; p = 0.022). In patients with no significant family history, there was a negative correlation between LDL-C and sphingosine levels (r = –0.351; p = 0.048) (Fig. 3).

DISCUSSION

There are few studies of the sphingomyelins' and ceramides' profile in patients with family hyperlipidemia. The animal model of family hyperlipidemia associated with LDL receptor gene mutations demonstrated the significant increase of total sphingomyeline and C18 : 0 ceramide in homozygotes [7]. In our study we noted only the SM 18 : 1/22 : 0 fraction and C20 : 1 ceramide increase.

It was shown that the level of ceramides is associated with other coronary heart disease risk factors (obesity and insulin resistance). It was believed that some ceramide fractions were able to stimulate the synthesis of pro-inflammatory cytokines (e.g., tumor necrosis factor) in case of increased consumption of saturated fat with food [8]. In patients after bariatric surgery, a decrease in the level of atherogenic sphinogomyelins and

ceramides was observed earlier and to a much greater extent than weight loss, which correlated with a decrease in coronary risks [9].

It was found that in oxidized LDL the content of total sphingolipids and ceramides was significantly higher, which could be an evidence of the role of sphingolipids in destabilization of atherosclerotic plaque and coronary heart disease and other disorders' complications manifestation [10]. Sphingosine causes aggregation of Cu^{2+} peroxide vesicles and accelerates LDL peroxidation, making them more atherogenic. Long chain ceramides can serve as catalysts for said process. Ceramides with chain length C6, C8, C10 do not possess such activity. Sphinganine, on the opposite, blocks peroxidation processes [11]. In our study we noted the significant increase of sphingosine level in patients with definite family dislipidemia. There were no significant differences in the sphinganine level in patients with low and high probability of family hyperlipidemia.

ApoE gene polymorphism (2/3/4) is associated with the increase of ceramide pathogenic fractions which may be related with increased coronary heart disease risk in young people [12].

The value of ceramides C 16 : 0, C 22 : 0, C 24 : 0, C 24 : 1 in the carotid atherosclerosis pathogenesis in HIV patients was shown. For the long chain ceramides C : 22 and C : 24 a positive correlation with the TC and LDL level was determined [13]. Positive correlation of sphingomyelines SM d16 : 0/28 : 5, SM d18 : 1/24 : 1 and SM d18 : 1/16 : 0 with the TC and LDL level was revealed in the animal model of dislipidemia (*ApoE*-deficient mice). The level of said fractions in animals with hyperlipidemia was elevated. Sphingolipides of such kind are considered pro-atherogenic [14]. There is evidence that oxidative stress and lipotoxicity are associated precisely with an increase in the level of long chain ceramides, which, for example, becomes apparent in patients with insulin resistance [15]. In our study the SM 18 : 1/22 : 0 sphingomyeline was increased in patients with definite/probable hyperlipidemia. Positive correlations of blood cholesterol with ceramides C24 : 0, C24 : 1 level were revealed.

Our study had a number of limitations: single site study, small sample size, lack of data from large studies on the epidemiological relationship between detected changes in lipid component and cardiovascular events (heart attacks, strokes, cardiovascular death).

CONCLUSION

Patients with definite/probable FH demonstrate not only high level of TC and LDL, but also the high level of pro-atherogenic sphingosine, sphingomyeline SM 18 : 1/22 : 0, and long chain ceramides (C 20 : 1, C 22 : 1). The revealed lipidome features require further clarification of their clinical significance.

Lipidome changes may help to explain the mechanism of increasing the risk and early onset of atherosclerosis in said group of patients.

Positive correlation of sphingosine with the LDL level in patients with significant family history is the evidence of the importance of sphingosine as an additional risk factor associated with the family nature of the disease.

References

1. Matanes F, Twal WO, Hammad SM. Sphingolipids as biomarkers of disease. Adv Exp Med Biol. 2019; (1159): 109–38. DOI: 10.1007/978-3-030-21162-2_7.
2. Anroedh S, Hilvo M, Akkerhuis KM, Kauhanen D, Koistinen K, Oemrawsingh R, et al. Plasma concentrations of molecular lipid species predict long-term clinical outcome in coronary artery disease patients. J Lipid Res. 2018; 59 (9): 1729–37. DOI: 10.1194/jlr.P081281.
3. Sutter I, Klingenberg R, Othman A, Rohrer L, Landmesser U, Heg D, et al. Decreased phosphatidylcholine plasmalogens — a putative novel lipid signature in patients with stable coronary artery disease and acute myocardial infarction. Atherosclerosis. 2016; (246): 130–40. DOI: 10.1016/j.atherosclerosis.2016.01.003.
4. Ng TW, Ooi EM, Watts GF, Chan DC, Meikle PJ, Barrett PH. Association of plasma ceramides and sphingomyelin with VLDL apoB-100 fractional catabolic rate before and after rosuvastatin treatment. J Clin Endocrinol Metab. 2015; 100 (6): 2497–501. DOI: 10.1210/jc.2014-4348. PubMed PMID: 25816050.
5. Tarasov K, Ekroos K, Suoniemi M, Kauhanen D, Sylvänne T, Hurme R, et al. Molecular lipids identify cardiovascular risk and are efficiently lowered by simvastatin and PCSK9 deficiency. J Clin Endocrinol Metab. 2014; 99 (1): E45–52. DOI:10.1210/jc.2013-2559. PubMed PMID: 24243630; PubMed Central PMCID: PMC3928964.
6. Bligh EG, Dyer WJ. A rapid method of total lipid extraction and purification. Can J Biochem Physiol. 1959; 37 (8): 911–7.
7. Hoogendoorn A, den Hoedt S, Hartman EMJ, Krabbendam-Peters I, Te Lintel Hekkert M, van der Zee L, et al. Variation in coronary atherosclerosis severity related to a distinct LDL (Low-Density Lipoprotein) profile: findings from a familial hypercholesterolemia pig model. Arterioscler Thromb Vasc Biol. 2019; 39 (11): 2338–52. DOI:10.1161/ATVBAHA.119.313246.
8. Sokolowska E, Blachnio-Zabielska A. The role of ceramides in insulin resistance. Front Endocrinol (Lausanne). 2019; (10): 577. DOI: 10.3389/fendo.2019.00577.
9. Kayser BD, Lhomme M, Dao MC, Ichou F, Bouillot JL, Prifti E, et al. Serum lipidomics reveals early differential effects of gastric bypass compared with banding on phospholipids and sphingolipids independent of differences in weight loss. Int J Obes (Lond). 2017; 41 (6): 917–25. DOI: 10.1038/ijo.2017.63.
10. Paul A, Lydic TA, Hogan R, Goo YH. Cholesterol acceptors regulate the lipidome of macrophage foam cells. Int J Mol Sci. 2019; 20 (15): E3784–801. DOI: 10.3390/ijms20153784.
11. Jiménez-Rojo N, Viguera AR, Collado MI, Sims KH, Constance C, Hill KS et al. Sphingosine induces the aggregation of imine-containing peroxidized vesicles. Biochim Biophys Acta. 2014; 1838 (8): 2071–7. DOI: 10.1016/j.bbamem.2014.04.028.
12. Karjalainen JP, Mononen N, Hutri-Kähönen N, Lehtimäki M, Hilvo M(4), Kauhanen D, et al. New evidence from plasma ceramides links apoE polymorphism to greater risk of coronary artery disease in Finnish adults. J Lipid Res. 2019; 60 (9): 1622–9. DOI: 10.1194/jlr.M092809.
13. Zhao W, Wang X, Deik AA, Hanna DB, Wang T, Haberlen SA et al. Elevated plasma ceramides are associated with antiretroviral therapy use and progression of carotid artery atherosclerosis in HIV infection. Circulation. 2019; 139 (17): 2003–11. DOI: 0.1161/CIRCULATIONAHA.118.037487.
14. Chen Y, Wen S, Jiang M, Zhu Y, Ding L, Shi H, et al. Atherosclerotic dyslipidemia revealed by plasma lipidomics on ApoE-/- mice fed a high-fat diet. Atherosclerosis. 2017; (262): 78–86. DOI: 10.1016/j.atherosclerosis.2017.05.010.
15. Law BA, Liao X, Moore KS, Southard A, Roddy P, Ji R, et al. Lipotoxic very-long-chain ceramides cause mitochondrial dysfunction, oxidative stress, and cell death in cardiomyocytes. FASEB J. 2018; 32 (3): 1403–16. DOI: 10.1096/fj.201700300R. PubMed PMID: 29127192; PubMed Central PMCID: PMC5892719.

Литература

1. Matanes F, Twal WO, Hammad SM. Sphingolipids as biomarkers of disease. Adv Exp Med Biol. 2019; (1159): 109–38. DOI: 10.1007/978-3-030-21162-2_7.
2. Anroedh S, Hilvo M, Akkerhuis KM, Kauhanen D, Koistinen K, Oemrawsingh R, et al. Plasma concentrations of molecular lipid species predict long-term clinical outcome in coronary artery disease patients. J Lipid Res. 2018; 59 (9): 1729–37. DOI: 10.1194/jlr.P081281
3. Sutter I, Klingenberg R, Othman A, Rohrer L, Landmesser U, Heg D, et al. Decreased phosphatidylcholine plasmalogens — a putative novel lipid signature in patients with stable coronary artery disease and acute myocardial infarction. Atherosclerosis. 2016; (246): 130–40. DOI: 10.1016/j.atherosclerosis.2016.01.003.
4. Ng TW, Ooi EM, Watts GF, Chan DC, Meikle PJ, Barrett PH. Association of plasma ceramides and sphingomyelin with VLDL apoB-100 fractional catabolic rate before and after rosuvastatin treatment. J Clin Endocrinol Metab. 2015; 100 (6): 2497–501. DOI: 10.1210/jc.2014-4348. PubMed PMID: 25816050.
5. Tarasov K, Ekroos K, Suoniemi M, Kauhanen D, Sylvänne T, Hurme R, et al. Molecular lipids identify cardiovascular risk and are efficiently lowered by simvastatin and PCSK9 deficiency. J Clin Endocrinol Metab. 2014; 99 (1): E45–52. DOI:10.1210/jc.2013-2559. PubMed PMID: 24243630; PubMed Central PMCID: PMC3928964.
6. Bligh EG, Dyer WJ. A rapid method of total lipid extraction and purification. Can J Biochem Physiol. 1959; 37 (8): 911–7.
7. Hoogendoorn A, den Hoedt S, Hartman EMJ, Krabbendam-Peters I, Te Lintel Hekkert M, van der Zee L, et al. Variation in coronary atherosclerosis severity related to a distinct LDL (Low-Density Lipoprotein) profile: findings from a familial hypercholesterolemia pig model. Arterioscler Thromb Vasc Biol. 2019; 39 (11): 2338–52. DOI:10.1161/ATVBAHA.119.313246.
8. Sokolowska E, Blachnio-Zabielska A. The role of ceramides in insulin resistance. Front Endocrinol (Lausanne). 2019; (10): 577. DOI: 10.3389/fendo.2019.00577.
9. Kayser BD, Lhomme M, Dao MC, Ichou F, Bouillot JL, Prifti E, et al. Serum lipidomics reveals early differential effects of gastric bypass compared with banding on phospholipids and sphingolipids independent of differences in weight loss. Int J Obes (Lond). 2017; 41 (6): 917–25. DOI: 10.1038/ijo.2017.63.
10. Paul A, Lydic TA, Hogan R, Goo YH. Cholesterol acceptors regulate the lipidome of macrophage foam cells. Int J Mol Sci. 2019; 20 (15): E3784–801. DOI: 10.3390/ijms20153784.
11. Jiménez-Rojo N, Viguera AR, Collado MI, Sims KH, Constance C,

Hill KS, et al. Sphingosine induces the aggregation of imine-containing peroxidized vesicles. Biochim Biophys Acta. 2014; 1838 (8): 2071–7. DOI: 10.1016/j.bbamem.2014.04.028.

12. Karjalainen JP, Mononen N, Hutri-Kähönen N, Lehtimäki M, Hilvo M(4), Kauhanen D, et al. New evidence from plasma ceramides links apoE polymorphism to greater risk of coronary artery disease in Finnish adults. J Lipid Res. 2019; 60 (9): 1622–9. DOI: 10.1194/jlr.M092809.

13. Zhao W, Wang X, Deik AA, Hanna DB, Wang T, Haberlen SA, et al. Elevated plasma ceramides are associated with antiretroviral therapy use and progression of carotid artery atherosclerosis in HIV infection. Circulation. 2019; 139 (17): 2003–11. DOI: 0.1161/CIRCULATIONAHA.118.037487.

14. Chen Y, Wen S, Jiang M, Zhu Y, Ding L, Shi H, et al. Atherosclerotic dyslipidemia revealed by plasma lipidomics on ApoE-/- mice fed a high-fat diet. Atherosclerosis. 2017; (262): 78–86. DOI: 10.1016/j.atherosclerosis.2017.05.010.

15. Law BA, Liao X, Moore KS, Southard A, Roddy P, Ji R, et al. Lipotoxic very-long-chain ceramides cause mitochondrial dysfunction, oxidative stress, and cell death in cardiomyocytes. FASEB J. 2018; 32 (3): 1403–16. DOI: 10.1096/fj.201700300R. PubMed PMID: 29127192; PubMed Central PMCID: PMC5892719.

REVERSE MERIDIONAL CYCLODIALYSIS *AB INTERNO* IN MANAGEMENT OF OPEN ANGLE GLAUCOMA — A PRELIMINARY REPORT

Kumar V[1,2,3] ✉, Frolov MA[1], Dushina GN[1,3], Shradqa AS[1,3], Bezzabotnov AI[2,3], Abu Zaalan KA[1]

[1] Peoples' Friendship University of Russia, Moscow, Russia

[2] Skhodnya City Hospital, Khimki, Moscow Region, Russia

[3] Centre for eye microsurgery "Pro zrenie", Khimki, Moscow Region, Russia

The uveoscleral outflow as an alternate route of aqueous drainage is of great interest in glaucoma surgical treatment. A cyclodialysis cleft allows one to create a direct connection between the anterior chamber (AC) and the suprachoroidal space (SCS) which is the key element of uveoscleral outflow. The purpose of the study was to evaluate the safety and effectiveness of reverse meridional cyclodialysis *ab interno* (RMCai) in decreasing intraocular pressure (IOP) in patients with primary open-angle glaucoma (POAG) and refractory glaucoma (RG). Fourteen patients who exhibited POAG and RG (11 men and 3 women, age 77.3 ± 7.8 years) were included in the study. All patients underwent RMCai with the help of custom-designed spatula. The spatula, inserted through a clear corneal incision, was used to detach the ciliary body from the scleral spur to create a 2.0–2.5 mm wide and 6.0–6.5 mm deep cleft. Outcome measures were IOP change, use of hypotensive medication(s), complications, and need for a second surgery. Decrease in IOP by more than 20% and IOP between 6 and 21 mmHg without hypotensive medication constituted complete success. Similar changes in IOP with medication constituted partial success. Need for second surgery constituted failure. The follow-up period was >3 months. Baseline IOP and hypotensive medication use were 22.0 ± 8.5 mmHg (95% confidence interval (CI), 17.6–26.4) and 2.6 ± 0.9 (95% CI, 2.2–3.1). At 3, 6, 12, 18, and 24 months, complete success was achieved in 64.3%, 77.8%, 55.6%, 37.5%, and 40% of patients respectively; partial success — in 14.3%, 22.2%, 44.4%, 50.0%, and 60.0%. Four patients required a second surgery. Failure occurred because of cleft closure by fibrosis. It was concluded that RMCai is safe and effective in decreasing IOP in POAG and RG patients.

Keywords: glaucoma, intraocular pressure, cyclodialysis, cyclodialysis *ab interno*, uveoscleral outflow

ОБРАТНЫЙ МЕРИДИОНАЛЬНЫЙ ЦИКЛОДИАЛИЗ *AB INTERNO* В ЛЕЧЕНИИ ОТКРЫТОУГОЛЬНОЙ ГЛАУКОМЫ — ПРЕДВАРИТЕЛЬНЫЕ РЕЗУЛЬТАТЫ

В. Кумар[1,2,3] ✉, М. А. Фролов[1], Г. Н. Душина[1,3], А. С. Шрадка[1,3], А. И. Беззаботнов[2,3], К. А. Абу Заалан[1]

[1] Российский университет дружбы народов, Москва, Россия

[2] Сходненская городская больница, Химки, Московская область, Россия

[3] Центр микрохирургии глаза «Про зрение», Химки, Московская область, Россия

Увеосклеральный путь оттока внутриглазной жидкости (ВГЖ) представляет большой интерес в хирургическом лечении глаукомы. Суть операции циклодиализа заключается в создании прямого сообщения между передней камерой (ПК) глаза и супрахориоидальным пространством (СХП), главным звеном увеосклерального пути оттока ВГЖ. Целью нашего исследования было оценить безопасность и эффективность обратного меридионального циклодиализа *ab interno* (ОМЦ*ai*) в снижении внутриглазного давления (ВГД) у пациентов с первичной открытоугольной глаукомой (ПОУГ) и рефракторной глаукомой (РГ). У 14 пациентов с ПОУГ (11 мужчин и 3 женщины в возрасте 77,3 ± 7,8 лет) был проведен ОМЦ*ai* с помощью специально разработанного шпателя. Шпателем создавали циклодиализную щель шириной 2,0–2,5 мм и глубиной 6,0–6,5 мм. Критериями оценки успеха операции были динамика ВГД, потребность в дополнительной гипотензивной терапии и повторном хирургическом вмешательстве, а также наличие осложнений. Успех считали полным, если ВГД снижалось более чем на 20% и оставалось в переделах 6–21 мм рт. ст. без применения гипотензивных средств. Признанный успех связывали с потребностью в гипотензивной терапии. Лечение считали неудачным, если возникала необходимость в повторном хирургическом вмешательстве. Пациенты оставались под наблюдением не менее трех месяцев. Исходное ВГД и количество используемых гипотензивных препаратов составляли 22,0 ± 8,5 мм рт. ст. и 2,6 ± 0,9 соответственно. Через 3, 6, 12, 18 и 24 месяца после операции полный успех был достигнут в 64,3, 77,8, 55,6, 37,5 и 40% случаев соответственно, признанный — в 14,3, 22,2, 44,4, 50 и 60% случаев. Повторная операция потребовалась 4 пациентам. Причиной неудачи стала фиброзная облитерация циклодиализной щели. Было установлено, что ОМЦ*ai* безопасен и эффективен в снижении ВГД у пациентов с ПОУГ и РГ.

Ключевые слова: глаукома, внутриглазное давление, циклодиализ, циклодиализ *ab interno*, увеосклеральный отток

Open-angle glaucoma (OAG) is the leading cause of irreversible blindness worldwide [1]. Although glaucoma is a multifactorial disease, its management primarily focuses on control of intraocular pressure (IOP). Notably, IOP can be controlled either medically or by laser treatment. For patients with glaucoma that is refractory to medical or laser treatment, surgical management is indicated.

In the past, surgical techniques focused on creation of an artificial pathway for aqueous humor to bypass obstacles in drainage from the anterior chamber (AC); this led to development of penetrating glaucoma surgeries. A classic form of these surgeries is trabeculectomy [2], which is regarded as the gold standard in surgical management of glaucoma; its hypotensive effect remains for an extended period, but many complications arise during surgery and in the postoperative period [3, 4]. Development of non-penetrating surgeries (deep sclerectomy and its various modifications) reduced the complication rate; however, these techniques provide only a short-term hypotensive effect [5].

Recently, minimally invasive glaucoma surgeries have been developed to enhance the natural trabecular outflow, which comprises the conventional route of aqueous drainage [6, 7]. These surgeries are safe, and patient rehabilitation is rapid; notably, such surgeries do not involve use of a bleb, which enables them to remain free from bleb-related complications, such as cosmesis, bleb leakage, bleb infection, and endophthalmitis [6]. However, there are certain limitations which are associated with these surgeries. Their IOP-lowering effects are dependent upon episcleral vein pressure, and IOP decrease is moderate [8].

There also exists an alternate route of aqueous drainage: uveoscleral outflow. Because of its anatomical and physiological characteristics, uveoscleral outflow has tremendous potential for use in controlling IOP. This outflow, which comprises approximately half of the aqueous drainage in normal human eyes [9, 10], occurs by bulk flow of aqueous humor through the ciliary muscle into the suprachoroidal space (SCS); then flows into the choroid and suprachoroidal clefts, subsequently exiting the eye through perivascular spaces of the emissarial scleral channels, or directly through permeable scleral collagen bundles. There is a possible connection between the uveoscleral outflow pathway and the lymphatic system of the eye and orbit, which maintains tissue fluid balance [11]. A gradient of negative pressure within the SCS serves as the conduit for this aqueous flow pathway. Notably, exploitation of this pathway may enable development of safer and less invasive techniques with improved surgical success, which may thus increase quality of life for glaucoma patients.

A technique for reverse meridional cyclodialysis ab interno (RMCai) has been developed (patent of Russian Federation N 2676967, dated 19.01.2019) and a pilot study was undertaken to evaluate its safety and effectiveness in decreasing IOP in patients with POAG and RG [12].

The purpose of the study was to evaluate the safety and effectiveness of RMCai in decreasing IOP in patients with POAG and RG.

METHODS

In a consecutive interventional case series, a total of 17 patients (11 men and 6 women) who exhibited POAG and RG were operated upon during the period from February 2015 to December 2017. The average age of the patients was 77.3 ± 7.8 years (95% CI 73.2–81.4). Inclusion criteria: POAG or RG, more than 3 months of follow-up. Glaucoma patients

having visually significant cataract, thus requiring a combined procedure (phacoemulsification and hypotensive surgery), were also included. Exclusion criteria: angle-closure glaucoma, neovascular glaucoma, secondary glaucoma, or crystalline lens-induced glaucoma.

A complete ophthalmological examination was performed before surgery including visual acuity evaluation, IOP measurement (by Maklakov's method or with tonometer), slit lamp biomicroscopy, 78 diopter ophthalmoscopy, perimetry, and gonioscopy. For statistical purposes, IOP values obtained by Maklakov's method were converted to P0, using a custom conversion table [13]. For IOP measurement by ICare tonometer ic100 (Icare Finland Oy; Finland) the median of 3 consecutive measurements per eye was analyzed [14, 15].

Surgical technique

Only 1 eye per patient was eligible for surgery. Retrobulbar anesthesia was preferred. After insertion of the lid speculum, a clear corneal incision (2.75 mm) was made at the 10–11 o'clock position. The AC was irrigated with 0.2–0.3 ml of 0.01% solution of carbachol (Appasamy Ocular Devices, Pvt. Ltd.; India) to constrict the pupil and pull the iris away from the angle. The AC was filled with cohesive viscoelastic device, the 1.4% solution of sodium hyaluronate (Beaver Visitec International, Inc.; USA). Two paracenteses were made at 180° apart from each other. The patient's head was turned away from the surgeon by approximately 30° and the optical head of the operating microscope was tilted by 30° toward the surgeon. A surgical goniolens, held in the left hand of the surgeon, was placed on the cornea and angle structures were identified and studied. A custom-designed cyclodialysis spatula (Fig. 1) was inserted into the AC through the corneal incision, and the ciliary body was gently detached from the scleral spur.

Through this cleft the spatula was further meridionally advanced via slight sideways movements until a 6–6.5-mm long and 2.0–2.5-mm wide tunnel was made in the SCS, thereby joining the AC with the SCS. The spatula and goniolens were withdrawn. The patient's head and the operating microscope were returned to their primary positions. If hemorrhage occurred from the cyclodialysis site, a "wait and watch" strategy was used. Typically, bleeding stopped spontaneously after some time. Viscoelastic device was irrigated out from the AC by using a bimanual technique with the aid of irrigating and aspirating cannulas inserted through the paracentesis. An air bubble was
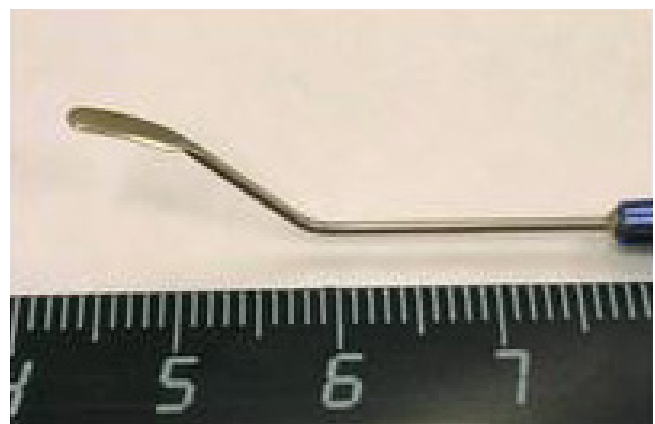

Fig. 1. Side view of the custom-designed spatula for reverse meridional cyclodialysis *ab interno*: distal end of the working portion of the spatula is 6.0–6.5 mm long and 2.0 mm wide; further, it is curved and repeats globe curvature

injected into the AC in order to prevent cleft closure. At the end of the operation, all incisions were sealed by hydration of the corneal stroma. Then, 0.2–0.3 ml of dexamethasone solution was injected subconjunctivally, and antibiotic ointment was placed in the conjunctival sac. A monocular patch was applied. In eyes with coexisting pathology, ultrasound phacoemulsification (phaco) was performed with initial implantation of a foldable hydrophilic intraocular lens (IOL). Before RMCai, all viscoelastic was removed from behind the IOL through irrigation. The pupil was constricted by irrigating the AC with carbachol solution and the AC was filled with cohesive viscoelastic. RMCai was performed as per the technique described above. Incisions were sealed by hydration of the corneal stroma.

Follow-up evaluation

Follow-up evaluation was performed as following. Patients discontinued IOP-lowering medications 1 day before surgery. Oral acetozolamide 0.25 g (Diacarb, Polpharma, Starogard Gdański; Poland) twice daily was prescribed for 1 day; patients were instructed to resume IOP-lowering medications only if the investigator determined that additional IOP lowering was needed. After surgery, patients were instructed to instill antibiotic and steroid eye drops for a period of 10–12 days. Patients were evaluated daily during hospital stay, after 1 week, and at 1, 3, 6, 12, 18, and 24 months after surgery. Postoperative assessment included visual acuity evaluation, tonometry, biomicroscopy, and ophthalmoscopy. If corneal condition allowed, eyes were evaluated via gonioscopy; wherever possible, findings were documented via photography and videography. Adverse events (if any) and number of glaucoma medications used were noted. Field of vision was tested with an interval of 6 months or 1 year.

Outcome measures and statistical analysis

The primary outcome was IOP change. The secondary outcomes were pre- and postoperatively used number of hypotensive medications, as well as complications and need for a second surgery. Reduction in IOP > 20% and IOP between 6 and 21 mmHg without medication constituted complete success; similar changes in IOP with medication constituted partial success. Failure constituted IOP < 6 mmHg or > 21 mmHg, IOP reduction <20%, or subsequent need for second glaucoma surgery. Success rates were evaluated at each follow-up visit, beginning 3 months after surgery.

Statistical analysis was performed using Microsoft Excel 2007 (Microsoft; USA) at each follow-up visit, considering changes in the number of patients. Paired Student's t-tests were used for IOP and medication analyses. Differences were significant when $p < 0.05$.

RESULTS

Fourteen eyes of 14 patients (11 man and 3 women) fulfilled the inclusion criteria. The baseline characteristics of the patients are described in Table 1.

Right eyes underwent operation in 5 patients, while left eyes — in 9 patients. Severe glaucomatous damage was present in 11 eyes (79%). Eight eyes (57%) had previously undergone surgery for glaucoma; of these, 3 underwent a combined surgical procedure in the present study: phaco with implantation of an acrylic hydrophilic IOL along with glaucoma surgery.

The mean follow-up period was 68.2 ± 44.2 weeks (95% CI 45.1–91.4). Two patients were lost to follow-up after 3 months; 1 patient was lost to follow-up after 18 months and 2 patients were lost to follow up after 24 months. Mean baseline IOP was 22.0 ± 8.5 mmHg (95% CI 17.6–26.4). A significant reduction in mean IOP and use of hypotensive medications was observed at each time point (Table 2). There were no cases of hypotony at any follow-up visits.

Success rate outcomes are described in Table 3.

Three eyes (21.4%) underwent repeat glaucoma surgery after 3 months following RMCai; 1 eye underwent repeat glaucoma surgery after 18 months. The Kaplan–Meier survival curve is shown in Fig. 2.

The mean best-corrected visual acuity before surgery was 1 ± 0.9 logarithm of the minimum angle of resolution (LogMAR). Mean LogMAR at 3, 6, 12, 18 and 24 months was 0.9 ± 0.9, 1.0 ± 1.0, 0.9 ± 1.0, 0.8 ± 1.0, and 0.6 ± 0.5, respectively.

In 11 of 14 eyes (79%), there was some hemorrhage at the cleft site, obscuring the view of the tunnel. In these eyes,

Table 1. Patient demographics

№	Sex / age	Eye	Previous glaucoma surgeries	Other ocular surgeries	Concomitant pathology
1	F / 74	LE	1. MTF 2. SDSC	–	Cataract
2	M / 82	RE	–	–	Cataract
3	F / 87	RE	–	–	Cataract
4	M / 87	RE	–	–	Cataract
5	M / 87	LE	1. Trabeculectomy	–	Cataract
6	M / 82	LE	–	–	Cataract
7	M / 64	RE	–	–	Cataract
8	M / 69	LE	1. Trabeculectomy	–	Cataract
9	M / 69	LE	1. Trabeculectomy	–	Cataract
10	M / 78	RE	1. Trabeculectomy	–	Cataract
11	M / 77	LE	1. Trabeculectomy	Phaco + IOL	Pseudophakia
12	M / 75	LE	–	–	Cataract
13	M / 64	LE	1. SDSC	Phaco + IOL	Pseudophakia
14	F / 82	LE	1. SDSC 2. Trabeculectomy	Phaco + IOL	Pseudophakia

Note: M — male; F — female; RE — right eye; LE — left eye; MTF — Singh's microtrack filtration operation; SDSC — segmental dilation of Schlemm's canal (implantation of Kumar's stainless-steel spiral expander in lumen of Schlemm's canal); Phaco — phacoemulsification; IOL — intraocular lens.

hemorrhage either stopped spontaneously after some time, or a bolus of viscoelastic was placed at the tunnel opening. In 3 eyes that underwent combined surgery, some blood reached the capsular bag behind the IOL. In these eyes, the blood was washed out with the aid of irrigating and aspirating cannulas.

In 11 of 14 eyes (79%), the early rehabilitative period was uneventful. In 3 eyes on the first postoperative day, hyphema was observed, which resolved within 1 week without any specific treatment. No second visit to the operation theatre was required because of hyphema. Furthermore, there were no noticeable complications in the late postoperative period. During gonioscopic evaluation of the cyclodialysis site at 3, 6, 12, 18, and 24 months after surgery, the cleft was open in 10, 8, 8, 5, and 3 eyes, respectively; moreover, the cleft was noticeably shallow in 3, 4, 6, 4, and 2 eyes, respectively, and completely closed in 4, 2, 1, 3, and 3 eyes, respectively (Fig. 3).

In all eyes with unsuccessful outcome, retrograde placement of the iris root at the cyclodialysis site was prevalent. During ultrasonic biomicroscopy of the AC angle in eyes with successful outcome, the cyclodialysis cleft could be easily identified.

DISCUSSION

Glaucoma surgery in the SCS has several important advantages relative to penetrating procedures. Some surgeons have attempted to improve supraciliary outflow using a non-penetrating deep sclerectomy procedure [16–18]. The results were encouraging, but not definitive. It is likely that the presence of a conjunctival bleb as a main filtration site for the aqueous humor did not completely open this pathway, thus affecting the final results.

The SCS offers the surgeon 2 surgical approaches: *ab externo* and ab interno. In the *ab externo* approach, a direct passage is created from the AC to the SCS by separation of the ciliary body from the scleral spur. This approach is easy to learn and does not require mastery of unfamiliar techniques and maneuvers. However, it requires extensive dissection of ocular tissues, and is thus very traumatic to the eye. There is a high risk of complications, such as postoperative hypotony and massive bleeding from scleral vessels. Several studies have demonstrated that when the SCS is reached through an *ab externo* approach, fibroblast activation is a primary cause of surgical failure [19, 20].

There are certain advantages with *ab interno* approach. This approach spares conjunctival dissection, retaining this structure in an intact state, which may be useful for future glaucoma procedures. It is minimally invasive and less traumatic; the resulting reduction in scarring leads to increased success rate. This surgery can be performed as an ambulatory procedure. The numbers of intraoperative and postoperative complications are negligible, and they are easily managed. The *ab interno* procedure can be performed, regardless of whether previous traditional glaucoma surgeries (e.g., trabeculectomy) have depleted viable conjunctiva tissue. The rehabilitation period is short [21–23]. However, this approach also involves limitations: it requires the use of costly instruments and apparatuses, such as an operating microscope in which the optical head can be tilted, as well as a surgical goniolens and viscoelastic devices; moreover, the surgeon should be familiar with the intraoperative gonioscopy procedure.

The concept of creating direct communication between the AC and SCS for reduction of IOP is not new. The first operative procedure to employ incision through insertion of the ciliary body to enable communication between the chambers of the anterior segment and the suprachoroid was performed by Hancock in 1861 [24], who described 6 cases in which the operation was used.

In 1905, a procedure was described for operative detachment of the ciliary body from its insertion, using an operation that was described as cyclodialysis [20]. Notably, the success of the operation depended upon communication

Table 2. Efficacy data

N of patients at follow-up visit	Follow-up visit					
	Pre-operative	3 months	6 months	12 months	18 months	24 months
	14	14	9	9	8	5
IOP change, mmHg	22.0 ± 8.5	13.8 ± 5.0	11.9 ± 3.4	10.1 ± 2.4	12.9 ± 3.9	13.0 ± 5.7
(95% CI)	(17.6–26.4)	(11.2–16.4)	(9.8–14.0)	(8.6–11.7)	(10.1–15.6)	(8.4–17.6)
% IOP decrease	–	30.8 ± 29.8	36.0 ± 35.1	48.0 ± 26.0	35.5 ± 35.6	34.5 ± 33.8
(95% CI)	–	(15.4–46.3)	(14.3–57.7)	(31.1–65.0)	(10.8–60.2)	(7.4–61.6)
N of medications	2.6 ± 0.9	0.5 ± 0.8	0.4 ± 0.7	0.6 ± 0.7	0.9 ± 0.8	1.0 ± 0.9
(95% CI)	(2.2–3.1)	(0.1–0.9)	(0–0.8)	(0.1–1.0)	(0.3–1.5)	(0.3–1.7)
N of eyes requiring hypotensive medication at baseline / N of eyes at follow-up visit (%)	14/14 (100)	2/14 (14.3)	2/9 (22.2)	4/9 (44.4)	4/8 (50.0)	3/5 (60.0)
N of patients requiring repeat surgery	0	2	1	0	0	0

Note: N — number; IOP — intraocular pressure; CI — confidence interval.

Table 3. Success rate

| N of patients at follow-up visit	Follow-up visit				
	3 months	6 months	12 months	18 months	24 months
	14	9	9	8	5
N of patients lost to follow-up	0	2	0	1	2
N of eyes with complete success (%)	9 (64.3)	7 (77.8)	5 (55.6)	3 (37.5)	2 (40)
N of eyes with partial success (%)	2 (14.3)	2 (22.2)	4 (44.4)	4 (50)	3 (60)
N of eyes with failure (%)	3 (21.4)	0	0	1 (12.5)	0
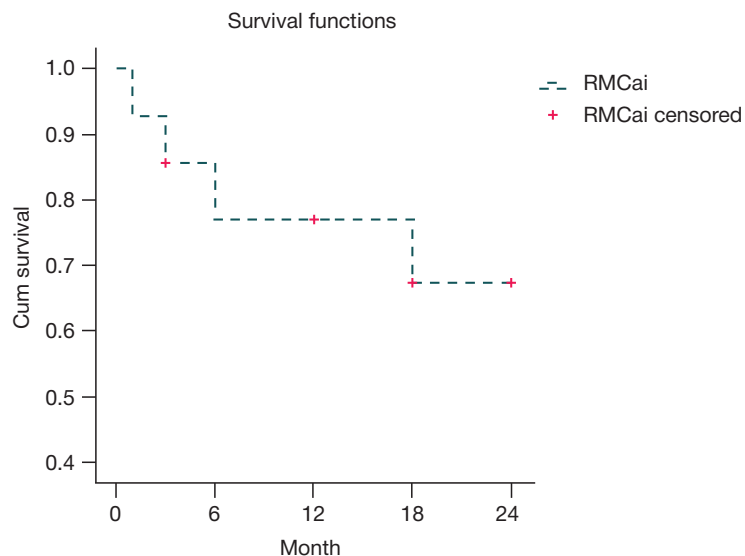
**Fig. 2.** Kaplan–Meier survival curve of eyes after RMCai
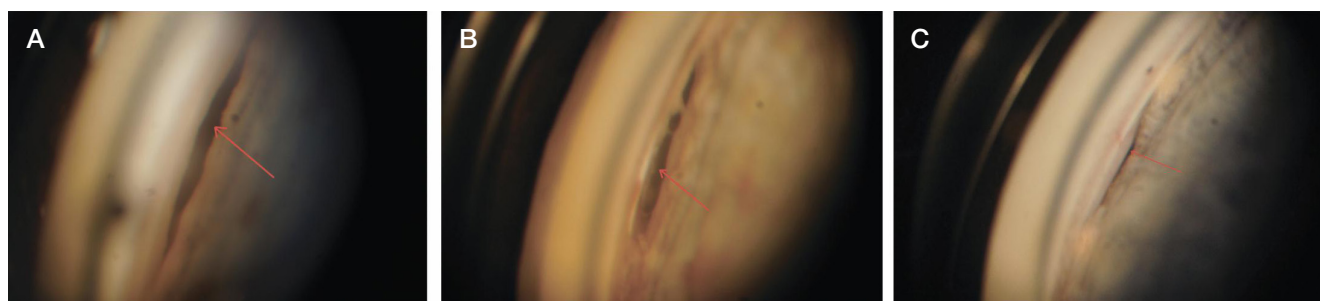
Fig. 3. Cyclodialysis cleft (*red arrow*) at different follow-up visits (different patients): 1 week (**A**); 1 month (**B**); 2 years (**C**); there are no signs of fibrosis or inflammation

between the AC and SCS. This hypothesis was supported by a number of works [25]. The other author [26] hypothesized that the operation acted by reducing pathologic accumulation of intraocular fluid by eliciting atrophy of the uveal tract.

The long-term success of this operation for reduction of IOP depends upon the patency of the cyclodialysis cleft. Notably, fibrosis of the cyclodialysis cleft may be the major factor for procedural failure; this has been reported by several authors [27–29]. Detailed morphological studies have demonstrated that fibroblasts and myofibroblasts are present throughout all layers of the choroid. These cells readily respond to trauma, surgical manipulation, and any foreign body by causing scar formation [30].

In our study, during gonioscopic evaluation of the cyclodialysis site, we noticed that in all eyes that showed procedural failure, there was reattachment of the iris root to the scleral wall. In most of these eyes, the reattachment site was posterior to its original anatomical attachment, constituting retrograde placement of the iris root. Our findings are like those reported by [27], who examined the angle of the AC in 14 eyes that underwent cyclodialysis. All eyes that underwent successful operation showed surgical cyclodialysis or detachment of the iris root, combined with communication between the AC and SCS. Three unsuccessful operations resulted in reattachment of the iris root to the scleral wall; the site of reattachment in these cases was posterior to its original anatomical attachment, constituting retrograde placement of the iris root (as noted in our study).

In a prospective, consecutive, case-control study, a group of authors [31] included 28 eyes of 20 patients with intractable glaucoma. Under gonioscopic control, cyclodialysis *ab interno* was performed over 2 clock hours to enable access to the SCS. After surgery, baseline IOP decreased from 34.3 ± 10.5 to 14.6 ± 12.4 mmHg. After a mean of 60 days, 21 eyes (75%) required further surgical intervention. Qualified success was observed in 4 eyes (14.3%); only 3 eyes (10.7%) demonstrated complete success. In their series, the authors obtained the best results for phakic eyes. In our study, at 12, 18, and 24 months of follow-up, absolute success was achieved in 55.6%, 37.5%, and 40% of eyes, whereas partial success was achieved in 44.4%, 50.0%, and 60.0% of eyes, respectively. Our results were more favorable than those of the prior study; this may be because minimum trauma occurred during surgery, due to the use of modern surgical microscopes and surgical goniolenses, which allowed identification of the anatomical structure of the angle.

There were several limitations to this study. These included absence of a control group, nonrandomized nature of the study, and small sample size ($n = 14$); further studies will require a larger sample of patients to confirm the findings reported here.

CONCLUSION

RMCai is an easy and safe procedure to perform, it effectively decreases IOP in patients with POAG and RG. Its success depends upon the patency of communication between the AC and SCS. Fibrosis of the cyclodialysis cleft is the primary reason for failure of this procedure. Use of measures to prevent its obliteration (e.g., implantation of various devices or materials to connect the AC with the SCS) may increase its success rate.

References

1. Quigley HA, Broman AT. The number of people with glaucoma worldwide in 2010 and 2020. Br J Ophthalmol. 2006; (90): 262–7. PubMed PMID: 16488940.
2. Cairns JE. Trabeculectomy. Preliminary report of a new method. Am J Ophthalmol. 1968; (66): 673–9. PubMed PMID: 4891876.
3. Jampel HD, Musch DC, Gillespie BW, Lichter PR, Wright MM, Guire KE, et al. Perioperative complications of trabeculectomy in the collaborative initial glaucoma treatment study (CIGTS). Am J Ophthalmol. 2005; (140): 16–22. PubMed PMID: 15939389.
4. Francis BA, Hong B, Winarko J, Kawji S, Dustin L, Chopra V. Vision loss and recovery after trabeculectomy: risk and associated risk factors. Arch Ophthalmol. 2011; (129): 1011–17. PubMed PMID: 21825185.
5. El Sayyad F, Helal M, El-Kholify H, Khalil M, El-Maghraby A. Nonpenetrating deep sclerectomy versus trabeculectomy in bilateral primary open-angle glaucoma. Ophthalmology. 2000; (107): 1671–4. PubMed PMID: 10964827.
6. Saheb H, Ahmed II. Micro-invasive glaucoma surgery: current perspectives and future directions. Curr Opin Ophthalmol. 2012; (23): 96–104. PubMed PMID: 22249233.
7. Kahook MY, Sarwat S, Seibold LK. MIGS: advances in glaucoma surgery. Thorofare: SLACK Incorporated, 2014; 122 p.
8. Francis BA, Sarkisian SR, Tan JC. Minimally Invasive Glaucoma Surgery: A practical guide. New York: Thieme Medical Publisher, Inc., 2017; 199 p.
9. Alm A, Nilsson SF. Uveoscleral outflow — a review. Exp Eye Res. 2009; (88): 760–8. PubMed PMID: 19150349.
10. Toris CB, Yablonski ME, Wang YL, Camras CB. Aqueous humor dynamics in the aging human eye. Am J Ophthalmol. 1999; (127): 407–12. PubMed PMID: 10218693.
11. Yucel Y, Gupta N. Lymphatic drainage from the eye: A new target for therapy. Prog Brain Res. 2015; (220): 185–98. PubMed PMID: 26497791.
12. Kumar V, Frolov MA, Dushina GN, Shradka AS, Bezzabotnov AI. Obratnyi meridional'nyi tsiklodializ ab interno v khirurgicheskom lechenii glaukomy razlichnoi etiologii: otdalennye rezul'taty. Natsional'nyi zhurnal glaukoma. 2018; 17 (4): 63–73. Russian.
13. Krasnov MM. Mikrokhirurgiya glaukom. 2-e izdanie. Moscow: Meditsina, 1980; 248 c. Russian.
14. Kato Y, Nakakura S, Matsuo N, Yoshitomi K, Handa M, Tabuchi H, et al. Agreement among Goldmann applanation tonometer, iCare, and Icare PRO rebound tonometers; non-contact tonometer; and Tonopen XL in healthy elderly subjects. Int Ophthalmol. 2018; (38): 687–96. PubMed PMID: 28393323
15. Wong B, Parikh D, Rosen L, Gorski M, Angelilli A, Shih C. Comparison of disposable Goldmann applanation tonometer, iCare ic100, and Tonopen XL to standards of care Goldmann nondisposable applanation tonometer for measuring intraocular pressure. J Glaucoma. 2018; (27): 1119–24. PubMed PMID: 30134367.

16. Chihara E, Hayashi K. Effect of a fenestration between an intrascleral lake and supraciliary space on deep sclerectomy. J Glaucoma. 2016 Apr; 25 (4): 299–307. DOI: 10.1097/IJG.0000000000000277.
17. Frolov MA, Frolov AM, Kazakova KA. Kombinirovannye metody lecheniya pri sochetanii katarakty i glaukomy. Vestnik oftal'mologii. 2017; 133 (4): 42–46. PubMed PMID: 28980565. Russian.
18. Lapochkin VI, Svirin AV, Korchuganova EA. Novaya operatsiya v lechenii refrakternykh glaukom — limbosklerektomiya s klapannym drenirovaniem supratsiliarnogo prostranstva. Vestnik oftal'mologii. 2001; (1): 9–11. Russian.
19. Tanito M, Chihara E. Safety and effectiveness of gold glaucoma micro shunt for reducing intraocular pressure in Japanese patients with open angle glaucoma. Jpn J Ophthalmol. 2017; 61 (5): 388–94. PubMed PMID: 28600745.
20. Rekas M, Pawlik B, Grala B et al. Clinical and morphological evaluation of gold micro shunt after unsuccessful surgical treatment of patients with primary open–angle glaucoma. Eye (Lond). 2013; (27): 1214–17. PubMed PMID: 2387717.
21. Heine L. Introduction of cyclodialysis in glaucoma. Dtsch Med Wochenschr. 1905; (31): 824–26.
22. Kammer JA, Mundy KM. Suprachoroidal devices in glaucoma surgery. Middle East Afr J Ophthalmol. 2015; (22): 45–52. PubMed PMID: 25624673.
23. Bailey AK, Sarkisian SR, Jr, Vold SD. Ab interno approach to the suprachoroidal space. J Cataract Refract Surg. 2014; (40): 1291–4. PubMed PMID: 25088626.
24. Hancock H. Division of the ciliary muscle for glaucoma. Lancet. 1861; (77): 137.
25. Galin MA, Baras I, Sambursky J. Glaucoma and cataract. A study of cyclodialysis-lens extraction. Am J Ophthalmol. 1969; (69): 522–6. PubMed PMID: 5778611.
26. Krauss W. Ueber die Zyklodialyse. Zeitschr. f. Augenh. 1907; (17): 318.
27. Barkan O. Cyclodialysis: its mode of action. Histologic observations in a case of glaucoma in which both eyes were successfully treated by cyclodialysis. Arch Ophthal. 1950; (43): 793–803.
28. Kolesnikova LN, Pantsyreva LP, Svirin AV. Dilyatatsiya suprakhorioidal'nogo prostranstva v kombinatsii s tsiklodializom. Vestnik oftal'mologii. 1976; (4): 18–20. PubMed PMID: 1021925. Russian.
29. Demeler U. Direct cyclopexy following operative and traumatic cyclodialysis. Fortschr Ophthalmol. 1984; (81): 466–8. PubMed PMID: 6500429.
30. Flügel-Koch C, May CA, Lütjen-Drecoll E. Presence of a contractile cell network in the human choroid. Ophthalmologica. 1996; (210): 296–302. PubMed PMID: 8878213.
31. Jordan JF, Dietlein TS, Dinslage S, Lüke C, Konen W, Krieglstein GK. Cyclodialysis ab interno as a surgical approach to intractable glaucoma. Graefes Arch Clin Exp Ophthalmol. 2007; (245): 1071–6. PubMed PMID: 17219126.

Литература

1. Quigley HA, Broman AT. The number of people with glaucoma worldwide in 2010 and 2020. Br J Ophthalmol. 2006; (90): 262–7. PubMed PMID: 16488940.
2. Cairns JE. Trabeculectomy. Preliminary report of a new method. Am J Ophthalmol. 1968; (66): 673–9. PubMed PMID: 4891876.
3. Jampel HD, Musch DC, Gillespie BW, Lichter PR, Wright MM, Guire KE, et al. Perioperative complications of trabeculectomy in the collaborative initial glaucoma treatment study (CIGTS). Am J Ophthalmol. 2005; (140): 16–22. PubMed PMID: 15939389.
4. Francis BA, Hong B, Winarko J, Kawji S, Dustin L, Chopra V. Vision loss and recovery after trabeculectomy: risk and associated risk factors. Arch Ophthalmol. 2011; (129): 1011–17. PubMed PMID: 21825185.
5. El Sayyad F, Helal M, El-Kholify H, Khalil M, El-Maghraby A. Nonpenetrating deep sclerectomy versus trabeculectomy in bilateral primary open-angle glaucoma. Ophthalmology. 2000; (107): 1671–4. PubMed PMID: 10964827.
6. Saheb H, Ahmed II. Micro-invasive glaucoma surgery: current perspectives and future directions. Curr Opin Ophthalmol. 2012; (23): 96–104. PubMed PMID: 22249233.
7. Kahook MY, Sarwat S, Seibold LK. MIGS: advances in glaucoma surgery. Thorofare: SLACK Incorporated, 2014; 122 p.
8. Francis BA, Sarkisian SR, Tan JC. Minimally Invasive Glaucoma Surgery: A practical guide. New York: Thieme Medical Publisher, Inc., 2017; 199 p.
9. Alm A, Nilsson SF. Uveoscleral outflow — a review. Exp Eye Res. 2009; (88): 760–8. PubMed PMID: 19150349.
10. Toris CB, Yablonski ME, Wang YL, Camras CB. Aqueous humor dynamics in the aging human eye. Am J Ophthalmol. 1999; (127): 407–12. PubMed PMID: 10218693.
11. Yucel Y, Gupta N. Lymphatic drainage from the eye: A new target for therapy. Prog Brain Res. 2015; (220): 185–98. PubMed PMID:

26497791.

12. Кумар В., Фролов М. А., Душина Г. Н., Шрадка А. С., Беззаботнов А. И. Обратный меридиональный циклодиализ *ab interno* в хирургическом лечении глаукомы различной этиологии: отдаленные результаты. Национальный журнал глаукома. 2018; 17 (4): 63–73.

13. Краснов М. М. Микрохирургия глауком. 2-е издание. М.: Медицина, 1980; 248 с.

14. Kato Y, Nakakura S, Matsuo N, Yoshitomi K, Handa M, Tabuchi H, et al. Agreement among Goldmann applanation tonometer, iCare, and Icare PRO rebound tonometers; non-contact tonometer; and Tonopen XL in healthy elderly subjects. Int Ophthalmol. 2018; (38): 687–96. PubMed PMID: 28393323

15. Wong B, Parikh D, Rosen L, Gorski M, Angelilli A, Shih C. Comparison of disposable Goldmann applanation tonometer, iCare ic100, and Tonopen XL to standards of care Goldmann nondisposable applanation tonometer for measuring intraocular pressure. J Glaucoma. 2018; (27): 1119–24. PubMed PMID: 30134367.

16. Chihara E, Hayashi K. Effect of a fenestration between an intrascleral lake and supraciliary space on deep sclerectomy. J Glaucoma. 2016 Apr; 25 4): 299-307. DOI: 10.1097/IJG.0000000000000277.

17. Фролов М. А., Фролов А. М., Казакова К. А. Комбинированные методы лечения при сочетании катаракты и глаукомы. Вестник офтальмологии. 2017; 133 (4): 42–6. PubMed PMID: 28980565.

18. Лапочкин В. И., Свирин А. В., Корчуганова Е. А. Новая операция в лечении рефрактерных глауком — лимбосклерэктомия с клапанным дренированием супрацилиарного пространства. Вестник офтальмологии. 2001; (1): 9–11.

19. Tanito M, Chihara E. Safety and effectiveness of gold glaucoma micro shunt for reducing intraocular pressure in Japanese patients with open angle glaucoma. Jpn J Ophthalmol. 2017; 61 (5): 388–94. PubMed PMID: 28600745.

20. Rekas M, Pawlik B, Grala B et al. Clinical and morphological evaluation of gold micro shunt after unsuccessful surgical treatment of patients with primary open–angle glaucoma. Eye (Lond). 2013; (27): 1214–17. PubMed PMID: 2387717.

21. Heine L. Introduction of cyclodialysis in glaucoma. Dtsch Med Wochenschr. 1905; (31): 824–26.

22. Kammer JA, Mundy KM. Suprachoroidal devices in glaucoma surgery. Middle East Afr J Ophthalmol. 2015; (22): 45–52. PubMed PMID: 25624673.

23. Bailey AK, Sarkisian SR, Jr, Vold SD. Ab interno approach to the suprachoroidal space. J Cataract Refract Surg. 2014; (40): 1291–4. PubMed PMID: 25088626.

24. Hancock H. Division of the ciliary muscle for glaucoma. Lancet. 1861; (77): 137.

25. Galin MA, Baras I, Sambursky J. Glaucoma and cataract. A study of cyclodialysis-lens extraction. Am J Ophthalmol. 1969; (69): 522–6. PubMed PMID: 5778611.

26. Krauss W. Ueber die Zyklodialyse. Zeitschr. f. Augenh. 1907; (17): 318.

27. Barkan O. Cyclodialysis: its mode of action. Histologic observations in a case of glaucoma in which both eyes were successfully treated by cyclodialysis. Arch Ophthal. 1950; (43): 793–803.

28. Колесникова Л. Н., Панцырева Л. П., Свирин А. В. Дилятация супрахориоидального пространства в комбинации с циклодиализом. Вестник офтальмологии. 1976; (4): 18–20. PubMed PMID: 1021925.

29. Demeler U. Direct cyclopexy following operative and traumatic cyclodialysis. Fortschr Ophthalmol. 1984; (81): 466–8. PubMed PMID: 6500429.

30. Flügel-Koch C, May CA, Lütjen-Drecoll E. Presence of a contractile cell network in the human choroid. Ophthalmologica. 1996; (210): 296–302. PubMed PMID: 8878213.

31. Jordan JF, Dietlein TS, Dinslage S, Lüke C, Konen W, Krieglstein GK. Cyclodialysis ab interno as a surgical approach to intractable glaucoma. Graefes Arch Clin Exp Ophthalmol. 2007; (245): 1071–6. PubMed PMID: 17219126.

RE-ESTABLISHING THE PATENCY OF THE HEPATIC VEIN AND THE PORTOSYSTEMIC SHUNT 10 YEARS AFTER THE TIPS PROCEDURE: A CLINICAL CASE

Tsitsiashvili MSh[1], Shipovskiy VN[1,2], Monakhov DV[1,2], Chelyapin AS[1,2] ✉, Huseynov AB[1]

[1] Pirogov Russian National Research Medical University, Moscow, Russia

[2] Pletnev City Clinical Hospital, Moscow, Russia

Transjugular intrahepatic portosystemic shunt is one of the few available options for treating complications of portal hypertension in patients with chronic diffuse liver diseases. Over time, shunt patency can become compromised, causing a recurrence of such complications. The clinical case presented below demonstrates the potential of TIPS and illustrates the use of an endovascular reintervention for re-establishing shunt patency, which improves the life expectancy of patients, as well as their quality of life.

Keywords: liver cirrhosis, portal hypertension, transjugular intrahepatic portosystemic shunt, dysfunction, reintervention

КЛИНИЧЕСКИЙ ПРИМЕР ВОССТАНОВЛЕНИЯ ПРОХОДИМОСТИ ПЕЧЕНОЧНОЙ ВЕНЫ И ПОРТОСИСТЕМНОГО ШУНТА ЧЕРЕЗ 10 ЛЕТ ПОСЛЕ TIPS

М. Ш. Цициашвили[1], В. Н. Шиповский[1,2], Д. В. Монахов[1,2], А. С. Челяпин[1,2] ✉, А. Б. Гусейнов[1]

[1] Российский национальный исследовательский университет имени Н. И. Пирогова, Москва, Россия

[2] Городская клиническая больница имени Д. Д. Плетнева, Москва, Россия

Одним из немногих доступных методов борьбы с осложнениями портальной гипертензии у пациентов с хроническими диффузными заболеваниями печени является трансъюгулярное портосистемное шунтирование. С течением времени имеется тенденция к развитию дисфункции внутрипеченочного шунта вследствие нарушения его проходимости, что вновь приводит к развитию осложнений портальной гипертензии. Описанный клинический случай демонстрирует возможности внутрипеченочного шунтирования, а также повторных эндоваскулярных вмешательств при дисфункции шунта, позволяющих значительно продлить жизнь пациента и сохранить ее качество.

Ключевые слова: цирроз печени, портальная гипертензия, трансъюгулярное внутрипеченочное портосистемное шунтирование, дисфункция, реинтервенция

Bleeding from esophageal (EVs) and gastric (GVs) varices is a life-threatening complication of portal hypertension. Mortality rates associated with first-time variceal hemorrhages and rebleeds are 50% and 70%, respectively [1, 2]. To reduce mortality, a special algorithm has been developed in Russia; it is detailed in the "clinical practice guidelines on the management of bleeding esophageal and gastric varices" [3]. According to this algorithm, endoscopic band ligation following emergency esophagogastroduodenoscopy (EGD) should be preferred over other endoscopic interventions because it allows achieving hemostasis in 80% of patients with refractory bleeding [3]. However, this treatment option works most effectively as primary prophylaxis for variceal bleeding and does not relieve portal pressure. Late recurrence of EVs and rebleeds occur in 50–60% of patients undergoing band ligation [4]. This necessitates the use of alternative treatments in relapsed patients, such as portosystemic shunts that relieve pressure in the portal venous system and azygoportal disconnection. Of all portosystemic

shunting options, transjugular intrahepatic portosystemic shunt (TIPS) is the treatment of choice for patients with class B/C cirrhosis. So far, we have performed 226 TIPS procedures in our clinic.

Intrahepatic shunt dysfunction can result in the recurrence of complications associated with portal hypertension and, therefore, is a relevant clinical problem [5–8]. Poor shunt patency can be caused by shunt thrombosis and pseudointimal hyperplasia, intimal hyperplasia of the hepatic vein, compression of the stent by high-density liver tissue, migration or disengagement of shunt components. On average, a shunt created from a stent-graft remains functional for 3–5 years; in extremely rare cases, it can retain its patency for up to 10 years.

To date, there are a variety of different endovascular techniques for restoring shunt patency. They help to extend the life of the shunt, reduce the risk of complications associated with portal hypertension and improve life expectancy in patients with end-stage diffuse chronic liver diseases.

Below, we describe a case of TIPS revision 10 years after stent implantation in the liver parenchyma.

Clinical case

Patient K., 40 years, was diagnosed with liver cirrhosis (LC) complicated by portal hypertension in 2006 at the Central Research Institute of Gastroenterology (Moscow). On December 10, 2007 the patient was urgently admitted to the Surgery Unit No. 4 of the City Clinical Hospital № 57 (Moscow). Diagnosis on admission: liver cirrhosis (class B on the Child-Pugh score) complicated by portal hypertension and recent grade III esophageal variceal bleeding.

The patient's condition was assessed as moderate. On physical examination, there was pallor and mild scleral icterus. Normal vesicular breathing was heard over both lungs. The respiratory rate was 14 breaths per minute. Heart tones were muffled. Blood pressure was 110/70. The patient's heart rate was 96 beats per minute. The abdomen was soft and nontender. The liver edge extended 3 cm below the costal margin. The patient showed no signs of urinary tract pathology.

Instrumental examinations revealed the following signs of portal hypertension: dilated portal (14 mm) and splenic (9 mm) veins, hepatosplenomegaly, grade III EVs. Blood tests revealed mild posthemorrhagic anemia (hemoglobin < 96 g/L), low red blood cell count (3.89×10^{12}/L), low platelet count (102×10^9/L), and unconjugated hyperbilirubinemia (34 µmol/L). The coagulation test came back normal.

On day 2 after admission to the hospital, there was a recurrence of gastrointestinal variceal bleeding confirmed by EGD. The bleeding was stopped using a Sengstaken–Blakemore tube. The patient was transferred to the Intensive Care Unit. Follow-up EGD revealed engorged varices (7–9 mm in diameter) in the middle and lower thirds of the esophagus. The mucosa above the varices was cyanotic-looking, with an overlayer of hemin. To reduce the risk of rebleeds, endoscopic band ligation was performed first on December 17, 2007; a total of 20 ligatures were placed. In the second step, on December 19, 2007 the patient underwent TIPS with a Viatorr TIPS Endoprosthesis stent-graft (Gore; USA). Intraoperatively, the portal pressure decreased from 520 to 300 mm H_2O.

The postoperative period was uneventful. On December 22, 2007, the patient underwent a Doppler ultrasound scan, which showed a normal blood flow throughout the entire length of the shunt with the intrashunt velocity of 85 cm/s. Postoperatively, the patient was receiving conventional medication therapy until he was stable; on December 25, 2007 the patient was discharged in a satisfactory condition.

In the 9-year follow-up period, the patient was hospitalized every 6 months to receive supportive therapy for his liver function. No clinical signs of complications associated with portal hypertension were observed during the entire follow-up period.

In December 2017 during one of such hospitalizations, a dupplex Doppler scan revealed a high-velocity flow in the proximal TIPS portion and a low-velocity flow in its distal segment, suggesting stenosis of the right hepatic vein (Fig. 1). EGD revealed grade III EVs indicative of the increasing pressure in the portal venous system.

In order to verify the diagnosis, a contrast-enhanced CT scan of the abdomen was performed, which confirmed stenosis of the right hepatic vein (Fig. 2).

Considering that there were signs of right hepatic vein stenosis, including the changed hemodynamics in the shunt and the portal vein (low velocity flow in the portal vein), as well
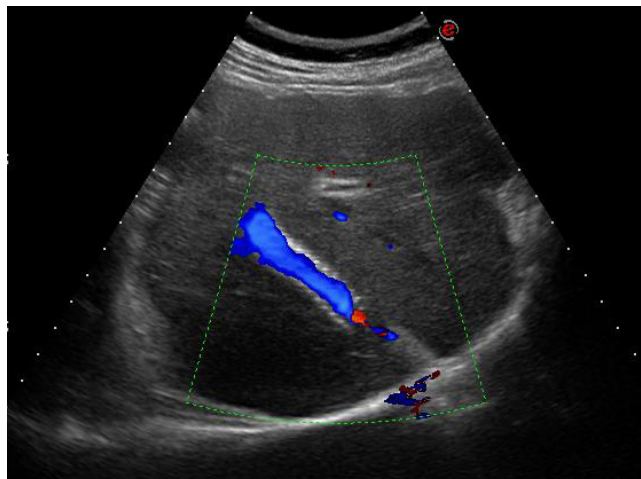

Fig. 1. Patient K. with class B liver cirrhosis, after TIPS. Stenosis of the proximal TIPS segment. Intrashunt velocity of 37 cm/s
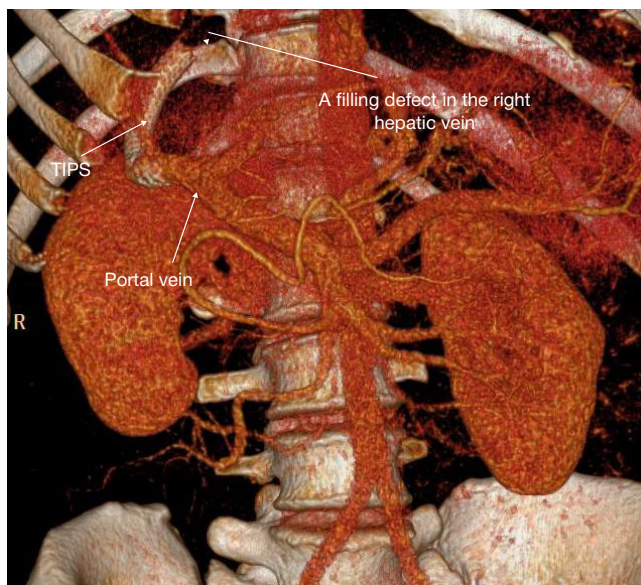

Fig. 2. A CT-angiography image showing intimal hyperplasia of the right hepatic vein
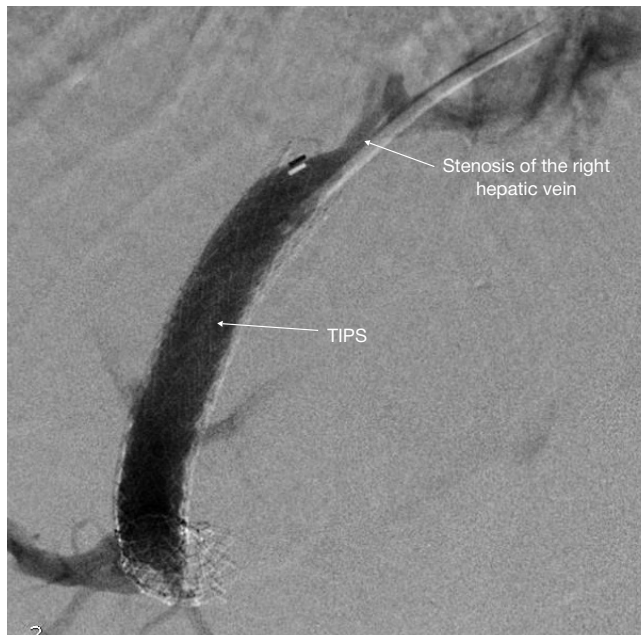

**Fig. 3.** Transjugular portal venogram of patient K
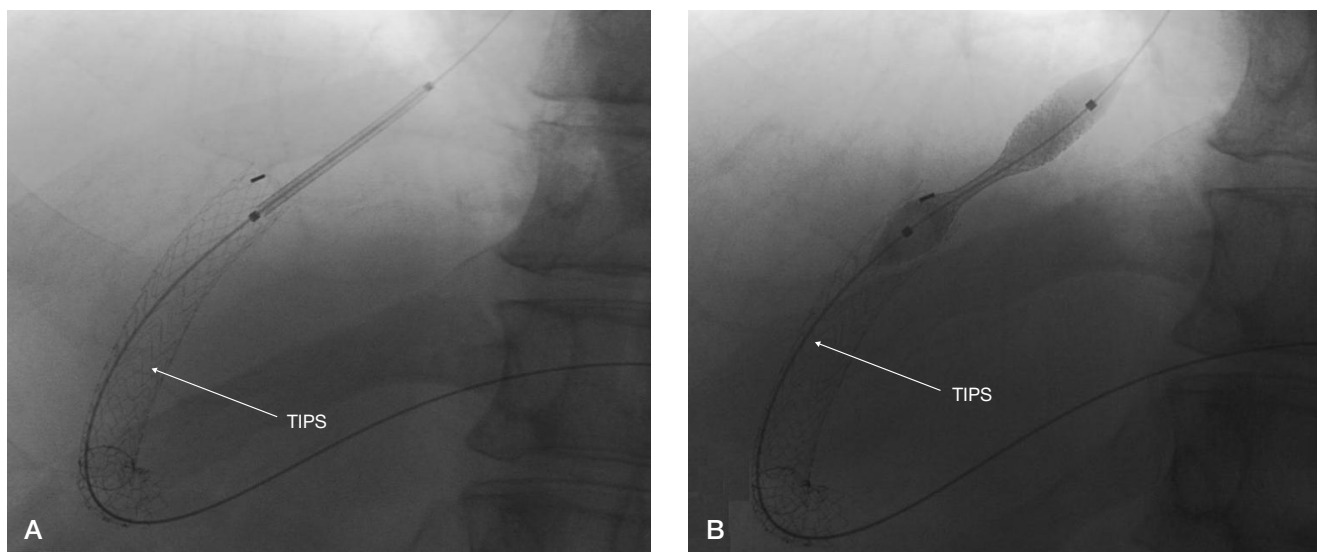
Fig. 4. Transjugular portal venogram of patient K. Stages of stent-in-stent placement. **A**. Stent implantation. **B**. Stent expansion

as progressing EVs, a decision was made to restore TIPS patency.

Stenosis was visualized by portal venography. After acquiring a portal venogram, it was decided to apply a stent-in-stent technique (Fig. 3 and 4).

Follow-up portal venography performed after the procedure revealed that the patency of the transjugular intrahepatic shunt had been re-established; no signs of stenosis were present on the venogram (Fig. 5).

The postoperative period was uneventful. On the Doppler image of the portal system, the intrashunt flow was normal, with a velocity of 112 cm/s. The patient received a course of medication therapy for his liver and was discharged when his condition was found to be satisfactory.

Since the procedure, the patient has been undergoing regular checkups in our clinic. His last hospitalization took place in August 2019. So far, no complications associated with portal hypertension have arisen in this 2-year follow-up period.

Discussion

As we were analyzing the literature and our own clinical experience, we arrived at the conclusion that stent-grafts are the best option for creating intrahepatic shunts during a TIPS procedure. The use of stent- grafts reduces the risk of shunt thrombosis in the early postoperative period and the incidence of TIPS dysfunction in the late postoperative period [8, 9].

However, in spite of all advantages of stent-grafts, shunt patency can deteriorate over time due to stenosis caused by intimal hyperplasia of the right hepatic vein. To reduce the risk of this complication, the stent should be placed in the ostium of the right hepatic vein [10, 11].

The clinical case presented in this article demonstrates that reinterventions after TIPS, including placement of stents in the
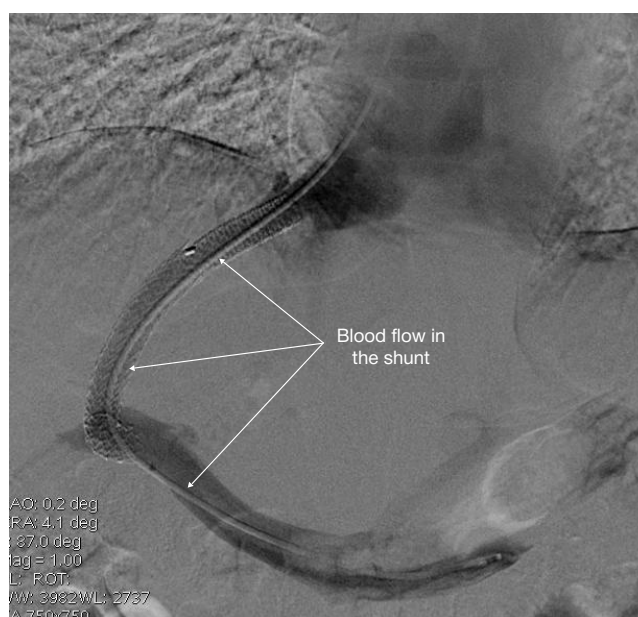

Fig. 5. Transjugular portal venogram of patient K. after TIPS revision and stent-in-stent placement

right hepatic vein, reduce the risk of complications associated with portal hypertension, improve life expectancy of the affected patients and the quality of their lives.

CONCLUSIONS

Re-establishing the patency of a compromised intrahepatic shunt has serious implications. A long-lasting TIPS allows liver transplant candidates to be on the waiting list for quite a long time without being at risk for variceal bleeding.

References

1. Elsebaey MA, et al. Endoscopic injection sclerotherapy versus N-Butyl-2 Cyanoacrylate injection in the management of actively bleeding esophageal varices: a randomized controlled trial. BMC gastroenterology. 2019; 19 (1): 23.
2. Shi L, et al. Favorable Effects of Endoscopic Ligation Combined with Drugs on Rebleeding and Mortality in Cirrhotic Patients: A Network Meta-Analysis. Digestive Diseases. 2018; 36 (2): 136–49.
3. Anisimov AYu, Vertkin AL, Devyatov AV, Dzidzava II, Zhigalova SB, Zatevakhin II, et al. Clinical guidelines on treatment of esophageal and stomach variceal bleeding. Available from: http://xn--

--9sbdbejx7bdduahou3a5d.xn--p1ai/stranica-pravlenija/unkr/urgentnaja-abdominalnaja-hirurgija/klinicheskie-rekomendaci-po-lecheniyu-krovotechenii-iz-varikozno-rasshirenyh-ven-pischevoda-i-zheludka.html.

4. Masalaite L, Valantinas J, Stanaitis J. Endoscopic ultrasound findings predict the recurrence of esophageal varices after endoscopic band ligation: a prospective cohort study. Scandinavian journal of gastroenterology. 2015; 50 (11): 1322–30.

5. Bureau C, et al. Transjugular intrahepatic portosystemic shunts with covered stents increase transplant-free survival of patients with cirrhosis and recurrent ascites. Gastroenterology. 2017; 152 (1): 157–63.

6. Lv Y, Han G, Fan D. Thrombosis after transjugular intrahepatic portosystemic shunt: an ominous sign? AME Medical Journal. 2017; 2 (40).

7. Li YH, et al. Long-term shunt patency and overall survival of transjugular intrahepatic portosystemic shunt placement using covered stents with bare stents versus covered stents alone // Clinical radiology. 2018; 73 (6): 580–7.

8. Saad WE. A. Portal Hypertension: Imaging, Diagnosis, and Endovascular Management. Thieme, 2017.

9. Luo, Xue-Feng, et al. Stent-Grafts for the Treatment of TIPS Dysfunction: Fluency Stent vs Wallgraft Stent. World Journal of Gastroenterology. 2013; 19 (30): 5000–5.

10. Wang Q, et al. Eight millimetre covered TIPS does not compromise shunt function but reduces hepatic encephalopathy in preventing variceal rebleeding. Journal of hepatology. 2017; 67 (3): 508–16.

11. Suhocki PV, et al. Transjugular intrahepatic portosystemic shunt complications: prevention and management // Seminars in interventional radiology. Thieme Medical Publishers. 2015; 32 (2): 123–32.

Литература

1. Elsebaey MA, et al. Endoscopic injection sclerotherapy versus N-Butyl-2 Cyanoacrylate injection in the management of actively bleeding esophageal varices: a randomized controlled trial. BMC gastroenterology. 2019; 19 (1): 23.

2. Shi L, et al. Favorable Effects of Endoscopic Ligation Combined with Drugs on Rebleeding and Mortality in Cirrhotic Patients: A Network Meta-Analysis. Digestive Diseases. 2018; 36 (2): 136–49.

3. Анисимов А. Ю., Верткин А. Л., Девятов А. В., Дзидзава И. И., Жигалова С. Б., Затевахин И. И., и др. Клинические рекомендации по лечению кровотечений из варикозно-расширенных вен пищевода и желудка. Доступно по ссылке: http://xn----9sbdbejx7bdduahou3a5d.xn--p1ai/stranica-pravlenija/unkr/urgentnaja-abdominalnaja-hirurgija/klinicheskie-rekomendaci-po-lecheniyu-krovotechenii-iz-varikozno-rasshirenyh-ven-pischevoda-i-zheludka.html.

4. Masalaite L, Valantinas J, Stanaitis J. Endoscopic ultrasound findings predict the recurrence of esophageal varices after endoscopic band ligation: a prospective cohort study. Scandinavian journal of gastroenterology. 2015; 50 (11): 1322–30.

5. Bureau C, et al. Transjugular intrahepatic portosystemic shunts with covered stents increase transplant-free survival of patients with cirrhosis and recurrent ascites. Gastroenterology. 2017; 152 (1): 157–63.

6. Lv Y, Han G, Fan D. Thrombosis after transjugular intrahepatic portosystemic shunt: an ominous sign? AME Medical Journal. 2017; 2 (40).

7. Li YH, et al. Long-term shunt patency and overall survival of transjugular intrahepatic portosystemic shunt placement using covered stents with bare stents versus covered stents alone // Clinical radiology. 2018; 73 (6): 580–7.

8. Saad WE. A. Portal Hypertension: Imaging, Diagnosis, and Endovascular Management. Thieme, 2017.

9. Luo, Xue-Feng, et al. Stent-Grafts for the Treatment of TIPS Dysfunction: Fluency Stent vs Wallgraft Stent. World Journal of Gastroenterology. 2013; 19 (30): 5000–5.

10. Wang Q, et al. Eight millimetre covered TIPS does not compromise shunt function but reduces hepatic encephalopathy in preventing variceal rebleeding. Journal of hepatology. 2017; 67 (3): 508–16.

11. Suhocki PV, et al. Transjugular intrahepatic portosystemic shunt complications: prevention and management // Seminars in interventional radiology. Thieme Medical Publishers. 2015; 32 (2): 123–32.

CASE REPORT: REMOVAL OF A PROLIFERATING PILOMATRICOMA WITH A CO_2 LASER

Gaydina TA ✉, Dvornikov AS, Skripkina PA

Pirogov Russian National Research Medical University, Moscow, Russia

Tumors of the skin/skin adnexa are astonishingly diverse. The diagnostic algorithms for skin neoplasms includes history taking, the assessment of clinical data, dermoscopy and a histopathological examination. Literature descriptions of a histologically confirmed pilomatricoma are scarce. If the lesion is localized to an esthetically sensitive body area, it is important to minimize the postoperative cosmetic defect. In the case described below, we were able to achieve a positive esthetic outcome in a patient with a facial pilomatricoma sized < 2 cm using a CO_2 laser.

Author contribution: Gaydina TA — surgery; literature analysis; data acquisition, analysis and interpretation; manuscript preparation; Dvornikov AS — literature analysis; data acquisition, analysis and interpretation; Skripkina PA — manuscript preparation.

Compliance with ethical standards: the patient gave informed consent to the surgical intervention and publication of her personal data.

✉ **Correspondence should be addressed:** Tatiana A. Gaydina
Ostrovityanova, 1, Moscow, 117997; doc429@yandex.ru

КЛИНИЧЕСКИЙ СЛУЧАЙ: УДАЛЕНИЕ ПРОЛИФЕРИРУЮЩЕЙ ПИЛОМАТРИКСОМЫ CO_2-ЛАЗЕРОМ

Т. А. Гайдина ✉, А. С. Дворников, П. А. Скрипкина

Российский национальный исследовательский медицинский университет имени Н. И. Пирогова, Москва, Россия

В клинической практике врачи разных специальностей наблюдают большое разнообразие новообразований кожи (НК) и ее придатков. Алгоритм диагностики включает оценку анамнестических и клинических данных, дерматоскопическое и гистологическое исследования. Описание пиломатриксомы с гистологическим подтверждением диагноза представляет собой редкий клинический случай. При локализации пиломатриксомы на эстетически значимом участке кожного покрова задача врача минимизировать косметический дефект после удаления. Мы получили положительный косметический результат после удаления пиломатриксомы диаметром менее 2 см² на коже лица методом CO_2-лазерной деструкции.

Информация о вкладе авторов: Т. А. Гайдина — проведение оперативного лечения, анализ литературы, сбор, анализ и интерпретация данных, подготовка черновика рукописи; А. С. Дворников — анализ литературы, сбор, анализ, интерпретация данных; П. А. Скрипкина — подготовка черновика рукописи.

Соблюдение этических стандартов: пациентка подписала добровольное информированное согласие на проведение оперативного лечения.

✉ **Для корреспонденции:** Татьяна Анатольевна Гайдина
ул. Островитянова, д. 1, г. Москва, 117997; doc429@yandex.ru

The diversity of clinical presentations of skin neoplasms (SN) seen on physical examination and the ensuing difficulty in their differential diagnosis necessitate the use of additional diagnostic techniques. The initial examination of SN includes dermoscopy [1]; ultrasonography, siascopy, confocal laser scanning microscopy, [2] and near-infrared multispectral imaging [3] can also facilitate the diagnosis, if available. However, the application of these tools does not eliminate the possibility of misdiagnosis; even the findings of a histopathological examination, the gold standard of modern medicine, can be subject to misinterpretation [4]. Dermoscopy is a widespread technique for diagnosing melanocytic skin tumors in the first place [5]. Dermoscopy images of rare SN, such as pilomatricoma, are underrepresented in the literature.

Pilomatricoma, also known as benign calcifying epithelioma, necrotizing epithelioma, calcifying epithelioma of Malherbe, and pilomatrixoma, is a rare benign skin neoplasm with follicular differentiation. In 1880, A. Malherbe and J. Chenantais hypothesized that the tumor derived from sebaceous glands [6]. In 1961, R. Forbis and E. Helwig coined the term "pilomatricoma" because they found that the tumor arose from the outer sheath cells of the hair follicle root [6]. F. Moehlenbeck reported that pilomatricoma accounted for 0.12% of 140,000 SN he had analyzed [6]. Today, it is known that pilomatricoma originates

from the hair follicle matrix [7]. It is usually localized to the head or neck and is more often seen in children, especially girls, although adults are also affected [8]. Its clinical manifestations are diverse. The tumor can present as a small, barely noticeable subcutaneous lesion, as well as a bigger, more aggressive and locally invasive growth [9]. Due to its varying clinical presentations, pilomatricoma can be mistaken for a malignancy. Unattractive postoperative scars can cause emotional distress in patients with facial pilomatricomas. Therefore, the size and location of the lesion, the risk of developing a hypertrophic or keloid scar, comorbidities, and the patient's age should all be taken into account when deciding on the best treatment option. It is important to minimize the postoperative cosmetic defect and achieve an esthetically acceptable result.

Clinical case

Female patient K., aged 52, presented with a skin lesion on her left cheek (Fig.1). She had first spotted the lesion 20 years before but never sought medical advice. The patient had tried to squeeze it on repeated occasions before she noticed the mass was growing.

Status localis: the patient's skin color was normal; her Fitzpatrick skin type was III. On the left cheek, there was

a nodular pink-pale mass sized 10.0 × 10.0 × 0.5 mm with a heterogenous lobular structure and yellow inclusions. The mass was soft and non-tender on palpation. The surrounding skin was intact.

Dermoscopy allowed a 20x magnification. The examination revealed a mass with clear margins and a lobular structure, symmetrical on two axes; the mass had homogenous yellow and pale pink inclusions, tortuous blood vessels and skin flakes (Fig. 2).

The analysis of the dermoscopy image by a convolution neural network suggested a benign tumor.

Clinical diagnosis: a benign skin neoplasm of the face (D23.3).

Differential diagnosis: basal cell carcinoma, epidermoid cyst, atheroma, xanthogranuloma, dermal cylindroma, dermatofibroma.

Considering the location of the neoplasm and its size (up to 2 cm^2), it was decided to remove it under local anesthesia using a CO_2 laser; the procedure was preceded by a scalpel biopsy.

Histopathology: D17.0 Proliferating pilomatricoma (necrotizing epithelioma of Malherbe) (Fig. 3). ICD-O code: 8110/0.

The follow-up examination conducted 2 weeks after surgery revealed formation of a neat scar (Fig. 4, 5)

Discussion

Patients with SN seek medical advice from both cancer specialists and non-oncologists. According to the literature, skin malignancies are the most common cancer type reported in the Russian Federation, amounting to 12.6% (excluding melanoma) or 14.2% (including melanoma) [10]. It is critical that the patient should be immediately referred to an oncologist if clinical examination is suspicious of a skin/skin adnexa malignancy in order to make a timely diagnosis and decide on an adequate treatment strategy [11]. Pilomatricoma is a rare skin lesion, and physical examination alone does not provide the accurate diagnosis. In the case described in this article, we performed dermoscopy and carried out a histopathological study of the excised mass. With rare SN, there is always a risk that dermoscopy findings can be misinterpreted. In this regard, the use of artificial intelligence (AI) for the initial screening for SN is a promising approach [12]. At present, AI is employed to analyze digital microphotographs; it demonstrates high sensitivity in detecting malignancies. A convolutional neural network (CNN) is trained on over 100,000 microphotographs

Fig. 2. Dermoscopy: a mass with a clear lobular structure, showing homogenous areas of yellow and pale pink, tortuous blood vessels and skin flakes (magnification: ×20)
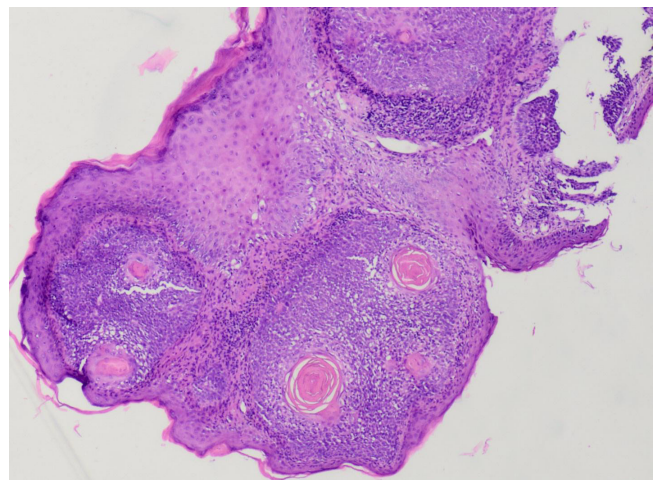
Fig. 3. A skin fragment with a nodule consisting of proliferating epithelial cells in a garland-resembling arrangement. Some of the cells are necrotic (the so-called shadow cells). Inflammatory cell infiltrate is seen around the layers of the epithelium (staining: hematoxylin and eosin; magnification ×40)

Fig. 1. A pale-pink skin nodule with yellow inclusions on the left cheek

Fig. 4. Dermoscopy: a well-demarcated symmetrical pale pink area (magnification: ×20)

of SN with a histologically confirmed diagnosis [13]. It can build its own algorithms for decision making during the analysis. A trained CNN demonstrates better specificity and sensitivity in comparison with dermatologists who have little (<2 years) or moderate (>5 years) experience in dermoscopy [13]. Of course, AI cannot replace humans in diagnosing SN, but it can assist fledgling doctors in decision making. In the nearest future CNNs will continue to develop and will be trained on real clinical data; this will improve the diagnostic accuracy for such rare SN as pilomatricoma.

Due to the risk of postoperative hypertrophic scarring, facial surgery can be a stressful factor for the affected patients. The arsenal of techniques for pilomatricoma removal is broad and includes surgical excision, curettage, cauterization, cryosurgery, photodynamic therapy, and laser ablation. It is reported that the use of a CO_2 laser for removing various SN and appendageal tumors of the face produces a good esthetic result [14, 15]. A CO_2 laser reduces the rate of pilomatricoma recurrence, the time needed for the surgical wound to epithelize, the incidence of intraoperative and postoperative complications, and increases the positive feedback rate. A CO_2 laser is highly effective in removing small (<2 cm^2) pilomatricomas, providing a good esthetic result.

CONCLUSIONS

Physical examination alone is not enough to diagnose a pilomatricoma; additional noninvasive diagnostic tools should be employed. Dermoscopy is the most common technique in dermatology; however, the literature shows a lack of dermoscopy images of rare skin neoplasms, such as pilomatricoma. There is a need for a dermoscopy images database of rare skin tumors for the subsequent computer-assisted analysis in order to improve the accuracy of diagnostic screening. Pilomatricomas less than 2 cm^2 in size, especially those located on esthetically sensitive body areas, should be removed using a CO_2 laser. This technique produces a good esthetic result and minimizes cosmetic defects.

Fig. 5. A neat postoperative scar is staring to form

References

1. Kubanov AA, Sysoeva TA, Gallyamova YuA, Bisharova AS, Mercalova IB. Algoritm obsledovanija pacientov s novoobrazovanijami kozhi. Lechashhij vrach. 2018; (3): 83–8. Russian.
2. Malishevskaya NP, Sokolova AV. Sovremennye metody neinvazivnoj diagnostiki melanomy kozhi. Vestnik dermatologii i venerologii. 2014; (4): 46–53. Russian.
3. Rey-Barroso L, Burgos-Fernández FJ, Delpueyo X, Ares M, Royo S, Malvehy, J, et al. Visible and Extended Near-Infrared Multispectral Imaging for Skin Cancer Diagnosis Sensors. 2018; 18 (5): 1441.
4. Kit OI, Fomenko YuA, Karnauhov NS, Lapteva TO. Chastota rashozhdenija diagnoza v prizhiznennoj patologoanatomicheskoj diagnostike onkologicheskih zabolevanij (po materialam peresmotra gotovyh gistologicheskih preparatov v patologoanatomicheskom otdelenii FGBU RNIOI MZ RF). Issledovanija i praktika v medicine. 2019; 6 (1S): 148. Russian.
5. Sinelnikov IE, Baryshnikov KA, Demidov LV. Klinicheskaja diagnostika melanomy kozhi. Vestnik RONC im. N. N. Blohina RAMN. 2017; 28 (1–2): 68–73. Russian.
6. Menshhikova GV, Ermilova AI, Abramov KS, Golubev SS. Sluchaj redkoj dobrokachestvennoj opuholi u rebenka. Rossijskij zhurnal kozhnyh i venericheskih boleznej. 2015; 18 (1): 15–17. Russian.
7. Junusbaeva MM, Junusbaev BB, Valiev RR, Hammatova AA, Husnutdinova YeK. Shirokoe mnogoobrazie keratinov cheloveka. Vestnik dermatologii i venerologii. 2015; (5): 42–52. Russian.
8. Sudip S, Pranaya K, Barnali C, Kisalay G. Pilomatricoma mimicking ruptured epidermal cyst in a middle aged woman. Indian Journal of Dermatology. 2016; 61 (1): 88–90.
9. Mainak D, Indranil C. A lesson learnt: retrospection in a case of pilomatricoma mimicking as parotid neoplasm. Einstein (Sao Paulo). 2016; 14 (1): 104–5.
10. Kaprin AD, Starinskij VV, Petrova GV. Zlokachestvennye novoobrazovanija v Rossii v 2014 godu (zabolevaemost' i smertnost'). M.: MNIOI im. P. A. Gercena — filial FGBU «NMIRC» Minzdrava Rossii; 2016; 250 s. Russian.
11. Prikaz Ministerstva zdravoohranenija i social'nogo razvitija Rossijskoj Federacii ot 18 aprelja 2012g. # 381n Ob utverzhdenii Porjadka okazanija medicinskoj pomoshhi naseleniju po profilju «Kosmetologija». Dostupno po ssylke: https://legalacts.ru/doc/prikaz-minzdravsotsrazvitija-rossii-ot-18042012-n-381n/.
12. Fujisawa Y, Inoue S, Nakamura Y. The Possibility of Deep Learning-Based, Computer-Aided Skin Tumor Classifiers. Front Med (Lausanne). 2019; 27 (6): 191.
13. Haenssle HA, Fink C, Schneiderbauer R, Toberer F, Buhl T, Blum A, et al. Man against machine: diagnostic performance of a deep learning convolutional neural network for dermoscopic melanoma recognition in comparison to 58 dermatologists. Annals of Oncology. 2018; (0): 1–7.
14. McGee JS, Suchter MF, Milgraum SS. Multiple Familial Trichoepithelioma Successfully Treated with CO_2-Laser and Imiquimod. Skinmed. 2016; Dec 1; 14 (6): 467–8.
15. Cho HJ, Lee W, Jeon MK, Park JO, Yang EJ. Staged Mosaic Punching Excision of a Kissing Nevus on the Eyelid. Aesthetic Plast Surg. 2019; Jun; 43 (3): 652–7.

Литература

1. Кубанов А. А., Сысоева Т.А., Галлямова Ю. А., Бишарова А. С., Мерцалова И. Б. Алгоритм обследования пациентов с новообразованиями кожи. Лечащий врач. 2018; (3): 83–8.
2. Малишевская Н. П., Соколова А. В. Современные методы неинвазивной диагностики меланомы кожи. Вестник дерматологии и венерологии. 2014; (4): 46–53.
3. Rey-Barroso L, Burgos-Fernández FJ, Delpueyo X, Ares M, Royo S, Malvehy, J, et al. Visible and Extended Near-Infrared Multispectral Imaging for Skin Cancer Diagnosis Sensors. 2018; 18 (5): 1441.
4. Кит О. И., Фоменко Ю. А., Карнаухов Н. С., Лаптева Т. О. Частота расхождения диагноза в прижизненной патологоанатомической диагностике онкологических заболеваний (по материалам пересмотра готовых гистологических препаратов в патологоанатомическом отделении ФГБУ РНИОИ МЗ РФ). Исследования и практика в медицине. 2019; 6 (1S): 148.
5. Синельников И. Е., Барышников К. А., Демидов Л. В. Клиническая диагностика меланомы кожи. Вестник РОНЦ им. Н. Н. Блохина РАМН. 2017; 28 (1–2): 68–73.
6. Меньщикова Г. В., Ермилова А. И., Абрамов К. С., Голубев С. С. Случаи редкой доброкачественной опухоли у ребенка. Российский журнал кожных и венерических болезней. 2015; 18 (1): 15–17.
7. Юнусбаева М. М., Юнусбаев Б. Б., Валиев Р. Р., Хамматова А. А., Хуснутдинова Э. К. Широкое многообразие кератинов человека. Вестник дерматологии и венерологии. 2015; (5): 42–52.
8. Sudip S, Pranaya K, Barnali C, Kisalay G. Pilomatricoma mimicking ruptured epidermal cyst in a middle aged woman. Indian Journal of Dermatology. 2016; 61 (1): 88–90.
9. Mainak D, Indranil C. A lesson learnt: retrospection in a case of pilomatricoma mimicking as parotid neoplasm. Einstein (Sao Paulo). 2016; 14 (1): 104–5.
10. Каприн А. Д., Старинский В. В., Петрова Г. В. Злокачественные новообразования в России в 2014 году (заболеваемость и смертность). М.: МНИОИ им. П. А. Герцена — филиал ФГБУ «НМИРЦ» Минздрава России; 2016; 250 с.
11. Приказ Министерства здравоохранения и социального развития Российской Федерации от 18 апреля 2012 г. № 381н Об утверждении Порядка оказания медицинской помощи населению по профилю «Косметология». Доступно по ссылке: https://legalacts.ru/doc/prikaz-minzdravsotsrazvitija-rossii-ot-18042012-n-381n/.
12. Fujisawa Y, Inoue S, Nakamura Y. The Possibility of Deep Learning-Based, Computer-Aided Skin Tumor Classifiers. Front Med (Lausanne). 2019; 27 (6): 191.
13. Haenssle HA, Fink C, Schneiderbauer R, Toberer F, Buhl T, Blum A, et al. Man against machine: diagnostic performance of a deep learning convolutional neural network for dermoscopic melanoma recognition in comparison to 58 dermatologists. Annals of Oncology. 2018; (0): 1–7.
14. McGee JS, Suchter MF, Milgraum SS. Multiple Familial Trichoepithelioma Successfully Treated with CO_2-Laser and Imiquimod. Skinmed. 2016; Dec 1; 14 (6): 467–8.
15. Cho HJ, Lee W, Jeon MK, Park JO, Yang EJ. Staged Mosaic Punching Excision of a Kissing Nevus on the Eyelid. Aesthetic Plast Surg. 2019; Jun; 43 (3): 652–7.

QUANTITATIVE PCR IN DIAGNOSING INFECTIOUS UROGENITAL PATHOLOGY

Rakhmatulina MR[1] ✉, Galkina IS[2]

[1] Burnasyan Federal Medical Biophysical Center of Federal Medical Biological Agency, Moscow, Russia

[2] Federal Research Institute for Health Organization and Informatics of Ministry of Health of the Russian Federation, Moscow, Russia

This article describes the contemporary methods of diagnosing sexually transmitted infections, their advantages and disadvantages, indications for use. The authors describe application of quantitative polymerase chain reaction in diagnosing inflammatory diseases and dysbiotic conditions in men and women. This method, which is currently the "golden standard" in urogenital pathology diagnostics, has undeniable advantages over microbiological methods and qualitative polymerase chain reaction: the preanalytical stage requirements (preservation of quantitative ratios between microorganisms or nucleic acids of microorganisms) are not as strict, the risk of contamination from outside environment and subsequent corruption of the results is significantly smaller, the conditions for all microorganisms, including those impossible and hard to cultivate, are the same sensitivity and specificity-wise, it is possible to sample materials and evaluate microbiota (ratios of microorganisms and their groups) and also possible to collect samples non-invasively, the speed of testing is high.

ДИАГНОСТИКА ИНФЕКЦИОННОЙ УРОГЕНИТАЛЬНОЙ ПАТОЛОГИИ МЕТОДОМ КОЛИЧЕСТВЕННОЙ ПЦР

М. Р. Рахматулина[1] ✉, И. С. Галкина[2]

[1] Федеральный медицинский биофизический центр имени А. И. Бурназяна, Москва, Россия

[2] Центральный научно-исследовательский институт организации и информатизации здравоохранения Минздрава России, Москва, Россия

В статье представлены современные методы диагностики инфекций, передаваемых половым путем, их преимущества и недостатки, показания к применению. Описаны возможности количественной полимеразной цепной реакции для диагностики воспалительных заболеваний и дисбиотических состояний у мужчин и женщин. Данный метод, являющийся в настоящее время «золотым стандартом» диагностики урогенитальной патологии, имеет неоспоримые преимущества перед микробиологическими методами и полимеразной цепной реакцией в качественном формате: менее жесткие требования к преаналитическому этапу для сохранения количественных соотношений между микроорганизмами (нуклеиновыми кислотами микроорганизмов), значительно меньший риск влияния на результат исследования контаминации образцов микроорганизмами из внешней среды, равные условия по чувствительности и специфичности для всех микроорганизмов, в том числе некультивируемых и труднокультивируемых, возможность контроля взятия материала и оценки состояния микробиоты по отношению микроорганизмов и их групп друг к другу, скорость получения результата и возможность исследования неинвазивно взятых образцов.

Contemporary researchers estimate that over 357 million people a year contract bacterial pathogens of sexually transmitted infections (STIs) [1, 2], and the frequency of inflammatory diseases of urogenital tract caused by aerobic and anaerobic opportunistic microorganisms reaches 80% among genital sphere pathologies [3-5].

With the aim to reduce incidence of and eliminate STIs there was developed the Global Health Sector Strategy on Sexually Transmitted Infections (2009–2016, 2016–2021). One of the missions pursued by the strategy is popularization of early diagnostics of such diseases, including symptom-free cases, since diagnosing an STI at an early stage creates optimal conditions for effective treatment and helps prevent further spread of the infectious agents [2].

Until recently, culture test was the "golden standard" in urogenital infections diagnostics. However, a significant number of etiological agents of urogenital tract infections and inflammations are hard to culture or unculturable. Besides, culture testing is labor intensive and time consuming, which significantly limits its use in routine clinical practice. Thus, there is a need for new diagnostic technology for urogenital pathology.

Diagnostic methods for urogenital infections

The current recommendation is to perform extra tests to confirm gonococcal infection diagnosed through microscopic examination only if the patient is male and the disease

manifests itself. Microscopy has a number of deficiencies that limit its applicability significantly: the assessments of results are subjective, the sensitivity is low (30–40%) when examining cervical, pharyngeal and rectal samples, as well as in cases of asymptomatic infections [6]. For children, pregnant women, women during menopause and in suspected cases of extragenital and complicated forms of the disease it is necessary to use culture and/or molecular biological testing methods. In *N. gonorrhoeae* identification, the specificity and sensitivity offered by molecular biological methods reaches 100%. They are given priority in the routines of diagnosing asymptomatic forms of the disease, when a mixed infection is suspected, in screening examinations and when there are anamnestic and/or clinical signs of gonococcal infection with negative results of microscopic examination or when there are altered gram-negative or gram-stable diplococci detected [7, 8].

The basic methods of diagnosing urogenital trichomoniasis are native preparation microscopy, molecular biological and culture methods. Native preparation microscopy is performed immediately after sampling biological material, which limits

applicability of this method. Microscopy of stained preparations is not recommended for diagnostic purposes since its sensitivity and specificity are the lowest (30–60%) compared to other laboratory methods (Trichomonas vaginalis are often round and resemble polymorphonuclear leukocytes, and its typical morphological signs are lost during fixation and staining) [6].

Culture method's sensitivity and specificity largely depend on the composition of culture media and conditions of Trichomonas culturing. This method is more labor intensive and time consuming than molecular biological methods, the sensitivity of which is 88–97% and specificity — 98–99%. Molecular biological testing is given priority in cases of asymptomatic trichomoniasis (most often observed in males), when there is a mixed infection suspected, in screening examinations, and also when there is a need to control the quality of microscopic examination [5, 8].

It is recommended to apply only the molecular biological methods, with their specificity and sensitivity approaching 100% [5, 9], to validate diagnosis of chlamydial infection, diseases caused by *M. genitalium*, and viral STIs (anogenital herpes virus and human papillomavirus infections).
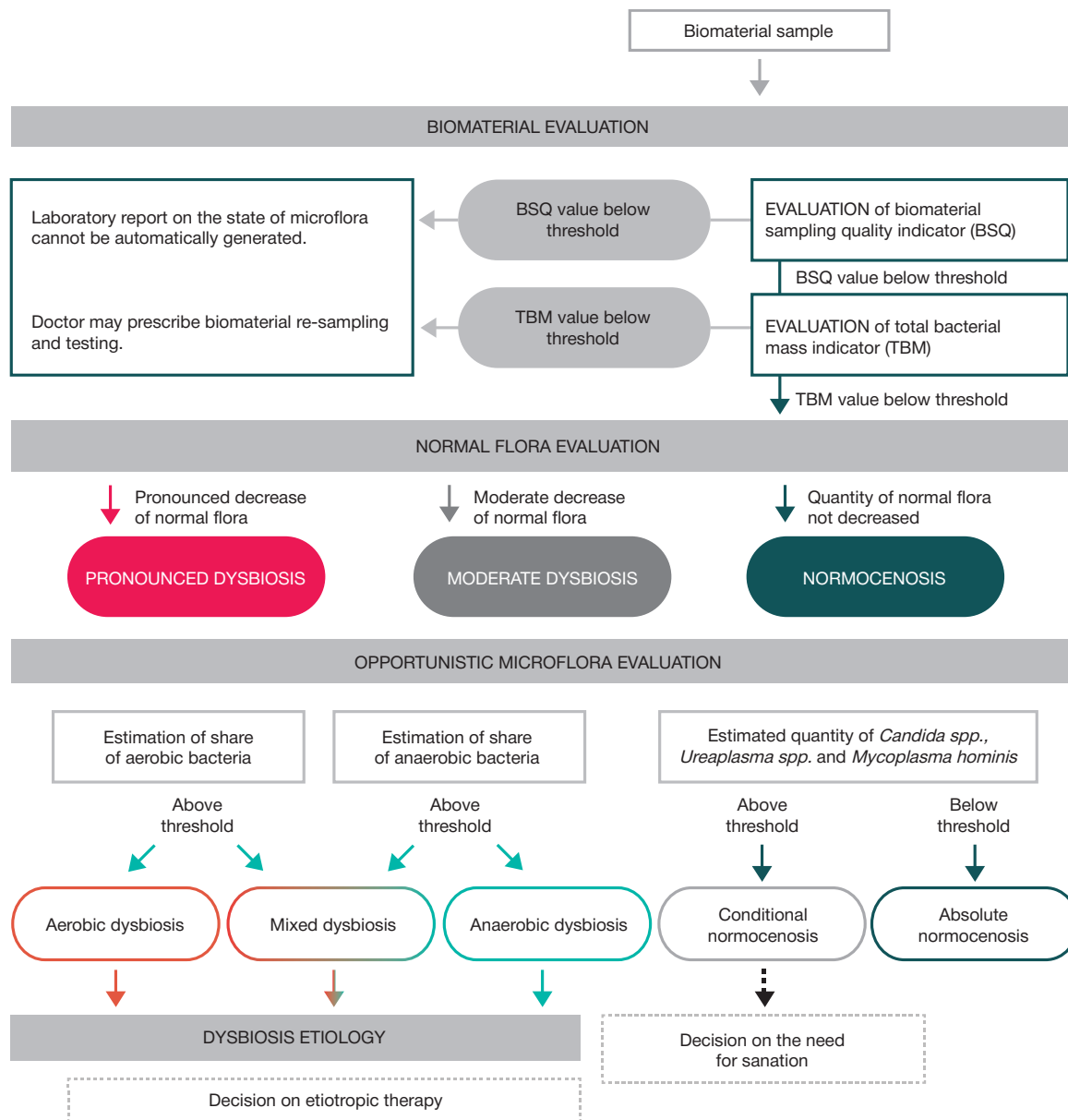

Fig. 1. The basic algorithm for interpreting urogenital tract microflora examination, female patients, real-time PCR

Thus, molecular biological methods — polymerase chain reaction (PCR), real-time PCR (RT PCR), NASBA — were added to the official lists as methods to diagnose all sexually transmitted infections.

Possibilities offered by molecular biological methods in diagnosing urogenital system pathologies

Introduction of PCR to clinical practice had a truly revolutionary effect on identification of STIs agents. However, improperly selected genetic targets and/or various inhibitory factors can affect sensitivity of PCR. Moreover, its specificity may also be hindered by non-pathogenic representatives of the same genus/family of microorganisms present in the sample. Besides, qualitative PCR does not provide sufficient information to identify opportunistic microorganisms.

Real-time PCR is a modification of PCR that combines amplification and simultaneous detection of accumulation of its products directly during the reaction. This method allows not only to determine DNA of the microorganism but also quantify its content in the sample. Real-time PCR does not involve post-amplification analysis of reaction products and extraction of the test tube contents, which significantly lowers the risk of sample contamination and eliminates the need for a separate laboratory zone, as well as reduces testing time and augments objectivity of interpretation of its results [10].

Until recently, only the culture method allowed identification of opportunistic aerobic microorganisms, while anaerobic microorganisms, which often cause inflammatory and dysbiotic diseases of genitourinary system, remained undetected. Meanwhile, it is known that this group of bacteria often competes with lactobacilli for biotope dominance, and with dysbiotic disorders in women, it is usually obligate-anaerobic microorganisms that colonize the vaginal epithelium [11].

Today, real-time PCR enables adequate diagnostics of STIs and simultaneous detection of dysbiotic conditions (aerobic/anaerobic vaginitis, urethritis, balanoposthitis, bacterial vaginosis, etc.) resulting from an imbalance between opportunistic microorganisms and normal urinary tract microbiota. There is a number of testing systems based on this method (Florocenosis, Ampliflor, Amplisens etc.) registered in Russia; they allow qualitative and quantitative assessment of pathogenic and opportunistic aerobic microorganisms. Florocenosis and Ampliflor enable identification of lactobacilli, representatives of the Candida genus, family *Enterobacteriaceae*, *Streptococcus spp.*, *Staphylococcus spp.*, *G.vaginalis, A.vaginae*, opportunistic mycoplasmas, but they do not allow detecting obligate anaerobic microorganisms. Femoflor-16 and Androflor testing systems offer the widest detected range of opportunistic aerobic and anaerobic microorganisms of all the systems available. Application of these unique "paired" tests, developed for women and men, allows developing an effective algorithm for laboratory examination of couples and selection of therapy if one or both partners have infectious diseases of reproductive system or reproductive function disorders (Fig. 1, 2) [12, 13].

From the clinical point of view, one of the most important features of these testing systems is sampling quality control: the marker of sufficiency of collected epithelial cells that enter transport medium when scraping. At the early stages of examination, this indicator allows assessing adequacy of biomaterial sampling and avoiding false positive and false negative results [14, 15].

Absolute quantitative results of real-time PCR are given in genome equivalents (GE), the values of which are proportional to microbial contamination of urogenital biotope. However, according to some researchers, absolute quantitative indicators do not always correlate with severity of clinical picture of the disease, and values in excess of their thresholds do not always
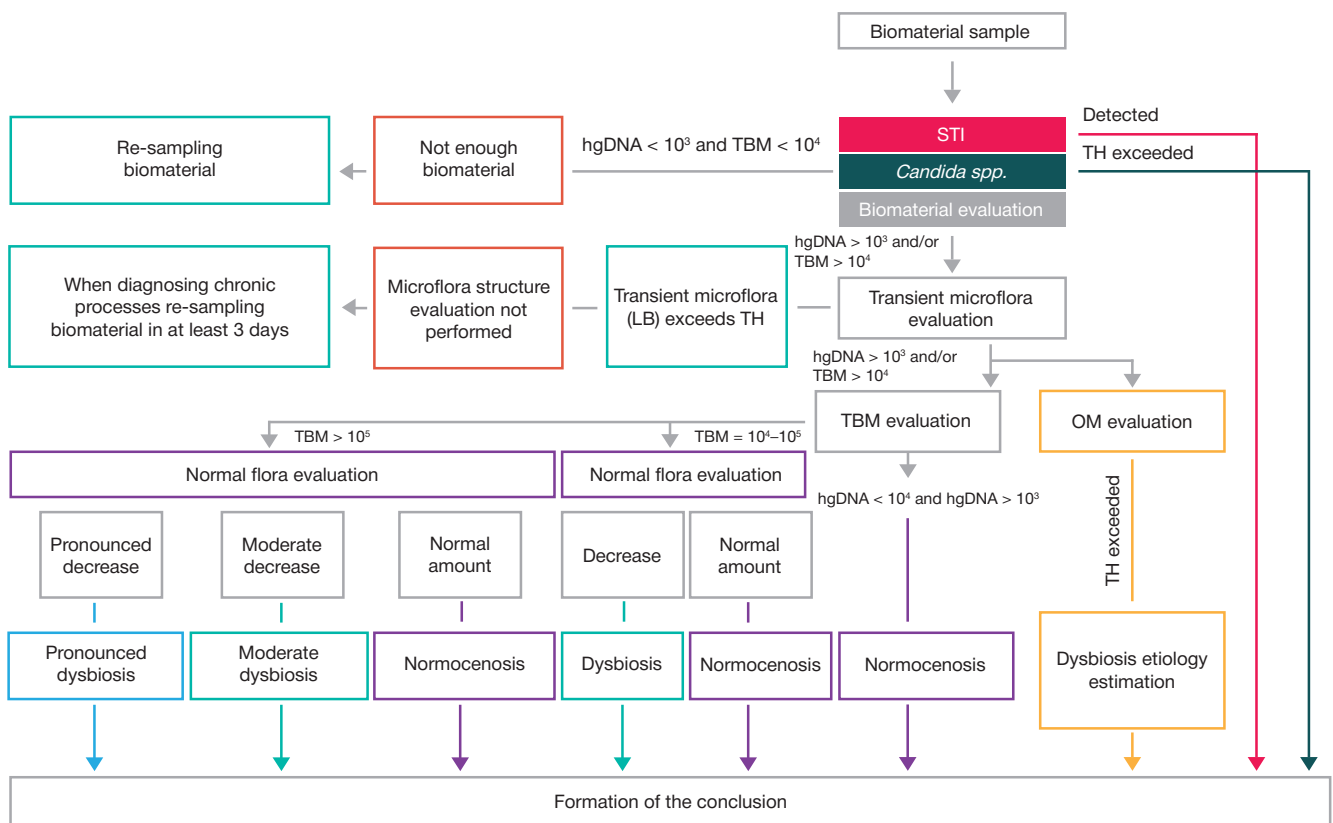
Abbreviations: TBM — total bacterial mass, hgDNA — human genomic DNA, LB — lactobacilli, OM — opportunistic microorganisms, TH — threshold value

Fig. 2. The basic algorithm for interpreting urogenital tract microflora examination, male patients, real-time PCR

signal of clinical manifestations of an infectious-inflammatory process. Back in 1986, F. J. Roberts found a bacteriuria level below significancy in 30% of patients with clinically and laboratory confirmed bacterial infections of genitourinary tract, and in 1987 J. A. Kellogg et al. found no correlation between clinical manifestations of urethritis and a significant level of bacteriuria. In this connection, determining the relative quantitative indicators (shares) of opportunistic microorganisms as a logarithmic difference and as a percentage of the total bacterial mass is of great practical interest. This indicator allows a specialist to assess the share of each microorganism or group of microorganisms in a specific biological sample, as well as evaluate their prevalence over other species, including

normoflora, which significantly increases clinical significance of the test.

CONCLUSIONS

PCR, previously discredited as oversensitive for urogenital pathology diagnosing, justifies itself through introduction of quantitative PCR tests into routine clinical practice, which enable express testing providing a comprehensive assessment of the state of urogenital biocenosis. This approach demonstrates the ratio of key representatives of the microbial community and reduces the share of false positive and false negative results.

References

1. Ye H, Song T, Zeng X, Li L, Hou M, Xi M. Association between genital mycoplasmas infection and human papillomavirus infection, abnormal cervical cytopathology, and cervical cancer: a systematic review and meta-analysis. Arch Gynecol Obstet. 2018 Jun; 297 (6): 1377–87.
2. Global Health Sector Strategy on Sexually Transmitted Infections. 2016–2021. World Health Organization, 2016. Available from: http://www.who.int/mediacentre/factsheets/fs110/ru/
3. Khan J, Farzand R. Prevalence of Mycoplasma hominis and Ureaplasma urealyticum among women with unexplaind infertility with and without vaginitis and cervicitis. African Journal of Microbiology Research. 2011; 5 (8): 861–64.
4. Krasnoselskikh TV, Manasheva EB, Gezey MA. Komorbidnost' sifilisa i VICh-infektsii: otritsatel'nyy epidemiologicheskiy i klinicheskiy sinergizm. VICh-infektsiya i immunosupressii. 2018; 10 (3): 7–16. Russian.
5. Klinicheskie rekomendatsii po vedeniyu bol'nykh infektsiyami, peredavaemymi polovym putem, i urogenital'nymi infektsiyami. M.: DEKS-press, 2012; 112 s. Russian.
6. Dolgov VV, redaktor. Klinicheskaya laboratornaya diagnostika. Uchebnik v 2 tomakh. M.: OOO «Labdiag», 2018; 624 s. Russian.
7. European Guideline on the Diagnosis and Treatment of Gonorrhoea in Adults 2012. Aavailable from: http://www.iusti.org/regions/Europe/pdf/2012/ Gonorrhoea_2012.pdf.
8. Sexually Transmitted Diseases Treatment Guidelines, 2015. MMWR, 2015; 64 (3).
9. Lanjouw E, Ouburg S, de Vries HJ, Stary A, Radcliffe K and

Unemo M. 2015 European guideline on the management of Chlamydia trachomatis infections. Int J STD AIDS. 2016 Apr; 27 (5): 333–48.
10. Rakhmatulina MR, Shatalova AYu. Sovremennye predstavleniya o mikrobiotsenoze vaginal'nogo biotopa i ego narusheniyakh u zhenshchin reproduktivnogo vozrasta. Vestnik dermatologii i venerologii. 2009; (3): 38–42. Russian.
11. Voroshilina ES, Donnikov AE, Plotko EE. Biotsenoz vlagalishcha s tochki zreniya kolichestvennoy polimeraznoy tsepnoy reaktsii: chto est' norma? Akusherstvo i ginekologiya. 2011; (1): 57–65. Russian.
12. Boldyreva MN, Galkina IS. Androflor® — novyy metod diagnostiki zabolevaniy urogenital'nogo trakta muzhchin. Meditsinskiy alfavit. 2016; 3 (282): 40–1. Russian.
13. Borovets SYu. Diagnosticheskaya znachimost' issledovaniya mikroflory eyakulyata u bol'nykh khronicheskim bakterial'nym prostatitom metodom PCR-RT «Androflor». Urologicheskie vedomosti. 2019; 9 (S): 22–3. Russian.
14. Shipitsyna EV, Martikaynen ZM, Vorobeva NE, Ermoshkina MS, Stepanova OS, Donnikov AE, i dr. Primenenie testa Femoflor dlya otsenki mikrobiotsenoza vlagalishcha. Zhurnal akusherstva i zhenskikh bolezney. 2009; 58 (3): 44–50. Russian.
15. Fomina OV, Bolotina ES. Opyt primeneniya test-sistemy «Femoflor-skrin» dlya otsenki vaginal'noy mikrobioty. V sbornike: IKh Vserossiyskoy nauchno-prakticheskoy konferentsii s mezhdunarodnym uchastiem. Molekulyarnaya diagnostika 2017. 2017 g. Moskva: 379–80. Russian.

Литература

1. Ye H, Song T, Zeng X, Li L, Hou M, Xi M. Association between genital mycoplasmas infection and human papillomavirus infection, abnormal cervical cytopathology, and cervical cancer: a systematic review and meta-analysis. Arch Gynecol Obstet. 2018 Jun; 297 (6): 1377–87.
2. Глобальная стратегия сектора здравоохранения по инфекциям, передаваемым половым путем. 2016–2021 гг. World Health Organization, 2016. Доступно по ссылке: http://www.who.int/mediacentre/factsheets/fs110/ru/
3. Khan J, Farzand R. Prevalence of Mycoplasma hominis and Ureaplasma urealyticum among women with unexplaind infertility with and without vaginitis and cervicitis. African Journal of Microbiology Research. 2011; 5 (8): 861–4.
4. Красносельских Т. В., Манашева Е. Б., Гезей М. А. Коморбидность сифилиса и ВИЧ-инфекции: отрицательный эпидемиологический и клинический синергизм. ВИЧ-инфекция и иммуносупрессии. 2018; 10 (3): 7–16.
5. Клинические рекомендации по ведению больных инфекциями, передаваемыми половым путем, и урогенитальными инфекциями. М.: ДЭКС-пресс, 2012; 112 с.

6. Долгов В. В., редактор. Клиническая лабораторная диагностика. Учебник в 2-х томах. М.: ООО «Лабдиаг», 2018; 624 с.
7. European Guideline on the Diagnosis and Treatment of Gonorrhoea in Adults 2012. Доступно по ссылке: http://www.iusti.org/regions/Europe/pdf/2012/ Gonorrhoea_2012.pdf.
8. Sexually Transmitted Diseases Treatment Guidelines, 2015. MMWR, 2015; 64 (3).
9. Lanjouw E, Ouburg S, de Vries HJ, Stary A, Radcliffe K, Unemo M. 2015 European guideline on the management of Chlamydia trachomatis infections. Int J STD AIDS. 2016 Apr; 27 (5): 333–48.
10. Рахматулина М. Р., Шаталова А. Ю. Современные представления о микробиоценозе вагинального биотопа и его нарушениях у женщин репродуктивного возраста. Вестник дерматологии и венерологии. 2009; (3): 38–42.
11. Ворошилина Е. С., Донников А. Е., Плотко Е. Э. Биоценоз влагалища с точки зрения количественной полимеразной цепной реакции: что есть норма? Акушерство и гинекология. 2011; (1): 57–65.
12. Болдырева М. Н., Галкина И. С. Андрофлор® – новый метод

диагностики заболеваний урогенитального тракта мужчин. Медицинский алфавит. 2016; 3 (282): 40–1.

13. Боровец С. Ю. Диагностическая значимость исследования микрофлоры эякулята у больных хроническим бактериальным простатитом методом PCR-RT «Андрофлор». Урологические ведомости. 2019; 9 (S): 22–3.

14. Шипицына Е. В., Мартикайнен З. М., Воробьева Н. Е., Ермошкина М. С., Степанова О. С., Донников А. Е., и др.

Применение теста Фемофлор для оценки микробиоценоза влагалища. Журнал акушерства и женских болезней. 2009; 58 (3): 44–50.

15. Фомина О. В., Болотина Е. С. Опыт применения тест-системы «Фемофлор-скрин» для оценки вагинальной микробиоты. В сборнике: IX Всероссийской научно-практической конференции с международным участием. Молекулярная диагностика 2017; 2017 г. Москва: 379–80.